



Trento Institute for  
Fundamental Physics  
and Applications



# ACTIVITY REPORT 2017



A collaborative centre for translational physics research



## **TIFPA Activity Report 2017**



**TIFPA**  
**Activity Report 2017**



Trento Institute for Fundamental Physics and Applications

Typeset in the Bitstream Charter typeface using the  $\text{\LaTeX}$  2<sub>ε</sub> document formatting system and markup language

Editor: Piero Spinnato (TIFPA)

Cover and overall graphics design: Francesca Cuicchio (Ufficio Comunicazione INFN, Rome)

Cover image: research activities at the experimental room of the APSS Protontherapy Centre in Trento, photograph courtesy of Marta Rovituso (TIFPA).

First print, May 2018

Printed and bound at Rotooffset Paganella, Trento

[www.rotooffset.it](http://www.rotooffset.it)

# Contents

Foreword	1	Nuclear Physics	55
Virtual Labs	3	AEgIS	57
Space Research	5	FOOT	59
Medical Technologies	13	Theoretical Physics	61
Sensors and Detectors	17	BELL	63
INFN Experiments	25	BIOPHYS	65
Particle Physics	27	FBS	67
ATLAS	29	FLAG	69
RD-FASE2	31	MANYBODY	72
Activities starting in 2018	33	NEMESYS	74
FASE2_ATLAS	33	NINPHA	76
Astroparticle Physics	35	TEONGRAV	78
AMS	37	Technological Research	81
DarkSide	40	APiX2	83
FISH	42	ARDESIA	85
HUMOR	44	AXIAL	87
LIMADOU	46	KIDS_RD	89
LISA Pathfinder and LISA	48	MoVe IT	91
QUAX	50	NADIR	94
Virgo	52	New Reflections	96
		Redsox2	98
		SEED	100

<b>SICILIA</b>	<b>101</b>	<b>LIDAL</b>	<b>119</b>
<b>Activities starting in 2018</b>	<b>103</b>	<b>MONDO</b>	<b>121</b>
ASAP	103	<b>MOPET</b>	<b>123</b>
DEEP 3D	103	<b>PLANT</b>	<b>125</b>
ELOFLEX	104	<b>Prima-RDH-IRPT</b>	<b>127</b>
ISOLPHARM-Ag	105	<b>Profiling</b>	<b>129</b>
TIMESPOT	106	<b>RIGHTABOVE</b>	<b>131</b>
XDET	106	<b>ROSSINI</b>	<b>133</b>
<b>Proton Beam-based R&amp;D</b>	<b>107</b>	<b>TIFPA Services</b>	<b>135</b>
<b>BUILDING</b>	<b>109</b>	<b>TIFPA Publications</b>	<b>139</b>
<b>ELOFLEX</b>	<b>111</b>	<b>Seminars</b>	<b>155</b>
<b>GammaRad</b>	<b>112</b>	<b>Events</b>	<b>164</b>
<b>iIMPACT</b>	<b>114</b>		
<b>KI-MARK</b>	<b>117</b>		



# Foreword

Marco Durante

Direttore,  
TIFPA

I am delighted to introduce the second Annual Report the Trento Institute for Fundamental Physics and Applications (TIFPA), a National research center of the National Institute for Nuclear Physics (INFN) in co-operation with Trento University (UNITN), Bruno Kessler Foundation, and the Healthcare Agency (APSS).

The year 2017 saw a rapid growth in the center in terms of budget and experiments. Compared to 2015, the budget has increased of 240%, the personnel by 400% and the number of INFN experiments with TIFPA participation by 180%. Most of the budget increase has been driven by external funds. The numbers themselves prove the enormous success of the center, which goes beyond the most optimistic expectations.

Yet the growth was not only quantitative, but qualitative as well. TIFPA is proud to offer to the scientific community a new accelerator facility, with two beamlines dedicated to research with 250 MeV protons. The use of the facility is now regulated by an agreement between TIFPA and APSS, and is an open, user facility, even if users are charged to contribute to the running costs. In 2017, we had 20 experiments in the TIFPA facility. We already have 10 in 2018, and counting. The facility has been rapidly noted in Europe and attracted great attention. It allowed TIFPA to enter the large Infrastructure project INSPIRE within Horizon2020. ESA has included TIFPA in the list of ground-based facilities for space radiation research, along with only other 4 accelerators in Europe (2 in Germany and one each in France and The Netherlands). The facility can gather funding from external sources and compensate the expenses by charging the users, a model which is new for clinical centers and is considered as an important example by IBA for other clinical centers worldwide with experimental rooms.

This tremendous growth and scientific achievements would not have been possible without the commitment of the TIFPA staff and associates. Not a single result could have been achieved without the hard work of Marta Perucci, Giuliana Pellizzari (seconded from the Trento Province), Christian Manea, the young Laura Chilovi, and Piero Spinnato, who also kindly prepared this document. Special thanks should go to Francesco Tommasino of UNITN, who has been instrumental in building the experimental room and is now chairing the Program Advisory Committee of the facility. I would like to thank all the other staff and associates, but I am limited in space. Just “thank you all”.

I hope you will enjoy reading the report, and I wish TIFPA a future filled of success.





# Virtual Labs





## Space Research

William Joseph Weber<sup>1,2</sup>  
williamjoseph.weber@unitn.it

with contributions by

William Jerome Burger,<sup>3,2</sup> Roberto Iuppa,<sup>1,2</sup> Chiara La Tessa<sup>1,2</sup>

2017 has been a year in which TIFPA has both consolidated existing strengths in long-running programs of space research and leveraged wide ranging local expertise to expand into new projects. Space technologies currently under development in TIFPA range from fundamental studies of the Universe, with observation of low frequency gravitational wave observation and astroparticles, to critical questions of applied space science including the radiation safety of astronauts, the removal of orbiting debris and earthquake detection from orbit.

While missions in orbit like LISA Pathfinder and AMS-02 continue to produce important scientific results, TIFPA is actively preparing the next generation AMS and the observatory LISA. Members of TIFPA are participating actively in important missions in various stages of development and operations, and serve at the highest levels in the scientific direction of both ESA and ASI. The unique environment of TIFPA provides a fertile ground for space research. Examples of this include the growing impact of the APSS beamline facility as a natural laboratory for a broad range of space radiation testing and collaboration with the materials science expertise in the Dipartimento di Fisica in the New Reflections laser ablation project.

This brief report presents the TIFPA contribution in developing technology for space research in 2017 and plans for the new year, divided into the main scientific and engineering

projects that will benefit from our research.

### Laser Interferometer Space Antenna (LISA)

Well before LISA Pathfinder was definitively turned off on July 18, 2017 (see report at p. 48), work on the orbiting gravitational wave observatory LISA was reaching full speed, and the TIFPA team has been rapidly shifting its focus to developing the necessary hardware and measurement techniques for LISA.

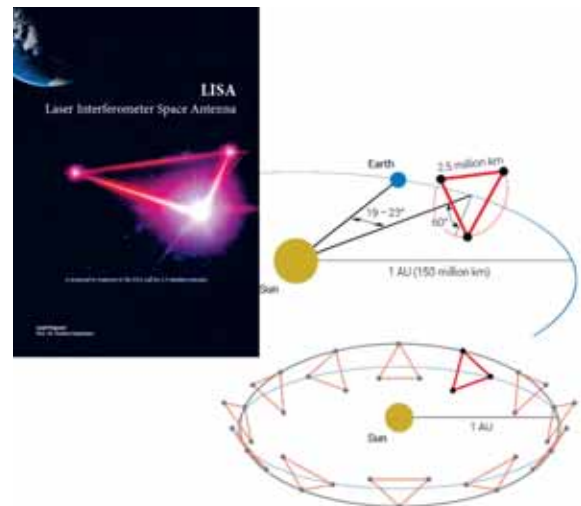


Figure 1: Proposal for the LASER Interferometer Space Antenna (LISA), since selected as the ESA L3 mission.

LISA<sup>1</sup> was proposed in January and selected by ESA in June, 2017, as the third Large Mission (L3) of the Cosmic Vision program, slated for launch in the early 2030s. LISA will initiate gravitational wave observation in the 20  $\mu$ Hz

<sup>1</sup>Danzmann, K. et al. (2017), [https://www.elisascience.org/files/publications/LISA\\_L3\\_20170120.pdf](https://www.elisascience.org/files/publications/LISA_L3_20170120.pdf).

<sup>1</sup>University of Trento, Italy

<sup>2</sup>INFN TIFPA, Trento, Italy

<sup>3</sup>FBK, Trento, Italy

to 0.1 Hz band. It is based on a constellation of free-falling test masses (TM) orbiting the Sun in a triangular formation (Fig. 1). A passing gravitational wave creates a tidal deformation of the TM constellation, producing differential accelerations along the three sides of the triangle that are measured with laser interferometry. The proposed design uses two TM freely-falling inside each of three spacecraft separated by 2.5 million km, with relative acceleration between distant TM measured in combinations of inter-spacecraft measurements of the varying laser Doppler shift and local TM to spacecraft measurements. The spacecraft are “drag-free” controlled to follow the two TM along the critical interferometry axes, leaving them as force-free references of geodesic motion.

From a measurement technology standpoint, interferometry between distant spacecraft is new to LISA, while the “local” challenges – the spacecraft drag-free control, the interferometric measurement the relative motion between TM and spacecraft, and particularly the use of TM as geodesic references – benefit from the LISA Pathfinder demonstrator hardware and measurement science heritage. The inter-spacecraft interferometry, which limits sensitivity above 5 mHz, will employ laser beams sent and received through a 30 cm diameter telescope, with 2 W output resulting in roughly 100 pW received light at the distant spacecraft, with precision tracking of the MHz doppler shifts caused by the differential orbital velocities between spacecraft.

The geodesic reference TM performance on the other hand sets the LISA sensitivity below 5 mHz, requiring that any spurious accelerations below

$$S_g^{1/2} < 3 \text{ fm/s}^2/\text{Hz}^{1/2} \times \left[ 1 + \left( \frac{0.4\text{mHz}}{f} \right)^2 \right]^{1/2} \quad (1)$$

LISA Pathfinder has demonstrated this, with margin, down to 20  $\mu\text{Hz}$ , but achieving this in the LISA constellation and hardware configuration, robustly and in a way that allows understanding and debugging in orbit, will demand design, analysis and experimental verification on ground in the next years. The Italian (ASI) contribution of the TM themselves

and the “gravitational reference sensor” (GRS) hardware that surrounds them, are the essential elements achieving this low noise geodesic reference system. This effort will have a large scientific impact: the low frequency acceleration noise level is critical for observations of super massive black holes, determining how long, to what distances, and with what precision these and other sources can be studied.

The LISA GRS will build upon the LPF hardware, illustrated in Fig. 2. Particular areas of measurement technology development in Trento in 2018 will include:

- **Vacuum**, designing the vacuum hardware and protocols to limit Brownian noise from residual gas and pressure gradients from outgassing
- **UV TM discharge**, analyzing and measuring the photoelectric discharge of the LISA TM inside the GRS
- **Gravitational balance**, with analysis and experimentation for the static field from the spacecraft mass and its fluctuations
- **GRS interface**, analysis contributing to the design for thermal and mechanical stability

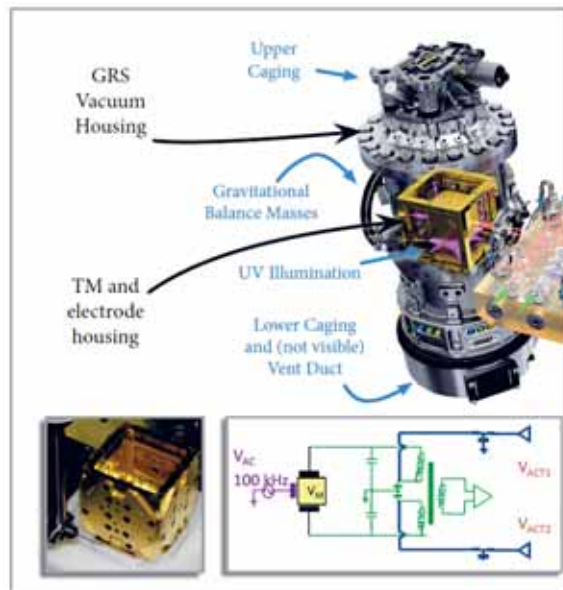


Figure 2: Illustration of GRS hardware heritage from LPF

In addition to hardware, the Trento group is designing techniques to measure, diagnose,

and correct for stray forces in the LISA constellation, addressing questions such as how to distinguish between a transient force on a single TM from a gravitational wave tidal deformation on the constellation, and how to measure a force on one TM using as a geodesic reference a TM in a spacecraft 2.5 million km away.

The LISA mission will begin, in Spring 2018, an industrial “phase A” top level study of the mission, from the measurement concept to the launcher, spacecraft, communications and power systems. In parallel, the “consortium” of European states that will provide the various measurement payload items – including the GRS – will develop these subsystems and their internal interface. An ESA “system engineering” team will oversee and harmonize these efforts, with participation by Trento and several other instrument PI groups, particularly for aspects regarding the free-fall metrology. The aim is to prepare the mission for possible adoption by ESA in the early 2020s, an important step towards opening the low frequency gravitational window on the Universe.

**Development of particle detectors** In 2017, the development of particle detectors in Trento was driven by the possibility of participating in the second CSES mission, scheduled for launch in 2020. Preliminary contacts of CNSA (Chinese National Space Agency) with ASI (Italian Space Agency) were aimed at exploring the possibility for the INFN Limadou collaboration to take charge of the second version of the High Energy Particle Detector (HEPD2). TIFPA team was asked to propose a new layout, drawing lessons from HEPD2 and improving both its sensitivity and operability. The most important request from the mission management is to lower the energy range accessible to the Italian payload. In fact, HEPD is sensitive to 10 – 200 MeV electrons and 30 – 300 MeV/n nuclei, whereas HEPD2 should go down to 5 MeV electrons and 15 MeV protons. As a consequence, the amount of material that particles have to pass through before triggering HEPD2 has to be much lower than for HEPD. Both the

tracker (currently made of two silicon detectors 300  $\mu\text{m}$  thick) and the trigger (currently made of plastic scintillators 0.5 cm thick) have to be replaced with thinner devices. Moreover, CSES2 is going to take data all along the orbit, differently from CSES, which is off for absolute latitudes higher than  $65^\circ$ . The higher the latitude, the less the shielding from the geomagnetic field, the higher the rate of particles triggering the detector. It follows that the HEPD trigger logic has to be suitably modified not to blind the HEPD2 around the poles, at least for electrons. In fact, electrons are the most promising physics channel to look at for correlations of ionosphere variations and violent phenomena in the lithosphere (e.g. large magnitude earthquakes).<sup>2</sup> A real-time separation of electrons and nuclei may be achieved by exploiting the time of flight (TOF) difference they exhibit from 5 MeV to 300 MeV. In this range, electrons’ velocity is practically  $c$  whereas protons are not faster than  $0.3c$ . This difference translates in a TOF difference of 770 ps along 10 cm. Trento’s Limadou team is proposing a new configuration, sketched in the Fig. 3. The HEPD2 has four trigger planes, paired to make the trigger position-sensitive. The two pairs are 10 cm apart from each other, to implement the TOF device. Behind the trigger, the energy detector is visible, about the same of HEPD1. Trigger bars hit by a nearly threshold proton are coloured in green.

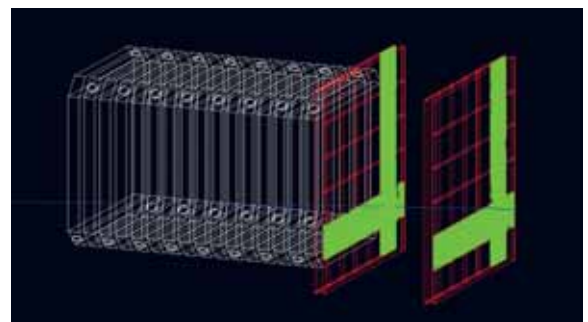


Figure 3: A GEANT4 simulation of a possible HEPD2 layout.

Trento’s proposal for the HEPD2 tracker, not reported in Fig. 3 to make trigger planes visible, relies on the use of Monolithic Active Pixel

<sup>2</sup>Fidani, C. et al. (2010), Remote sensing 2, pp. 2170–2184.

Sensors (MAPS) instead of double-sided silicon microstrip detectors (as in HEPD1). MAPS are silicon detectors fabricated with CMOS technology, profiting from all related advantages:

- (i) extremely low pixel size (down to few  $\mu\text{m}^2$ );
- (ii) charge collection by diffusion;
- (iii) fully embedded front-end electronics, determining very high signal-to-noise ratio, low power consumption, high scalability;
- (iv) possibility to zero-suppress the signal directly on chip.

Feature (ii) is particularly important, as it allows for very thin detectors. For instance, the ALPIDE chip pictured in Fig. 4 is only 100  $\mu\text{m}$  thick. ALPIDE<sup>3</sup> has been developed with a 180 nm CMOS Imaging Process for the upgrade of the ALICE Inner Tracking System. The chip size is  $3 \times 1.5 \text{ cm}^2$ , featuring a matrix of  $1024 \times 512$  squared pixels. The chip embeds a sparsifying readout architecture (priority encoder) that can work in both triggered and continuous modes. It has been designed to perform tracking at high rates and high occupancy, as expected for Pb-Pb collisions at the LHC. That environment is very different from space, where particles hit the detector with lower rates and events are characterised by lower occupancy. On the other hand, the power budget of an LHC experiment is order of magnitudes higher than that of a small satellite. The picture in Fig. 4 was taken in the TIFPA clean room, where an intensive test



Figure 4: The ALPIDE sensor on the carrier board.

<sup>3</sup>Aglieri Rinella, G. (2017), Nucl. Instrum. Meth. Proceedings, 14th Vienna Conference on Instrumentation (VCI 2016): Vienna, Austria, February 15-19, 2016 A845, pp. 583–587.

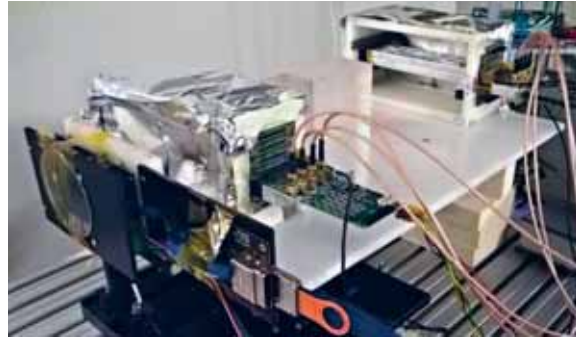


Figure 5: Picture of the setup used at the APSS proton beamline. The ALPIDE chip is the leftmost part of the setup. Courtesy of Dr. S. Mattiazzo and the iMPACT project team.

campaign to qualify the ALPIDE sensor for space applications is in progress.

Activities are mainly aimed at minimising power consumption and characterising detector response for low energy particles. Fig. 5 shows the experimental setup of a test at the APSS proton beamline in collaboration with the iMPACT group from University-INFN of Padova: testing ALPIDE with nuclei of energy lower than 100 MeV/n has been extremely important, as the ALICE inner detector is designed to track hadrons with higher momenta, up to few GeV.

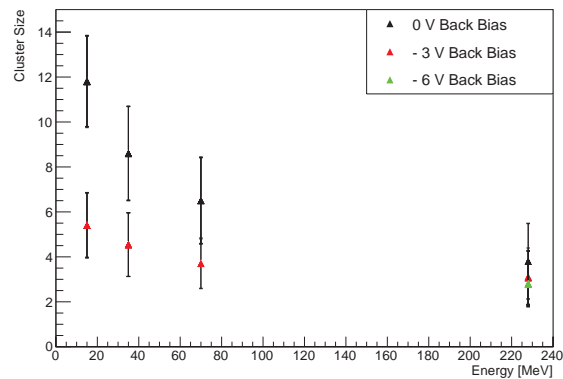


Figure 6: Evolution of the cluster size as a function of the proton.

Fig. 6 reports the number of fired pixels (the cluster size) as a function of the proton kinetic energy. Error bars represent the RMS of distributions. ALPIDE may also work with low back-bias voltage (−3 or −6 V), to speed

up the charge collection and reduce the cluster size. The purely diffusive working regime (0 V) shows the clearest dependence of cluster size on primary energy, with a moderate sensitivity to replace the  $dE/dx$  information.

**Development of high temperature superconducting magnets** The activity started in 2016 to design prototype YBCO coils has continued in 2017, becoming the *HDMS project* (HTS Demonstrator Magnet for Space). Funded by CERN and ASI, it is aimed at demonstrating technical feasibility for using high field high temperature superconducting (HTS) magnets technologies under development for particle accelerators in aerospace applications for science. The target mission is a high resolution astroparticle spectrometer in space and the most important secondary application is the shielding of astronauts from cosmic radiation. The project has developed in strong synergy with the EuCARD2/ARIES initiative and the CERN HTS program for High Field HTS magnets.<sup>4</sup> The base for the application is the EuCARD2 dipole wound with roebel cable, as pictured in Fig. 7.



Figure 7: High luminosity LHC dipole test at CERN. Courtesy of Dr. G. De Rijk.

Technical objectives of the HDMS project are:

- (i) to design a compact dipole field demonstrator, racetrack-type and based on CERN Accelerator Technology under development for future colliders;

- (ii) to develop the conductor suitable for the space environment;
- (iii) to manufacture a small demonstrator to test the conductor and most of related technologies (cooling, quenching, protection);
- (iv) to test the demonstrator in a wide temperature range, namely  $4\text{ K} < T_{op} < 80\text{ K}$ .

Fig. 8 reports the preliminary design of the coil made in Trento: the calculation was made using specs of a Bruker HTS tape, with coil size  $1.0 \times 0.3\text{ m}^2$  and 200 windings per pancake. The coil mass is 17.5 kg. Accounting for a maximum tape length of 90 m, and joint resistance of  $30\text{ n}\Omega$ , the maximum cryo power needed at 20 K is 400 W (COP 150 assumed).

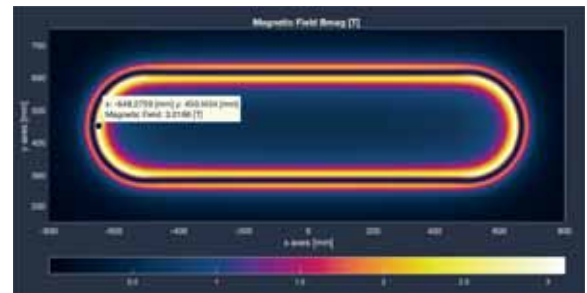


Figure 8: Expected magnetic field intensity for the test coil at maximal engineering current density  $J_{c,en} = 330\text{ A/mm}^2$ . No background field considered.

**Rossini** Future human exploration into interplanetary space will place astronaut crews at increased health hazards compared to the current Low-Earth Orbit (LEO) missions on the International Space Station (ISS). It is now generally acknowledged that exposure to space radiation represents the main health risk for exploration-class missions.<sup>5</sup> In deep space, astronauts will be exposed to the full spectrum of Galactic Cosmic Rays (GCR) and Solar Particle Events (SPE).<sup>6</sup> The radiation hazard is further aggravated by the mission length. Currently, a journey to Mars is estimated to last at least one and half year, much longer than typical space journeys to date. The combination of increased mission length with the deep space radiation

<sup>4</sup>Rossi, L. and Bottura, L. (2013), Rev. Accel. Sci. Technol. **5**(CERN-ATS-2013-019), pp. 51–89.

<sup>5</sup>Chancellor, J. et al. (2014), Life **4**, pp. 419–510.

<sup>6</sup>Durante, M. and Cucinotta, F. A. (2011), Rev. Mod. Phys. **83**, pp. 1245–81.

environment will result in exceeding the currently accepted radiation dose limits.<sup>7</sup> As time in space should be increased, rather than decreased, according to the plans of exploration and colonization, the best tools for minimizing the risk to the crew members are mission planning and spacecraft design. Shielding optimization plays a major role in this strategy as all other alternative countermeasures are still in a preliminary phase.

The ROSSINI project of the European Space Agency (ESA) is a ground-based study of shielding for space travel. It started in 2011 and has now completed its second phase. Its approach is based on the use of a single high-energy heavy ion beam attenuation to estimate the shielding effectiveness of a variety of single and multi-layer materials of interest for different space scenarios.

**Test campaigns** The choice of candidate materials for this study was guided by the physics of particles interaction (electromagnetic and nuclear) and by their usability in spacecraft design. Different kinds of samples were considered: standard materials already used for structural and shielding purposes in space vehicles, innovative materials optimized for radio-protection applications, simulants of Moon and Mars soil and multilayers configurations to reproduce both hard and soft (inflatable) structures for deep-space or planetary mission scenarios. Together with the estimated nuclear fragmentation probability per mass, the trade-off method for the selection of materials to be tested is based on the analytical hierarchy process, which takes into account the following elements:

- **reliability** - accuracy of deterministic and Monte Carlo codes in reproducing the material chemical structure and in simulating their behavior (dose reduction, production of secondary particles, etc...);
- **multifunctionality** - capability of a material to perform other functions in addition

to radiation shielding;

- **environment compatibility** - it includes the external, internal and the launch environment compatibility;
- **availability** - it considers the material status on the European market in terms of resources amount, cost and fabrication time;
- **processability** - feasibility of the application of a given material in a Space mission in terms of basic safety requirements (toxicity, flammability, etc...);
- **Technology Readiness Level (TRL)** - according to the ESA definition.

The shielding effectiveness of all materials was assessed by measuring their performance in reducing the dose when exposed to high-energy charged particles. The samples were exposed to 1000 MeV/u <sup>4</sup>He and 962-972 MeV/u <sup>56</sup>Fe beams at the NASA Space Radiation Laboratory (NSRL) in Brookhaven National Laboratory (Upton NY, USA) and to 430 MeV/u <sup>12</sup>C ions at the Heavy Ion Therapy (HIT) center (Heidelberg, Germany). The beams selected for the test campaign were identified as a proxy for the GCRs and SPEs.

The dose reduction (partial or full Bragg curves when enough material was available) were measured for all selected candidates (Fig. 9) to obtain their shielding effectiveness.

Further measurements were performed with the most promising materials to study the primary beam fragmentation, the neutron yield and the microdosimetry spectra to characterize the quality of the radiation field behind the shielding.

The outputs of this study represent a useful database for benchmarking Monte Carlo and analytical transport codes used for space radiation transport calculations. The experimental results have been compared with simulations from GRAS/Geant4<sup>8</sup> and PHITS.<sup>9</sup> Furthermore, TRiP98 (TReatment PlannIng for Particles),<sup>10</sup> the first treatment planning system for scanned heavy ion beams, has been used to reproduce

<sup>7</sup>McKenna-Lawlor, S. et al. (2014), *Acta Astronaut.* **104**, pp. 565–73.

<sup>8</sup>Agostinelli, S. et al. (2003), *Nucl. Inst. Meth. A* **506**, p. 250.

<sup>9</sup>Sato, T. et al. (2013), *J. Nucl. Sci. Technol.* **50**, pp. 913–923.

<sup>10</sup>Krämer, M. et al. (2000), *Phys. Med. Bio.* **45**, pp. 3299–317.

the HIT dose reduction set up and SPE spectrum 1D simulations for selected materials. The objective of this activity was an exploratory approach to evaluate a possible extension of this code to high energy heavy ions, to test its applicability with different shielding materials and compound geometries, in order to study with a deterministic code the transport of space HZE particles through space structures.

The results obtained within ROSSINI provides recommendations for optimizing the design of space vessels and habitats in different radiation environments. The development of innovative materials represents a technological advance and may very well find applications beyond space radioprotection purposes.

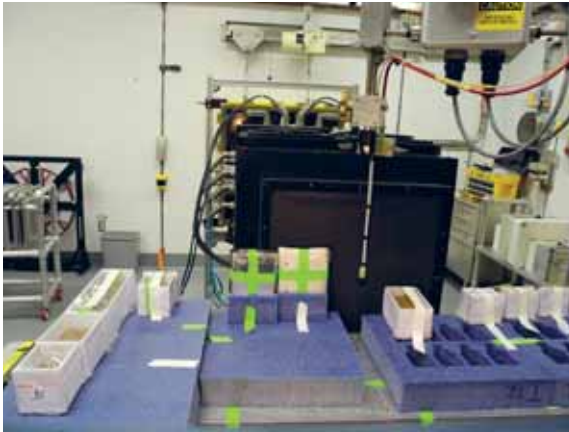


Figure 9: Candidate shielding materials exposed to high-energy heavy ions at the NASA Space Radiation Laboratory (NSRL) for measuring dose reduction.

**New Reflections** New Reflections in the Solar System is an experiment in the INFN technological research group CSN5. The experiment has received funding (2016-2018) to develop innovative laser technology for space applications. The TIFPA participation concerns the potential applications of laser ablation which may be used for spacecraft propulsion or the deviation of the trajectories of artificial and natural satellites.

The first year of the program at TIFPA was devoted to developing a simulation program to assess the performance required by ground and space laser systems to eliminate space debris,

non-functional satellites and their fragments in near Earth orbit, in function of mass and orbit.<sup>11</sup>

The IdEA laboratory of the University of Trento has joined the TIFPA group this year. The Pulsed Laser Deposition (PLD) laboratory of IdEA is equipped with a nanosecond pulse width KrF excimer laser with a variable 1-100 Hz repetition rate. The group has important experience, theoretical as well as experimental, in laser ablation.

Laser ablation refers to the removal of material from the surface of a solid which is heated to high temperatures by a laser beam. The total momentum of the ejected material results in an equivalent impulse directed in the opposite direction, normal to the surface of the object. The impulse delivered to a solid mass  $m$  may be written,

$$m\Delta v = \left( \frac{E_o}{\pi r^2} \right) SC_m \quad (2)$$

where  $E_o$  is the energy of laser pulse,  $\pi r^2$  is the size of a circular beam spot,  $S$  is surface area of the solid mass, and  $C_m$  is the coupling coefficient (N/W) for the conversion of the incident laser pulse energy to impulse.

For debris mitigation, the important parameters are the ablation threshold and coupling coefficient for aluminum, a common space construction material. The coupling coefficient has been measured at the PLD laboratory using the observed angular deflection of a  $1.5 \times 1.5 \times 0.5 \text{ cm}^3$  Al target mounted on a ballistic pendulum in a vacuum chamber. The ballistic pendulum is shown in Fig. 10.

The experimental set-up in the PLD laboratory is shown in Fig. 11. The angular deflection is measured at distance of 3.5m from the pendulum. A preliminary result,  $5.3 \cdot 10^{-5} \text{ N/W}$  obtained with a laser pulse energy density of  $0.8 \text{ GW/cm}^2$ , may be compared to the values used in (Battiston et al. 2017a)<sup>11</sup> for evaluating ground and space laser configurations,  $2 \cdot 10^{-5} \text{ N/W}$  between  $0.5$  and  $0.8 \text{ GW/cm}^2$ .

<sup>11</sup>Battiston, R. et al. (2017), Journal of Space Safety Engineering 4, pp. 36-44.



Figure 10: The aluminum target mounted on the ballistic pendulum in the KrF laser beam. The angular deflection of the Al target is obtained from the displacement of a second, reflected laser beam, in the vertical direction.

A second experimental set-up consisting of pivoting pendulum containing two Al targets mounted on either side of the central support column is shown in Fig. 12. The KrF laser beam is incident on the top (left) Al target position shown in the upper (lower) photograph. The ejection of material produced by KrF laser beam in the irradiated target is visible in the lower photograph.

The primary objectives for the coming year are optimizing the coupling coefficient measurement, and extending the measurement to materials suited to propulsion and asteroid deflection applications.

In order to be a viable alternative for asteroid impact avoidance, the intervention should begin well in advance of the expected impact date. Consequently the laser system would be deployed in space. Ablation also plays an

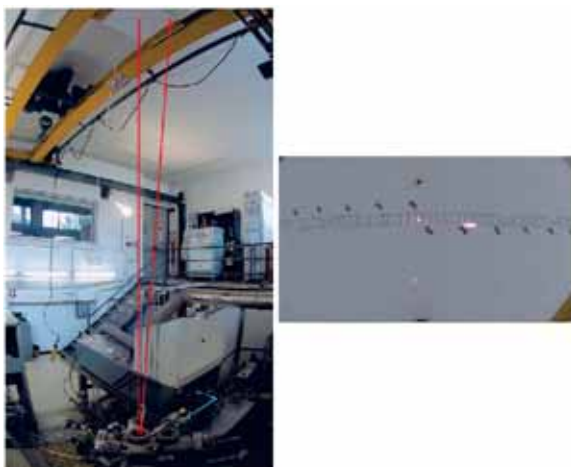


Figure 11: View of the experimental set-up in the PLD laboratory (left). The angular deflection of the reflected laser beam observed on the screen located 3.5 m above the vacuum chamber (right).

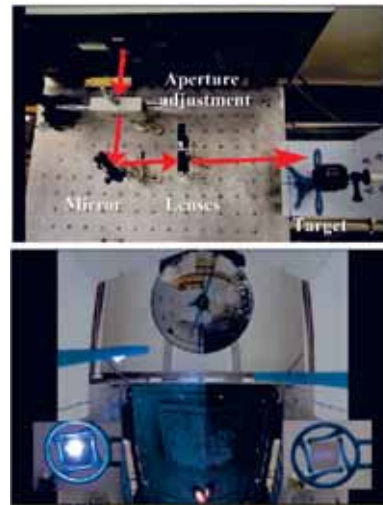


Figure 12: View of a second experimental set-up consisting of the pivoting pendulum containing two Al target (upper photograph). The material ejected by the ablation produced by the KrF laser beam is visible at left-side target position in the lower photograph.

important role during the breakup of meteorites in the atmosphere. The coupling coefficients and ablation thresholds of meteorite material are important input parameters for simulations which trace meteorites through the atmosphere to predict the mass, velocity and trajectory of the remnants which would reach the surface of the Earth.

We have recently received from the University of Central Florida in Orlando, USA, in collaboration with NASA, samples of asteroid simulant material, which mimic the mineralogy of the type C1 carbonaceous chondrite meteorites. For the propulsion application, the candidate materials will be evaluated for efficiency and required launch mass. Laser propulsion may be considered for satellites in space, small or micro satellite launches and interplanetary travel. Carbon composite materials are among the interesting candidates.

For both applications the measurements should be performed with different atmospheric densities, requiring measurement and control of the mass density in the vacuum chamber. The ability to vary both the pulse width and frequency of the pulsed laser are important to optimize the design of the laser system. The upgrades of the facility, which are not contained in the 2018 budget allocated to New Reflections, are projected for a future effort dedicated to laser ablation.



## Medical Technologies

Marco Schwarz<sup>1,2</sup>

marco.schwarz@apss.tn.it

During 2016 and 2017 the activity of the protontherapy centre went through a phase of consolidation and growth on several aspects, with an increasing number of patients treated in the two gantry rooms, the design and clinical implementation of new planning and treatment techniques, and the developments ongoing in the experimental room concerning the two lines for physics and radiobiology research. In this report we will shortly describe a few of these developments, namely

- Experimental validation of a Monte Carlo code for clinical practice
- First treatment of moving targets.
- Planning studies to evaluate the benefits of protontherapy for breast cancer patients.
- Characterization of the fixed line for biological experiments.
- Analysis of protontherapy treatment outcomes.

**Experimental validation of a Monte Carlo code for clinical practice.** Nowadays, the most common method to calculate and optimize dose distributions treatment planning for proton therapy clinical practice is based on analytical algorithms. However, Monte Carlo (MC) methods are considered the gold standard to describe particle interactions and to calculate the resulting doses. Several MC algorithms to compute proton dose distribution have been

tested and compared to analytical pencil beam algorithms in a research settings over the past few years. The superiority of MC algorithms is particularly evident whenever beam modifiers are used (such as a pre-absorber, also known as range shifter, or an aperture) and/or when the beam has to traverse highly heterogeneous regions. The main reason for the absence of MC algorithm in clinical practice is the dose calculation time, which in most cases is incompatible with clinical needs. In early 2017, a MC algorithm was made available in our treatment planning systems, that was supposed to find a good balance between accuracy and speed. Since this was a total novelty, no literature data were available to estimate its calculation accuracy. We therefore carried-out a full validation procedure, consisting in

- a) carrying out tests both in an anthropomorphic head phantom and in a biological sample,
- b) investigating the role of air gap and of minimizing the use of a pre-absorber to improve the agreement between measurement and TPS predictions and
- c) finding practical solutions for an optimal management of a pre-absorber in PBS proton therapy.

The results confirmed a much improved accuracy of the MC code for challenging geometries, as shown for example in Fig. 1.

<sup>1</sup>Agenzia Provinciale per i Servizi Sanitari, Trento

<sup>2</sup>INFN TIFPA, Trento, Italy

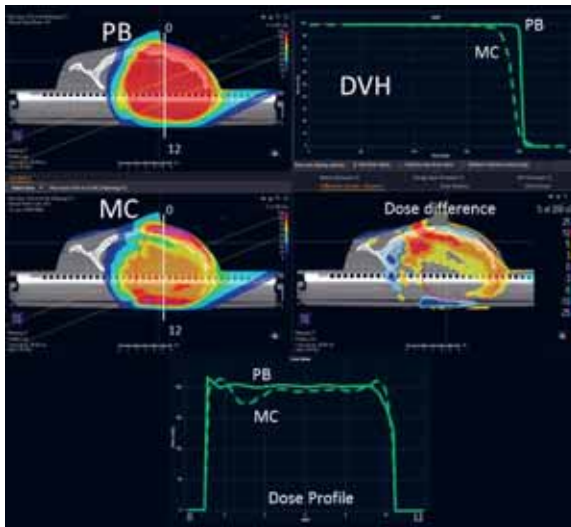


Figure 1: Comparison between Pencil Beam (PB), Monte Carlo (MC) calculations and measurements for a simulated target volume in an antropomorphic phantom

**First treatment of moving targets.** Proton-therapy dose distribution may be severely affected by any kind of motion that introduces differences between the patient anatomy during planning and during treatment delivery. Respiratory motion is a cause of particular concern in protontherapy with pencil beam scanning. We started the treatments of moving targets by implementing techniques for time-resolved computed tomography acquisition (also known as 4DCT), and for evaluating the impact of breathing motion on the planned dose distribution. A real time optical tracking system was used to monitor the patient during the CT scan and treatment. This system can trigger the beam during the treatment. Validation measurements on the machine were performed. A 4DCT (10 phases) and a free-breathing CT (FBCT) were used for planning. The physician used the 4DCT for target delineation on the FBCT. The planning was performed on the FBCT and the approved plan was evaluated in two ways: a) dose recalculation on each 4DCT phase and b) Interplay effect evaluation: every spot was assigned to a phase according to the beam delivery time and the breathing curve of the patient. The 10 doses were then deformed and summed on the FBCT. The highest breathing amplitude recorded during 4DCT

scan was used as gating threshold during treatment delivery. We then defined, validated and used for two patients a protocol for the treatment of small amplitude moving targets. An example of the breathing signal for the two patients is shown in Fig. 2. The planning and delivery of the treatments gave very good results in terms of coverage, OARs sparing, 4D dose evaluation of the plan and interplay effect assessment.

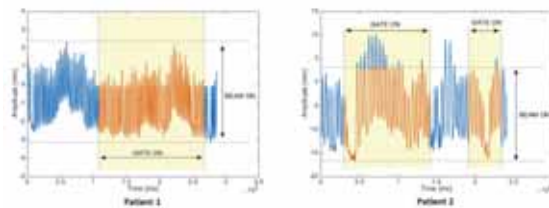


Figure 2: Example of breathing cycles for the two patients treated with motion monitoring. The beam-on and gating-on windows are highlighted. On the left, the breathing curve for the first patient, which shows little variability and does not cause beam interruptions. On the right, a much more irregular curve which was quite typical for the second patient.

**Planning studies to evaluate the benefits of protontherapy for breast cancer patients.**

The interest in proton beam therapy (PBT) for the treatment of breast cancer has substantially increased in the radiation therapy community over recent years. Taking into account the good survival obtained with photon RT for breast cancer patients (estimated overall 5-year survival of about 89%, the main motivation for the use of protons lies in the potential reduction of radiation-induced side effects such as cardiac toxicity risks which is higher for left-side BC patients. Indeed, PBT delivers the lowest mean heart dose (MHD) when compared with any other photon technique, including breathing control. Radiation induced skin toxicity (RIST) is however another important end point impacting on patient quality of life. While in photon RT the skin-sparing effect is due to the initial dose buildup, this is not the case for protons where the skin lies in the dose profile plateau region. Nowadays with proton pencil beam scanning (PBS) becoming more accessible, a reduction can be expected in the dose released to the skin as a consequence of higher

flexibility and enhanced modulation capability in treatment planning. We therefore applied a recently developed skin normal tissue complication probability (NTCP) model to guide proton PBS treatment plan optimization for left-side breast cancer. Our analysis suggests that protons may be safely applied without increasing the risk of severe acute radiation induced skin toxicity (Fig. 3). The quantitative risk estimates also support the potential clinical benefits of IMPT for left-side BC irradiation due to lower risk of cardiac and pulmonary morbidity. The applied approach might be relevant on the long term for the setup of cost-effectiveness evaluation strategies based on NTCP predictions.

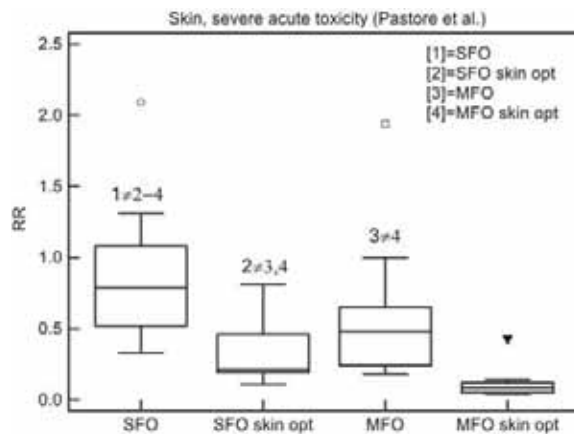


Figure 3: Relative risk (RR) ratio comparison according to normal tissue complication probability (NTCP) analysis for acute severe skin toxicity. SFO: single field optimization; MFO: multi-field optimization; skin opt.: skin included in the cost function.

**Characterization of the fixed line for biological experiments.** While the fix pencil beam available at the physics line in the experimental room allows performing a large spectrum of experiments (e.g. detector testing, radiation hardness, radiation shielding), it is not suited for the setup of radiobiology experiments, for which different requirements have to be satisfied. To that purpose, a large field in the order of several squared centimeters is needed, ensuring high dose homogeneity and a reasonable and adjustable dose rate. To that purpose, we worked on the design and setup of a passive scattering line, allowing fulfilling these requirements. After tuning and characterization, beam parameters were in agreement with those

obtained at the physics beam line (see e.g. spot size in Fig. 4). Based on these data, a preliminary design was proposed for a passive scattering line for large field irradiation. By combining a tantalum scattering foil with a collimation system, we were able to obtain homogeneity higher than 90% in a  $6 \times 6 \text{ cm}^2$  irradiation area with 148 MeV initial proton beam energy. Starting from initial promising results, we are currently considering further upgrades of the beam line, which will include the use of ridge filters for Spread Out Bragg Peak (SOBP) modulation and the eventual upgrade to a double-scattering system. At the same time, the beam line geometry will be implemented in the Geant4 Monte Carlo code. Future plans include an extensive dosimetric characterization of the large irradiation field. A radiobiological characterization of the beam line will then be performed, which will allow opening the facility also to external users.

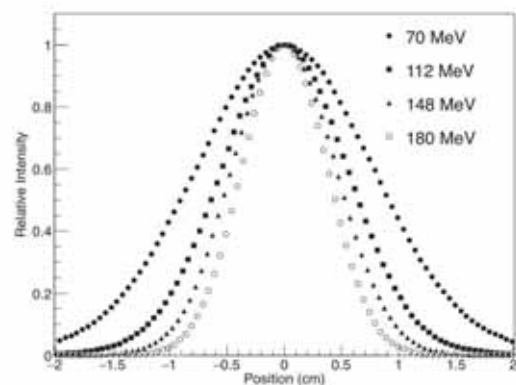


Figure 4: Beam spot profiles at the isocenter for four different energies.

**Analysis of protontherapy treatment outcomes.** Within the MoveIt project, a dose effect relation study was performed, aimed at modeling skin toxicity in brain cancer patients after protontherapy. We evaluated 72 consecutive brain tumor patients undergoing protontherapy at our center to assessing acute and late radiation induced alopecia. Dose-surface histograms (DSHs) of the body structure were extracted as representative of scalp irradiation. Patient and treatment-related characteristics were analyzed along with relative/absolute

Dose Surface Histograms parameters. Acute Grade 2 alopecia was found in 49% of patients, while late Grade 2 alopecia was found in 31% of the patients. Acute and late events were highly correlated and younger age at irradiation was the only clinical risk factor for acute alopecia. The relative scalp surface receiving at least 20 Gy (RS20) was significantly associated to late

G2 toxicity. Median RS20 was on average 11% in patients developing G2 toxicity and 2.9% in those who did not. Following studies will be aimed at both studying the evolution of this toxicity over longer period of time and at analyzing dose–effect relation for other treatment related side effects.



## Sensors and Detectors

Maurizio Boscardin<sup>1,2</sup>  
boscardi@fbk.eu

The TIFPA Virtual Lab for Sensors and Detectors is a sum of skills and facilities focused on the realization of silicon radiation particles detectors that have their applications in different contexts such as high energy physics both in-ground facility and in space experiments than in biology and medicine.

In these contexts, the virtual laboratory of TIFPA aims to build a large technological platform that makes available to the Italian and international scientific community a set of skills and infrastructures that allow the development of silicon sensors. The presence in the same Institute of researchers that deal with detectors with the capability to realize silicon devices for various fields of application allows to be innovative and to be able to respond quickly to the technological challenges that the research activity requires.

The main contributions to the Virtual Lab for Sensors and Detectors are given by the Center for Materials and Microsystems (CMM) of FBK, the Department of Industrial Engineering of the University of Trento and TIFPA. These groups provide the Virtual Lab more than 20 years experience in the development of radiation sensors exploiting the microelectronics technology.

The key to the success of the laboratory is the presence inside FBK of a large technological facility that adds two main infrastructures:

- More than 500mq of clean room fully

- equipped to process silicon devices
- a microanalysis capability based on the availability of various physical/chemistry characterization technologies.

Whereby the Virtual Lab thanks to the presence of an internal silicon foundry combined with the use of external state-of-the-art CMOS foundries, has the capability to simulate, design, produce and test semiconductor sensors. The operating model, therefore, allows the access to a large number of competencies/technologies that allow both to develop new devices but also to realize a pre-production of custom devices. The technologies/skills available are described in the following sections.

**Simulation and design** In case of full-custom technology, we start from physics-based TCAD simulation of the device. It is possible to evaluate numerically both the electrical parameters inside the device and the measurable quantities at the electrodes. The device can also be stimulated with light or ionizing particles to model the induced electrical signal. Furthermore, to emulate as close as possible a real device, we simulate also the fabrication technology. The tools used are commercial ones (SILVACO or SENTAURUS). This software can be used both to predict the functioning of a device as well as to understand anomalous behavior or failures of existing ones. The output of the simulations

<sup>1</sup>FBK, Trento, Italy

<sup>2</sup>INFN TIFPA, Trento, Italy

is used to design the geometry of all the sensor components (layers) with the proper CAD software and to define the technology process flow. Geometry and process sequence are used to build the device(s) on the silicon wafers in the internal foundry.

In case of the standard CMOS approach, usually, there is limited access to fabrication technology. So our competencies are mainly on circuit simulations and Integrated Circuit (IC) design. We have dedicated software tools to this purpose: CADENCE and MENTOR GRAPHICS. We design both analog and digital architectures. Quite important in this case is the capability of firmware design based on FPGA to control and read the ASIC.



Figure 1: In line inspection area.

**FBK technological Facility** The Microfabrication Area runs two separate cleanrooms that process 6-inch wafers: the Detector Cleanroom (500m<sup>2</sup> ISO 3-4 class) dedicated to the development of radiation sensors and the MEMS cleanroom (100m<sup>2</sup> ISO 4-5 class) where microdevices and sensors for different applications are developed. The Detectors cleanroom is a fully equipped CMOS like pilot line with lithographic capabilities down to a few hundred nanometers with a rather strict list of materials to be processed to avoid cross-contamination. The MEMS cleanroom a much more flexible laboratory devoted to the development of devices where the integration of different materials with silicon is needed. Strategic, in the sensor field, is the capability to perform low leakage and double-side processing.



Figure 2: Litho area.

Main equipment include:

- Ion implanter Varian Exitron 220, with energy range up to 200 KeV; Ions As75, B11, 49, P31, N, Ar40
- Deep reactive ion etching Alcatel AMS200 for silicon deep etching based on Bosch process
- Plasma etching of silicon oxide, silicon nitride, polysilicon dry and metal.
- Magnetron sputter (Eclipse MRC Mark II) for Al, AlSi1%, Ti/TiN deposition
- Stepper Nikon with a resolution of 350nm
- Mask aligner Karl Sues with backside alignment (2.5  $\mu$ m resolution)
- PECVD system (STS - MPS CVD) for deposition of Si Oxide, Si Nitride, SiON, Si-rich Oxide and Amorphous Si
- 5 Atmospheric Furnaces Centrotherm for dry and wet oxidation, N<sub>2</sub> annealing, doping from BBr<sub>3</sub> or POCl<sub>3</sub> and H<sub>2</sub> alloying/sintering
- 3 LPCV furnaces Centrotherm for TEOS doped and undoped, SiN standard and low stress - SiN, PolySi doped and undoped deposition.
- Isotropic silicon wet etching based on TMAH Bulk Si Wet
- Wet bench for wet etch process
- Wafer bonding AML for anodic and adhesive bonding
- Metrology in line: Interferometer, mechanical and optical profilometer, 4 point probe, Lifetime Sinton system, ellipsometer, SEM.

The packaging lab has been recently upgraded to a clean environment. It is dedicated to the development of prototype packages for mounting the silicon devices. It is equipped with ball and wedge wire bonders, die bonder, stencil screen printer, and tools necessary for encapsulation in resins and hermetic packaging.



Figure 3: Wet etching area.

**Device Characterization** Finally, there is a transversal know-how on device characterization. This includes competencies in parametric testing which is usually done at the wafer level contacting it with probes. It is mostly used to evaluate the functionality of the device measuring current and impedance. The testing labs are divided in wafer-level parametric testing and functional characterization. The first consists of 2 manual and 4 automatic probe-stations. The automatic ones allow a full wafer characterization to identify functional devices and to monitor the uniformity of electrical parameters. Two of that feature also a temperature-controlled chuck that allows setting the wafer temperature from  $-40$  to  $100$  °C.

The functional testing laboratories are equipped with state-of-the-art instrumentation for a variety of characterizations. In particular: the electro-optical testing, that includes measurement of sensor efficiency/noise in the controlled environment and of time-of-flight with fast lasers and a test with radioactive sources. It includes coupling the photosensor with scintillators to measure energy and timing resolution in case of X-ray/Gamma radiation. Main

instruments are : multi-channel semiconductor analyzers; high-speed, four-channel digitizing oscilloscopes (600 MHz - 2.5 GHz; up to 40 GS/s); 3 PC-controlled thermostatic chambers; cooled CCD cameras for emission microscopy; fast lasers for time-of-flight measurements; integrating sphere and optical bench; pyroelectric detector; THz kit with drive synthesizer; radioactive sources of different energies; digital pattern generator; logic and network analyser and NI acquisition boards.

In addition, a range of skills and equipment are available within the FBK facility for the physical-chemical characterization of materials, techniques that allow an in-depth analysis on technological aspects of the devices created, such as the possibility of measuring doping profiles using SIMS techniques. The techniques available include Secondary Ion Mass spectrometry (SIMS), Proton Transfer Mass Spectrometry (PTRMS), X-Ray Fluorescence (XRF), X-ray Diffraction (XRD), X-Ray Photoelectron spectroscopy (XPS), Scanning Electron Microscopy (SEM) with Energy Dispersive Spectroscopy (EDS) and Electron Back Scatter Diffraction (EBSD), Scanning Probe Microscopy (SPM) with Atomic Force Microscopy (AFM), Scanning Spreading Resistance Microscopy (SSRM), Kelvin Probe Force Microscopy (KPFM), Scanning Capacitance Microscopy (SCM).



Figure 4: PE-CVD equipment.



Figure 5: Testing area

Within the virtual lab, a series of technological platforms have been developed that have allowed the realization of detectors for various applications/experiments. The main available technologies are:

**Planar Detectors** Planar devices for high-energy radiation detectors exploiting direct ionization of the particle in silicon are realized in FBK. These sensors are produced in the internal foundry on high-purity high-resistivity silicon material. According to the electrode geometry, they are classified in pixel (SPD), strip (SSD) or drift detectors (SDD). As for pixels, p-on-n, n-su-p, and even n-on-n technologies are available; for the isolation, p-spray and/or p-stop are available. Regarding the microstrip, we have the capability to realize low leakage large area double side detector, AC or DC coupling and polarized by polysilicon resistor or punch through. These technologies are available on 6-inch substrates, such as Si-Fz, SOI

and Si-Si with a wafer thickness of  $275\mu\text{m}$  to 1mm. FBK has also the capability to develop an optimize entrance window for the specific wavelength required by each specific application. FBK also has capabilities to realize medium quantity productions of detectors: as an example, in the past we have realized about 800 double sided microstrip detectors for AMS-02 experiment and a similar quantity for ALICE - LHC (microstrip and pixel); more recently we have realized the microstrip double side, large area (about  $7\times 10$  cm) detectors for LIMADOU for the Chinese space agency.<sup>1</sup>

A process module was developed on planar technologies to reduce the lateral dead area in order to obtain an "edgeless" detector. This process is based on the capability to define a deep and doped trench that surrounds the detector itself. The trenches can be both continuous and trimmed.<sup>2</sup> Finally, it is possible to realize an "Active Edge" device based on the realization of a termination zone based on a "columns fence". This solution is based on the realization of a series of doped columns that surround the detector.

**Silicon Drift Detectors** The Silicon Drift Detectors (SDD)<sup>3</sup> are currently mainly used for X-ray spectroscopy, thanks to the outstanding energy resolution that they can achieve. The most common application for SDD is in the field of analytical instrumentation, where they are employed in many different techniques such as X-ray fluorescence (XRF) analysis, energy dispersive x-ray spectroscopy (EDS) combined with electron microscopy, x-ray reflectivity (XRR), etc. Besides these applications, SDDs are also used for x-ray spectroscopy in astrophysics experiments and particle physics experiments and they are also considered as photosensors for scintillation detectors in gamma-ray spectroscopy, thanks to their high quantum efficiency for visible light. By starting this kind

<sup>1</sup>Rashevskaya, I. et al. (2016), *Proceedings of the 25th International workshop on vertex detectors (Vertex 2016)*, p. 64.

<sup>2</sup>Calderini, G. et al. (2016), *Nuclear Instruments and Methods in Physics Research, Section A* **831**, pp. 133–136.

<sup>3</sup>Quaglia, R. et al. (2016), *Nuclear Instruments and Methods in Physics Research, Section A* **824**, pp. 449–451; Bufon, J. et al. (2017), *X-Ray Spectrometry* **46**(5), pp. 313–318.

of detectors, FBK has developed the following internal technologies:

- realization of devices with a really low leakage current, in order to achieve the best energy resolutions and to reduce the requirements for the sensor cooling.
- process to obtain a thin entrance window, which makes possible to extend the SDD energy detection range to low energy x-rays (few hundreds of eV).
- adaptation of the SDD technology to many different applications, creating sensors with dedicated layouts and geometries: developing custom multi-pixel detectors, which are of the utmost importance to cover large areas in high-count-rate experiments at high luminosity facilities such as synchrotrons and x-ray free electron lasers (XFELs); recently FBK has also produced the largest SDD sensor ever made, which has an active area of  $\sim 11 \times 7 \text{ cm}^2$  and is being developed for astrophysics applications.

**UFSD** Ultra-Fast Silicon Detector (UFSD) is an innovative silicon sensor optimized for timing measurements, based on the Low-Gain Avalanche Diode technology (LGAD). LGAD merges the best characteristics of traditional silicon sensor with the main features of Avalanche Photodiode (APD). LGAD is a silicon detector with output signal about a factor 10 larger than that of standard silicon detector and with noise comparable with that of traditional silicon sensor. UFSD recently obtained a time resolution of  $\sim 30 \text{ ps}$  in beam tests and are now being considered in the upgrade of the CMS and ATLAS experiments as timing detectors. Over the last few years, Fondazione Bruno Kessler, in collaboration with the universities of Trento and Turin, have been involved in developing of UFSD. The first production batch (completed in 2016) was fabricated on 275 $\mu\text{m}$  thick Silicon substrates. It was aimed at testing both the functionality and the reliability of the new proposed fabrication technology, showing excellent results in

terms of gain and timing resolution.<sup>4</sup> A second pilot batch (completed in late spring 2017) has been produced on Silicon-to-Silicon wafers with a thickness of 50 $\mu\text{m}$ , in order to improve the timing performance. In this production, we tested also new techniques to improve the radiation hardness of the devices. Two different dopant elements (Boron and Gallium) have been used to realize the multiplication junction, as well as carbon co-implant has been tested on some wafers. The first results obtained on irradiated samples show very promising results that allowing the use of such detectors for equivalent doses beyond the  $10^{15} \text{ neq/cm}^2$ .

**Si-3D** First introduced by Sherwood Parker in 1997, 3D silicon detectors consist of an array of columnar electrodes of both doping types, oriented perpendicularly to the wafer surface and penetrating entirely through the substrate. This unique structure enables to decouple the active sensor thickness from the electrode distance, offering important advantages in terms of low operation voltage, fast time response and high radiation tolerance. Additionally, 3D technology allows for "active edges", i.e., deep trenches heavily doped to act as ohmic terminations of the sensors, able to reduce the insensitive edge region to a few micrometers. Obviously this is gained at the expense of a complex and expensive technology, due to the use of several non standard techniques, such as Wafer Bonding (WB) and Deep Reactive Ion Etching (DRIE).

The first Si-3D technology developed in FBK is a two-sided process, where the junction columns are engraved from the front side, the ohmic columns from the back side, without the presence of a wafer support. The columns are completely passing through the thickness of the wafer. We used this approach in the production of sensors for ATLAS IBL. In terms of functional characteristics, remarkable performance has been demonstrated for IBL 3D sensors: in particular, they have demonstrated a reconstruction efficiency of  $>98\%$  for  $15^\circ$  slopes inclined to 160 V bias after  $5 \times 10^{15} \text{ neq/cm}^2$ .<sup>5</sup>

<sup>4</sup>Paternoster, G. et al. (2017), Journal of Instrumentation **12**(02), p. C02077.

<sup>5</sup>Da Vià, C. et al. (2013), Nuclear Instruments and Methods in Physics Research, Section A **699**, pp. 18–21.

As an alternative, a single-sided 3D technology with handle wafer has been proposed by FBK with modifications allowing for back-side sensor bias. The wafers is composed by two parts: a device layer of high quality and High resistivity silicon and a support wafers with low resistivity material.

The ohmic columns are etched deep enough to reach the highly doped handle wafer, so that a good ohmic contact is achieved on the sensor back-side and the junction column has a lower depth than the thickness of the device layer. FBK also demonstrated the feasibility of this technology with Silicon on Insulator (SOI) wafers: to this purpose, it was proved that the p+ columns can be etched by DRIE also through the bonding oxide, thus reaching the heavily doped handle wafer. Among the advantages offered by the single-sided solutions are the mechanical robustness provided by the thick handle wafer, which is also compatible with active edges; moreover, the active layer thickness can be tailored to the desired value. With a thin active layer ( $\sim 100 \mu\text{m}$ ), narrow columns can be etched even though the aspect ratio is not improved, and all the device dimensions can be more easily downscaled.<sup>6</sup>

**SPAD/SiPM** SPAD and SiPMs are based on the Geiger-mode operation of photodiodes biased above the breakdown voltage. Single photo-diodes operated in this condition as photo-detectors are commonly known as SPADs (single-photon avalanche diodes). A densely packed array of SPADs is referred to as Silicon Photomultiplier (SiPM).

SiPMs are gradually replacing Photomultiplier Tubes (PMTs) in a number of applications, offering, among other features, higher sensitivity, ruggedness, lower operating voltage, lower cost and higher gain uniformity, insensitivity to magnetic fields, making them an excellent candidate for single and few-photon counting applications, with extremely good timing resolution. Typically, SiPMs are employed in the scintillation light readout in applications such as:

- Medical Imaging: Time-of-Flight PET, MRI-compatible ToF-PET, Gamma Cameras, Prompt-Gamma Imaging, intra-operative probes;
- Big Physics Experiments: calorimetry and timing measurements in High-energy physics experiments, Cherenkov light detection, readout of liquid scintillators (LAr and LXe);
- Ionizing Radiation Spectroscopy: Low-energy to high-energy Gamma-ray spectroscopy and X-ray spectroscopy;
- Security and Safety: homeland security, cargo inspection, radiation dosimetry and environmental monitoring.

Other applications of SiPMs include the measurement of fluorescence light intensity and lifetime and analytical instrumentation. Finally, thanks to recent extension of sensitivity to the NIR, SiPMs are currently one of the most promising photo-detectors for LiDAR, including automotive LiDAR.

We follow two approaches for this sensor development:

- custom design and technology developed by FBK, sensors are usually fabricated in FBK;
- sensor design provided by FBK, fabrication in standard CMOS technology at an external silicon foundry.

In the first case, the detector is fully developed in house with optimized microelectronic processes, obtaining a custom SiPM technology. This allows to optimize the device performance such as efficiency and noise and to customize it to a specific application. In such solution, the technology does not allow the integration of the readout electronics on the same substrate as the SiPM and FBK fabricates what is called Analog SiPMs, which provides an analog signal that has to be processed by an external electronics.

In the second case, the standard CMOS technology allows for the sensor and electronics to be integrated. This means that maximum compactness and integrated intelligence can be

<sup>6</sup>Sultan, D. et al. (2017), Journal of Instrumentation 12(01), p. C01022.

achieved. Clearly, the SPADs realized with this approach have sub-optimal performance since the technology is not accessible. Depending on the application, one or the other may be preferred. As an example, in the field of gamma-ray detection with scintillators (both in high-energy physics and medical equipment) the custom solution is preferred because of the better performance and the relatively relaxed requirements on the compactness.

Considering custom SiPM technologies, FBK started analog SiPM development more than one decade ago and now can offer different state-of-the-art technologies for different applications. Among them, Near Ultra Violet, High Density (NUV-HD) SiPM technology features a peak photon-detection efficiency (PDE) of 65 at 410 nm (including the fill factor), Dark Count Rate (DCR) in the order of 50 kHz/mm<sup>2</sup>, correlated noise of 10% at 55% PDE, and microcell pitch ranging from 15  $\mu$ m to 40  $\mu$ m.<sup>7</sup> Sensitivity remains high in the near ultra violet, with a PDE of 48% at 320 nm. NUV-HD SiPMs provide state-of-the-art 85 ps FWHM coincidence resolving time (CRT) in PET applications, reading out the light of a Ca co-doped LYSO crystal.<sup>8</sup> Single Photon Timing Resolution (SPTR) of NUV-HD SiPMs was below 30 ps FWHM, when measured on single SPAD with covered edges, and increased to 75 and 180 ps FWHM for SiPMs with active areas of 1  $\times$  1 mm<sup>2</sup> and 3  $\times$  3 mm<sup>2</sup>, respectively, because of the electronic noise.<sup>9</sup> FBK also developed the capability of fabricating large-area NUV-HD devices, with a size up to 1 cm<sup>2</sup>.

Recent interest in the SiPM readout of liquid scintillators (mainly LAr and LXe) triggered the development of a Low-Field variant of the NUV-HD technology (NUV-HD-LF), which is optimized for operation at cryogenic temperatures and features a DCR of a few mHz/mm<sup>2</sup> at 77 K.<sup>10</sup> At this temperature, few-photon counting capability was demonstrated with very large

sensitive areas, obtaining an S/N of 13.8 using a 24 cm<sup>2</sup> SiPM array coupled to a single analog readout channel (DarkSide collaboration). Other ongoing optimizations of the NUV-HD technology include the development of devices with extended deep-UV sensitivity: preliminary measurements show a PDE of approximately 20% at  $\sim$ 178 nm.

At FBK, we also developed the RGB-HD SiPMs with peak sensitivity of 45% at 550 nm and of  $\sim$ 10% at 900 nm. Based on the RGB-HD technology, we developed the Linearly-Graded SiPMs (LG-SiPMs), which provides XY position sensitivity over the active area down to the microcell level using only four analog readout channels.<sup>11</sup> Ongoing developments aim at increasing the sensitivity in the near-infrared (NIR-HD technology): preliminary results show a PDE higher than 20% at 850 nm.

Ultra-High-Density SiPMs (RGB-UHD) are an evolution of RGB-HD SiPMs, characterized by an even smaller cell size to reduce the SiPM non-linearity. Cell pitch ranges from a 12.5  $\mu$ m down to 5  $\mu$ m, corresponding to the remarkable cell density of 7400 and up to 46000 cells/mm<sup>2</sup>. The 10  $\mu$ m cell reaches a PDE of 35% at 515 nm, while the microcell recharge time constant is below 5 ns for the 7.5 microcells.

Considering CMOS-based SPADs and SiPMs, FBK skills are such that the entire flow can be managed, from the high-level simulation of the device into the physical system to the circuit-level design, simulation and layout, from the electrical and electro-optical characterization to the prototype implementation. On the other hand, fabrication is subcontracted to external foundries, exploiting existing cooperation and selecting the more appropriate technology for the specific task to be solved. Typical architectures of CMOS-based SPAD sensors include array arrangement with local (per-pixel) or global special processing features, such as time-stamping (time-to-digital con-

<sup>7</sup>Piemonte, C. et al. (2016), IEEE Transactions on Electron Devices **63**(3), pp. 1111–1116.

<sup>8</sup>Nemallapudi, M. V. et al. (2015), Physics in Medicine & Biology **60**(12), p. 4635.

<sup>9</sup>Acerbi, F. et al. (2015), Nuclear Instruments and Methods in Physics Research, Section A **787**, pp. 34–37.

<sup>10</sup>Acerbi, F. et al. (2017), IEEE Transactions on Electron Devices **64**(2), pp. 521–526.

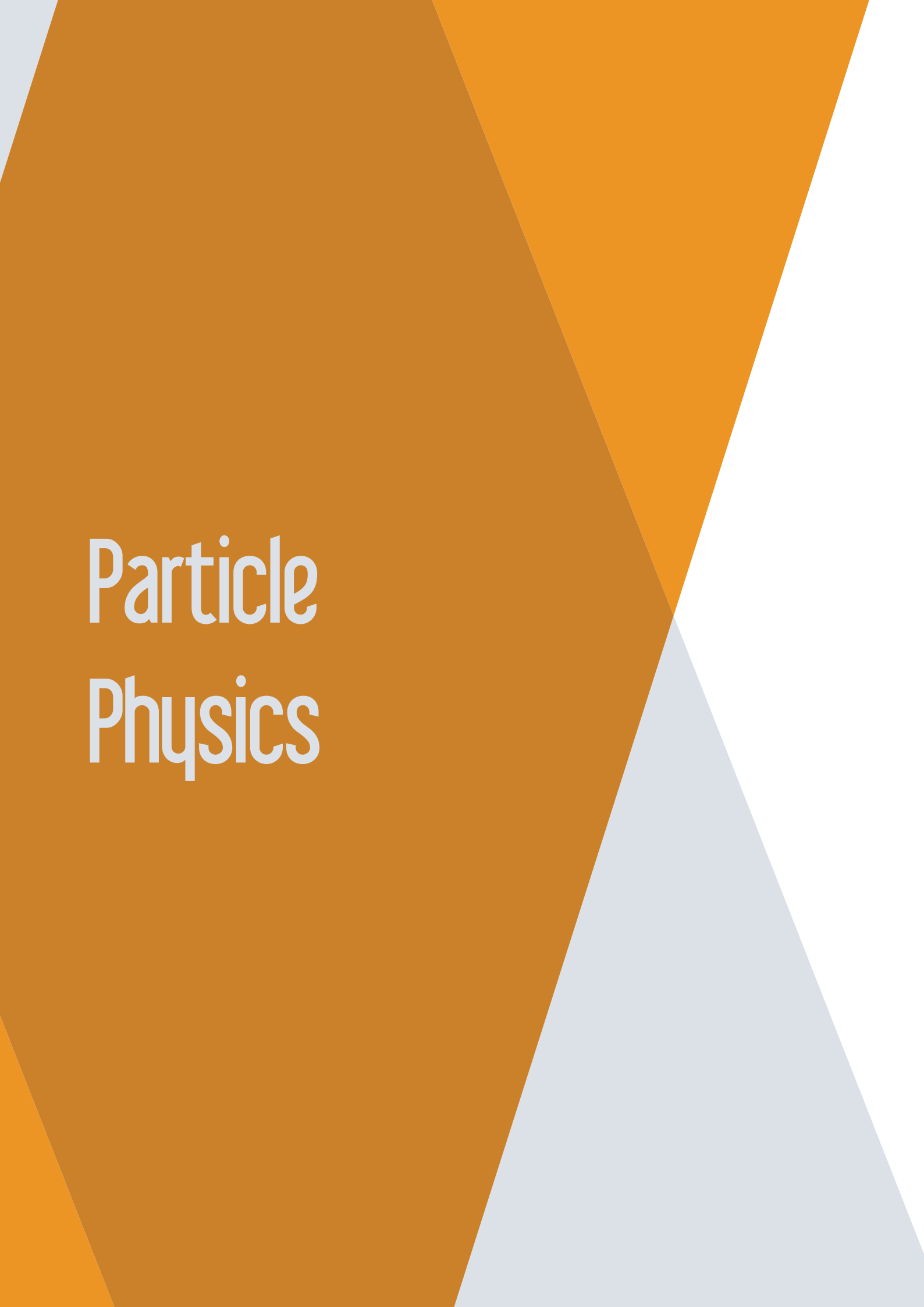
<sup>11</sup>Gola, A. et al. (2013), 2013 IEEE Nuclear Science Symposium and Medical Imaging Conference (2013 NSS/MIC), pp. 1–4.

verters, TDC, with tens of picoseconds timing resolution), energy evaluation through digital-SiPM topologies, high-speed readout and event-

based operation for minimization of the data transfer load.

# INFN Experiments





# Particle Physics

## Gian-Franco Dalla Betta

gianfranco.dallabetta@unitn.it

Coordinator,  
TIFPA Particle Physics Activities



The research activities of the INFN National Scientific Committee 1 (CSN1) deal with fundamental interactions of matter in experiments using particle accelerators, of which the Large Hadron Collider (LHC) is currently the largest and most powerful in the world. The LHC was built at CERN between 1998 and 2008 and its primary objectives are the discovery of the Higgs boson and other particles predicted by supersymmetric theories. The LHC is designed for proton-proton collisions delivering an unprecedented luminosity of  $10^{34} \text{ cm}^{-2}\text{s}^{-1}$  and a maximum energy of energy 14 TeV in the center of mass. The particle beams are not continuous but in bunches with a repetition rate never shorter than 25 ns.

ATLAS (A Toroidal LHC ApparatuS) and CMS (Compact Muon Solenoid) are the two general-purpose particle detectors built at the LHC. ATLAS has many objectives, spacing between the discovery of new particles, the confirmation of current theories and the discovery of new physics models. The most famous of these objectives is, of course, the discovery of the Higgs Boson, which was announced, jointly with CMS, in July 2012. When looking for very rare events, like the Higgs boson, the luminosity must be very high in order to increase the probability of generating such events. Hence, the High Luminosity LHC (HL-LHC) is currently planned for 2022 and is referred to as Phase-2 upgrade. Many hardware upgrades will be required in order to go beyond the initially designed luminosity and reach  $5 \times 10^{34} \text{ cm}^{-2}\text{s}^{-1}$  while maintaining the same energy in the center of mass. In particular, the ATLAS Inner Detector will be completely replaced with a new and more modern one.

The Trento group has collaborated with the ATLAS experiment since 2007, first within the CERN ATLAS 3D Collaboration and later, since 2011, also within INFN ATLAS Italy. The involvement with ATLAS has regarded the development of 3D pixel sensors for the Insertable B-Layer (IBL), the fourth layer of pixel sensors which was installed within the inner tracker in 2013: in particular, the group was responsible for the design of the 3D pixels fabricated at FBK. Following this successful contribution, since June 2015 the University of Trento / TIFPA Group has been officially an ATLAS institute.

The main commitment of the Trento group has been mainly on the engineering side: in particular, within the "INFN RD-FASE2" project, TIFPA has led the italian effort, in collaboration with FBK, towards a new generation of 3D pixel sensors for the Inner Tracker (ITk) of the ATLAS detector "Phase 2" upgrade.

More recently, since 2016, the group started to be involved also with the ATLAS physics program. In particular, in 2017 the Trento ATLAS team joined the Inner Detector (ID) performance group and it focused on data analysis aimed at improving the alignment of the ATLAS ID.

The most significant outcomes of the research activities in 2017 are summarised in the ATLAS and RD-FASE2 reports.

# ATLAS

Gian-Franco Dalla Betta, Francesco Maria Follega, Roberto Iuppa,<sup>†</sup> Ester Ricci

In 2017 the Trento ATLAS team joined the Inner Detector (ID) performance group and it focused on data analysis aimed at improving the alignment of the ATLAS ID. The ID is immersed in a solenoidal 2 T magnetic field, and it is made of three distinct subsystems: in order of proximity to the interaction region, they are the pixel detector (usually referred to as Pixel), the semiconductor tracker (SCT) and the transition radiation tracker (TRT). Since the beginning of Run 2, Pixel comprehends the innermost Insertable B-Layer (IBL), using also 3D silicon sensors with  $50\ \mu\text{m}$  pitch, fabricated by FBK (Trento) and CNM (Barcelona). The outermost three Pixel layers feature a more traditional planar technology.  $55\text{--}95\ \mu\text{m}$  pitch silicon microstrips are distributed over 8 (9) layers in the SCT barrel (endcaps). Proportional drift tubes with resolution as good as  $150\ \mu\text{m}$  are used to measure tracks in the TRT (30 points on average). The spaces between the straws are filled with polymer fibres, which act as radiator and allow to separate hadrons and electrons by detecting the transition radiation.

Every track is reconstructed from about 40 points and its curvature radius  $R$  allows to determine the transverse component of its momentum via the well-known relation  $p_T[\text{GeV}/c] = 0.3 B[\text{T}]R[\text{m}]$ . Any bias in the measurement of  $R$  directly impacts on the accuracy of the  $p_T$  measurement, which in turn impacts on the reconstruction of kinematic observables like momentum, energy and invariant mass. For tracks with momenta as high as those detected by ATLAS, the most important source

of bias is the misalignment of detector modules. Detectors may be misaligned because of permanent reasons (e.g. mechanical assembly) or due to transitory issues (thermal expansion, magnetic field induced torsions, long-term settling). Alignment is largely recovered by looking at data and computing the correction factors necessary to make experimental points aligned at best for each track. This result is usually achieved by iteratively minimising the  $\chi^2$  of residuals to the the best fit track. At each iteration, all hits too distant from the best fit track are taken out and the fit is improved. In principle, the number of degrees of freedom that the

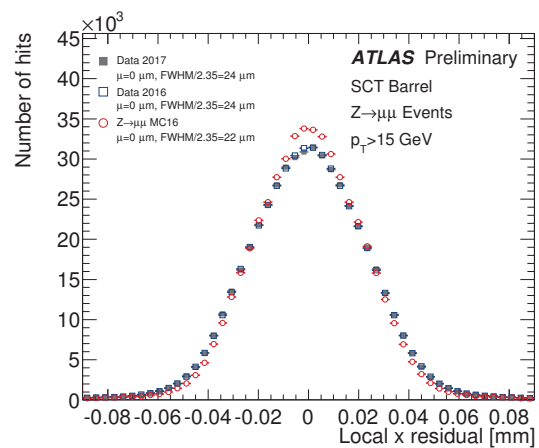


Figure 1: Residual of the SCT barrel for early 2017 data compared to a run from 2016 and to simulated  $Z \rightarrow \mu\mu$  events. Simulated events and 2016 data are normalised to 2017 data number of tracks. The residuals have been extracted refitting the muon tracks in the Inner Detector (with  $p_T > 15\ \text{GeV}/c$ ) from  $Z \rightarrow \mu\mu$  events. 2017 data is shown in gray full squares, 2016 data in blue open squares and the Monte Carlo in red open circles.

<sup>†</sup>Contact Author: roberto.iuppa@unitn.it

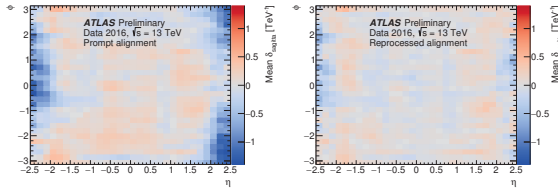


Figure 2: Average sagitta bias as a function of  $\eta$  and  $\phi$  for the 2016 proton-proton dataset. Corrections obtained with the reprocessed alignment (right) are compared to corrections obtained with the prompt alignment (left).

$\chi^2$  is computed over may be equal to the total number of pixels, strips and straw tubes to be aligned. This number being too large, distortions are parametrised via analytical expressions, looked for and corrected for. Further residuals are corrected for in small regions of  $\eta$ ,  $\phi$  and  $p_T$ . These solutions allow for quasi-real-time corrections, computed down to few hours after data taking (“prompt alignment”). More detailed and time-consuming analyses are performed offline by the tracking performance group of the ATLAS collaboration, improving by a factor of three or more the prompt alignment. As visible in Fig. 1 the alignment makes the residual distribution compatible with predictions from Monte Carlo. More details about the ATLAS ID alignment can be found in (ATLAS Collaboration 2010)<sup>1</sup> and (ATLAS Collaboration 2011).<sup>2</sup>

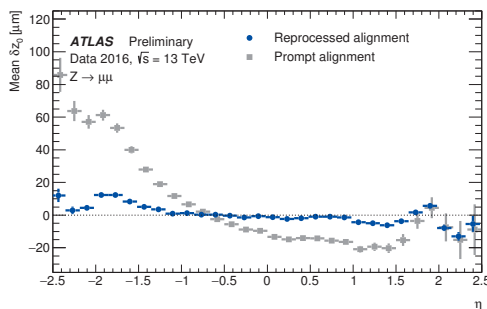


Figure 3: Average bias of the track parameter  $z_0$  as a function of  $\eta$  for the 2016 proton-proton dataset, averaged over  $\phi$ . The vertical bars indicate the variance along the azimuthal direction. Corrections obtained with the reprocessed alignment (blue circles) are compared to corrections obtained with the prompt alignment (grey squares).

The quality of the alignment is usually quantified by the distance of the track perigee to the nominal interaction point, which is expected to be zero. The FWHM of its projections on the transverse plane ( $d_0$ ) and the longitudinal plane ( $z_0$ ) are good figures of merit of how good the tracker alignment is. Moreover,  $Z \rightarrow \mu\mu$  events are kinematically closed and allow to estimate the charge-dependent bias in the sagitta estimation ( $s \propto 1/p_T$ ). Also  $Z \rightarrow ee$  events allow for an estimation of this bias, but the calorimeter response has to be considered also ( $E/p$  method). More details are reported in (ATLAS Collaboration 2012).<sup>3</sup> Figs. 2 and 3 were made public in mid 2017 and show an example of the sagitta bias in the  $(\eta, \phi)$  plane.

Trento’s team was assigned two tasks by the ATLAS ID alignment group: (a) to improve the alignment in the calibration loop and (b) to consolidate the offline data quality monitoring. Concerning (a), the team introduced new types of plots summarising the track-to-hit residual information over many runs and showing the temporal development of these residuals over many runs. The plots were initially prepared using 2016 data, and tests with 2017 data were performed as well. These plots are going to be included in the ID tracking alignment tool (ATLAS internal). Concerning (b), the team prepared invariant mass plots of reconstructed muon pairs as a first test, before proceeding to the production of weak mode maps showing the sagitta,  $d_0$ , and  $z_0$  biases present in the updated 2016 alignment. It introduced alternative variables and ways to present the bias information obtained from  $Z \rightarrow \mu\mu$  samples, by extracting the  $Z$  decay width rather than the  $Z$  mass. Further improvement was obtained by using an  $(\eta, \phi)$  dependent  $Z$  mass for reference, accounting for material effects all along the muons’ path.

Trento’s team has played an important role in the ATLAS alignment group, and the contribution of its young members is held in high consideration, earning them the qualification of ATLAS authors.

<sup>1</sup>ATLAS Collaboration (2010), <http://cds.cern.ch/record/1281342> ATLAS-CONF-2010-067.

<sup>2</sup>ATLAS Collaboration (2011), <http://cds.cern.ch/record/1334582> ATLAS-CONF-2011-012.

<sup>3</sup>ATLAS Collaboration (2012), <http://cds.cern.ch/record/1483518> ATLAS-CONF-2012-141.

## RD-FASE2

Gian-Franco Dalla Betta,<sup>†</sup> Maurizio Boscardin, Mostafa El Khatib, Roberto Iuppa, David Macii, Roberto Mendicino, D M S Sultan, Giovanni Verzellesi

Since 2014, the RD-FASE2 project within CSN1 has addressed the technological developments for the ATLAS and CMS detector upgrades at the High Luminosity LHC. The role of TIFPA has been concerned with the development of a new generation of 3D sensors aimed at the innermost tracking layers. This application requires very high hit-rate capabilities, increased pixel granularity (e.g.,  $50 \times 50$  or  $25 \times 100 \mu\text{m}^2$  pixel size) and extreme radiation hardness (up to  $2 \times 10^{16} \text{ n}_{eq} \text{ cm}^{-2}$  fluence). New 3D sensors are made with a single-sided process with thinner active regions ( $\sim 100 \mu\text{m}$ ), narrower columnar electrodes ( $\sim 100 \mu\text{m}$ ) with reduced inter-electrode spacing ( $\sim 30 \mu\text{m}$ ), and very slim edges ( $\sim 100 \mu\text{m}$ ).

3D sensors from the first batch fabricated at FBK in 2016 were extensively tested. Their electrical characteristics measured at wafer level are very good, as reported in (Sultan et al. 2017a). The best two wafers underwent bump bonding at Leonardo (Rome). Several pixel modules were assembled with FEI4 and PSI46dig read-out circuits (ROCs), and tested in laboratory and in beam tests at CERN and Fermilab during the last year. Results were as expected, with relatively low noise figures ( $\sim 100 \text{ e}^-$  rms, compatible with the pixel capacitance), and hit efficiency higher than 99% already at low voltage.

In 2017, the main effort was devoted to the characterisation of irradiated samples. An irradiation campaign was carried out for both the FEI4 and PSI46dig modules, with irradiations

at CERN (24 GeV/c protons), KIT (25 MeV protons), and JSI (reactor neutrons). Preliminary results from the irradiation of test structures (3D diodes and strips) up to very large fluences ( $3.5 \times 10^{16} \text{ n}_{eq} \text{ cm}^{-2}$ ) anticipate that sensors can be operated at a voltage high enough to allow for full depletion (hence high efficiency) with an increase of the leakage current following the expected (SRH related) trend with neutron and proton fluence (Dalla Betta et al. 2017a).

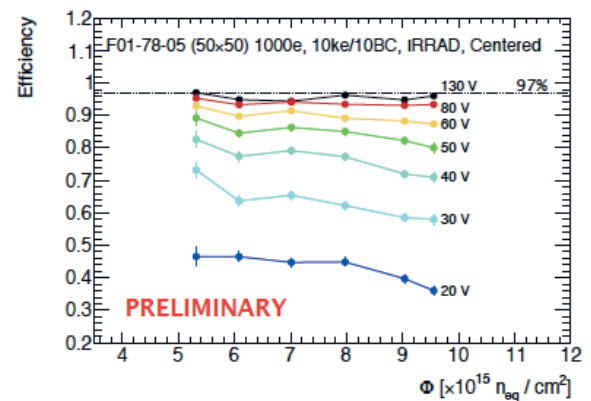


Figure 1: Hit efficiency of a  $50 \times 50$  pixel detector irradiated at CERN IRRAD as a function of fluence for different bias voltages.

Proton irradiated pixel modules with FEI4 ROCs were measured in beam tests using 120 GeV pions at CERN SPS H6A beam line in August and October 2017, with encouraging results. As an example, Fig. 1 shows the hit efficiency of a  $50 \times 50$  pixel detector irradiated at CERN IRRAD as a function of fluence for different bias voltages. Data refer to a module calibration setting with a threshold of  $1000 \text{ e}^-$

<sup>†</sup>Contact Author: gianfranco.dallabetta@unitn.it

and a Time-over-Threshold (ToT) of 10 bunch crossings at  $10 \text{ ke}^{-\text{s}}$  signal. It can be seen that, if the bias voltage is high enough, the sensor retains an efficiency of  $\sim 97\%$  in the entire fluence range. Such a value is close to the one expected theoretically for normally incident particles, taking into account that the columnar electrodes are dead regions. After the October test beam, selected modules have been chosen to be further irradiated at CERN IRRAD up to larger fluences, and will be measured again in a test beam in spring 2018. Other irradiated pixel modules with PSI46dig ROCs were measured in a beam test at FERMILAB MTest area in November 2017. Data analysis is under way.

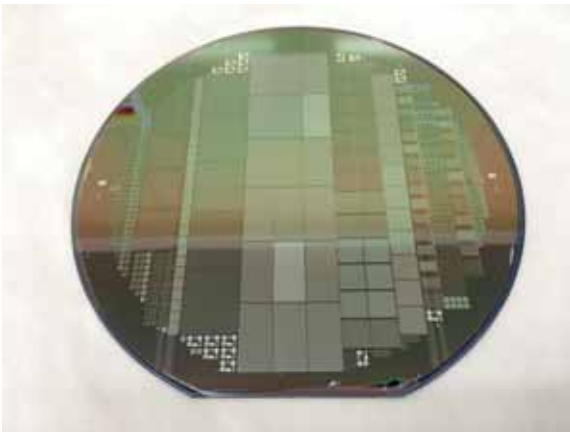


Figure 2: Photograph of a wafer from the second batch fabricated at FBK.

In parallel, a new batch of 3D sensors was designed at UniTN and fabricated at FBK. Twelve wafers were completed, including both Si-Si DWB and SOI substrates. The wafer layout (see the photograph in Fig. 2) includes several different small-pitch pixel sensors, among them those compatible with the new RD53A ROC that will be available by the end of 2017 (the RD53A compatible sensors are visible in the centre of the wafer in Fig. 2). Initial results from the electrical characterization of sensors at the wafer level are good both in terms of leakage currents, of the order of 1 pA per column like in the first batch, and breakdown voltage as large as 120 V. Results also confirmed that the  $25 \times 100 \mu\text{m}^2$  pixel with two read-out electrodes is critical for the yield, suggesting that an improved lithography system should be used for its fabrication. Five selected wafers were sent for bump bonding to Leonardo (Rome) and IZM (Berlin). Pixel modules with RD53A ROC will be available soon and will be extensively tested in 2018.

## Selected Papers

- Dalla Betta, G.-F., Mendicino, R., Boscardin, M., Hoferkamp, M., Mendicino, R., Seidel, S., and Sultan, D. (2017a). *Electrical characterization of FBK small-pitch 3D sensors after  $\gamma$ -ray, neutron and proton irradiations*. *Journal Instrum.* **12**, p. C11028.
- Sultan, D., Dalla Betta, G.-F., Mendicino, R., Boscardin, M., Ronchin, S., and Zorzi, N. (2017a). *First Production of New Thin 3D Sensors for HL-LHC at FBK*. *Journal Instrum.* **12**, p. C01022.

# Activities starting in 2018

## FASE2\_ATLAS

**Research outline** The project is aimed at completing the R&D activities previously started in the “RD-FASE2” Project, with a more focused approach aimed at solving some specific remaining issues in view of the construction of the new ATLAS detector for High-Luminosity LHC. Within the Inner Tracker sub-project, TIFPA will work at the optimization of 3D pixel sensors for the innermost layer. Extensive tests will be carried out on modules equipped with the new RD53A read-out chip, both before and after irradiation. New batches of 3D sensors will be processed at FBK also using stepper lithography, in order to improve the yield for future production.

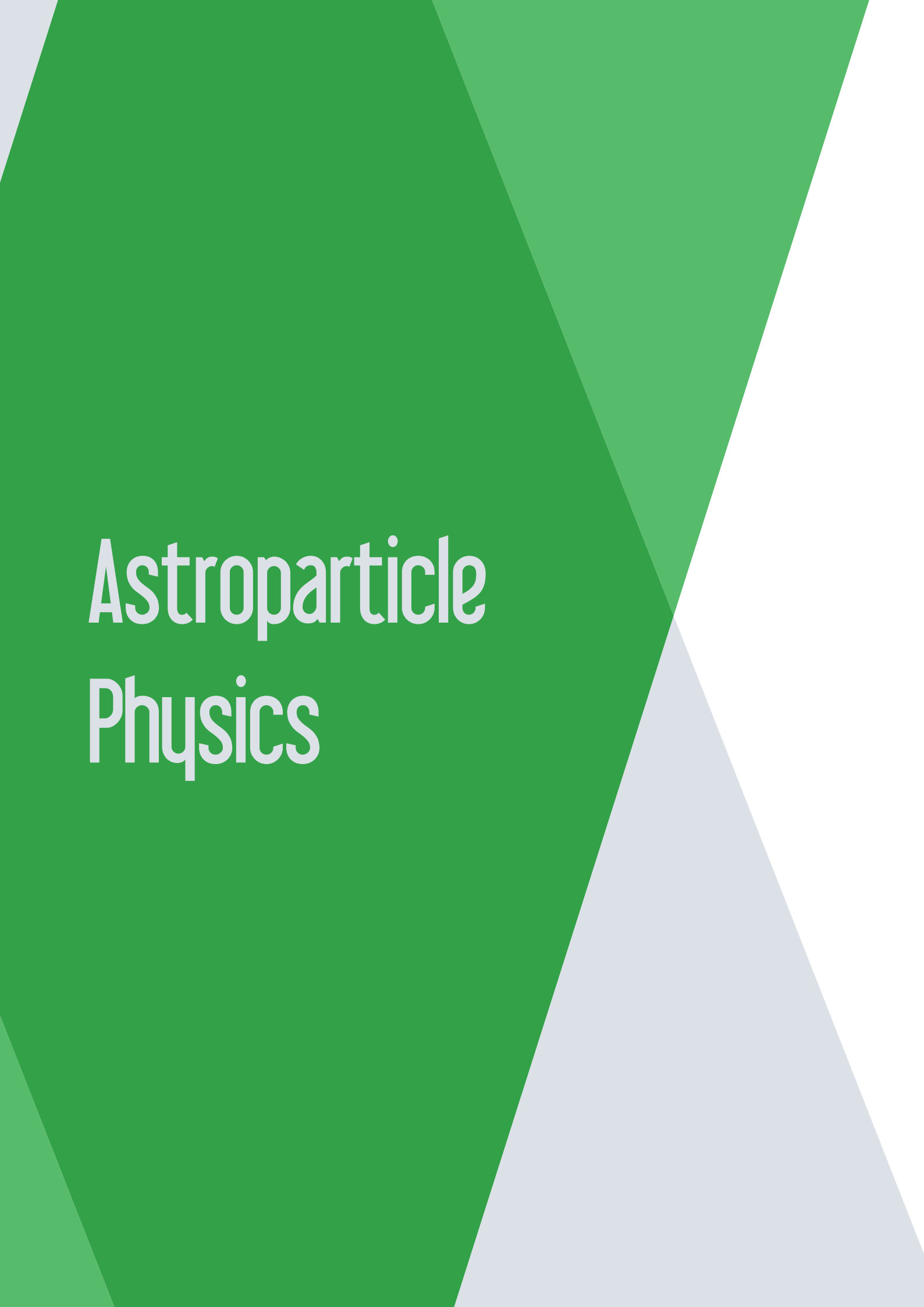
**involved external institutions** FBK, Leonardo SpA, IFAE

**INFN groups** Bologna, Cosenza, Genova, Lecce, LNF, Milano, Napoli, Pisa, Roma1, Roma2, Roma3, TIFPA, Udine

**Principal Investigator** Marina Cobal, INFN Trieste — Gruppo Collegato di Udine

**TIFPA team** Gian-Franco Dalla Betta (coordinator), Giacomo Baldi, Maurizio Boscardin, Mostafa El-Khatib, Roberto Iuppa, David Macii, Giulio Monaco, Kenji Nardone, Giovanni Verzellesi





# Astroparticle Physics

Rita Dolesi

rita.dolesi@unitn.it

Coordinator,  
TIFPA Astroparticle Physics Activities



Astroparticle physics is an interdisciplinary field at the intersection of particle physics, astrophysics, cosmology and fundamental physics. Within INFN, this field is competence of the Commissione Scientifica Nazionale II, that deals in fact with a wide spectrum of experimental investigations. They range from studies of the neutrino properties to experiments probing the dark Universe, from studies of radiation and gravitational waves from the Universe to experiments addressing the foundation of general and quantum physics. These activities differ for the topics, for the employed technologies and involve researchers working in various fields. Therefore they greatly benefit from the synergy between INFN and other research institutes, as happens at the TIFPA where INFN, Università di Trento, CNR, FBK and Trento Proton Therapy Center can work efficiently in joint projects. Lively and productive is obviously also the collaboration with ASI for the space based experiments.

At the TIFPA, the activities related to astroparticle physics currently involve about 40 researchers in 8 experiments briefly presented in this section, together with their recent highlights. It is noteworthy the high quality of the contribution of the TIFPA members in these projects: their remarkable ability to simulate, to design and then to fabricate cutting-edge devices and to realize challenging novel experimental apparatus allow for pushing the experimental performance to their limits and therefore to enhance the overall scientific return.

In 2107, several events of extraordinary scientific relevance and general significant advances characterized these activities.

Virgo and LISA-LISA Pathfinder are the leading INFN experiments in the detection of gravitational waves field which is opening a new window for the exploration of the Universe. In 2017, two years from the LIGO/Virgo collaboration announcement of first direct detection of the gravitational sound of two coalescing stellar black holes, and just two weeks after the awarding of the Nobel Prize for Physics for that goal, LIGO and Virgo announced a second result of enormous scientific relevance: the observation of the coalescence of two neutron stars in both gravitational and electromagnetic waves that opens the era of the multi-messenger astronomy. In 2017 moreover, LISA Pathfinder successfully completed its adventure in space with outstanding performance, that demonstrated the ability to realize the science potential of the LISA mission that is now progressing toward its implementation.

On the International Space Station (ISS), AMS-02 is a state-of-the-art particle physics detector successfully performing precision measurements of cosmic ray composition and flux , and investigating the Universe and its origin by searching for antimatter and dark matter.

LIMADOU, a particle detector designed to study the correlation observed between seismic phenomena and changes in the trapped particle populations of the inner Van Allen radiation belt, that was successfully launched at the beginning of February 2018 and already started the preliminary phases of the in-flight operations.

The detection of a possible dark matter candidate is the goal of DARKSIDE and QUAX while, in the domain of quantum simulations operates FISH, modelling interactions and mechanism at the basis of high energy system by means of quantum gases of ultra-cold atoms. HUMOR focuses on probing the granularity of space-time at the Planck scale expected by theory trying to unify General Relativity with Quantum Physics.

# AMS

Laurent Basara, Roberto Battiston, William Jerome Burger, Francesco Dimiccoli, Konstantin Kanishev, Ignazio Lazzizzera, Francesco Nozzoli<sup>†</sup>

AMS-02 is a state-of-the-art particle physics detector designed to operate as an external module on the International Space Station (ISS). It is studying the universe and its origin by searching for antimatter and dark matter, while performing precision measurements of cosmic ray composition and flux.

The high statistics of the measurements, along with the high precision of the experiment, allow to study the detailed variations with rigidity of the flux spectral indices and flux ratios, important in understanding the origin, acceleration and propagation of cosmic rays in our galaxy. As an example, the knowledge of the rigidity dependence of the boron to carbon flux ratio (B/C) is a fundamental measurement for the understanding of the propagation of cosmic rays. AMS-02 has recently published the precise measurement of the B/C ratio from 1.9 GV to 2.6 TV, based on 2.3 million boron and 8.3 million carbon nuclei collected during the first 5 years of operation (Aguilar et al. 2016). The B/C ratio, shown in Fig. 1 does not show any significant structures in contrast to many cosmic ray models that require such structures at high rigidities. Remarkably, above 65 GV, the B/C ratio is well described by a single power law  $R^\Delta$  with index  $\Delta = -0.333 \pm 0.014(stat) \pm 0.005(syst)$ , in good agreement with the Kolmogorov theory of turbulence which predicts  $\Delta = -1/3$  asymptotically.

AMS-02 results for the Proton and Helium fluxes show a surprisingly similar behaviour,

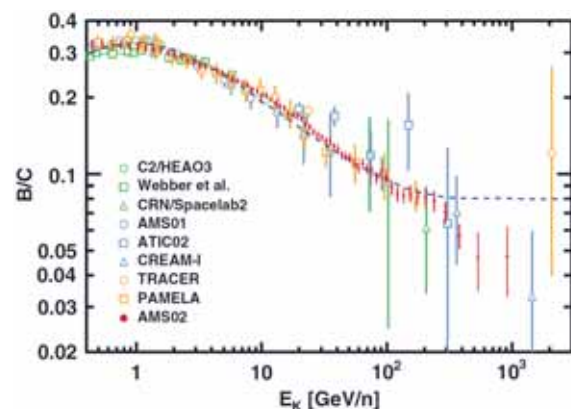


Figure 1: The AMS-02 Boron to Carbon ratio as a function of kinetic energy per nucleon  $E_K$  compared with previous measurements. The dashed line shows an example of the B/C ratio required by the models that would explain the AMS results for the positron fraction,  $e^+/(e^+ + e^-)$ , and antiproton-to-proton ratio (Nozzoli 2016) as purely due to secondary production. These models are ruled out by the AMS measurement of B/C ratio.

where the spectral index progressively hardens at rigidities larger than 100 GV. A recent study of the light nuclei cosmic ray component (He, C, and O) measured in the rigidity range 2 GV to 3 TV has been published by AMS (Aguilar et al. 2017). A total of 90 million helium, 8.4 million carbon, and 7.0 million oxygen nuclei have been collected by AMS during the first 5 years of operation. Unexpectedly, above 60 GV, these three spectra have identical rigidity dependence. They all deviate from a single power law above 200 GV and harden in an identical way. Results, with comparison of the fluxes, are summarized in Fig. 2.

<sup>†</sup>Contact Author: francesco.nozzoli@tifpa.infn.it

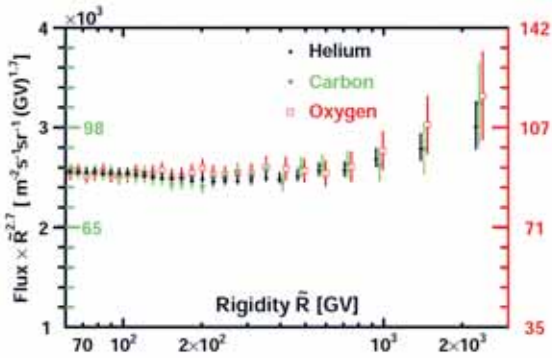


Figure 2: The rigidity dependence of the helium (left black axis), carbon (left green axis), and oxygen (right red axis) fluxes. For clarity, horizontal positions of the helium and oxygen data points above 400 GV are displaced with respect to the carbon. As seen, above 60 GV the three fluxes have identical rigidity dependence.

Helium, carbon, and oxygen are among the most abundant nuclei in cosmic rays. They are called primary cosmic rays and are thought to be mainly produced and accelerated in astrophysical sources. Precise knowledge of their spectra in the GV - TV rigidity region, measured by AMS-02, would provide important insights to the origin, acceleration, and subsequent propagation processes of cosmic rays in the Galaxy.

Beyond the detailed study of nuclear composition of the cosmic rays, the AMS collaboration is improving the existing analysis for the measurements of electron and positrons at high energy and for the first measurements of Anti-Deuterons in cosmic rays. Both channels are good candidates for the indirect detection of Dark Matter particles, in particular the primary Anti-Deuteron flux due to Dark Matter annihilation.

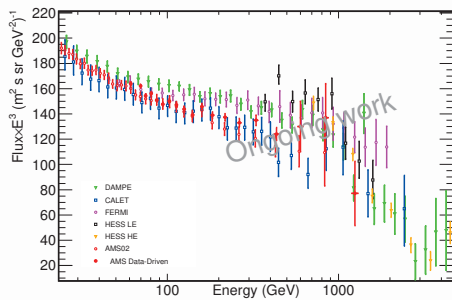


Figure 3: Preliminary status of the “MC-Free” data-driven measurement for the  $(e^+ + e^-)$  flux, compared with the recent results from HESS, FERMI-LAT, DAMPE and CALET.

tion might be up to three orders of magnitude higher with the respect to the expected secondary production in a wide range of possible annihilating Dark Matter masses.

The TIFPA-AMS02 group plays a leading in the measurement of the Deuteron and Anti-Deuteron fluxes and is now also working on the measurement of the Electron and Positron sum flux at high energy. In particular, for the measurement of  $(e^+ + e^-)$  flux, a data-driven method has been developed with the aim of reduction of the systematic errors due to the Monte Carlo simulation of multivariate classifiers. These classifiers are necessary to reject the large proton background at high energy. Preliminary results are shown in Fig. 3; the data-driven approach is able to extend the flux measurement up to 1.5 TeV, with a possible confirmation of the break in the  $(e^+ + e^-)$  flux observed by HESS and DAMPE experiments but not observed by FERMI-LAT and CALET.

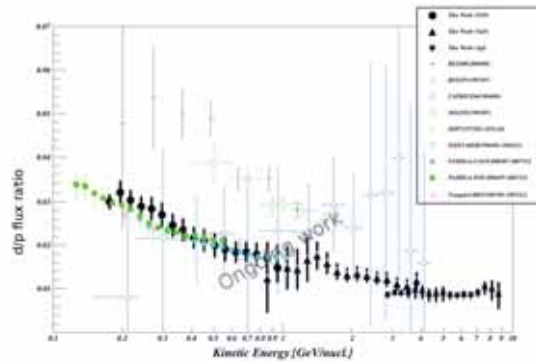


Figure 4: Preliminary Deuteron over Proton flux ratio measured with AMS-02 compared with previous measurements.

The perspectives for AMS-02 is to measure the  $(e^+ + e^-)$  flux up to  $\sim 2$  TeV, this limitation is due to the relatively smaller exposure with respect to FERMI-LAT, DAMPE and CALET. However, due to the redundancy of the energy measurement provided by the magnetic spectrometer and calorimeter the AMS-02 result has smaller systematic errors and may provide an interesting crosscheck regarding the position of the break in the  $(e^+ + e^-)$  flux reported at  $E \sim$  TeV by some experiments.

The TIFPA group is currently analyzing the Deuteron flux as a first step for the study of the cosmic Anti-Deuteron flux, allowing the opti-

mization of the detector performances and selection strategy. Moreover, the deuteron flux measure is itself very important, because the flux ratio between exclusively secondary and primary produced CR particles gives important constraints to the propagation models of CR in the Galaxy.

We developed both multivariate approach than a simple cut analysis for the distinction of deuterons from the overwhelming proton back-

ground. Fig. 4 shows a preliminary result of the measurement of the Deuteron to Proton flux ratio.

Moreover analysis tools developed for the Deuteron flux measurement may be applied also for other isotope mass separations,  $^3\text{He}/^4\text{He}$  ratio and  $^{10}\text{Be}/^9\text{Be}/^7\text{Be}$  abundances in cosmic rays, as well as for the search for strangelets.

## Selected Papers

- Aguilar, M. et al., AMS collaboration (2017). *Observation of the Identical Rigidity Dependence of He, C, and O Cosmic Rays at High Rigidities by the Alpha Magnetic Spectrometer on the International Space Station*. Phys. Rev. Lett. **119**(25), p. 251101.
- AMS collaboration (2016). *Precision Measurement of the Boron to Carbon Flux Ratio in Cosmic Rays from 1.9 GV to 2.6 TV with the Alpha Magnetic Spectrometer on the International Space Station*. Phys. Rev. Lett. **117**(23), p. 231102.
- Nozzoli, F. (2016). “Precision measurement of antiproton to proton ratio with the Alpha Magnetic Spectrometer on the International Space Station”. *25th European Cosmic Ray Symposium (ECRS 2016) Turin, Italy, September 04-09, 2016*.

# DarkSide

Fabio Acerbi, Alberto Gola,<sup>†</sup> Marco Marcante, Alberto Mazzi, Giovanni Paternoster, Claudio Piemonte, Veronica Regazzoni

The existence of dark matter in the Universe is commonly accepted as the explanation of many phenomena, ranging from internal motions of galaxies to the large scale inhomogeneities in the cosmic microwave background radiation and the dynamics of colliding galaxy clusters.

A favored hypothesis that explains these observations is that dark matter is made of weakly interacting massive particles (WIMPs). However, no such particles exist in the Standard Model and none has been observed directly at particle accelerators or elsewhere. Hence the nature of the dark matter remains unknown.

DarkSide 20k experiment (DS-20k) is a direct detection experiment based on a shielded underground detector with 20 tons of liquid argon target mass. It will be based on a two-phase Time projection Chamber (TPC) filled with low-background, depleted Argon (DAR) and will be deployed in in the underground Hall C at National Laboratory Gran Sasso, LNGS, inside a newly constructed Liquid Scintillator Veto, LSV, and Water Cherenkov Veto, WCV, see Fig.1. DS-20k constitutes an expanded version of the DS50 experiment, currently running at LNGS.

**DS20k Time Projection Chamber** In the TPC, events in the Liquid Argon result in electron or nuclear recoils that deposit energy in the argon, resulting in excitation and ionization. The direct excitation, and that due to recombining ions, results in a prompt scintillation signal, called S1. LAr scintillation has a wavelength of 128 nm, in the far UV, thus

a wavelength shifter (TPC) will cover all surfaces that the UV light hits. Ionization electrons escaping recombination are drifted by an applied electric field to the top of the LAr, where a stronger applied field extracts the electrons into the argon gas above the liquid. Here the strong field accelerates the electrons enough for them to excite (but not ionize) the argon gas, producing a secondary scintillation signal, S2, that is proportional to the initial ionization. Photosensors at the top and bottom of the TPC read out both scintillation signals in each event.

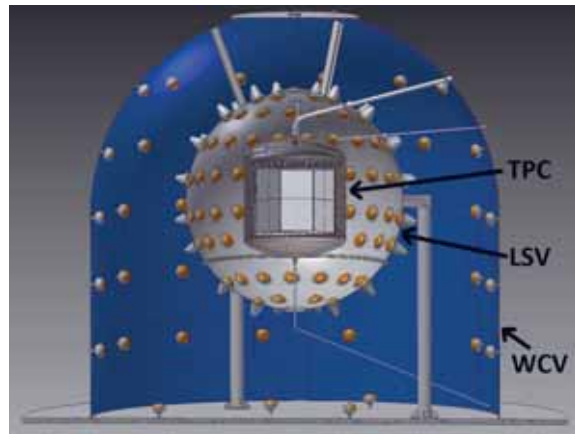


Figure 1: Cross sectional view of the DS20k experiment through its center plane, showing the water tank and the WCV detector, the stainless steel sphere and LSV detector, and the DarkSide-20k cryostat and LAr TPC.

S1 is used for energy determination and pulse-shape discrimination. S2 is used for energy and 3D position measurement of the event,

<sup>†</sup>Contact Author: gola@fbk.eu

obtaining the vertical coordinate from the drift time between S1 and S2, and the horizontal coordinates from the pattern of light in the top photosensors.

**Silicon Photo Multipliers** The use of Silicon Photomultipliers (SiPMs) instead of Photo Multiplier Tubes as photodetectors is one of the main technological challenges of the experiment, the other being the production of ultra-low-background DAR. There are several advantages in using these detectors in DS-20k, among them: low bias voltage (25 - 40 V), efficient integration into tiles to cover large areas, customizable size and performance, excellent photon counting capabilities and high Photon Detection Efficiency (PDE). The most important one, however, is that SiPMs are virtually radioactivity free (silicon is very radio pure material). SiPMs will be grouped in tiles and integrated in several photo-detection modules, to cover a total area of approximately 10 square meters.

**DS-20k Activity at TIFPA** The use of SiPMs at cryogenic temperatures is innovative and very few studies have been carried out on their characterization and optimization at cryogenic temperatures. Furthermore, the readout of such large active areas poses several challenges in the design and optimization of both SiPMs and front-end electronics, developed at LNGS, and in packaging techniques. In this context, TIFPA started the DS-20k activity in 2016, collaborating mainly with Fondazione Bruno Kessler (FBK), LNGS, Naples INFN section and Princeton University. The activity was focused on cryogenic characterization of different SiPMs technologies developed by FBK to:

- (i) verify and characterize their functionality at cryogenic temperatures and, in particular, at 87 K;
- (ii) select the most suitable one for DS-20k;

- (iii) provide information to optimize the SiPM parameters and layout for the best possible performance in DS-20k.

To this aim, one of the most important results obtained in 2016 and confirmed in later SiPM productions is the exceptionally low Dark Count Rate (DCR) of NUV-HD-LF (low electric field variant) technology at 87 K, which is at the state of the art with a value of a few mHz/mm<sup>2</sup>. Using cryogenic electronics finalized at LNGS in 2017, remarkable few-photon counting capability was demonstrated at 77 K, with S/N of 13.8, using a 24 cm<sup>2</sup> SiPM array coupled to a single analog readout channel, as shown in Fig. 2. In 2017, TIFPA commissioned new R&D runs of SiPMs to FBK, to test a technological split aimed at further improving their cryogenic performance. Experimental characterization of the new split showed that it is effective in suppressing the increase of the correlated noise previously observed at cryogenic temperatures, therefore increasing the maximum operating over-voltage of SiPMs at 87 K by a factor of 3. This result is very important to increase the S/N ratio in photon counting, to relax the specifications on the readout electronics and to improve the stability of the photo-detection system. This confirms the choice SiPMs as a valid alternative to PMTs for the readout of the large photosensitive areas required by DS20k.

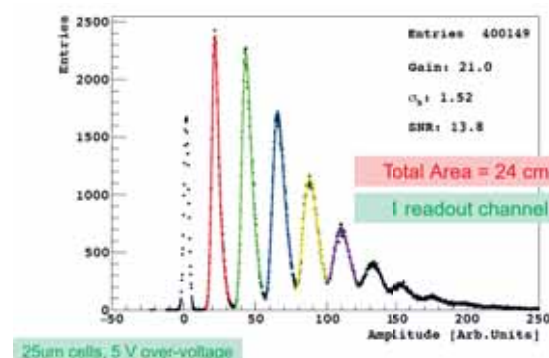


Figure 2: Few-photon spectrum measured at 77 K with a 24 cm<sup>2</sup> SiPM array and a single analog channel readout.

# FISH

Giacomo Colzi, Eleonora Fava, Carmelo Mordini, Arturo Farolfi, Sandro Stringari, Giacomo Lamporesi, Gabriele Ferrari <sup>†</sup>

FISH, Fundamental Interaction Simulations with quantum gases, focuses on the dynamics of quantum gases of ultracold atoms with the aim to model interactions and mechanisms at the basis of high energy physics. This research field belongs to the domain of quantum simulation, where physical systems difficult to address experimentally are studied through analogies with simpler systems. In particular we focus on the study of vortices in a system made of two Rabi-coupled atomic Bose-Einstein condensates to simulate quark confinement.<sup>1</sup>

Spinor Bose-Einstein condensates, whose wavefunction has a spin term, play a crucial role within the community of ultracold/quantum gases. Since the early demonstration of Bose-Einstein condensation, these systems were studied mainly in the absence of stationary driving among the internal states, focusing on mean-field effects as, for instance, the stability of polarization, the miscibility, and the many-body dynamics of the superfluids under the action of external parameters such as the symmetry of the interactions, the confining potential, or the energy splitting of the internal states. The case of Hamiltonians containing a coupling term among the spin states has been fairly unexplored so far, at least experimentally, because of technical constraints imposed by the stability of the magnetic fields. On the other hand, binary condensates under the action of a resonant coupling among internal states have attracted a substantial theoretical interest since it was rec-

ognized that in such systems the additional degrees of freedom (i.e., the relative phase) give access to new kinds of topological excitations, such as domain walls and vortex molecules.<sup>1</sup>

In Trento we plan to realize bound states of vortices in binary condensates under the action of a resonant coupling. The interaction among the constituents of the vortex molecule will be studied as a function of the accessible experimental parameters, such as the intensity of the coupling, the intra- and inter-species mean-field interactions, or the confining external potential. Quantum simulation of quark confinement will be performed by introducing terms which may result in the breaking of the vortex-molecules, such as time-dependent perturbations of the

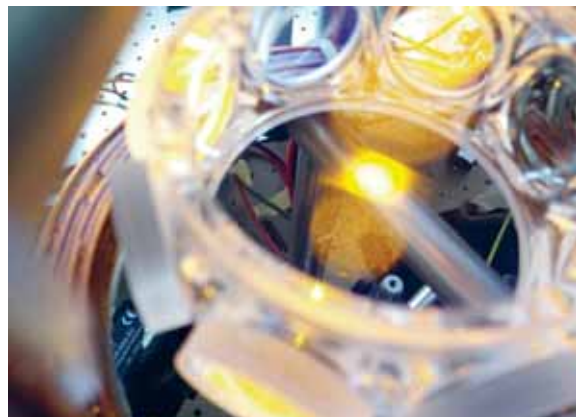


Figure 1: Magneto-optic trap (yellow spot in the center of the octagonal cell) containing  $5 \times 10^9$  sodium atoms laser cooled to temperatures of about  $10\mu K$ , reaching a phase-space density of the order of  $10^{-4}$ .

<sup>†</sup>Contact Author: gabriele.ferrari@unitn.it

<sup>1</sup>Son, D. T. and Stephanov, M. A. (2002), Phys. Rev. A 65(6), p. 063621.

external potential or high temperature of the sample, and observing how additional molecules are generated after individual processes of molecule-breaking.

During the last year the activities mainly focused on the realization of the novel dedicated experimental apparatus, by means of the

- setting up of an atomic source of sodium atoms, its loading into a 3D Magneto-Optic Trap, and laser cooling in a gray molasses (Colzi et al. 2016) (see Fig. 1),
- setting up of a far-off resonance optical dipole trap, which was initially intended to be loaded directly from the gray molasses. Various attempts made in the course of the year showed the low efficiency of this approach due to incompatibilities in the simultaneous operation of the gray molasses and the optical dipole trap,
- the issue was solved by means of the development of a novel hybrid magnetic and optical dipole trap which also takes into account the constraints resulting from the employ of a  $\mu$ -metal shield enclosing the science cell,
- in the hybrid trap evaporative cooling was demonstrated and optimized in order to enter into the quantum degenerate regime, resulting in Bose-Einstein

condensates of up to  $7 \times 10^6$  atoms (see Fig. 2).

On an existing experimental apparatus we also completed a series of measurements to characterize the static and dynamic response of superfluid mixtures in the linear regime and near to the miscible-immiscible transition, extending the measurements performed at zero temperature (Bienaimé et al. 2016) to the finite temperature case (Fava et al. 2017).

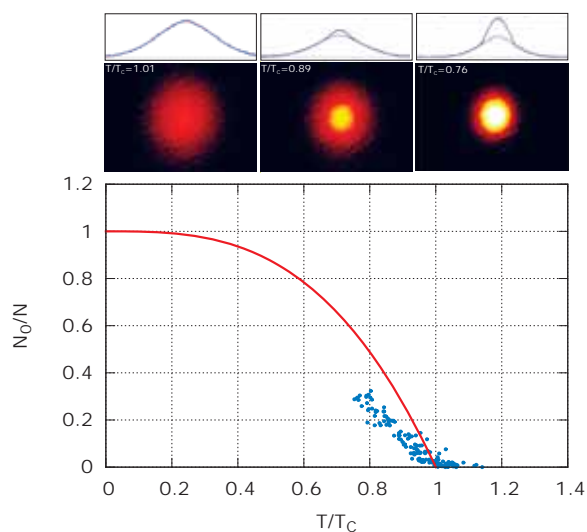


Figure 2: Condensed fraction as a function of the reduced temperature  $T/T_c$ , where  $T_c$  is the ideal harmonically trapped gas transition temperature. The orange solid line is the analytic formula for the ideal gas.

## Selected Papers

Bienaimé, T., Fava, E., Colzi, G., Mordini, C., Serafini, S., Qu, C., Stringari, S., Lamporesi, G., and Ferrari, G. (2016). *Spin-Dipole Oscillation and Polarizability of a Binary Bose-Einstein Condensate near the Miscible-Immiscible Phase Transition*. Phys. Rev. A **94**, p. 063652.

Colzi, G., Durastante, G., Fava, E., Serafini, S., Lamporesi, G., and Ferrari, G. (2016). *Sub-Doppler cooling of sodium atoms in gray molasses*. Phys. Rev. A **93**(2), p. 023421.

Fava, E., Bienaimé, T., Mordini, C., Colzi, G., Qu, C., Stringari, S., Lamporesi, G., and Ferrari, G. (2017). *Spin Superfluidity of a Bose Gas Mixture at Finite Temperature*. arXiv:1708.03923.

# HUMOR

Michele Bonaldi, Antonio Borrielli, Enrico Serra,<sup>†</sup> Giovanni Andrea Prodi

One of the open questions in physics is to reconcile the two most successful theories of physics, Einstein's general relativity and quantum physics. Currently, there are many theories that aspire to achieve this unification, but none of them is convincing and it is not clear how they can be verified experimentally. A common feature of these theories is that the space-time changes nature, become "granular" at a very small length, called "Planck scale" ( $L_P = \sqrt{\hbar G/c^3} = 10^{-35}$  m). The HUMOR (Heisenberg Uncertainty Measured with Optomechanical Resonators) experiment uses a new method for probing the space-time: the microscopic vibrations of oscillators of different sizes and masses, from a few nanogram up to a few milligrams, are measured with great accuracy, using lasers and/or electromagnetic sensors. The presence of a granularity of space-time at the Planck scale should be reflected in a nonlinear behavior of the oscillators, up to the dimensional scale currently measurable in the laboratory. In fact, in the framework of quantum mechanics, the measurement accuracy is at the heart of the Heisenberg relations, that, however, do not imply an absolute minimum uncertainty in the position. An arbitrarily precise measurement of the position of a particle is indeed possible at the cost of our knowledge about its momentum. This consideration motivated the introduction of generalized uncertainty principles (GUPs), such as

$$\Delta q \Delta p \geq \frac{\hbar}{2} \left( 1 + \beta_0 \left( \frac{L_P \Delta p}{\hbar} \right)^2 \right), \quad (3)$$

<sup>†</sup>Contact Author: [enrico.serra@tifpa.infn.it](mailto:enrico.serra@tifpa.infn.it)

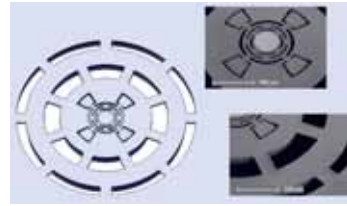


Figure 1: CAD drawings and SEM details of an optomechanical oscillators. The mirror is deposited over the central disk.

that implies indeed a nonzero minimal uncertainty  $\Delta q_{min} = \sqrt{\beta_0} L_P$ . The dimensionless parameter  $\beta_0$  is assumed to be around unity, in which case the corrections are negligible unless lengths are close to the Planck length. Any experimental upper limit for  $\beta_0 > 1$  would constrain new physics below the length scale  $\sqrt{\beta_0} L_P$ . This GUP implies two relevant effects with respect to a harmonic oscillator: the appearance of the third harmonic and a dependence of the oscillation frequency on the amplitude. Therefore, to set a limit on the value of  $\beta_0$ , we can measure the frequency of highly isolated oscillators at different oscillation amplitudes.

The micro-mechanical oscillators were built with micro-lithography on silicon wafers. In Fig. 1 we show for instance a device with a typical mass of  $100 \mu\text{g}$ , with a shape designed to best isolate it from the external environment. The oscillators are then cooled down to a few degrees above absolute zero, to limit heat induced vibrations. The movement is measured with laser beams and low noise electrostatic sensors, with sensitivity to the displacement comparable to the size of

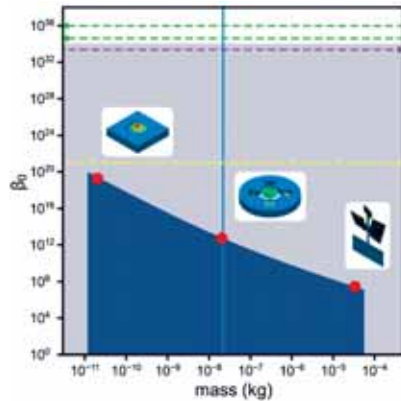


Figure 2: Red dots: upper limits to the parameter  $\beta_0$ . Gray shows the area below the electroweak scale, dark blue the area that remains unexplored. Dashed lines reports some previously estimated upper limits, obtained in mass ranges outside this graph (as indicated by the arrows).<sup>1</sup> The vertical line corresponds to the Planck mass (22  $\mu\text{g}$ ).

the atomic nucleus. The setup can measure changes in the oscillation frequency of some part in a billion during the free decay of the oscillation after a resonant drive. In Fig. 2 we report the results obtained with oscillators of different dimensions and shapes (as shown in the insets near the experimental points).<sup>1</sup> The resonators show their quantum behaviours in a Quantum Non Demolition (QND) measurement scheme: exploiting the light field intensity as observable in the QND optical scheme we have demonstrated a reduced uncertainty on intensity fluctuations actually achieving a sub-shot noise level (Pontin et al. 2017).

These results improve the previous upper limits to quantum gravity effects by many or-

ders of magnitude. The next challenge is to further cool an oscillator using laser light. At ultracryogenic temperature the behavior of the oscillator should be markedly quantum-like and it will thus be possible to highlight in the most direct manner any anomalies due to effects of quantum gravity. For this experiment we have designed and produced a membrane resonator, equipped with a specific on-chip loss shield for a circular membrane (Fig. 3), that achieve a mechanical quality factor of  $10^7$ . Nanomembranes were successfully tested in advanced optical schemes (M. Rossi et al. 2017) and (Kralj et al. 2017) for improving cooling efficiency. By the membrane's surface functionalization with high-reflectivity metasurface (Fig. 3) we are able to improve the cooling efficiency of the resonator.

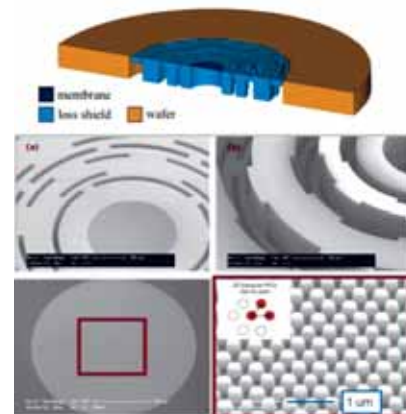


Figure 3: (Top): SEM image of the membrane resonator equipped a “loss shield” structure. (Bottom): large area metasurface reflector and detailed view of the hexagonal sub-micron pattern made of Si pillars.

## Selected Papers

Kralj, N., Rossi, M., Zippilli, S., Natali, R., Borrielli, A., Pandraud, G., Serra, E., Di Giuseppe, G., and Vitali, D. (2017). *Enhancement of three-mode optomechanical interaction by feedback-controlled light*. *Quantum Science and Technology* 2(3).

Pontin, A., Bonaldi, M., Borrielli, A., Marconi, L., Marino, F., Pandraud, G., Prodi, G., Sarro, P., Serra, E., and Marin, F. (2017). “Quantum nondemolition measurement of light intensity fluctuations in an optomechanical experiment”. *2017 European Conference on Lasers and Electro-Optics and European Quantum Electronics Conference*. Vol. F81-EQEC 2017. Optical Society of America, IEEE.

Rossi, M., Kralj, N., Zippilli, S., Natali, R., Borrielli, A., Pandraud, G., Serra, E., Di Giuseppe, G., and Vitali, D. (2017). *Enhancing Sideband Cooling by Feedback-Controlled Light*. *Physical Review Letters* 119(12).

<sup>1</sup>Bawaj, M. et al. (2015), *Nature Comm.* 6, p. 7503.

# LIMADOU

William Jerome Burger,<sup>†</sup> Laurent Basara, Francesco Dimiccoli, Francesco Follega, Roberto Iuppa, Ignazio Lazzizzera, Christian Manea, Matteo Puel, Ester Ricci

Limadou is the High Energy Particle Detector (HEPD) of the Chinese Seismo-Electromagnetic Satellite (CSES). The HEPD is designed to study the correlation between seismic activity and the trapped particle populations in the Van Allen radiation belts reported by instruments on different satellites.<sup>1</sup>

The trapped particle populations are characterized by three adiabatic invariants of their motion in the Earth's dipole magnetic field: the conservation of the magnetic moment during the gyration orbit around the field line, the invariance of the field integral between the mirror points, and the flux invariance of the longitudinal drift shell. The particles may be classified according to their drift shell defined by the height of the field line at the equator  $L$ , and the equatorial pitch angle  $\alpha_{eq}$ .

The HEPD is designed to measure with good resolution the pitch angle and energy of the electrons and protons in the radiation belts. The detector includes a silicon tracker, a segmented scintillator trigger plane, a scintillator-LYSO calorimeter, and 5 scintillator veto planes which surround the calorimeter volume.

The two tracker planes, composed 0.300 mm thick double-sided silicon microstrip sensors, are located at the top of the detector in order to minimize the influence of multiple Coulomb scattering on the pitch angle measurement. The segmented plane (T1) is composed of 6,  $3.0 \times 24.2 \times 0.5 \text{ cm}^3$ , plastic scintillators. The calorimeter consists of 16,

$17.7 \times 17.7 \times 1.0 \text{ cm}^3$  scintillator planes, and a  $3 \times 3$  array of  $4.8 \times 4.8 \times 4.0 \text{ cm}^3$  LYSO crystals.

The CSES will be placed in a sun-synchronous, circular orbit at 500 km with a  $98^\circ$  inclination. The HEPD is positioned on the satellite to point toward the zenith. The local pitch angle defined by the line-of-sight of the detector varies between  $90^\circ$  at the equator and  $\sim 0^\circ$  near the poles. The dimensions of the HEPD were chosen to maintain a wide angular acceptance throughout the orbit.

The HEPD was calibrated with protons in the research beam line at the Trento Proton Therapy Center in November 2016. The HEPD Monte Carlo simulation used for the data analysis is shown in Fig. 1.

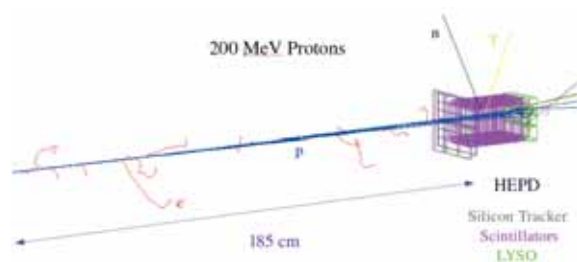


Figure 1: The HEPD Monte Carlo simulation of the proton test beam in Trento. Particle types of the generated beam (5 events) and secondaries are indicated: protons (blue), electrons (red), neutrons (black) and photons (yellow).

The mean energy loss at the output of the analog-digital-convertors (ADC) of the tracker electronics are compared to the expected mean energy loss (MeV)

<sup>†</sup>Contact Author: william.burger@tifpa.infn.it

<sup>1</sup>Aleksandrin, S. et al. (2003), Annales Geophysicae 21, pp. 597–602.

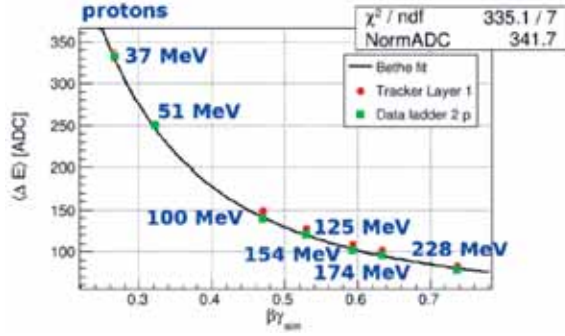


Figure 2: The measured mean energy loss in the silicon tracker (green) and the corresponding energy loss recorded in the Monte Carlo simulation (red), expressed in ADC counts using the conversion factor of the energy calibration. The results are compared to the behavior predicted by the Bethe equation. The kinetic energy of the proton beam is indicated.

of the Monte Carlo simulation to obtain the ADC-to-MeV conversion factor. Fig. 2 shows the experimental and Monte Carlo ADC values after calibration, as a function of the proton momentum ( $\beta\gamma$ ) at the upstream silicon tracker plane in the Monte Carlo. The momentum dependence agrees well with the expected behavior described by the Bethe equation.

The energy calibration of the calorimeter scintillators is obtained in a similar fashion. Fig. 3 shows the energy losses recorded in the Monte Carlo simulation in the scintillator planes and the LYSO crystals for 154 MeV protons.

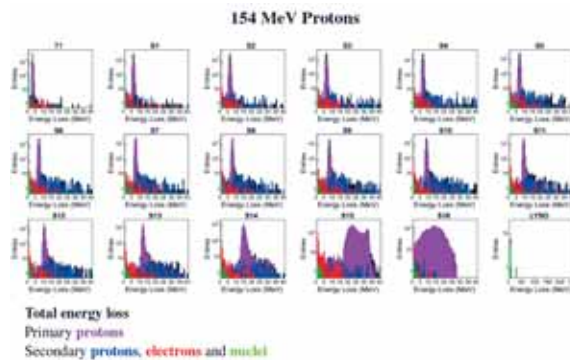


Figure 3: The energy losses recorded in the segmented trigger plane T1, the calorimeter scintillator planes (S1-S16) and the LYSO crystals in the Monte Carlo simulation for the 154 MeV proton beam. The color coded distributions are indicated.

The energy loss peaks of the primary beam protons are distinguished in the T1 scintillator and the first calorimeter scintillator planes S1-S13. The Monte Carlo peak positions are compared to the measured peak positions to obtain the energy conversion factors.

The energy dependence of the conversion factors are shown in Fig. 4. The calibration results for proton energy losses above  $\sim 12$  MeV, near the Bragg peak, are affected by the presence of the passive material of the segmented calorimeter planes, as illustrated in the last two scintillator planes S15 and S16 in Fig. 3. The scintillators may be calibrated up to  $\sim 15$  MeV.

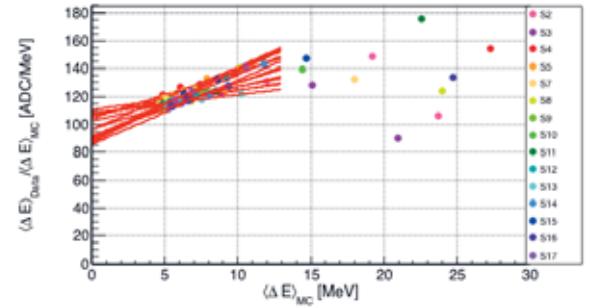


Figure 4: The energy calibration of the 16 calorimeter scintillators, labeled S2-S17. The quoted  $\Delta E$  refers to the peak values of the energy loss distributions.

The TIFPA Limadou group is responsible for the HEPD Geant4 Monte Carlo simulation, the offline software which converts the online data and the Monte Carlo generated data to a common format for the data analysis, and the online program which monitors the physics data. The group has provided the results of the silicon tracker performance obtained in the proton test beam in Trento and with atmospheric muons.

A second satellite CSES2 is programmed. The TIFPA Limadou group has begun to study possible modifications of the HEPD, notably the replacement of the present microstrip silicon detectors of the tracker with monolithic active pixel sensors. The change implies a redistribution of the contributions of the different sub-detectors to the overall performance.

## LISA Pathfinder and LISA

Daniele Bortoluzzi, Eleonora Castelli, Antonella Cavalleri, Rita Dolesi,<sup>†</sup> Valerio Ferroni, Ferran Gibert, Roberta Giusteri, Mauro Hueller, Martina Muratore, Paolo Pivato, Giuliana Rusano, Daniele Vetrugno, Stefano Vitale, William Joseph Weber

Our current image of the Universe is essentially based on the observation of electromagnetic waves in a broad frequency spectrum. Much of the Universe, however, does not emit electromagnetic radiation, while everything interacts gravitationally. Despite being the weakest of the fundamental interactions, it is gravity that dominates the Universe on a large scale and regulates its expansion since the Big-Bang. As predicted by Einstein's General Relativity, gravity has its messenger: gravitational waves produced by massive accelerating bodies, such as coalescing black holes binaries or violent phenomena like stellar core collapse. Gravitational waves propagate at the speed of light, essentially undisturbed, bringing often not otherwise accessible information about events across all cosmic ages, from Cosmic Dawn to the present. The observation of gravitational waves promises to open new extraordinary perspectives for investigation of crucial issues like the nature of gravity in weak and in strong field regime, the nature of black holes, the formation and evolution of stellar binary system, the formation and evolution of cosmic structures since the earliest stages of the Universe.

While the ground-based observatories of the LIGO-VIRGO collaboration open the era of "multi-messenger" astronomy with the detection of the coalescence of two neutron stars observed also in electromagnetic radiation, the project of LISA is rapidly progressing toward the implementation of the first space-based ob-

servatory devoted to the low-frequency sources that can not be detected from ground.

Einstein's theory describes gravity in terms of the curvature of space-time that is deformed by the passing of gravitational waves. These effect can be detected in space by measuring with great precision the relative acceleration of masses in free fall, i.e. reference masses subject to gravity field but well-isolated from other types of disturbing forces. In order to test the feasibility of reference masses geodesic motion at the level required for a high sensitivity space-based gravitational wave observatory, that correspond to an improvement of several orders of magnitude relative to of what had been attained before, ESA and its partners - including the Italian Space Agency, the National Institute of Nuclear Physics and the University of Trento - realized the precursor mission LISA Pathfinder, which ended successfully in 2017.

The Trento Group, led by the Principal Investigator prof. Stefano Vitale, has contributed in a leadership role in all phases of the mission, including hardware design and prototyping, laboratory torsion pendulum testing, scientific guidance of the industrial aerospace contractors, and finally to the design and operation of the flight measurement campaign. To achieve its goals, LISA Pathfinder measured the relative acceleration of two 2 kg test masses in near-perfect geodesic motion, 38 cm apart in a single spacecraft (see p. 5 for more details). Its outstanding performance (Armano

---

<sup>†</sup>Contact Author: [rita.dolesi@unitn.it](mailto:rita.dolesi@unitn.it)

et al. 2018), shown in Fig. 1, provides an experimental benchmark demonstrating the ability to realize the low-frequency science potential of the LISA mission. LISA Pathfinder team has therefore successfully completed its adventure in space, acknowledged also with the ESA Team Award for 2017 and the Space Technology Award 2017 from the American Astronautical Society.

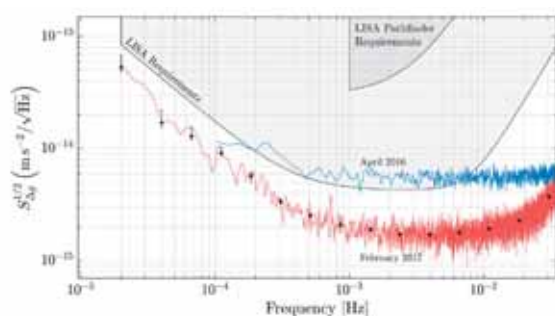


Figure 1: Spectrum of differential acceleration noise measured by LISA Pathfinder shown together with the LISA Pathfinder and the LISA requirement (Armano et al. 2018)

As internationally recognized leader in development and realization systems of free-falling geodesic reference test masses for space based gravitational wave detector, the Trento Group has played a critical role within the consortium of European institution that prepared the LISA's proposal.<sup>1</sup> LISA consists of three identical satellite in a triangular constellation, with arms of several million km, orbiting around the Sun, shown in Fig. 2 with its strain sensitivity. It should allow for the observation of thousands of gravitational wave sources with high signal-to-noise, and in many cases very

well characterized in terms of frequency, position in the sky, and luminosity distance. It targets massive sources emitting in the 0.1 mHz to 1 Hz band not accessible from ground due to the gravitationally noise Terrestrial environment, ranging from stellar mass binaries in our own Galaxy to the merger of two galactic-core black holes, from  $10^5$  to  $10^7$  solar masses, from the recent Universe back to the epoch of the first galaxies.

In June 2017 LISA has been selected by the ESA Scientific Program Committee as the L3 Mission of the ESA Cosmic Vision program. In November 2017 LISA passed the Mission Definition Review that validates its feasibility and its compatibility with the scientific objectives detailed in the proposal. After an in-depth study of the implementation of the mission lasting about two years, the adoption of the mission is scheduled for 2020-2022 for a launch in 2030-2034.

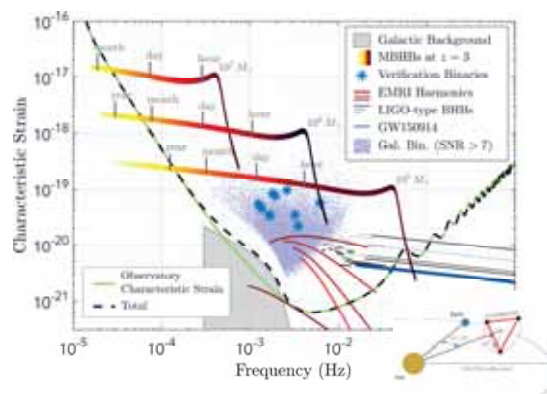


Figure 2: LISA's sensitivity curve plotted with the signal levels for several GW sources. In the inset a schematic of the LISA-concept.

## Selected Papers

Armano, M. et al., LISA Pathfinder Collaboration (2018). *Beyond the Required LISA Free-Fall Performance: New LISA Pathfinder Results down to 20  $\mu$ m/Hz*. Physical Review Letter **120**, p. 061101.

<sup>1</sup>[www.lisamission.org/proposal/LISA.pdf](http://www.lisamission.org/proposal/LISA.pdf)

# QUAX

Paolo Falferi,<sup>†</sup> Renato Mezzena

The signature of symmetry breaking at extremely high energies can be highlighted by the presence of long-range ultra-weak forces mediated by pseudo-Goldstone bosons. In particular, the pseudo-boson can be either the QCD axion or an axion-like-particle (ALP), which involves P and T violating forces with strength proportional to the product of the couplings at the pseudo-boson vertices. There are two options for coupling pseudo-scalar bosons with fundamental fermions. In a multipole expansion, these two fields are described by the "dipole" (pseudo-scalar coupling  $g_p$ ) and "monopole" (scalar coupling  $g_s$ ) moments, respectively. For instance, exchange of virtual axions - a possible solution of the strong CP problem - mediates a monopole-dipole force where  $g_s$  is proportional to the QCD vacuum angle  $\theta \simeq 10^{-10} \sim 10^{-14}$ . The  $g_p^e g_s^N$  interaction between an electron  $e$  and a nucleus  $N$  mediated by an axion or ALP can be represented by an effective magnetic field (Crescini et al. 2017b). Clearly, this field is not a genuine magnetic field, as the interaction potential is generated by pseudoscalar exchange rather than by photon exchange, and so it does not satisfy the Maxwell's equations. Once this effect is integrated over a macroscopic monopole source, the resulting total effective magnetic field can have a measurable amplitude or at least permit to improve current upper limits on  $g_p^e g_s^N$ .

The experiment (see Fig. 1) is performed by measuring the magnetization of a cubic sample of gadolinium oxyorthosilicate  $\text{Gd}_2\text{SiO}_5$  crystal (GSO) with 1cm edge length ("detector"), in-

duced by 4 disk shaped lead masses ("sources"). GSO is a paramagnetic material with a magnetic susceptibility  $\chi \simeq 0.7$  at cryogenic temperatures. The crystal is housed in the lower part of a liquid helium cryostat and cooled down to  $\simeq 4\text{K}$ . The distance between the center of mass of each "source" of effective magnetic field and the GSO crystal is modulated in time by mounting the masses on a rotating aluminum wheel as illustrated in Fig. 1. The aluminum wheel is 70 cm in diameter and rotates at a constant angular velocity ( $\sim 300\text{s}^{-1}$ ). The minimum distance between each "source" and detector is 3.7 cm. To detect the variation of magnetization we use a dc-SQUID operated at  $\simeq 4\text{K}$ . The superconducting input coil of the SQUID is connected to a superconducting pick-up coil, which is optimally wound (8 turns of a NbTi wire) around the GSO crystal. The two coils in series transfer the magnetic flux from the pick-up coil to the SQUID loop. As the effective magnetic field is not a true magnetic field, we can reduce the environmental magnetic disturbances around the GSO with magnetic ( $\mu$ -metal + superconducting) shields with an estimated overall rejection factor of  $10^{12}$ , which is sufficient to make environmental magnetic disturbances negligible. As a consequence, in our experimental setup, the dominant noise source is the additive flux noise of the SQUID, which therefore represents the sensitivity limit of the magnetometer.

We tested the hypothesis whether the wheel rotation may introduce an excess noise by comparing measurements obtained with rotating or

<sup>†</sup>Contact Author: falferi@fbk.eu

non-rotating wheel. We found no modification of the magnetic noise level in the frequency band of the measurement. In addition, multiple measurements were taken and no time dependence of the output has been found. To obtain an optimal estimate of the amplitude of the modulated effective magnetic field, we performed a phase sensitive detection of the SQUID signal with a digital lock-in with reference phase given by the rotating wheel.

The long-term stability of our apparatus allows us to integrate the lock-in output for  $1.5 \times 10^4$  s estimating the corresponding mean  $\langle B_{eff} \rangle = 1.8 \times 10^{-17}$  T and standard deviation  $\sigma_{B_{eff}} = 2.9 \times 10^{-17}$  T, expressed in equivalent magnetic field at the pickup coil. The mean value is compatible with zero within one standard deviation, and so we conclude that

we have observed no induced magnetization in the GSO crystal due to monopole-dipole interaction mediated by axions or ALPs. Using numerical integration over the volume of the lead "sources" and taking into account the geometry of the apparatus, we can convert our measurements of the effective magnetic field in an upper limit of  $g_p^e g_s^N / (\hbar c) \leq 4.3 \times 10^{-30}$  at 95% of confidence level in the range  $1\text{cm} < \lambda_a < 20\text{cm}$  where  $\lambda_a$  is the Compton wavelength of the axion (interaction range) (Crescini et al. 2017a). Currently, our limit is the best for spin-dependent forces mediated by axions or ALPs, as we obtained an enhancement of magnetic field sensitivity of one order of magnitude with respect to other experiments reported in the literature.

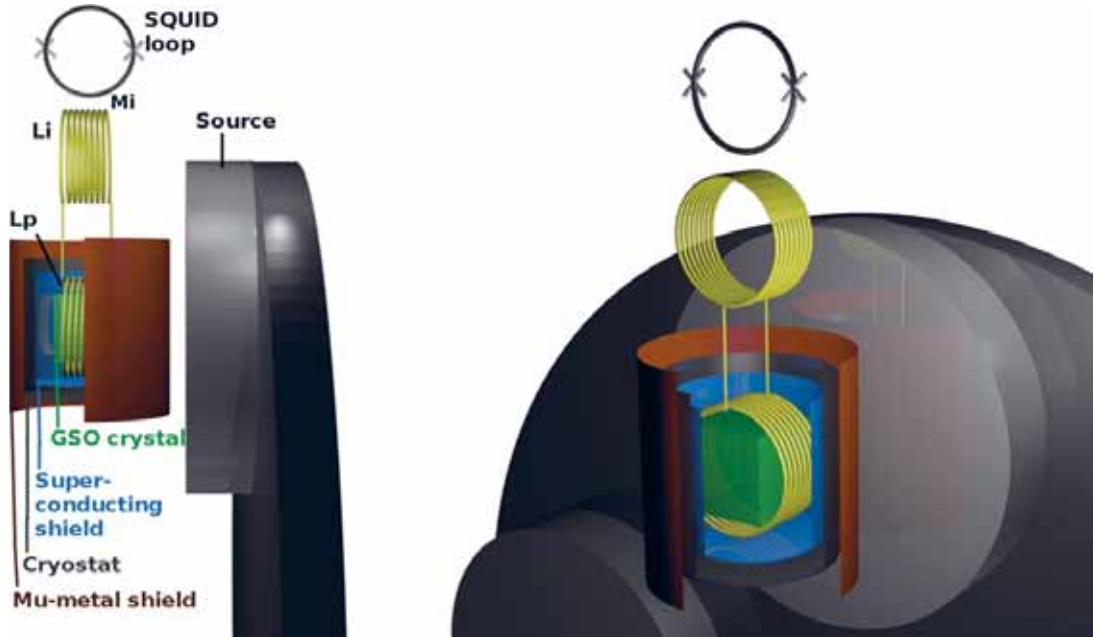


Figure 1: Schematic model of the apparatus.  $L_i = 1.8\mu\text{H}$  is the input coil of the SQUID,  $L_p \simeq 1.8\mu\text{H}$  is the pick-up coil wound on the GSO crystal. On the right side of the figure is represented a lead "source" mounted on the rotating wheel.

## Selected Papers

Crescini, N., Braggio, C., Carugno, G., Falferi, P., Ortolan, A., and Ruoso, G. (2017a). *Improved constraints on monopole-dipole interaction mediated by pseudo-scalar bosons*. Physics Letters B 773(Supplement C), pp. 677–680.

Crescini, N., Braggio, C., Carugno, G., Falferi, P., Ortolan, A., and Ruoso, G. (2017b). *The QUAX- $g_p g_s$  experiment to search for monopole-dipole Axion interaction*. Nucl. Instrum. Meth. A842, pp. 109–113.

# Virgo

## The gravitational wave observatory becomes worldwide and enables a new astronomy

Giovanni A. Prodi,<sup>†</sup> Riccardo Ciolfi, Bruno Giacomazzo, Antonio Perreca, Matteo Di Giovanni, Andrea Miani, Maria C. Tringali, Shubhanshu Tiwari, Michele Valentini

Year 2017 will be remembered in the history of astronomy as the dawn of multi-messenger observations, specifically of the observation of an astrophysical phenomena across the gravitational wave (GW) channel and light at all the surveyed wavelengths of the spectrum, from Gamma to radio. This historic breakthrough has been enabled by the GW observatory LIGO-Virgo: thanks to the fact that in August 2017 the Advanced Virgo detector joined the observation run started by the twin Advanced LIGO detectors, the localization performances of the GW sources achieved unprecedented accuracy in both angular position and distance. In fact, a network of three distant detectors enables to reconstruct the wavefront direction by a triangulation analysis which exploits both amplitude and phase coherence. Moreover, since Virgo detector is not aligned to the twin LIGO detectors, it catches a different component of the polarization of the GW; this enables a better coverage of the sky, but most importantly it enables the reconstruction of the polarization state and distance in the case of standard gravitational wave sirens.

The first published detection of a GW registered in Virgo data has been a Binary Black Hole (BBH) coalescence, passing the Earth on August 14, 2017 and named GW170814. Fig. 1

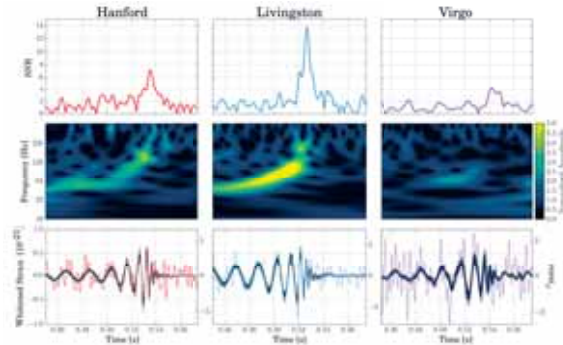


Figure 1: The first published high confidence GW detection involving the Advanced Virgo detector, BBH coalescence GW170814. Top row: Signal-to-noise ratio as a function of time in the three detectors. Middle row: Time-frequency representation of the GW strain amplitude. Note the characteristic "chirp" pattern of increasing frequency with time. Bottom row: GW strain time series with the best waveforms selected by the matched filtering (black solid curves) and unmodeled search methods (grey bands) superimposed.

summarizes the measured traces in the three detectors; even if the amplitude sensitivity of Virgo was about 1/4 of the best LIGO detector (Livingston), it made a huge difference in the reconstructed localization of the source, by decreasing the volume uncertainty by more than a factor 30 with respect to the uncertainty achievable by LIGO only detectors, see Fig. 2. This results adds to the other BBH mergers detected and published by LIGO-Virgo in 2017, namely GW170104 and GW170608. The full

<sup>†</sup>Contact Author: giovanniandrea.prodi@unitn.it

analysis of the population of BBH mergers detected in 2017 is still ongoing, both to extend the fundamental physics tests performed in previous analysis and to unveil the astrophysical properties of stellar mass Black Holes.

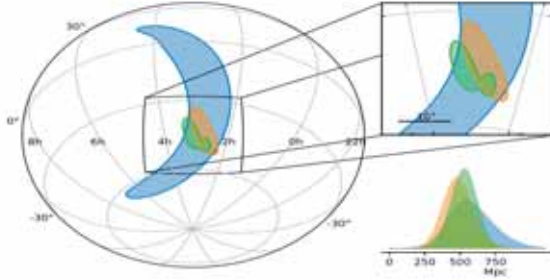


Figure 2: Localization of BBH merger GW170814. Left: 90% credible angular regions in the sky (blue area: rapid localization based on data from the two LIGO detectors only; orange area: adding Virgo; green area: deeper off-line analysis using all three detectors). Bottom right: probability distributions for the luminosity distance of the source.

The most serendipitous discovery has been the Binary Neutron Star (BNS) coalescence GW170817, which is the first and only direct observation of this kind. The morphology of the GW signal brings the fingerprints of the tidal deformability and more generally of the equation of state of Neutron Stars, thus opening a new window to study matter at higher density than in atomic nuclei. An even more impactful result has been the association of the very weak Gamma Ray Burst GRBA 170817 with GW170817, demonstrating that short Gamma Ray Bursts are indeed powered by BNS mergers and enabling the first high precision test of propagation speed of GWs, which indeed travel at light speed within  $\sim 1$  part in  $10^{15}$ . Also in this case Virgo data has been crucial for providing the localization of the source, which

led to a volume including only about 50 possible host galaxies, see Fig. 3. This enabled the most important counterpart search of the history of astronomy so far, pursued by about 70 ground- and space-based electromagnetic and neutrino observatories. The counterpart was identified, a transient object interpreted as a kilonova, a region where the matter ejected from the merger is experiencing nucleosynthesis of the heavier elements.

The Virgo group at TIFPA in 2017 contributed to the searches for GW transients in LIGO-Virgo surveys, to the investigation of the gravitational wave emissions from BNS coalescences and remnants, and to studies of the noise and data quality of the Advanced Virgo detector.

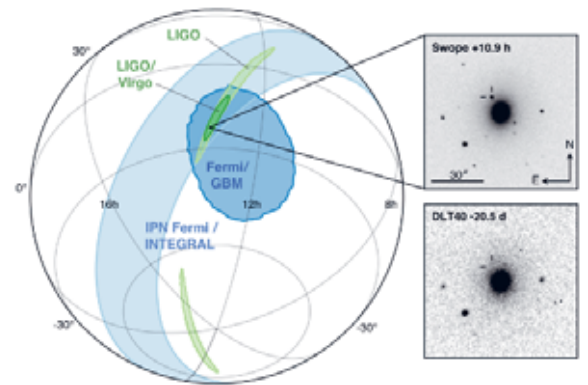
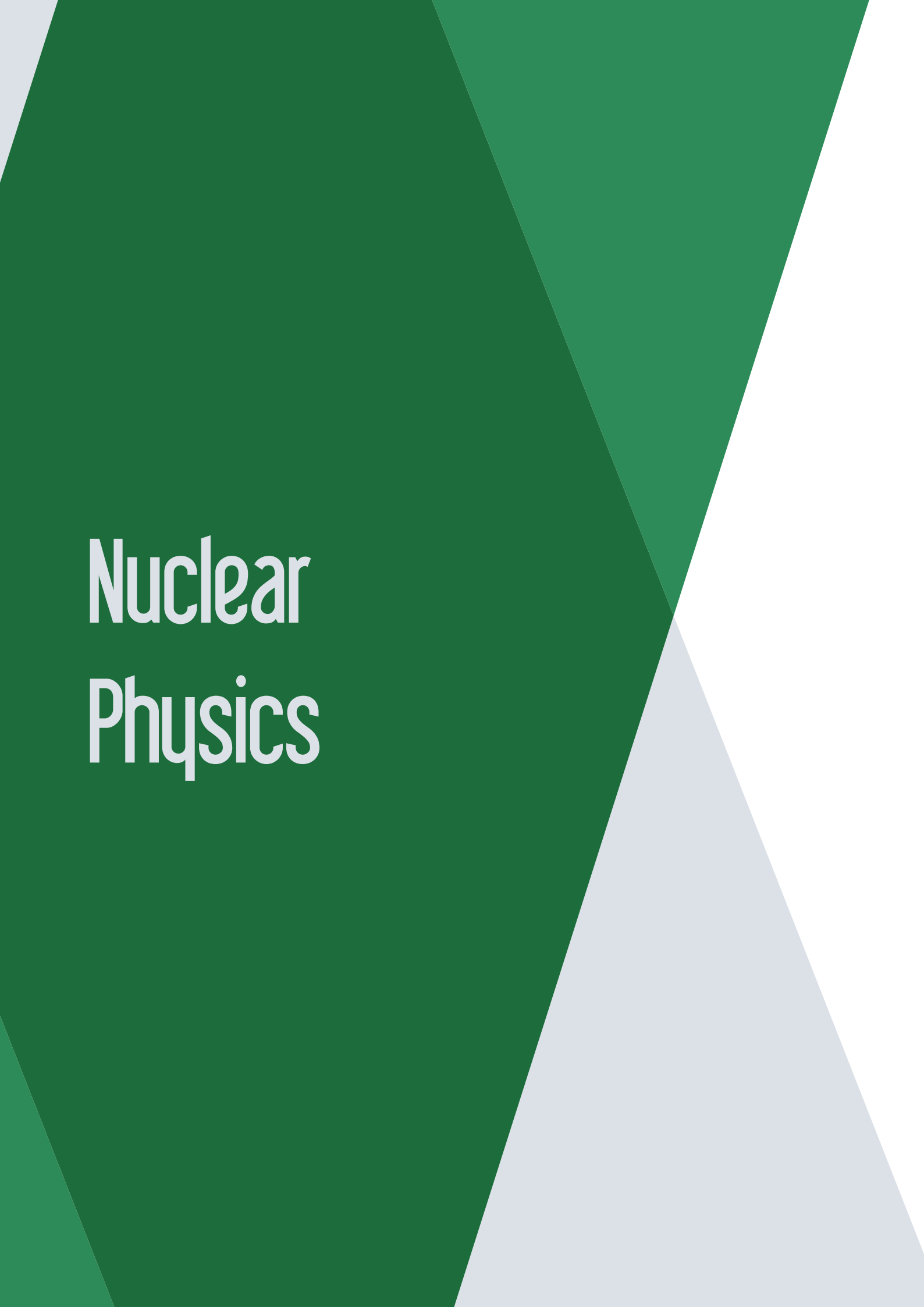


Figure 3: Localization of GW170817 (by LIGO-Virgo), of GRBA 170817 (by the Fermi and INTEGRAL satellites) and optical (the Swope discovery image) signals. The colored areas show the sky localization regions estimated by the gamma-ray observatories (in blue) and by the gravitational-wave detectors (in green). The insert shows the location of the known galaxy NGC4993: on the top image, recorded almost 11 hours after the gravitational-wave and gamma-ray signals had been detected, a new source (marked by a reticle) is visible: it was not there on the bottom picture, taken about three weeks before the event.





# Nuclear Physics

## Roberto Sennen Brusa

robertosennen.brusa@unitn.it

Coordinator,  
TIFPA Nuclear Physics Activities



Two INFN-TIFPA experimental research groups have activities belonging to the Research Line 3, Nuclear Physics of INFN. One group works in antimatter physics carrying out fundamental and applied studies, the second one deals with nuclear fragmentation experiments in an energy range that is of interest for particle therapy. Research Line 3 fund AEGIS (Antimatter Experiment: gravity, Interferometry, Spectroscopy) and FOOT (FragmentatiOn Of Target) experiments.

AEGIS experiment aims to cast some light on one of the great mystery in physics: why only matter survived after the Big Bang? At the origin of the Universe we expect that, by symmetry, the same amount of matter and antimatter would have been produced. But for each particle, composing ordinary matter, exists an anti-particle that has the same mass but opposite charge and if a particle and its antiparticle collide, they annihilate giving rise to energy. To look if the existence of our world is due to asymmetry between matter and antimatter, AEGIS main goal is to produce a beam of anti-hydrogen (the antimatter of a hydrogen atom, formed by a positron and an antiproton) and to study if antimatter falls with the same acceleration as the ordinary matter in the Earth gravitational field. The experiment is set up at the antiproton facility at CERN. Differently from many other experiments at CERN, AEGIS needs to store very low energy antiprotons and to produce a very slow positronium (atom formed by a positron and an electron) beam for obtaining antihydrogen by charge exchange, as it is detailed in the following information box. The main tasks of the Trento-TIFPA group is the manipulation of positrons (production, cooling, storing, dumping) and the production of the positronium beam from specific targets at CERN. R&D and applied works are carried out by the group, with the slow positron beam set up at the Trento Department of Physics.

The main goal of the FOOT experiment is the elucidation of the target fragmentation in a proton therapy scenario. One of the main advantages of proton therapy stays in the improved dose deposition compared to photon radiation therapy. By exploiting the physics of the Bragg peak, protons (as well as heavier particles) allow precisely targeting the tumor while sparing surrounding healthy tissues, especially in the entrance channel. However, inelastic nuclear interactions with the patient result into the production of target fragments, which might be heavier than protons. Due to the high charge and low residual energy, an enhanced biological effectiveness can be attributed to those fragments. An accurate description of the role of target fragments is currently missing. This is mainly due to the lack of reliable cross data for production of heavy recoils. The extremely low residual range hinders the detection of target fragment. FOOT aims at filling this gap, by adopting an inverse-kinematic approach, thus studying the fragmentation of different ion beams (e.g. C, O, Ca) onto hydrogen enriched targets, such as  $C_2H_4$ . The data provided by the FOOT experiment will thus be also useful to improve the characterization of projectile fragmentation for C and O beams, which also have increasing therapeutic applications. The Trento-TIFPA group contributes to the experiment by studying and optimizing the performances of the Beam Monitor detector (i.e. a drift chamber) that is in charge of measuring the direction and impinging point of the ion beam on the target. At the same time, the group collaborates to test beam activities involving different part of the detector and taking place at the Trento Proton Therapy Center.

# AEgIS

Francesco Guatieri,<sup>†</sup> Sebastiano Mariazzi, Luca Penasa, Roberto S. Brusa

AEgIS (Antimatter Experiment: Gravity, Interferometry, Spectroscopy) is one among the few experiments set up at the antiproton decelerator (AD) at CERN. The Big Bang is expected to have produced an equal amount of matter and antimatter but only matter survived and gave rise to the existing world. The experiments at the AD are searching for asymmetries between matter and antimatter. One of these asymmetries could be a different action of gravity on antimatter.

The AEgIS experiment (Brusa et al. 2017) aims to test the weak equivalence principle (WEP) by studying the free fall of antihydrogen ( $\bar{H}$ ) in the Earth's gravitational field. The measurement of the gravitational acceleration  $\bar{g}$  on  $\bar{H}$  will be performed by measuring the time of flight and the vertical displacement of each  $\bar{H}$  after its passage through a moiré deflectometer. The AEgIS method and set up to produce a pulsed  $\bar{H}$  beam is illustrated in Fig.1. Antiprotons ( $\bar{p}$ ) of 5.3 MeV delivered by AD are slowed down to a few keV passing through a degrader and then caught in a Penning-Malmberg traps in the 5 T magnet where they are cooled by sympathetic cooling with electrons. Cooled  $\bar{p}$  are transferred into a second Penning-Malmberg trap in the 1 T magnet where  $\bar{H}^*$  is to be formed. Positrons ( $e^+$ ) are cooled in a two-stage Surko buffer trap and stored in a Penning-Malmberg accumulator delivering  $e^+$  bunches that are transferred in the 5 T and then in the 1 T magnet where they are injected in a  $e^+$ /Ps (positronium) porous silica converter. The fraction of formed Ps that is cooled by collisions in silica and emitted into vacuum is laser excited

in long living Rydberg states. Rydberg Ps fly into the antiproton trap, where  $\bar{H}$  can be formed in an excited state by the charge exchange reaction:  $\text{Ps}^* + \bar{p} \rightarrow \bar{H}^* + e^-$ . Excited  $\bar{H}$  is Stark accelerated and decays to ground state along its path towards the moiré deflectometer.

A secondary chamber to perform R&D experiments on Ps is connected to the  $e^+$  accumulator.<sup>1</sup>

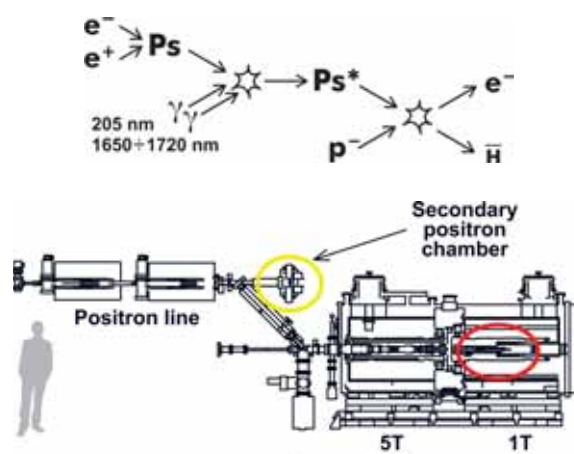


Figure 1: The AEgIS method and the AEgIS experimental set-up for the production of a pulsed cold  $\bar{H}$  beam. The chamber for Ps experiments and the  $\bar{H}$  production region are indicated by yellow and red circles, respectively.

**Status of the experiment** The AEgIS activity during 2017 focused on the manipulation of  $\bar{p}$  and Ps in the 1 T  $\bar{H}$  production region. A sketch of the production region is reported in Fig. 2.

A procedure for trapping  $\bar{p}$  in the Penning-Malmberg trap in the 5 T region and the following adiabatic transport and re-trapping in the

<sup>†</sup>Contact Author: fguatier@cern.ch

<sup>1</sup>Aghion, S. et al. (2015), Nucl. Instrum. Methods Phys. Res. B **362**, p. 86.

1 T  $\bar{H}$  production trap was devised during the 2017 AD run. Around  $3 \cdot 10^5$   $\bar{p}$  were stored in the production trap ( $\bar{p}$  trap in Fig. 2) and cooled with electrons at few hundreds of kelvin.

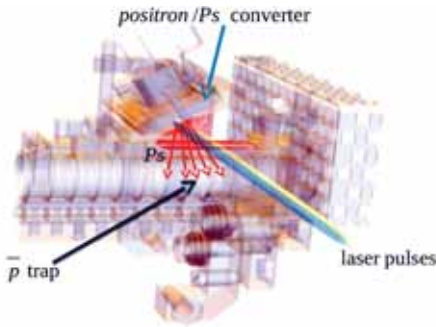


Figure 2: Sketch of the AEGIS  $\bar{H}$  production region in the 1 T.

The Ps excitation to Rydberg states via a two-step  $1^3S \rightarrow 3^3P$ ,  $3^3P \rightarrow Rydberg$  has been previously demonstrated in the secondary chamber for Ps experiments<sup>2</sup> (see also Caravita et al. 2017). In 2017, the experiment has been successfully repeated in the cryogenic environment of the 1 T  $\bar{H}$  production region. Pulses of  $e^+$  with a duration of  $\approx 20$  ns were injected in a nanochannelled Si target with oriented oxidized nanochannels with high  $e^+$ /Ps conversion efficiency. Ps emitted into vacuum was then excited to  $n = 3$  with an UV laser pulse (205 nm) and then to  $n = 17$  by shooting an IR laser (wavelength  $\approx 1695$  nm). Ps excitation was measured by the SSPALS (Single Shot Positron Annihilation Lifetime Spectroscopy). In Fig. 3, SSPALS spectra (divided by  $e^{-t/142\text{ns}}$ ) measured with laser on and off are shown. The normalized difference below the areas, reported in the inset, is a fingerprint of Ps excitation to long living Rydberg states.

Alongside the main activity of particle manipulation in the 1 T  $\bar{H}$  production region, the characterization of different kinds of  $e^+$ /Ps

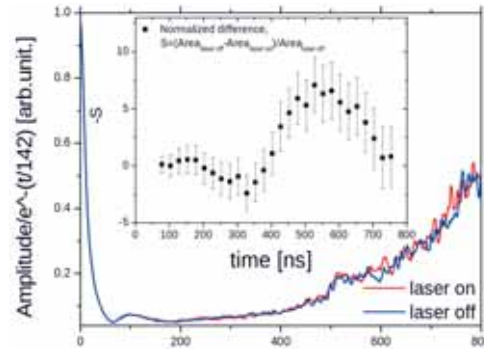


Figure 3: SSPALS spectra divided by  $e^{-t/142\text{ns}}$  measured in the  $\bar{H}$  production region. The normalized difference below the curves is reported in the inset.

converters have been performed.  $e^+$ /Ps converters in transmission geometry (i.e. with Ps emitted from the opposite side of the target with respect to the positron implantation) hold great promise in the maximization of the overlap between  $\text{Ps}^*$  and  $\bar{p}$ . Preliminary tests of this novel kind of converters have been carried out in the Ps experimental chamber (Aghion et al. 2017). In Fig. 4, SSPALS spectra measured at different positron implantation energy in a transmission  $e^+$ /Ps converter are reported.

Further studies of Ps cooling in targets with nanochannels at cryogenic temperature are going on at the Trento slow continuous positron beam.

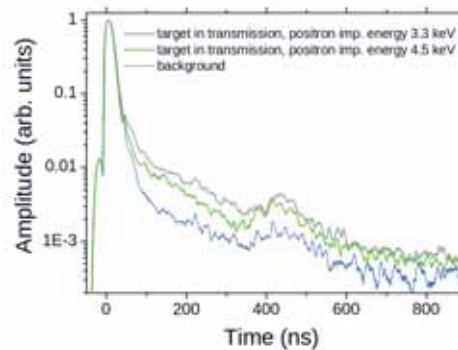


Figure 4: SSPALS spectra in a transmission  $e^+$ /Ps converter.

## Selected Papers

- Aghion, S. et al. (2017). *Characterization of a transmission positron/positronium converter for anti-hydrogen production*. Nucl. Instrum. Methods Phys. Res. B **407**, p. 55.
- Brusa, R. S. et al. (2017). *The AEGIS experiment at CERN: Measuring antihydrogen free-fall in earth's gravitational field to test WEP with antimatter*. J. of Phys. Conf **791**, p. 012014.
- Caravita, R. et al. (2017). *Advances in Ps Manipulations and Laser Studies in the AEGIS Experiment*. Acta Phys Pol B **48**, p. 1583.

<sup>2</sup>Aghion, S. et al. (2016), Phys. Rev. A **94**, p. 012507.

# FOOT

Francesco Tommasino,<sup>†</sup> Marco Durante, Sebastian Hild, Chiara La Tessa, Marta Rovituro, Enrico Verroi

The FOOT (FragmentatiOn Of Target) experiment aims at improving the accuracy of proton therapy cancer treatments, by studying the inelastic nuclear interactions taking place between the primary beam and the patient tissues. Target fragments that originate from such interactions can have high charge (i.e. high biological effectiveness) and low residual range. Consequently, a biological effect might be associated to target fragments, especially in terms on normal tissue damage in the entrance channel before reaching the tumour. Currently, these interactions are not accurately considered by treatment planning softwares, due to the lack of cross section data to describe target fragments production. The residual range of heavy fragments is limited to tens of micrometers. This hinders their detection since in most of the cases they cannot exit the target. For this reason, FOOT will adopt an inverse kinematic approach, studying the fragmentation of different ions beams (e.g. C, O, Ca) onto hydrogen enriched target, such as C<sub>2</sub>H<sub>4</sub>, as already adopted in (Dudouet et al. 2013)<sup>1</sup> and (Webber et al. 1990).<sup>2</sup> Secondary fragments will have boosted energy and longer range, making the detection easier. The choice of the inverse kinematics forces the measurement of the beam momentum in each direction: for this reason a Beam Monitor (BM) detector has been adopted in the pre-target region, which will allow the determination of the Lorentz boost to be applied to

the produced fragments. The final goal of the FOOT experiment will be the measurement of the heavy fragment ( $Z > 2$ ) cross section with maximum uncertainty of 5% and the fragment energy spectrum with an energy resolution of the order of 1-2 MeV/u. The charge and isotopic identification (at the level of 3% and 5% respectively) are also important goals of this measurement. Beyond the analysis in terms of direct kinematics, FOOT will also contribute to extend and complete the measurements of projectile fragmentation cross sections induced by C and O beams. Such measurements are needed to improve the projectile fragmentation description of these beams in ion therapy and their specific Treatment Planning Systems.

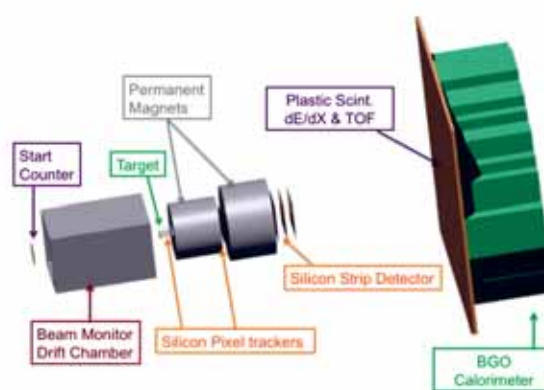


Figure 1: Schematic view of the FOOT electronic apparatus.

The activities of the Collaboration during 2017 have been mainly focused on the optimization of the experimental apparatus and

<sup>†</sup>Contact Author: francesco.tommasino@unitn.it

<sup>1</sup>Dudouet, J. et al. (2013), Phys Rev C 88, p. 064615.

<sup>2</sup>Webber, W. et al. (1990), Phys Rev C 41, p. 547.

on the analysis of the expected performances. The FOOT experimental setup must be easily movable and fit the space limitations set by the different experimental and treatment rooms where ion beams of therapeutic energies are available.

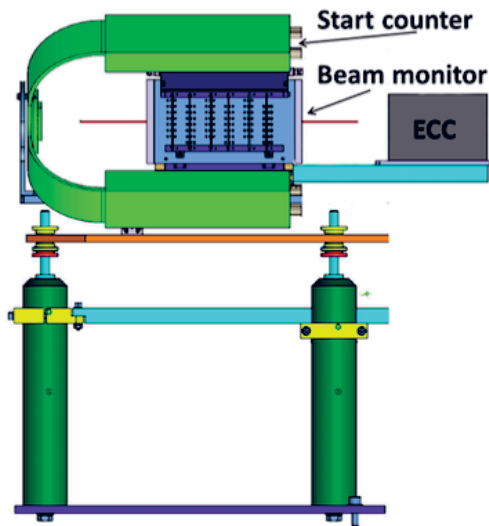


Figure 2: Emulsion spectrometer setup of the FOOT apparatus.

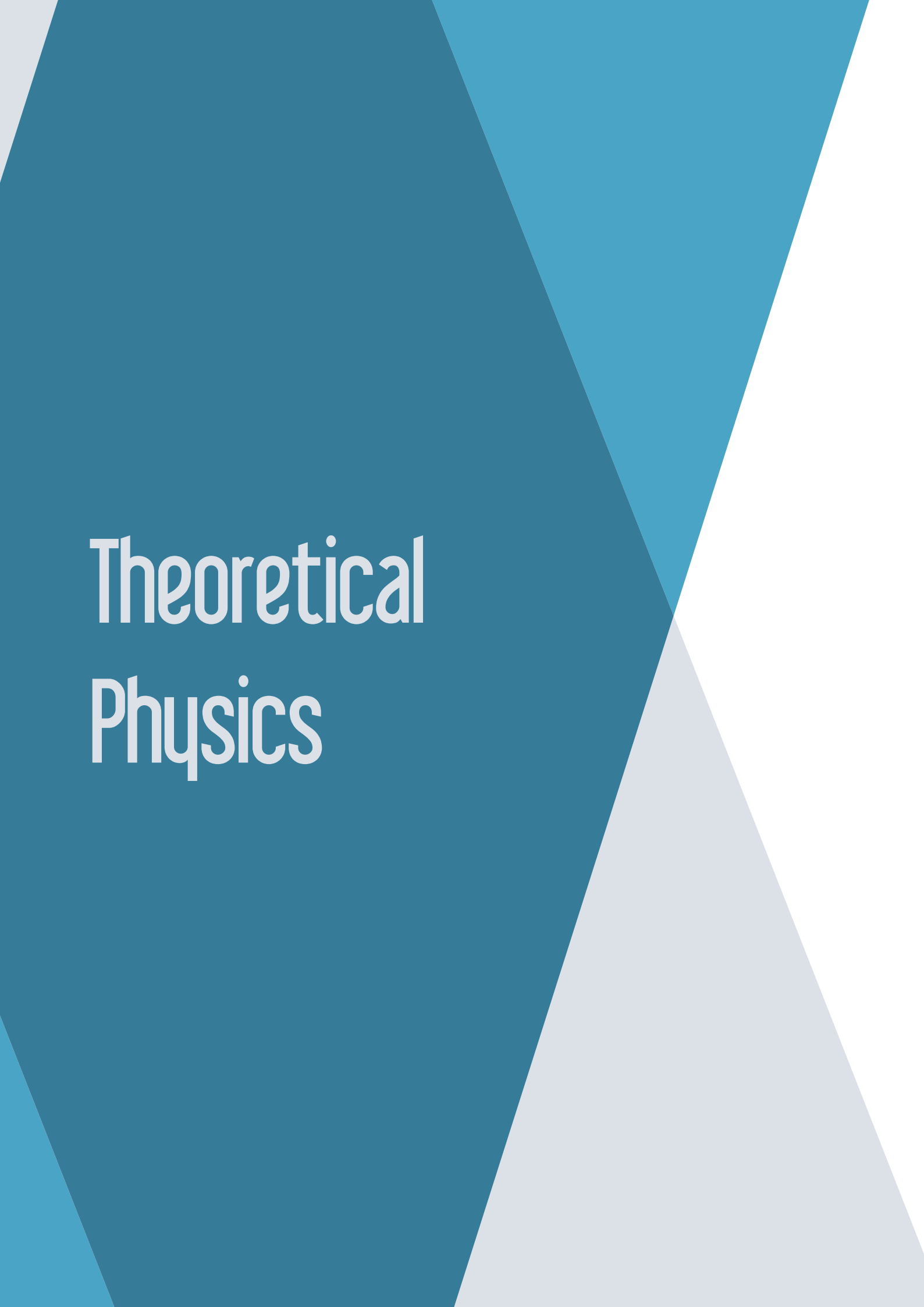
Taking into account a good balancing between the detector cost, its portability and the need of high performances, the FOOT experiment will consider two alternative setups:

- A setup based on electronic detectors and a magnetic spectrometer, aiming to the identification and measurement of fragments heavier than the  $4\text{He}$ , covering an angular acceptance of  $\pm 10^\circ$ , with respect to the beam axis (Fig. 1).
- A setup exploiting the emulsion chamber capabilities (Fig. 2). As already tested in

the FIRST experiment,<sup>3</sup> a specific emulsion chamber will be coupled with the pre-target devices of the FOOT setup to measure the production in target fragmentation of light charged fragments as protons, deuterons, tritons and Helium nuclei. The emulsion spectrometer supplies complementary measurements for fragments emitted at large angle with respect to the electronic detector, extending the angular acceptance up to  $\pm 70^\circ$ .

The TIFPA unit of the FOOT experiment is currently dedicated to the study of the performances of the BM detector. The BM is a drift chamber consisting of twelve layers of wires, with three drift cells per layer. Planes with wires oriented along the x and y axes are alterned in such a way to reconstruct the beam profile. The cell shape is rectangular (16 mm x 10 mm) with the long side orthogonal to the beam. In each view two consecutive layers are staggered by half a cell to solve left-right ambiguities in track reconstruction. The BM detector will be placed between the Start Counter and the target and will be used to measure the direction and impinging point of the ion beam on the target. Simulation and experimental work will be performed in the coming months, in order to find the optimal working conditions for the BM (e.g. gas mixtures, high voltage settings) according to the FOOT requirements. In parallel, TIFPA is supporting the testing of several sub-detectors of the apparatus, taking place at the Experimental Room of the Trento Proton Therapy center.

<sup>3</sup>Toppi, M. et al. (2016), Phys Rev C 93, p. 064601.

The background features abstract geometric shapes in various shades of teal and light blue, set against a white background. The shapes are angular and layered, creating a modern, minimalist aesthetic.

# Theoretical Physics

Francesco Pederiva

francesco.pederiva@unitn.it

Coordinator,  
TIFPA Theoretical Physics Activities



During the year 2017 the theory group at TIFPA has seen a substantial evolution in its composition. For the first time a staff INFN researcher (Alessandro Lovato) has joined the group after winning one of the positions that were assigned at the end of 2016 in a national competition. This is an important achievement and one of the concrete signs of how TIFPA has changed the range of opportunities for the development of the scientific activity.

The group related to the IS FLAG has also seen quite a change, since Sergio Zerbini has retired, and Massimiliano Rinaldi has joined the Department staff, ensuring the continuation of a lively scientific activity in this topic.

We want to remind that, due to the specific characterization of the Physics Department, the TIFPA theory group does not follow the standard composition found elsewhere in Italy. At present we have activated seven different groups referring to the national projects (“Iniziativa Specifiche”) approved and financed by the national scientific committee for theoretical physics.

The composition of the research lines in 2017 has seen very few changes.

We still have a strong group of people working on the theory of fundamental interactions. In particular there is a unit carrying on modern views and perspectives in gravitation and cosmology (FLAG), and one working on the numerical solution of General Relativity equations related to the investigation of gravitational waves emission (TEONGRAV).

Nuclear physics has always played an important role in Trento. The structure and dynamics of nuclei, and the connections of nuclear theory to stellar physics and the more fundamental quantum chromodynamics theory are investigated with modern few-body (FBS) and many-body (MANY-BODY) numerical techniques.

An interesting development occurred after the establishment of TIFPA was the creation of a research team within the Mathematics Department working on fundamental aspects of quantum theory and extensions of quantum field theory in curved spaces (BELL).

A strong identification mark of the TIFPA group is the presence of interdisciplinary activities, which are of great importance in the context of the center. In particular, there is a well established activity in theoretical biophysics, looking for innovative tools in the description of the kinetics of complex molecules (BIOPHYS). Very important has always been the fundamental research and the application to condensed matter problems which will be made more visible through the opening of a new project focussed on solid state physics (NEMESYS).

The TIFPA theory group has always been connected to the INFN experimental activity in Italy and abroad, and is open to the new developments and new challenges brought by the center. Presently it counts 42 researchers. About half of them are University of Trento, FBK, INFN and other institutions staff members, and rest are M.Sc. and Ph.D. students, and post-docs.

# BELL

Valter Moretti,<sup>†</sup> Romeo Brunetti, Riccardo Ghiloni, Sonia Mazzucchi, Alessandro Perotti, Davide Pastorello, Nicolò Cangini, Alberto Melati, Marco Oppio

BELL research group at TIFPA studies various foundational, axiomatic and mathematical topics of Quantum Theories, also in relation with quantum field theory and quantum gravity. Mathematical advanced technologies are exploited to solve difficult problems of theoretical physics or to construct physically significant, non-trivial, mathematical models, completely solvable which can be used as starting points for physical applications. During 2016-2017 we published several research papers on international research journals, a monograph and another monograph is in print. Just to have a (not exhaustive) look of our intensive production we focus attention on three relevant works about three corresponding topics of mathematical methods for physics.

## Foundational aspects of Quantum Theories

The first paper (Moretti and Oppio 2017), by Valter Moretti and Marco Oppio concerns a longstanding issue about the formulation of quantum theories in Hilbert spaces. As is known from a celebrated 1995 theorem by Solér and an earlier conjecture by von Neumann himself, quantum theories can be formulated into real, complex or quaternionic Hilbert spaces. However up to now no quantum systems with real or quaternionic formulations are known. What is the physical reason for the absence of these systems though permitted by the general mathematical theory? Without entering into the details of the aforementioned paper, that is only the former of a couple of

works on the subject, we established the remarkable result that the deep reason for the lack of real quantum theories is nothing but Poincaré symmetry. A quantum relativistically elementary (in Wigner sense) system pictured in a real Hilbert space always admits an equivalent standard description in a complex Hilbert space, whose complex structure is Poincaré invariant and fixed by relativistic symmetry. A second paper on the quaternionic variant has been submitted for publication by the same authors.

## Feynman Functional Methods for Quantum Theories

Another result achieved by Sonia Mazzucchi (Mazzucchi 2017) regards the so called functional integral technology applied to physics (Euclidean and Feynman path integral). This elegant and definitely powerful mathematical approach to the formulation of quantum theories was invented by R. Feynmann in 1948 and since then it has been fruitfully applied to Quantum Mechanics and Quantum Field Theory. Essentially, the crucial idea is to replace the classical notion of a single, unique temporal evolution for a system with a sum, or functional integral, over an infinity of possible evolutions to compute a quantum amplitude. In spite of the powerfulness of this approach, its rigorous mathematical formulation has always been very challenging due to the well-known deep differences between the path-integral machinery, exploited in quantum physics, and the standard probability measure theory on infinite dimen-

<sup>†</sup>Contact Author: [valter.moretti@unitn.it](mailto:valter.moretti@unitn.it)

sional spaces. The same procedure can be exploited to construct solutions of other physically relevant equations like the heat equation. Formally, this can be achieved by an analytic continuation from real to imaginary values of the time variable within a mathematical machinery called Wick rotation. However this procedure is mathematically non-trivial and need a deep theoretical technology. In (Mazzucchi 2017) the definition of infinite dimensional Fresnel integrals is generalized to the case of polynomial phase functions of any degree and applied to the construction of a functional integral representation for solutions of a general class of higher-order differential equations with various physical applications, a generalized heat equation in particular.

**Quantum Control** Last but not least, Davide Pastorello's paper (Pastorello 2017a) concerns quantum control of physical systems described

in finite dimensional Hilbert spaces. These system have a big impact in recent technological applications. An issue of utmost relevance concerns controllability of these systems: they must be prepared and driven into specific states to start and finish their quantum job. As is known, quantum theory in a finite-dimensional Hilbert space can be geometrically formulated as a proper Hamiltonian theory. From this point of view a quantum system can be described in a classical-like framework where quantum dynamics is represented by a Hamiltonian flow in the phase space given by projective Hilbert space. This paper by D. Pastorello is devoted to investigate how the notion of accessibility algebra from classical control theory can be applied within geometric Hamiltonian formulation of Quantum Mechanics to study controllability of a quantum system. A new characterization of quantum controllability in terms of Killing vector fields w.r.t. Fubini-Study metric on projective space is also presented.

## Selected Papers

- Mazzucchi, S. (2017). *Infinite Dimensional Oscillatory Integrals with Polynomial Phase and Applications to Higher-Order Heat-Type Equations*. Potential Analysis.
- Moretti, V. and Oppio, M. (2017). *Quantum theory in real Hilbert space: How the complex Hilbert space structure emerges from Poincaré symmetry*. Reviews in Mathematical Physics **29**(06), p. 1750021.
- Pastorello, D. (2017a). *A geometric approach to quantum control in projective Hilbert spaces*. Reports in Mathematical Physics **79**, pp. 53–56.

# BIOPHYS

Gianfranco Abruscio, Giovanni Garberoglio, Pietro Faccioli,<sup>†</sup> Simone Orioli, Gianluca Lattanzi, Michele Turelli

The 2017 research activity within the BIOPHYS INFN scientific initiative at TIFPA has proceeded along the following directions:

**Investigation of rare biomolecular transitions** We continued our development of high-performance theoretical and computational techniques investigate the dynamics and kinetics of slow and complex biomolecular transitions, using theoretical physics methods. In particular, we developed and validated a new approach called “Self-Consistent Path Sampling” which provides a major improvement with respect to our previous approaches, since its results do not depend on a pre-determined choice of reaction coordinate. Instead the reaction coordinate is evaluated self-consistently and represents an output of the calculation. Furthermore we developed a technique to efficiently and accurately evaluate the potential of mean force along the reaction coordinate.

**Electronic excitations in biologic and organic matter** In the past several years the Trento BIOPHYS team developed the theory called Molecular Quantum Field Theory, which can be used to compute the density matrix for electronic excitations propagating in macromolecules embedded in a solvent. In 2017 we showed how this theory can be used to compute the absorption spectrum in linear spectroscopy experiments. In a different project, we have successfully applied computational methods (in particular DFT calculations) to the investigation

of molecular materials employed in organic solar cells. Finally, we completed a project in collaboration with the team lead by Prof. Mennucci at Pisa University, which aims at directly computing time-resolved circular dichroism spectra of protein in the near UV regime. This method can be used to test microscopic calculation of protein folding pathways, since the near UV spectrum carries information about the formation of tertiary structures between aromatic residues.

**Nanotechnology and Material Science** We continued the on-going collaboration for the ab-initio calculation of virial coefficients of molecular gases. We validated state-of-the-art potentials for the interaction of molecular hydrogen with carbon monoxide, a mixture of interest in astrophysical research. We also proposed a novel structure of carbon-based nanofoams, inspired by carbon-fullerene nanotruss networks. The resulting frameworks show very similar properties under traction, but under compressive regimes peculiar instabilities are found, leading to negative values of the Poisson ratios. We reported on the comparison between calculated and measured electron energy-loss spectra in diamond and graphite. We compared various models including a fully ab-initio calculation using time-dependent density functional theory. The results show the sizeable effect that some approximation can have on the final result. Finally, we contributed to an experimental/numerical investigation on

<sup>†</sup>Contact Author: [pietro.faccioli@unitn.it](mailto:pietro.faccioli@unitn.it)

the effect of graphene and carbon-nanotube doping on the tensile properties of spider silk. Experiments seem to indicate an increment of the mechanical properties of doped silk with respect to the pristine one. However, the actual reason for this increase is not fully understood from the theoretical point of view.

**Computational Biophysics** The research activity in 2017 has mainly dealt with the application of molecular dynamics simulations to the investigation of systems of biological and/or technological interest. In particular, we have continued our studies on the membrane protein aquaporin-4 (AQP4) that is responsible for the onset of the autoimmune disease Neuromyelitis optica: our computational studies identified the molecular rationale for the binding affinity of immunoglobulin-G with different AQP4 mutants. Our computational protocol on membrane proteins has been also applied to another important protein, the human monoamine oxidase (hMAO), that is implied in depression, anxiety and neurodegenerative diseases. Our

study was the first attempt to explain at molecular level the selectivity of the two available isoforms of hMAO and thus contribute to the design of new and highly selective hMAO inhibitors. We have also started a novel study on the motor protein prestin, that is involved in our hearing system (see Fig. 1). Finally, we have successfully applied computational methods (in particular DFT calculations) to the investigation of molecular materials employed in organic solar cells.

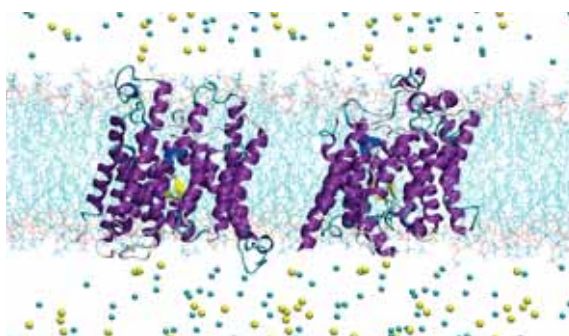


Figure 1: Snapshot taken from the molecular dynamics simulation of the mammalian membrane protein prestin in two different conformations.

# FBS

Giuseppina Orlandini,<sup>†</sup> Winfried Leidemann, Fabrizio Ferrari Ruffino, Paolo Andreatta

The main goal of this research activity is the theoretical investigation of the **structure and dynamics of nuclear few-body systems**. This investigation includes structure properties of light nuclei and hypernuclei, as well as reactions involving continuum states. The motivation for this research is twofold. First to connect the properties of such nuclear/hypernuclear systems to the microscopic interactions among the constituents. Therefore, part of the activity is devoted to provide a better understanding of the nuclear interaction, in particular its three-body component, by comparing the results of *ab initio* approaches and experimental observables. Second, to develop new methods adapted to solve the quantum mechanical many-body problem for increasing mass num-

ber.

What characterizes the Trento activity (and which makes it a recognized leader group in the field of Few-Body Physics) is the development and application of an original integral transform approach, which is known as the **LIT method** (LIT=Lorentz Integral Transform)<sup>1</sup> to study reactions involving states in the continuum. In the following recent results, obtained by applying such a method are presented:

(i) A fundamental quantity in nuclear physics is represented by the electric dipole polarizability. In fact it is related to critical observables such as the radii of the proton and neutron distributions. However, an accurate calculation of this quantity is most

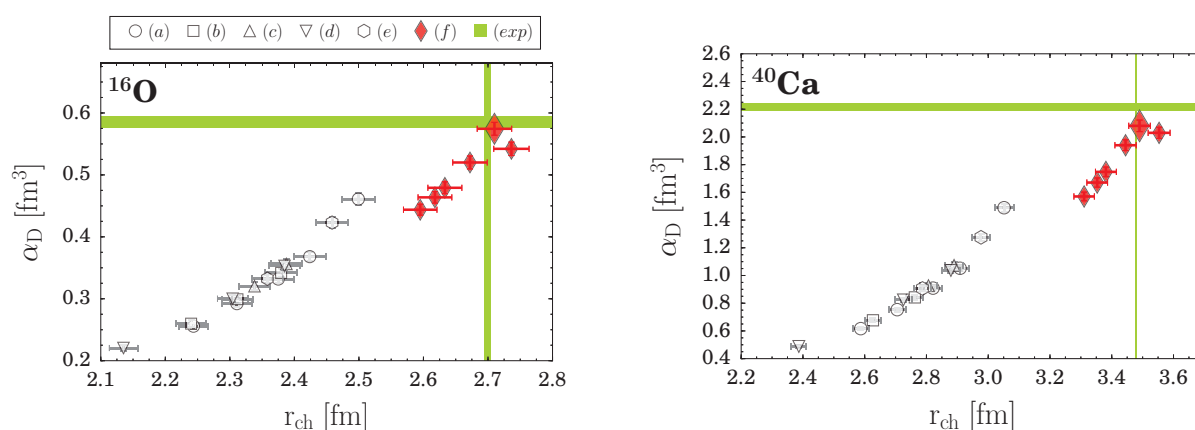


Figure 1: Dipole polarizabilities versus charge radii in  $^{16}\text{O}$  and  $^{40}\text{Ca}$  from different chiral potentials.

<sup>†</sup>Contact Author: giuseppina.orlandini@unitn.it

<sup>1</sup>Efros, V. D. et al. (1994), Physics Letters B **338**(2-3), pp. 130–133;  
Efros, V. D. et al. (2007), Journal of Physics G: Nuclear and Particle Physics **34**(12), R459.

challenging, since it requires the knowledge of the dipole strength in the scattering continuum. Combining the Lorentz integral transform approach and the coupled-cluster method we have been able to compute this quantity using bound-state techniques. The strong correlation between the dipole polarizability and the charge radius is confirmed for all the interactions used, obtained from chiral effective field theory, see Fig. 1. The dependence on three-nucleon forces has been studied, and good agreement with data has been found for the  $^4\text{He}$ ,  $^{40}\text{Ca}$  and  $^{16}\text{O}$  nuclei, see (Bacca and Orlandini 2016) in the general bibliography, p. 151. Moreover we have been able to predict the dipole polarizability for the rare nucleus  $^{22}\text{O}$ .

ii) The LIT approach has been tested for the calculation of astrophysical S-factors, considering the reaction  $^2\text{H}(p,\gamma)^3\text{He}$  (Deflorian et al. 2017). If one aims at a precise determination of S-factors it is necessary to obtain a sufficiently high density of LIT states at low energies, resulting from the hamiltonian matrix diagonalization. In particular it has been shown that the HH basis is not very well suited for such a calculation and that a different basis is much more advantageous. With the latter the comparison of LIT results with calculations, where continuum wave functions are explicitly used, has been quite successful.

(iii) A very important progress has been made in the technique of the Hyperspherical Harmonics (HH), a typical bound state method

for ab initio calculations of few body bound states. In fact the Non-Symmetrized Hyperspherical Harmonics method (NSHH) has been generalized in order to make it possible to deal with systems containing constituents of different masses. This progress is particularly relevant for the field of hypernuclei, where the hypernuclear force is still largely unknown. First results have been obtained for  $^3\text{H}_\Lambda$ ,  $^3\text{He}_\Lambda$  (Ferrari Ruffino et al. 2017) and  $^5\text{He}_\Lambda$  and successfully benchmarked, when possible, to results obtained with other techniques. The generalized NSHH (GNSHH) opens the possibility to deal also with hypernuclei of a larger number of constituents and even strangeness  $S > 1$ . Also those heavier nuclear systems that present a clusterized structure (e.g. the interesting  $^9\text{Be}$ ) can be treated by the GNSHH.

iv) The integral transform approach is especially useful when it is possible to calculate, by matrix diagonalization, the integral transform of a physical quantity of interest (e.g. cross sections in the continuum), whilst a direct calculation of the latter is very cumbersome or out of reach. However, this depends on the kind of kernel of the transform. Which kernels are suitable for that has been discussed in (Orlandini and Turro 2017). In particular special kernels have been advocated as best in order to avoid at the same time the ill-posedness of the inversion problem. The results of a model study show that some *wavelet* kernels are very promising in this respect.

## Selected Papers

- Deflorian, S., Efras, V., and Leidemann, W. (2017). *Calculation of the Astrophysical S-Factor S-12 with the Lorentz Integral Transform*. *Few-Body Syst.* **58**, pp. 1–12.
- Ferrari Ruffino, F., Lonardonì, D., Barnea, N., Deflorian, S., Leidemann, W., Orlandini, G., and Pederiva, F. (2017). *Benchmark Results for Few-Body Hypernuclei*. *Few-Body Syst.* **58**, UNSP 113.
- Orlandini, G. and Turro, F. (2017). *Integral Transform Methods: A Critical Review of Various Kernels*. *Few-Body Syst.* **58**, UNSP 76.

# FLAG

Luciano Vanzo,<sup>†</sup> Massimiliano Rinaldi, Sergio Zerbini, Lorenzo Sebastiani, Alessandro Casalino, Stefano Chinaglia, Aimeric Colleaux

**Scientific Activity** The scientific activity has been greatly enhanced by the new INFN post-doc position won by Lorenzo Sebastiani, who began service in July 2017. Most of the research activity 2016/2017 focussed on the following research areas:

- (i) Black holes in the light of information complexity
- (ii) scale invariant models of inflation, reheating and Horndeski gravity
- (iii) Regularity and stability problems of Cauchy horizons and black holes
- (iv) The Euclid project

(i) Black holes are among the most amazing objects predicted by general relativity or more general metric theories of gravity, both for theoretical as well as observational reasons. An interesting question is to see how much complexity is hidden in the objects, in contrast with the apparent simplicity suggested by the no-hair theorems. Recently there has been a flood of activity aiming to understand the measure of complexity for black holes. It turned out that the horizon quantum states, attributed to these objects by the holographic description of black holes in anti-de Sitter space, have a sort of Kolmogorov complexity. More exactly, a quantum version of this complexity. It evolves with time as the black hole evaporates, and one problem is to study the time evolution of this complexity as time goes on.

There are many benefits in obtaining such evolution, one is the hope to clarify the nature

of the information loss paradox afflicting black hole quantum physics since its beginning. We undertook this study, and we obtained the interesting result (previously unknown to the best of our knowledge) that asymptotically anti-de Sitter boundary conditions are not required, provided one computes the complexity grow in the interior of the black hole in a so called Wheeler-De Witt patch. Moreover, it all depends on the validity of the generalized second law, because this implies the energy bound on complexity grow long known in information theory for communication channels, another good result. A paper on this (“Action growth for black holes in modified gravity”, ArXiv: 1710:05686 [hep-th]) is presently waiting a response from Physical Review D.

(ii) In the theory of inflation, we continued to analyze several attractor mechanism for generating primordial density fluctuations with the spectrum compatible with the data collected by the Planck satellite. We also continued the study of the role of scale invariance of the underlying theory, which we began in 2016, and extended them to study the reheating process thought to be responsible of the creation of standard model and dark matter particles. Results were presented in (Tambalo and Rinaldi 2017).

With the collaboration of a PhD student, we undertook the task of pushing the Theory of Horndeski gravity beyond the homogeneous isotropic limit, in order to apply it to the real universe. This theory gained recently some in-

<sup>†</sup>Contact Author: [luciano.vanzo@unitn.it](mailto:luciano.vanzo@unitn.it)

terest as a model of dark matter. Results were not encouraging and point to rule out the theory, or more precisely the particular subclass here studied. The role of scalar tensor Horndeski gravity as a model for dark matter has been investigated too. Results are presented in (Rinaldi 2017a), see general bibliography, p. 151. It is just to go beyond the results in this paper that cosmological perturbations were studied, using the hi-class software recently developed for help in this kind of problems.

The study of compact objects in Horndeski gravity is another subject of interest to our group. Neutron stars and axionic black hole solutions have been investigated throughly, see (Cisterna et al. 2017) in the general bibliography, p. 151.

Inflation based on logarithmic  $R^2$  corrections to GR have been investigated too, with interesting output (Odintsov et al. 2017).

(iii) An old question with still has no general answer is what happen inside black holes. In particular, the embarrassing presence of a central space-time singularity has always generated concern among experts in the field. It was Sakharov conjecture that to avoid the singularity in gravitational collapse the black hole should have a de Sitter core, namely looks like de Sitter space near the center. But it is not so easy to produce such a behavior. Among the many proposals, smoothing out the singularity, non commutative geometry, modified gravitational interactions, et cetera, models have been investigated in our group with exotic matter content and/or electromagnetic fields with non linear dynamics.

It turned out that a de Sitter core can be obtained by using negative radial pressure and non vanishing transversal pressure, which is not in conflict with spherical symmetry. But there are drawbacks: one was the presence of growing modes, i.e. instability, and the presence of Cauchy horizons, making the black hole interior unpredictable to some extent. Both are problematic features of black hole solutions, to which we found no cure. Results are presented in (Chinaglia and Zerbini 2017).

(iv) *The Euclid project* One of us in FLAG

(M. Rinaldi) is a founder member of the Euclid Theory Working Group, namely an international group of more than 50 theoreticians engaged to give a theoretical support to the ESA Euclid mission to be launched in 2021. The main activity is to systematically study models of dark matter and dark energy and to produce the related forecasts to be confronted with data. The results of this collaborations are continuously reported an updated in Living Review of Relativity. A paper entitled *Cosmology and Fundamental Physics with the Euclid Satellite*<sup>1</sup> has been accepted by Living Review of Relativity as an update of an earlier 2013 version.

**Seminars and Events** The annual FLAG meeting has been held in Como, Palazzo San Abbondio, owned by Insubria University, during a two day meeting on December 14-15. Among the participants, the Field medalist Lafforgue was invited to speak about the Langlands Program. The meeting hosted about 20 people and delivered 15 talks on various aspects of the FLAG activity, including a measurement of the gravitational constant variability by monitoring solar activity (see the talk of A. Buonanno from INAF and INFN Catania).

Various people delivered talks to various conferences:

- The “Karl Schwarzschild meeting 2017”. Title: “Thermodynamical aspects of black holes in modified gravity”. Proceedings to appear.
- FLAG annual Meeting, Como, December 14-15/2017, “Action grow for black holes in modified gravity”.
- IV Cosmology and the Quantum Vacuum, Segovia September 4-8, 2017, with title: “A model of regular black holes satisfying the weak energy condition”. Proceedings to appear.
- M. Rinaldi seminar: “Scale invariant inflation”, Modified Gravity Day, University of Padova, 16 giugno 2017 (invited talk).
- M. Rinaldi seminar: “Scale invariant gravity and inflation”, Oskar Klein Centre, Stockholm, June 13, 2017 (invited

<sup>1</sup>Amendola, L. et al. (2016), arXiv (1606.00180).

- talk).
- M. Rinaldi seminar: "The scale-invariant inflationary Universe", University of Helsinki, January 25, 2017 (invited talk). See also (Rinaldi 2017b) in the general

bibliography, p. 151.

We mention also some activity in public outreach, to spread scientific ideas and achievements, both in schools and cultural foundations.

## Selected Papers

- Chinaglia, S. and Zerbini, S. (2017). *A note on singular and non-singular black holes*. Gen. Rel. Gravitation **49**, p. 75.
- Odintsov, S. D., Oikonomou, V., and Sebastiani, L. (2017). *Unification of Constant-roll Inflation and Dark Energy with Logarithmic  $R^2$ -corrected and Exponential  $F(R)$  Gravity*. Nuclear Physics B **923**, p. 608.
- Tambalo, G. and Rinaldi, M. (2017). *Inflation and reheating in scale-invariant scalar-tensor gravity*. Gen. Rel. Gravitation **49**, p. 52.

# MANYBODY

Francesco Pederiva,<sup>†</sup> Alessandro Lovato, Maurizio Dapor, Simone Taioli, Chen Ji, Lorenzo Contessi, Lorenzo Andreoli

The TIFPA unit of the MANYBODY collaboration pursues development and applications of quantum many-body techniques to both systems of interest for nuclear physics and nuclear astrophysics (Lovato, Ji, Contessi, Andreoli, Pederiva), and applications to condensed matter physics (Dapor, Taioli, Pederiva). The methods toolbox is quite diverse, ranging from Quantum Monte Carlo and transport Monte Carlo to density functional theory and direct diagonalization of the Hamiltonian.

Another important research line concerns the development of a systematic way of directly deriving nuclear interactions from Lattice QCD calculations. At present LQCD can estimate binding energy of multi-baryon systems, but only for artificially large quark masses, leading to pion masses in a range between 400 and 800 MeV, and an extrapolation would be needed to describe the physical case. In this context it is interesting to understand how the nuclear systematics evolves as a function of the pion mass. In particular one would like to understand as properties like saturation, or the binding of heavier nuclei evolve, and if extrapolation is at all possible. Together with N. Barnea and D. Gazit of the Hebrew University in Jerusalem, and U. van Kolck from Orsay, we developed a pion-less effective field theory leading to a description of interactions between lattice nucleons, and performed calculations on a few lattice nuclei, showing that the potential developed in this scheme is indeed predictive and consistent with lattice results.<sup>1</sup> In a subsequent work, we have extended the formalism and carried out an

analysis of the ground state of  $^{16}\text{O}$  (Contessi et al. 2017). The nuclear many-body Schrödinger equation is solved with the Auxiliary Field Diffusion Monte Carlo method. For the first time in a nuclear quantum Monte Carlo calculation, a linear optimization procedure, which allows us to devise an accurate trial wave function with a large number of variational parameters, is adopted. The method yields a binding energy of  $^4\text{He}$  which is in good agreement with experiment at physical pion mass and with lattice calculations at larger pion masses. At leading order we do not find any evidence of a  $^{16}\text{O}$  state which is stable against breakup into four  $^4\text{He}$ , although higher-order terms could bind  $^{16}\text{O}$ . The clusterization of the  $^{16}\text{O}$  wave function can be appreciated in Fig. 1, where we display the position of the nucleons during the imaginary-time evolution. The fact that nucleons forming the four  $^4\text{He}$  clusters remain close to the corresponding centers of mass is a clear evidence of clustering. This imaginary-time propagation refers to a specific value of

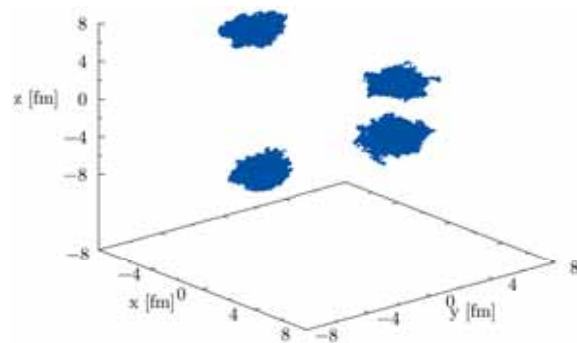


Figure 1: Imaginary-time diffusion of the  $^{16}\text{O}$  wave function for pionless-EFT potentials at  $m_\pi = 510 \text{ MeV}$ .

<sup>†</sup>Contact Author: francesco.pederiva@unitn.it

<sup>1</sup>Barnea, N. et al. (2015), Physical Review Letters 114(5).

the cutoff used to regularize the pionless-EFT potential, but analogous results are found for other cutoff values. It has to be noted that, within the pionless framework, next-to-leading order (NLO) and next-to-next-to-leading order (N<sup>2</sup>LO) terms could move <sup>16</sup>O with respect to the four- <sup>4</sup>He threshold.

A main effort of the MANYBODY group consists in providing precise calculations of neutrino- nucleus cross sections, which is critical for the success of current and next generation neutrino experiments. Experimental studies of neutrino- nucleus interactions carried out over the past decade have provided ample evidence of the inadequacy of the relativistic Fermi gas model, routinely employed in event generators. The complexity of nuclear dynamics and the variety of reaction mechanisms are such that ab-initio calculations of nuclear structure and electroweak interactions with nuclei are necessary. To attack this problem, we performed Green's function Monte Carlo (GFMC) calculations of the quasi-elastic neutral-current response functions of <sup>12</sup>C in the moderate momentum transfer regime, using realistic nuclear two- and three-body forces and consistent one- and two- body electroweak currents. By employing an improved version of the maximum entropy technique, based on Bayesian statistical inference, we were able to invert the Euclidean response function, achieving the first ab-initio calculation of the neutral-current response functions of <sup>12</sup>C. As shown in Fig. 2, two-body current contributions substantially increase in magnitude the one-body electroweak responses, and may well explain the axial mass puzzle, raised by the MiniBooNE experimental collaboration. The main shortcoming of the GFMC calculations resides in their non-relativistic nature, which limits their applicability to moderate momentum transfer. In collaboration with G. Orlandini, W. Leidemann

(FEWBODY) and N. Rocco (University of Surrey), we have extended the applicability range of the GFMC calculations employing the two-fragment model of (Efros et al. 2005).<sup>2</sup> Our theoretical calculations for the <sup>4</sup>He(*e*, *e'*) inclusive cross-section data are in excellent agreement with experiments for initial electron energies ranging from 0.3 GeV to 1.1 GeV.

As previously mentioned, the activity of the MANYBODY group, also encompass applications to other fields. Particularly important is the research in condensed matter theory. A substantial part of this work is developed within the ECT\*-LISC unit, whose activity are described elsewhere. However, the group also deals with the development of novel Quantum Monte Carlo techniques, such as the recently introduced Configuration Interaction Monte Carlo (CIMC), or general algorithms to deal with spin-dependent Hamiltonians. In this context, the first natural applications are on Coulombic systems, and therefore part of our scientific production did and will concern applications to many-electron systems such as the electron gas or atoms and molecules.

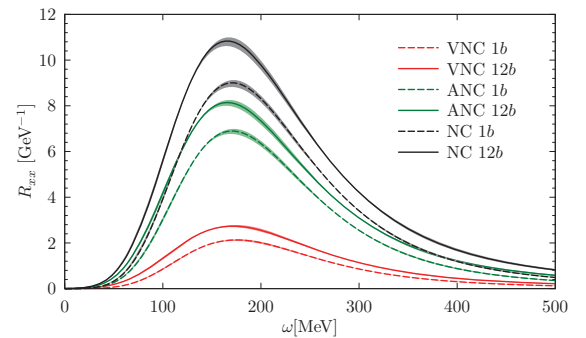


Figure 2: Neutral-current (NC) response functions in <sup>12</sup>C at momentum transfer  $q = 570$  MeV/c, obtained with one-body only (dashed lines) and one- and two-body (solid lines) currents. The narrow bands indicate the uncertainty in the maximum- entropy inversion. The vector (VNC) and axial (ANC) contributions are shown separately.

## Selected Papers

Contessi, L., Lovato, A., Pederiva, F., Roggero, A., Kirscher, J., and van Kolck, U. (2017). *Ground-state properties of <sup>4</sup>He and <sup>16</sup>O extrapolated from lattice QCD with pionless EFT*. Phys. Lett. **B772**, pp. 839–848.

<sup>2</sup>Efros, V. D. et al. (2005), Phys. Rev. **C72**, p. 011002.

# NEMESYS

Simone Taioli,<sup>†</sup> Maurizio Dapor, Giovanni Garberoglio

The research activity of this year was focussed along five different lines.

First, we study the ballistic properties of two-dimensional materials upon the hypervelocity impacts of C<sub>60</sub> fullerene molecules combining ab initio density functional tight binding and finite element simulations (Signetti et al. 2017). The critical penetration energy of monolayer membranes is determined using graphene and the 2D allotrope of boron nitride as case studies. Furthermore, the energy absorption scaling laws with a variable number of layers and interlayer spacing are investigated, for homogeneous or hybrid configurations (alternated stacking of graphene and boron nitride). At the nanolevel, a synergistic interaction between the layers emerges, not observed at the micro- and macro-scale for graphene armors. This size-scale transition in the impact behavior toward higher dimensional scales is rationalized in terms of scaling of the damaged volume and material strength. An optimal number of layers, between 5 and 10, emerges demonstrating that few-layered 2D material armors possess impact strength even higher than their monolayer counterparts. These results provide fundamental understanding for the design of ultralightweight multilayer armors using enhanced 2D material-based nanocomposites.

Second, we study Pillared Graphene Frameworks, which are a novel class of microporous materials made by graphene sheets separated by organic spacers. One of their main features is that the pillar type and density can be chosen to tune the material properties. In

this work, we present a computer simulation study of adsorption and dynamics of H<sub>2</sub>, CH<sub>4</sub>, CO<sub>2</sub>, N<sub>2</sub> and O<sub>2</sub> and binary mixtures thereof, in Pillared Graphene Frameworks with nitrogen-containing organic spacers. In general, we find that pillar density plays the most important role in determining gas adsorption. In the low-pressure regime ( $\leq 10$  bar) the amount of gas adsorbed is an increasing function of pillar density. At higher pressure the opposite trend is observed. Diffusion coefficients were computed for representative structures taking into account the framework flexibility that is essential for assessing the dynamical properties of the adsorbed gases. Good performance for the gas separation in CH<sub>4</sub>/H<sub>2</sub>, CO<sub>2</sub>/H<sub>2</sub> and CO<sub>2</sub>/N<sub>2</sub> mixtures was found, with values comparable to those of metal-organic frameworks and zeolites.

Third, we compare Monte Carlo (MC) simulations of electron-transport properties with reflection electron energy-loss measurements in diamond and graphite films (Azzolini et al. 2017b). We assess the impact of different approximations of the dielectric response on the observables of interest for the characterization of carbon-based materials. We calculate the frequency-dependent dielectric response and energy-loss functions of these materials in two ways: a full ab initio approach, in which we carry out time-dependent density functional simulations in linear response for different momentum transfers, and a semi-classical model, based on the Drude–Lorentz extension to finite momenta of the optical dielectric function. Ab

<sup>†</sup>Contact Author: taioli@ectstar.eu

initio calculated dielectric functions lead to better agreement with measured energy-loss spectra compared to the widely used Drude–Lorentz model. This discrepancy is particularly evident for insulators and semiconductors beyond the optical limit ( $\mathbf{q} \neq 0$ ), where single-particle excitations become relevant. Furthermore, we show that the behaviour of the energy-loss function obtained at different accuracy levels has a dramatic effect on other physical observables, such as the inelastic mean free path and the stopping power in the low energy ( $< 100$  eV) regime and thus on the accuracy of MC simulations.

Fourth, nonlinear electronic spectroscopies represent one of the most powerful techniques to study complex multi-chromophoric architectures. For these systems, in fact, linear spectra are too congested to be used to disentangle the many coupled vibroelectronic processes that are activated. By using a 2D approach, instead, a clear picture can be achieved, but only when the recorded spectra are combined with a proper interpretative model. So far, this has been almost always achieved through parametrized exciton Hamiltonians that necessarily introduce biases and/or arbitrary assumptions. In this study (Segatta et al. 2017), a first-principles approach is presented that combines accurate quantum chemical descriptions with state-of-the-art models for the environment through the use of atomistic and polarizable embeddings. Slow and fast bath dynamics, along with exciton transport between the pigments, are included. This approach is ap-

plied to the 2DES spectroscopy of the Light-Harvesting 2 (LH2) complex of purple bacteria (see Fig. 1). Simulations are extended over the entire visible-near-infrared spectral region to cover both carotenoid and bacteriochlorophyll signals. Our results provide an accurate description of excitonic properties and relaxation pathways, and give an unprecedented insight into the interpretation of the spectral signatures of the measured 2D signals.

Finally, Spider silk has promising mechanical properties, since it conjugates high strength ( $\simeq 1.5$  GPa) and toughness ( $\simeq 150$  J g $^{-1}$ ). We report the production of silk incorporating graphene and carbon nanotubes by spider spinning, after feeding spiders with the corresponding aqueous dispersions. We observe an increment of the mechanical properties with respect to pristine silk, up to a fracture strength  $\simeq 5.4$  GPa and a toughness modulus  $\simeq 1570$  J g $^{-1}$ . This approach could be extended to other biological systems and lead to a new class of artificially modified biological, or “bionic”, materials.

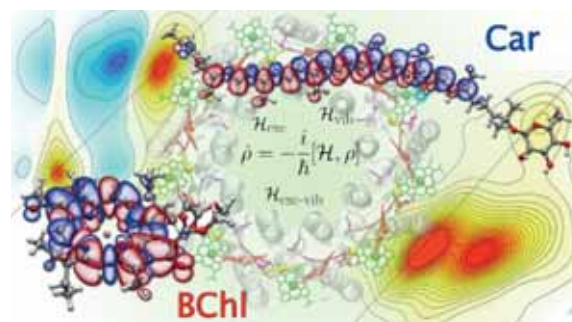


Figure 1: 2DES spectrum of the Light-Harvesting 2 (LH2) complex of purple bacteria

## Selected Papers

- Azzolini, M., Morresi, T., Garberoglio, G., Calliari, L., Pugno, N. M., Taioli, S., and Dapor, M. (2017b). Monte Carlo simulations of measured electron energy-loss spectra of diamond and graphite: Role of dielectric-response models. *Carbon* **118**(Supplement C), pp. 299–309.
- Segatta, F., Cupellini, L., Jurinovich, S., Mukamel, S., Dapor, M., Taioli, S., Garavelli, M., and Menucci, B. (2017). A Quantum Chemical Interpretation of Two-Dimensional Electronic Spectroscopy of Light-Harvesting Complexes. *Journal of the American Chemical Society* **139**(22). PMID: 28513172, pp. 7558–7567.
- Signetti, S., Taioli, S., and Pugno, N. M. (2017). 2D Material Armors Showing Superior Impact Strength of Few Layers. *ACS Applied Materials & Interfaces* **9**(46). PMID: 29120161, pp. 40820–40830.

# NINPHA

Marco Claudio Traini<sup>†</sup>

**Deep Inelastic Scattering in AdS/QCD** Generalized Parton Distributions are investigated in (M. Traini 2017) within a holographic approach where the string modes in the fifth dimension describe the nucleon in a bottom-up or AdS/QCD framework. The aim is to bring the AdS/QCD results in the realm of phenomenology in order to extract consequences and predictions.

A first attempt to apply the AdS/QCD framework for a bottom-up approach to the evaluation of the effective cross section for double parton scattering in proton-proton collisions is presented in (M. Traini et al. 2017). The main goal is the analytic evaluation of the dependence of the effective cross section on the longitudinal momenta of the involved partons, obtained within the holographic Soft-Wall model. If measured in high-energy processes at hadron colliders, this momentum dependence could open a new window on two-parton correlations in a proton as illustrated in Fig. 1 where a new effect is shown, namely the  $x$ -dependence of the effective cross section.

**Double Parton Distributions** The correct description of Double Parton Scattering (DPS), which represents a background in several channels for the search of new Physics at the LHC, requires the knowledge of double parton distribution functions (dPDFs). In (Rinaldi et al. 2016b) we studied to what extent factorized expressions for dPDFs, which neglect, at least in part, two-parton correlations, can be used. We show that they fail in reproducing the cal-

culated dPDFs, in particular in the valence region. Actually measurable processes at existing facilities occur at low longitudinal momenta of the interacting partons; to have contact with these processes we have analyzed correlations between pairs of partons of different kind, finding that, in some cases, they are strongly suppressed at low longitudinal momenta, while for other distributions they can be sizeable. For example, the effect of gluon-gluon correlations can be as large as 20%. We have shown that these behaviors can be understood in terms of a delicate interference of non-perturbative correlations, generated by the dynamics of the model, and perturbative ones, generated by the model independent evolution procedure. Our analysis shows that at LHC kinematics two-parton correlations can be relevant in DPS, and therefore we address the possibility to study them experimentally.

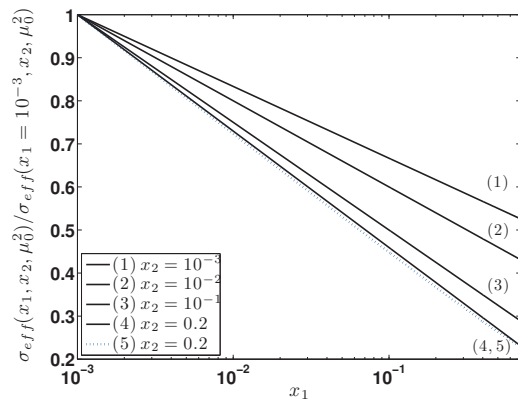


Figure 1:  $\sigma_{eff}(x_1, x_2, \mu_0^2)$  (normalized at  $x_1 = x_2 = 10^{-3}$ ), as a function of  $x_1$  at fixed  $x_2 = 0.001, 0.01, 0.1, 0.2$ .

<sup>†</sup>Contact Author: marcoclaudio.traini@unitn.it

## Selected Papers

- Rinaldi, M., Scopetta, S., Traini, M., and Vento, V. (2016b). *Correlations in double parton distributions: perturbative and non-perturbative effects*. *Journal of High Energy Physics* **10**, 063 (35 pages).
- Traini, M. (2017). *Generalized parton distributions: confining potential effects within AdS/QCD*. *European Physics Journal C* **77**, pp. 246–260.
- Traini, M., Rinaldi, M., Scopetta, S., and Vento, V. (2017). *The effective cross section for double parton scattering within a holographic AdS/QCD approach*. *Physics Letter B* **768**, pp. 270–273.

# TEONGRAV

Bruno Giacomazzo,<sup>†</sup> Riccardo Ciolfi, Andrea Endrizzi

The main research activity of the TEONGRAV group in Trento concerns fully general relativistic simulations of compact binaries, either neutron stars or black holes. We here very briefly summarize the main results from two representative papers published by our group in 2017 and that considered in particular possible electromagnetic counterparts of astrophysical events that can be detected by gravitational wave interferometers such as Virgo and LISA.

mass of the Sun within a radius of only around 10 km. Because of their extreme gravity a proper description of neutron stars requires Einstein’s theory of General Relativity. Investigating neutron star properties can shed light on the behavior of matter at very high densities, which is not yet understood well by nuclear physics. Two neutron stars can also bind together in a binary system, and orbit around each other for millions of years with a smaller and smaller separation. Eventually, the two merge together in an instant (just a few milliseconds) resulting either in a black hole or in a rapidly rotating neutron star, which can still collapse to a black hole later on.

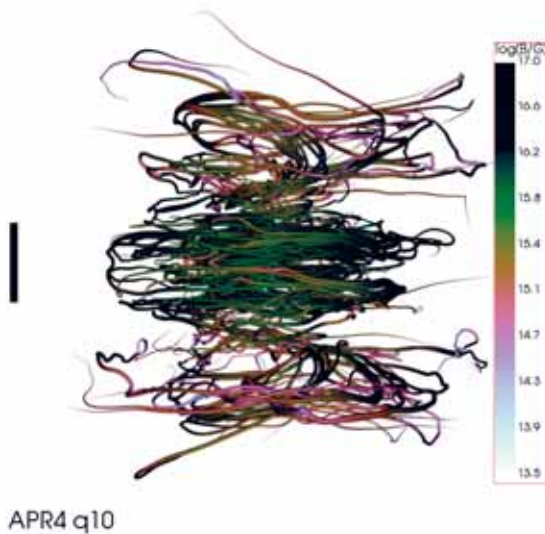


Figure 1: Structure of magnetic field 45 ms after merger for the equal-mass APR4 model. The coloring indicates the magnetic field strength. The black bar provides a length scale of 20 km.

**Binary Neutron Stars** Neutron stars are the remnants of supernova explosions (the spectacular deaths of massive stars) and the densest objects in the universe besides black holes. A typical neutron star concentrates more than the

Binary neutron star mergers are among the most violent astrophysical phenomena, which give rise to powerful gravitational wave signals and bright electromagnetic emission. The first binary neutron star merger was detected on August 17<sup>th</sup> 2017 by the gravitational wave detectors LIGO and Virgo. A simultaneous detection of a short gamma-ray burst and the following observations in all the other bands of the electromagnetic spectrum, from radio to X-rays, also confirmed that these mergers are responsible for at least some short gamma-ray bursts and that they are the site for the production of the most heavy elements in the universe.

In (Ciolfi et al. 2017) we investigated the merger of six different binary neutron star systems all having the same initial gravitational mass and magnetic energy. The systems differ in mass ratios (one equal- and one unequal-mass model) and in the equation of state (H4, APR4, MS1). The total initial gravitational

<sup>†</sup>Contact Author: [bruno.giacomazzo@unitn.it](mailto:bruno.giacomazzo@unitn.it)

mass was chosen such that a long-lived neutron star was produced when using the APR4 and MS1 equations of state and a short-lived (hypermassive) one when using H4 instead.

In Fig. 1 we show the resulting magnetic field configuration at the end of one of these simulations. None of the simulations showed the formation of a magnetically-dominated funnel, nor of a jet, along the spin-axis of the final remnant. Moreover, when a long-lived neutron star is formed, the regions above and below the remnant are strongly baryon polluted, possibly preventing the launch of a strongly relativistic jet and hence of a short gamma-ray burst. Interestingly, even when employing large magnetic fields of up to  $\sim 10^{16}\text{G}$  after merger, the post-merger gravitational wave signal seems to be almost unaffected by the magnetic field. Future simulations will include a better description of finite-temperature effects and of neutrino emission in order to provide more robust estimates for the gravitational and electromagnetic emission.

**Supermassive Black Holes** In (Kelly et al. 2017) we studied instead the accretion of magnetized matter onto merging supermassive black holes. Supermassive binary black holes will be powerful sources of gravitational waves for the LISA mission and they are formed after the merger of galaxies. In this scenario the two black holes may merge in a matter-rich environment that can produce bright electromagnetic signals.

In collaboration with colleagues at NASA Goddard Space Flight Center and at West Virginia University in the USA we studied the role of magnetic fields in the accretion of matter onto supermassive black hole binaries and the emission of relativistic jets and electromagnetic

signals.

Fig. 2 shows as an example the ratio between magnetic pressure and gas pressure after the merger in one of the simulations and it provides evidence for the formation of a collimated and magnetically-dominated jet.

We showed that this scenario seems to be insensitive to the initial magnetic field strength and number of orbits before merger. The luminosity, in the case of two  $10^8 M_\odot$  black holes surrounded by a plasma with densities of  $\sim 10^{-13}\text{gcm}^{-3}$ , can reach values of up to  $\sim 10^{46}\text{ergs}^{-1}$ . Our simulations focused though only on equal-mass non-spinning black hole binaries and a rather simple initial matter distribution. Future simulations will need to address also the effects of different mass ratios, black hole spins, and different matter configurations in order to improve our understanding of the electromagnetic emission that may come from these systems.

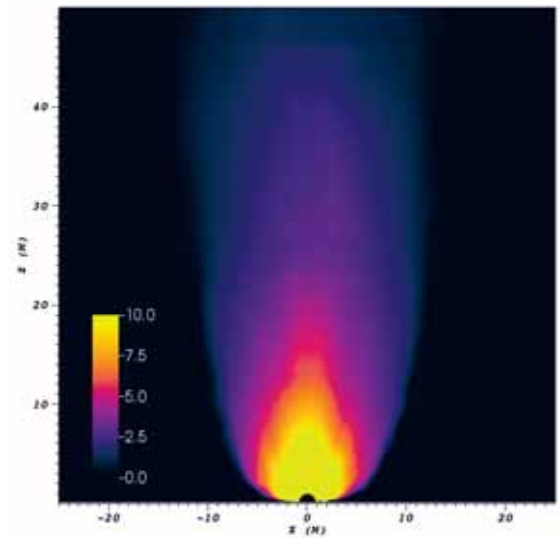


Figure 2: Magnetic-to-gas pressure ratio  $\beta^{-1} \equiv b^2/2P_{\text{gas}}$  about 150 hours after the merger of two black holes of  $10^8 M_\odot$ .

## Selected Papers

- Ciolfi, R., Kastaun, W., Giacomazzo, B., Endrizzi, A., Siegel, D. M., and Perna, R. (2017). *General relativistic magnetohydrodynamic simulations of binary neutron star mergers forming a long-lived neutron star*. Phys. Rev. D **95**(6), 063016, p. 063016.
- Kelly, B. J., Baker, J. G., Etienne, Z. B., Giacomazzo, B., and Schnittman, J. (2017). *Prompt Electromagnetic Transients from Binary Black Hole Mergers*. Phys. Rev. D **96**(12), 123003, p. 123003.





# Technological Research

Alberto Quaranta

alberto.quaranta@unitn.it

Coordinator,

TIFPA Technological Research Activities

In the second year from the foundation of the CSN5 group at TIFPA, 10 official projects, 3 calls, 1 sub-project (under endowment) and 1 Young Researcher Grant, are active at TIFPA in the technology and interdisciplinary field. Concerning CSN5, this number of activities is one of the highest among the INFN Italian Units. Moreover, at present CSN5 TIFPA group involves 39 researchers from three Departments, that are Physics (DF), Industrial Engineering (DII), Civil, Mechanics and Environment (DICAM), and Bruno Kessler Foundation (FBK). These institutions, together with INFN persons in charge at TIFPA, contribute to all the projects with a total amount of 29.5 Researcher Equivalent Time (FTE).

Most of the projects, enriched by the collaboration with FBK, are devoted to research on innovative detectors for particle physics and radiotherapy, while some other projects are more focused on interdisciplinary aspects involving medical physics and radiation application in this field. The projects acronyms are: ARDESIA, ASAP, ELOFLEX, AXIAL, REDSOX2, SEED, XDET, KIDS\_RD, HI-BRAD, ISOLPHARM\_AG, call acronyms are MOVE\_IT, SICILIA and TIMESPOT, and the Young Researcher Grant acronym is DEEP\_3D. Among them, ASAP, DEEP\_3D, ELOFLEX, ISOLPHARM\_AG, TIMESPOT and XDET are new projects, starting on 2018, which have been approved by the CSN5 commission.

Concerning new projects, ASAP works on the refinement of the detectors realized during a previous experiment (APIX2), by improving the resolution from 150 nm to 110 nm; DEEP\_3D project intends to develop an high spatial resolution and high gamma rejection neutron imager device by using silicon detectors coupled to neutron reactive materials; ELOFLEX has the aim to realize a hybrid flexible conductive-optical detector for the detection of radiation in mixed fields; ISOLPHARM\_AG has the focus to obtain new chemical transducers for the exploitation of an innovative isotope for radiotherapy, that is  $^{111}\text{Ag}$ ; TIMESPOT is a call involving a network of 10 Units whose objective is the development and implementation of a complete integrated system for tracking having very high precision both in space (100  $\mu\text{m}$  or less) and in time (100 ps or less) per detection channel; finally XDET wants to produce a pixel detector for X-ray imaging suitable for FEL and synchrotron measurements.

It is worth noting that after 2 years from its constitution the CSN5 activity at TIFPA reached a great maturity and productivity, collecting a huge number of experienced researchers in the field of detectors, interdisciplinary physics and materials science and engineering.

# APiX2

Lucio Pancheri,<sup>†</sup> Andrea Ficorella, Moustafa Khatib, Gian-Franco Dalla Betta

Goal of the APiX2 project is the development of an innovative position-sensitive pixelated sensor for the detection of ionizing particles. The APiX sensor is based on Geiger-mode avalanche pixels operated in fully digital mode with on-chip embedded electronics. In the Geiger-mode operation, a single electron-hole pair can trigger an avalanche event and thus there is no possibility to distinguish a particle-triggered event from a dark count. The proposed device is formed by two vertically-aligned pixelated detectors and exploits the coincidence between two simultaneous avalanche events to discriminate between particle-triggered events and dark counts.

ing in medicine and biology. A sensor based on this concept can have low noise, low power consumption and a good tolerance to electromagnetic interference. In addition, a timing resolution in the order of tens of picoseconds can be achieved thanks to the fast onset of avalanche multiplication in Geiger-mode regime.

The first demonstrator, a two-tier sensor assembly, was designed and fabricated in a commercial  $0.15\mu\text{m}$  CMOS process (Pancheri et al. 2017a). The sensor consists of a  $48 \times 16$  pixel array, and includes avalanche diodes of different sizes to evaluate the detection efficiency for different fill factors. Each pixel, having a  $50 \times 75\mu\text{m}^2$  area, includes detectors and electronics on both layers, with the top-layer signal transmitted to the bottom layer using a vertical interconnection per pixel. The pixel schematic diagram is shown in Fig. 1. In the pixel, the detectors are passively quenched and their output signals are digitized by means of a low-threshold comparator. The resulting pulses are shortened by a programmable-length monostable circuit, providing a minimum pulse width in the nanosecond range. The pixels can be independently enabled or disabled with an arbitrary pattern, defined by a configuration register. The output of the monostable in the top half-pixel feeds a coincidence detector located in the bottom layer, and the coincidence output is stored in a 1-bit memory. Data can be transferred in parallel to an output register for readout. In this way, signal detection and data readout can be run in parallel, thereby avoiding any dead time in the data acquisition process.

A micrograph of the bottom chip is shown in Fig. 2, together with a concept view of the two-layer assembly. Electrical tests showed the

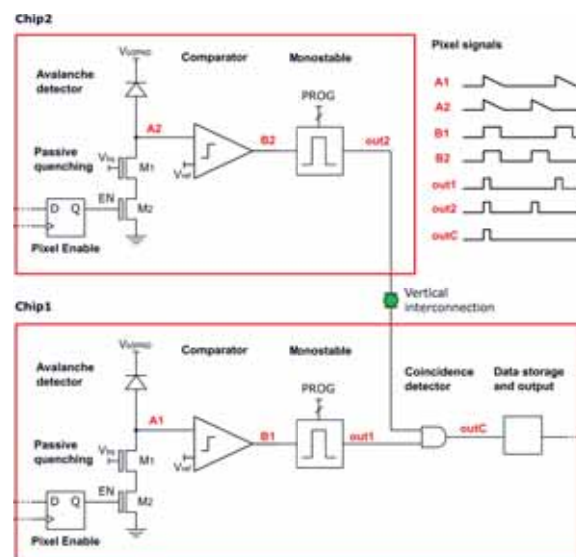


Figure 1: Simplified schematic of the pixel and illustration of pixel signals timing.

This approach offers several advantages in applications requiring low material budget and fine detector segmentation as, for instance, for tracking and vertex reconstruction in particle physics experiments and charged particle imag-

<sup>†</sup>Contact Author: lucio.pancheri@unitn.it

correct functionality of both avalanche detectors and electronics in the two chips. A complete characterization of Dark Count Rate and pixel optical cross-talk has been carried out on single layers (Pancheri et al. 2017a; Pancheri et al. 2017b).

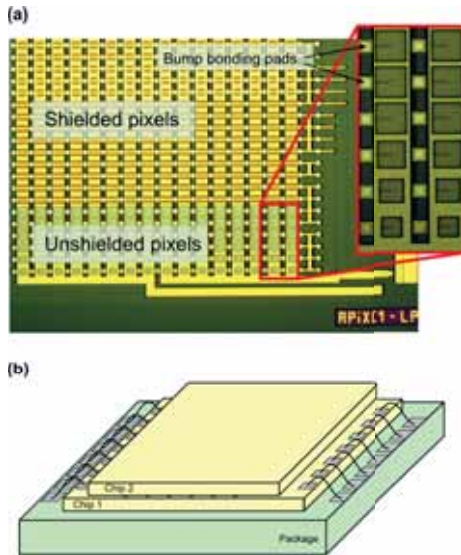


Figure 2: (a) Micrograph of the bottom chip (partial view) with detail of a group of pixel (b) Concept view of the vertically-integrated sensor assembly.

Several samples have been processed for vertical integration using bump bonding technique. The detectors were covered with a metal shield to avoid inter-layer optical cross-talk. The dark count rate per unit area has been substantially reduced from the range of MHz/mm<sup>2</sup> of the single layers to few 10s or 100s Hz/mm<sup>2</sup> at room temperature of the vertically integrated sensors, depending on the operation parameters. The variation of DCR on coincidence time,

temperature and overvoltage was assessed experimentally (Ficorella et al. 2018). A characterization with beta particles from a 90-Sr source demonstrates the correct sensor functionality (Fig. 3). A test beam at CERN has been conducted to calculate the efficiency of the sensor, confirming that it is basically due to the pixel fill factor, i.e. to the geometrical efficiency of the device. Irradiation tests with neutrons at different fluences indicate that the main source of degradation is due to the increase of the device Dark Count Rate. Measurements with protons are planned for the first months of 2018.

On the basis of these results, a new prototype has been designed and submitted to the foundry in 2017, to inspect the limits of the proposed approach in terms of efficiency, power consumption, timing resolution and scalability. The new prototype will be available for testing in early 2018.

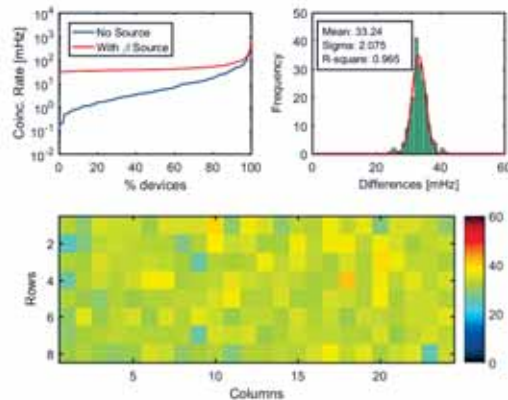


Figure 3: (a) Count rate distribution with and without  $\beta$  source. (b) Distribution of the count rate difference. (c) Map of the count rate difference.

## Selected Papers

- Ficorella, A., Pancheri, L., Brogi, P., Collazuol, G., Dalla Betta, G.-F., Marrocchesi, P., Morsani, F., Ratti, L., and Savoy-Navarro, A. (2018). *Crosstalk Characterization of a Two-Tier Pixelated Avalanche Sensor for Charged Particle Detection*. IEEE Journal of Selected Topics in Quantum Electronics 24(2).
- Pancheri, L., Brogi, P., Collazuol, G., Dalla Betta, G.-F., Ficorella, A., Marrocchesi, P., Morsani, F., Ratti, L., and Savoy-Navarro, A. (2017a). *First prototypes of two-tier avalanche pixel sensors for particle detection*. Nuclear Instruments and Methods in Physics Research, Section A: Accelerators, Spectrometers, Detectors and Associated Equipment 845, pp. 143–146.
- Pancheri, L., Ficorella, A., Brogi, P., Collazuol, G., Dalla Betta, G.-F., Marrocchesi, P., Morsani, F., Ratti, L., Savoy-Navarro, A., and Sulaj, A. (2017b). *First Demonstration of a Two-Tier Pixelated Avalanche Sensor for Charged Particle Detection*. IEEE Journal of the Electron Devices Society 5(5), pp. 404–410.

# ARDESIA

Nicola Zorzi,<sup>†</sup> Giacomo Borghi, Francesco Ficorella, Antonino Picciotto, Claudio Piemonte

ARDESIA project aims at the realization of a versatile and high-performance X-ray Spectroscopy detection system for synchrotron experiments in the energy range between 0.2 keV and 25 keV. The basic detection module is built around a 2×2 monolithic array of Silicon Drift Detectors (SDDs) realized using the technology available at FBK (Trento). The readout chain is based on a monolithic version with four channels of the CMOS preamplifier CUBE developed by Politecnico di Milano. Both the analog and the digital processing systems are developed to be compatible with several filtering and data acquisition interfaces available in different synchrotron facilities.

The role of INFN-TIFPA in the project concerns simulation, design, development of the fabrication technology, production and preliminary characterization of the SDD array detectors in close collaboration with the FBK micro-fabrication laboratory. The other INFN units involved in the project and their corresponding roles and tasks are as follows: INFN-Milan (overall project coordination, supervision of detector design, detection module development, integrated electronics and DAQ, spectroscopic measurements, support to experimentation in final applications) and INFN-LNF Frascati (detector module development, DAQ, installation of the detection modules in the synchrotron facilities, X-ray characterization measurements).

Very promising results were obtained by the spectroscopic characterization of the prototype detection modules fabricated in the previous year (Bellotti et al. 2017). In particular, the best

energy resolution (FWHM at the 5.9 keV Mn-K $\alpha$  of a <sup>55</sup>Fe source) obtained at -27°C and with a peaking time of 3  $\mu$ s is lower than 130 eV. In addition, the spectroscopic performances have been studied as a function of the filter width of the processing electronics, obtaining good results at short time widths well below 1  $\mu$ s, thus assuring operation in the Mcps range.

The activity in the 2017 was aimed at the optimization of the detection module and the construction of the spectrometer (Bellotti 2017). An electrical crosstalk among the channels of the preamplifier was discovered, mainly affecting the operation at high count rates. It was due to the stray bonding capacitances and was fixed in a second release of the 4 channels CUBE preamplifier, where the position of the pads have been changed to physically avoid the crosstalk. A study was performed to evaluate the charge sharing contribution among the adjacent channels. Thanks to the planned adoption of a collimator this effect was demonstrated to be of no concern for ARDESIA. A fully working single module spectrometer has been designed and constructed consisting of a cold finger structure that can be inserted inside the scattering chamber at the DaΦne beam-line in INFN-LNF. In a preliminary measurement session adopting a multi-element calibration source and an X-ray tube the spectrometer was fully functioning and all the 4 channels were able to acquire signals and to produce spectra. The results pointed out also the presence of electrical disturbances degrading the overall performances. After careful analy-

<sup>†</sup>Contact Author: zorzi@fbk.eu

sis a second release of the spectrometer with improved ground loops and a new strategy to connect the sensitive signals to the outputs has been manufactured and new tests in Frascati beamline have been planned.

The specific TIFPA activity was mainly focused to the development of SDD detectors with increased thickness in order to improve the X-ray detection efficiency in the energy range above 15 keV. In collaboration with FBK it was verified that wafers up to a thickness of 1mm can be effectively handled in the fabrication line. Proper silicon substrates were selected after a careful balance of technical specifications, costs and minimum order quantities. The main parameter affecting the operating conditions of the SDDs would be the silicon resistivity, defining the required bias voltage. For the acquired silicon wafers the estimated full depletion voltages are  $\sim 200$  V for the 0.8 mm thickness and  $\sim 320$  V for the 1 mm one. These high voltage values, combined with the increased thickness pose new requirements on the layout of the SDD devices, in particular with respect to the multi-guard rings termination structures and the chip border. To support a proper design, specific device simulations have been carried out in order to evaluate the lateral extension of the depletion region, the collection efficiency for photo-carriers generated close to the borders and the charge sharing between array elements. An example of the performed simulations is reported in Fig. 1, where it is shown the potential distribution inside the device when bi-

ased at operating conditions, indicating that a border region of 1.5 mm would be enough to prevent the depletion region from reaching the device border.

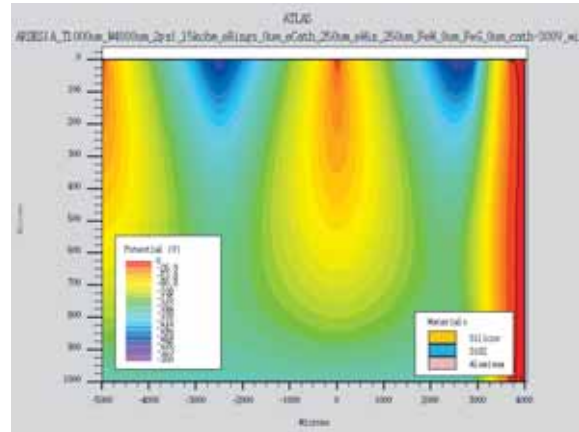


Figure 1: Simulated distribution of the electric potential in a cross section connecting two anodes of a 1 mm thick array and extending towards the chip edge. The anodes are at  $X = -5000$  and  $X = 0$  of the top surface ( $Y = 0$ ). The chip edge is at  $X = 4000$ . The applied bias is  $-300$  V at the cathodes ( $X = \pm 2500$ , top surface) and  $-180$  V at the entrance window (bottom surface).

The thick version of the ARDESIA SDD arrays has the same basic design of the previous one (with both circular and square elements of 5mm radius/side), while the chip dimension is increased by 1.5 mm with respect to the thin one so as to host a more robust termination structure and to avoid the lateral depletion region to reach the physical edge of the sensor. The estimated completion of thick ARDESIA arrays fabrication is by June 2018.

## Selected Papers

- Bellotti, G., Butt, A., Carminati, M., Fiorini, C., Balerna, A., Piemonte, C., Zorzi, N., and Bombelli, L. (2017). “The Detection Module of ARDESIA: A New, Versatile Array of SDDs for X-Ray Spectroscopy Synchrotron Applications”. *Conference Record of the 2016 Nuclear Science Symposium (NSS/MIC/RTSD), Strasbourg (France)*. IEEE.
- Bellotti, G. (2017). “ARDESIA: 4-Channels Fast SDD X-ray Spectrometer for Synchrotron Applications”. *IEEE Nuclear Science Symposium and Medical Imaging Conference (NSS/MIC), Atlanta, GA, USA, October, 21-28*.

# AXIAL

Alberto Quaranta,<sup>†</sup> Enrico Zanazzi, Viviana Mulloni, Lorenza Ferrario

The aim of project AXIAL is to study the coherent axial and quasi-axial channeling of particle within a very wide energy range, from 100 MeV to 400 GeV. From a fundamental point of view this experiment study the interaction between charged particle beams and crystals at energy ranges unexplored up to now, evidencing coherent behaviors of particles channeled through crystal planes. From a technological point of view, the coherent channeling allows the bending of energetic particle beams paving the way to the realization of beam manipulation devices. Moreover, the oscillations of charged particles between the crystal planes can be ex-

ploited for the production of electromagnetic radiation.

This year some experiments have been performed at CERN. In particular, a short bent Si crystal aligned with its main  $\langle 110 \rangle$  axes has been investigated for axial channeling steering and radiation enhancement by 120 GeV/c  $e^+/e^-$ . A comparison with a higher Z crystal (Ge) has been done, highlighting the difference in scattering and radiation generation. In fact, Ge crystals give rise to a higher radiation emission with respect to Si due to higher scattering induced by the higher Z value.

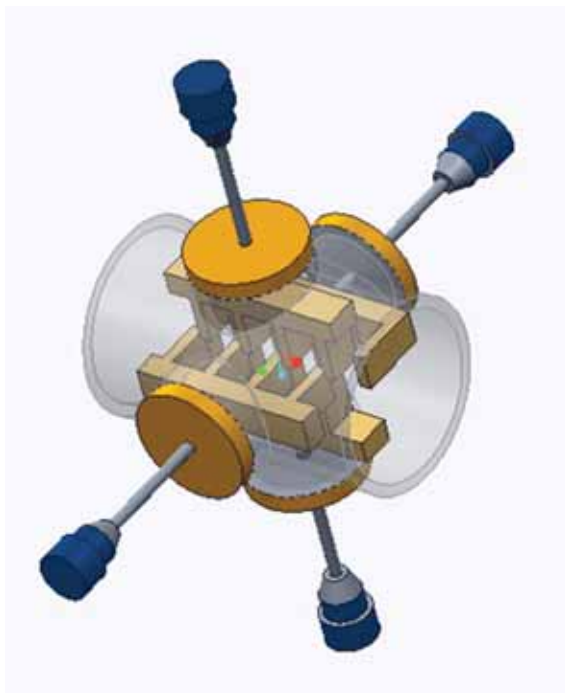


Figure 1: Sketch of the slits.

<sup>†</sup>Contact Author: [alberto.quaranta@unitn.it](mailto:alberto.quaranta@unitn.it)

As far as TIFPA is concerned, this year the activity was focused on the design for a collimation system suitable for producing beam with a divergence around 0.1 mrad at the APSS proton therapy facility. The system is based on two remotely controlled 4 jaw slit systems. The jaws are made by brass pieces modeled in order to shrink the beam cross section down to 0.1 mm or lower with a resolution of 20 microns (see Fig. 1a,b). So, two slits at a distance of 1 m should allow a beam divergence of 0.1 mrad. In order to avoid air molecules scattering worsening the divergence, the path between the two slits have to be at least in low

vacuum ( $10^{-3}$  mTorr). So, next step will be the production of a vacuum pipe with entrance and exit thin kapton windows; at the two extremities of the pipe the slits will be connected, both of them in vacuum two, and the beam cross section and divergence will be remotely controlled from the control room in order to set the better working parameters.

For the next year, after the production of the final collimator, tests at the APSS proton therapy are planned and channeling experiments through Si and Ge crystals at energies never explored before will be realized.

# KIDS\_RD

Renato Mezzena,<sup>†</sup> Benno Margesin

The main target of the KIDS\_RD project is the development of Microwave Kinetic Inductance Detectors (MKIDs) for broad band high energy resolution X-ray spectroscopy. These sensors, proposed for the first time in 2003, are thin film, superconducting microwave microresonators operating at a temperature  $T \leq T_c/10$ , where  $T_c$  is the critical temperature of the constituting material. They are called pair breaking detectors because incident photons with an energy  $h\nu > 2\Delta$  can be absorbed by breaking up Cooper pairs and creating a number of quasiparticle excitations  $N_{qp} = \eta h\nu/\Delta$  with  $\eta \simeq 0.59$  is the efficiency of creating quasiparticles and  $\Delta$  is the energy gap of the superconductor. The quasiparticles population above the thermal equilibrium changes the complex surface impedance of the superconductor  $Z_s = R_s + j\omega L_s$  where  $R_s$  is a resistive component associated with the quasiparticles, and  $L_s$  is the kinetic inductance due to the Cooper pairs. This impedance change causes a change of the quality factor and the resonant frequency of the superconducting microresonator which is coupled to a superconducting feed line. The feed line transmits a microwave probe signal at a frequency (typically 1 - 10 GHz) very close to the microresonator resonant frequency. Radiation absorbed results in a change of the transmitted signal magnitude and phase. An homodyne detection scheme is typically employed wherein an IQ-mixer produces as an output value the real part of the transmission signal in the I channel and the imaginary part in the Q channel. This readout scheme is very advantageous, because frequency domain multiplexing can be exploited in order to read hundreds of resonators. Only two coaxial lines are required to send a multi-tone probe signal to the

low temperature device and to receive, amplified by a cryogenic amplifier, the output signal. High detector Q values are required to achieve high responsivity, high sensitivity, and high multiplexing factors. Properly designed MKIDS have been demonstrated for several different application detecting electromagnetic radiation ranging from X-ray to mm waves.

The KIDS\_RD project investigates MKIDs working in both athermal and thermal mode. In the first mode, the most widely used, the electromagnetic radiation is absorbed directly by the most sensitive part (inductive) of the microresonator. In the second mode the electromagnetic radiation is absorbed by a thermal coupled absorber (pure calorimeter); the detector in this case is called TKID.

The INFN units involved in the KIDS\_RD project and their corresponding tasks are the following:

**Unit 1 - Milano-Bicocca** overall project coordination, detector design, film production and device microfabrication (in collaboration with the FBK foundation), cryogenics, device testing and data analysis.

**Unit 2 - Roma1** detector design, cryogenics, device testing.

**Unit 3 - Genova** readout and multiplexing development, data handling and analysis software development.

**Unit 4 - TIFPA** film production and device microfabrication (FBK foundation), low temperature device testing.

For the detector fabrication the Ti/TiN multilayer technology was adopted, exploiting the considerable experience gained by the Trento and Milano groups (Giachero et al. 2014) in recent years. In order to optimize the detector

<sup>†</sup>Contact Author: [renato.mezzena@unitn.it](mailto:renato.mezzena@unitn.it)



# MoVe IT

Emanuele Scifoni,<sup>†</sup> on behalf of the MoVe IT collaboration<sup>1</sup>

MoVe IT, "Modeling and Verification for Ion beam Treatment planning", is an INFN Call project aiming at exploiting particle therapy through developing new modeling approaches for physics and radiobiology of ion beams in treatment planning systems (TPS), as well as new verification devices, allowing a higher characterization of the beam, including a new dosimetry for accounting biological effects (see Fig. 1 for a graphical summary).

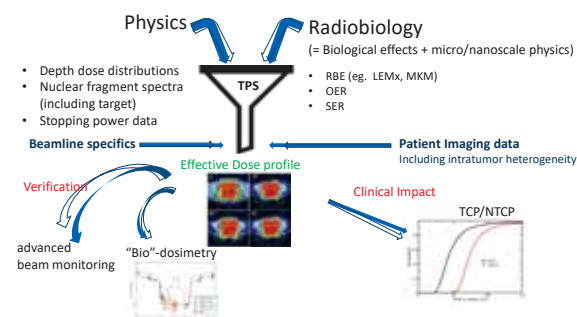


Figure 1: A graphical summary of the MoVe IT project

The first year of the MoVe IT activity was extremely intense and involved massively the TIFPA unit, which is the national responsible one, together with their strict collaborators from GSI Darmstadt and APSS protontherapy center (PTC). TIFPA researchers were involved on first line in all the 4 scientific workpackages (WP1-4) of the project, as well as in the managerial one (WPO). A short summary of the performed activities, divided in the corresponding WPs, is listed below, while more details are available in the cited publications, in

<sup>†</sup>Contact Author: [emanuele.scifoni@tifpa.infn.it](mailto:emanuele.scifoni@tifpa.infn.it)  
<sup>1</sup>for full list of contributors see [www.tifpa.infn.it/projects/move-it/](http://www.tifpa.infn.it/projects/move-it/)

the project webpage (<https://www.tifpa.infn.it/projects/move-it>) and in the First Activity Report.<sup>1</sup>

**WP1 - Radiobiological modeling for treatment planning.** The work performed in this package was benefiting from intense exchanges with the APSS PTC, as well as with the long-standing collaboration with the Biophysics department at GSI, Darmstadt (in particular Michael Kraemer and Olga Sokol). The task of the TIFPA unit was dedicated to improvements in the TRiP98 code. As a first step, several new software tools were developed, to convert different formats used for clinical data and in research TPS. The patients plans computed

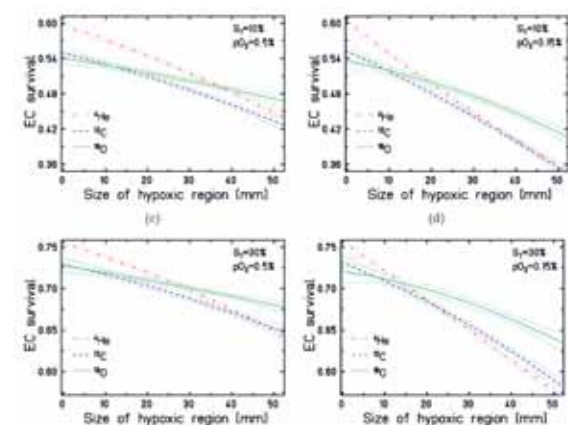


Figure 2: First full radiobiological based comparison of different ion beams in terms of entrance channel survival per same effect in the target, for different oxygenation conditions (Sokol et al. 2017).

<sup>1</sup>available at: [http://www.tifpa.infn.it/wp-content/uploads/2016/11/MOVE\\_IT\\_all\\_4.pdf](http://www.tifpa.infn.it/wp-content/uploads/2016/11/MOVE_IT_all_4.pdf)

with RayStation, the certified TPS in use at PTC, were then made possible to be imported in TRiP98. The native beam model was adapted in order to describe the proton beam in use in the center. At the same time, the study of the RBE arising from nuclear fragmentation of the target atoms has started, and Monte Carlo simulated fragment spectra, obtained by collaboration with Catania Unit (WP4), have been generated and analysed. Two approaches for radiobiological calculations of the impact of these fragments have been set up.

In the second task, related to hypoxia-oriented TPS, the first Milestone was accomplished, dedicated to the development of a method for importing functional PET data as oxygenation maps in the planning code. The new method was tested both in forward and inverse planning, allowing the generation of arbitrarily complex heterogeneous targets and testing the performance of the optimization code in restoring in any case an homogeneous survival profile, as well as in generating an optimal LET distribution.

In the meantime TIFPA unit and GSI finalized the first complete radiobiological charac-

terization of Oxygen ion beams for possible therapeutic applications (Sokol et al. 2017), including relevant comparisons with other beam modalities (Fig. 2). Finally a strong collaboration with the Torino Unit was also established for comparison of the different biophysical models and planning environments.

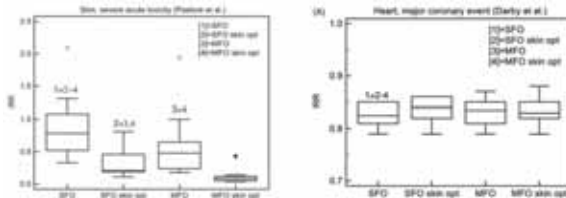


Figure 3: Relative risk, protons vs photons, for NTCP of skin and heart, in a breast tumor irradiation with different optimization methods (from Tommasino et al. 2017a).

**WP2 - NTCP and TCP.** The first task of this package was aiming at developing normal tissue complication probability (NTCP) models for exploiting and clinically characterizing dosimetric differences arising from pure TPS calculations, and in this the TIFPA unit was collaborating with the Naples unit and the APSS PTC.

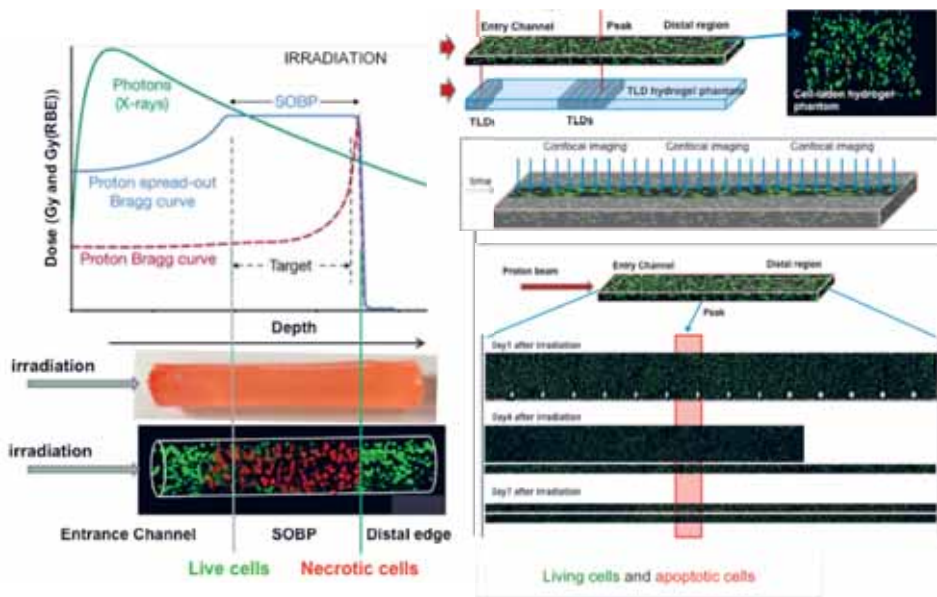


Figure 4: 3D biological phantom developed for high spatial resolution measurement of RBE and biological range extension in a proton beam, and confocal microscopy analysis procedure.

Among the first relevant results, there was a report analyzing *in silico* several toxicities in breast tumor irradiation with photons and protons (Tommasino et al. 2017a), emphasizing an almost overall advantage of the newest modality (Fig. 3). Next, a thorough analysis of patient data at the PTC was performed and a pool of patients has been selected for testing the NTCP approaches used for photons in a proton cohort, for selected case of toxicities (erythema and alopecia). Finally a set of plans and follow-up data from MD Anderson (Houston, USA) has been transferred for the comparative study of photon and proton toxicities in lung, for NSCLC patients, with the aim to interpret them and possibly provide insights for designing a more appropriate clinical trial.

**WP3 - Biological Dosimetry.** The TIFPA work in this part was dedicated to development of new devices for biological effects measurements, beyond pure physical dosimetry. Thanks also to the work performed in WP4, in upgrading the facility (see next section), it was then possible to perform the first biological experiments at the TIFPA experimental cave. The exploratory test was coupling pure physical dosimetric devices (TLD, realized and analyzed by the Naples Unit) and advanced cell supports developed with the BioTech (UniTN) partner (see Fig. 4).

## Selected Papers

- Sokol, O., Scifoni, E., Tinganelli, W., Kraft-Weyrather, W., Wiedemann, J., Maier, A., Boscolo, D., Friedrich, T., Brons, S., Durante, M., and Kämer, M. (2017). *Oxygen beams for therapy: Advanced biological treatment planning and experimental verification*. *Physics in Medicine and Biology* **62**(19), pp. 7798–7813.
- Tommasino, F., Durante, M., D’Avino, V., Liuzzi, R., Conson, M., Farace, P., Palma, G., Schwarz, M., Cella, L., and Pacelli, R. (2017a). *Model-based approach for quantitative estimates of skin, heart, and lung toxicity risk for left-side photon and proton irradiation after breast-conserving surgery*. *Acta Oncologica* **56**(5), pp. 730–736.
- Tommasino, F., Rovituro, M., Fabiano, S., Piffer, S., Manea, C., Lorentini, S., Lanzone, S., Wang, Z., Pasini, M., Burger, W., La Tessa, C., Scifoni, E., Schwarz, M., and Durante, M. (2017b). *Proton beam characterization in the experimental room of the Trento Proton Therapy facility*. *Nuclear Instruments and Methods in Physics Research, Section A: Accelerators, Spectrometers, Detectors and Associated Equipment* **869**, pp. 15–20.

## WP4 - Facilities and beamline simulations.

This WP was essential for the present and the next project advances. In particular, both hardware and software implementations for exploiting and accurately describing the beam in the TIFPA experimental cave, in collaboration with the LNS-Catania unit, have been performed. Among the important advances: the first setup of the physics line (30°) at TIFPA cave (Tommasino et al. 2017b), the initial installation of a single scattering device for spreading the beam for the biology line (0°), the full implementation and commitment of the new irradiation line in the public repository of the GEANT4 Hadrontherapy Class, allowing a tool for preparing experiments for the project as well as for external researchers (Fig. 5).

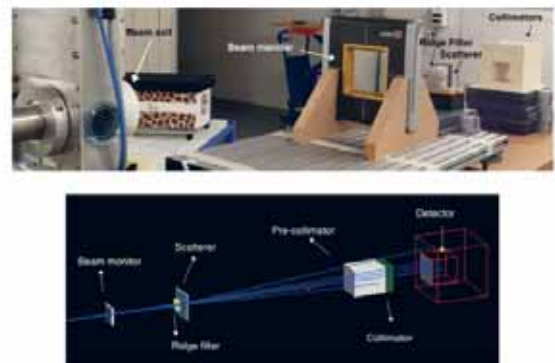


Figure 5: First experimental set up of the TIFPA "radiobiology" beamline at PTC, including scattering and energy spreading devices, with corresponding software class implemented in GEANT4.

# NADIR

Alberto Quaranta,<sup>†</sup> Marco Durante, Andrea Ficorella, Viviana Mulloni

In ion beam treatment of cancer, the early radiation-induced damage to cells begins with the damage of DNA segments and it is the result of the spatial distribution of inelastic interactions of single ionizing particles (track structure). For this reason, radiation damage cannot be accurately described by conventional dosimetric quantities, such as absorbed dose and linear energy transfer. Recent investigations on the stochastic of particle interactions in nanometre-sized volumes demonstrated the possibility to correlate quantities derived from the ionization cluster-size distributions to radiobiological effects. The development of gas-based apparatus, for example the Startrack at the Legnaro National Laboratories (Padova, Italy), paved the way for the investigation of the ionization cluster-size distributions of different particles and ions on a nanoscopic DNA level. Experimental investigations combined with Monte Carlo simulations demonstrated

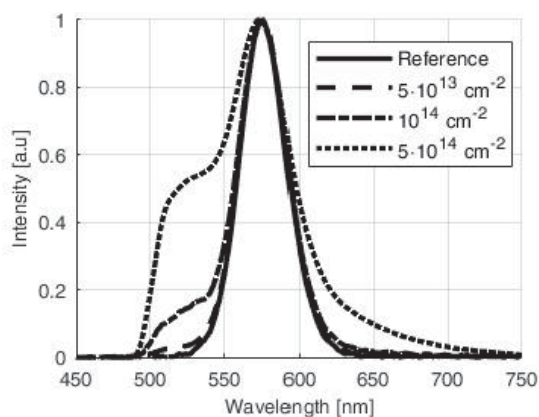


Figure 1: Spectra from quantum dots embedded in PVA after different proton irradiation fluences.

<sup>†</sup>Contact Author: [alberto.quaranta@unitn.it](mailto:alberto.quaranta@unitn.it)

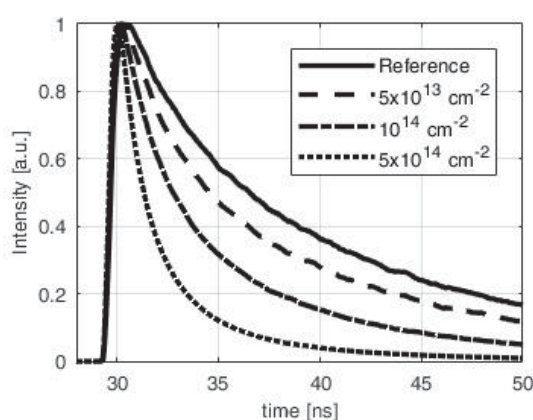


Figure 2: Lifetimes from quantum dots embedded in PVA after different proton irradiation fluences.

the possibility of a new metrology of ionizing radiation based on nanodosimetric descriptors.

In this framework, medical radiation treatments would benefit from the development of portable nanodosimeters, i.e. relatively compact and light devices that quantify the energy released by ionizing radiation within nanometric volumes. A possibility could be the use of Quantum Dots (QDs) as active material, since their size is comparable with those of the most probable radio-sensitive volumes of biological systems.

In our study, CdSeS/ZnS quantum dots (-COOH functionalized) with an emission wavelength of 575 nm were embedded in a polyvinyl alcohol matrix with a QD concentration of  $4.5 \times 10^{14} \text{ cm}^{-3}$ . Drop-casted films with 20  $\mu\text{m}$  thickness were irradiated at the Legnaro National Laboratories (Padova, Italy) using the

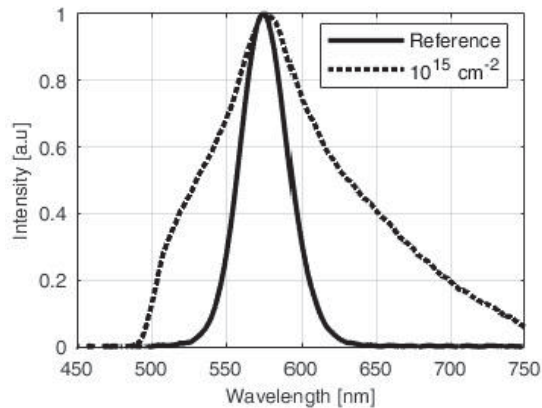


Figure 3: Spectra from quantum dots embedded in PVA before and after Helium irradiation .

AN2000 Van de Graaff accelerator. Three samples were irradiated with 2 MeV  $H^+$  ions at three different ion fluences, namely  $5 \times 10^{13} \text{ cm}^{-2}$ ;  $10^{14} \text{ cm}^{-2}$ ;  $5 \times 10^{14} \text{ cm}^{-2}$  while the other three samples were irradiated with 2 MeV  $He^+$  ions at ion fluences of  $10^{14} \text{ cm}^{-2}$ ;  $2 \times 10^{14} \text{ cm}^{-2}$ ;  $10^{15} \text{ cm}^{-2}$ . The range of  $H^+$  and  $He^+$  in polyvinyl alcohol, calculated with SRIM2013, is of  $68 \mu\text{m}$  and  $9.6 \mu\text{m}$ , respectively. So, protons go through the whole film thickness releasing an amount of energy of 365 keV, while  $He^+$  ions are implanted in the target releasing their entire energy (2 MeV). Steady-state and time-resolved fluorescence measurements were acquired using an optical setup equipped with a PicoQuant PCL 800-B picosecond pulsed laser diode with emission wavelength of 470 nm, a working frequency of 10 MHz and a pulse width of 300 ps. Steady-state measurements were acquired with an OceanOptics QE65000 high-efficiency portable spectrometer equipped with a silica fiber. Time-resolved measurements were carried out using a PicoQuant PicoHarp 300 accessory based on a silicon photomultiplier detector (NUV from AdvanSiD). Samples irradiated with  $H^+$  showed no significant changes in their luminescence spectra for ion fluences up to  $10^{14} \text{ cm}^{-2}$  (Fig. 1). On the other hand, an evident lowering of the luminescence lifetimes was measured with the increasing flu-

ence (Fig. 2). This effect can be attributed to the formation of dangling orbitals resulting either from radiation-induced break of -COOH ligand units or from network defects near the surface, which act as charge trapping centres at the QD surface. In samples irradiated with  $He^+$  a higher damage and a broadening of the QD emission spectrum were observed and correlated to the contribution from radiation-induced defects within the PVA matrix (Fig. 3). Moreover, a more marked decrease of luminescence lifetime is observed due to the higher damage level induced by the ion species (Fig. 4).

Summarizing, these tests outline for the first time how QD luminescence decay times are more sensitive to radiation damage, evidencing how this parameter can be used for dose monitoring systems. Further studies are needed in order to correlate the observed changes of the optical properties with the dose and more detailed structural analyses are necessary for identifying the point defects which are responsible of the observed trends. In the meantime, a Monte Carlo analysis has been developed in order to characterize the damage effects on carbon dots induced by proton beams, and proper ionization cross sections containing the Mermin solution for the dielectric function has been used for the first time for evaluating the radial dose within nanometric carbon volumes.

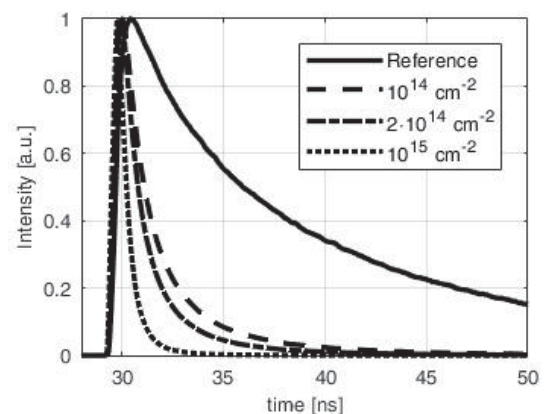


Figure 4: Lifetimes from quantum dots embedded in PVA after different Helium irradiation fluences.

# New Reflections

William Jerome Burger,<sup>†</sup> Roberto Battiston, Nicola Bazzanella, Claudio Cesari, Riccardo Checchetto, Roberto Iuppa, Christian Manea, Antonio Miotello

The TIFPA participates in the interdisciplinary 3-year experiment New Reflections in the Solar System of the INFN technological research group CSN5. The experiment has received funding to develop innovative laser technology for space applications.

The activity at Trento concerns the potential applications of laser ablation. Laser ablation refers to the ejection of material in the form of vapor and gas from the surface of a solid which is heated to high temperature by a laser beam. The momentum of the ejected material results in an equivalent impulse in the opposite direction, normal to the surface of the object. The impulse may be used to propulse a spacecraft, or to deviate the trajectories of artificial and natural satellites.

Laser ablation represents an interesting solution for the problem of space debris, i.e. the population of non-functional, artificial satellites and their fragments in low Earth orbit (LEO). The mass of the LEO population is estimated to be 3000t composed of objects ranging in size from small collision fragments (1-10 cm) to spent rockets and fully intact satellites.

The debris population with dimensions of 1-10 cm in LEO has increased the most rapidly in the last decade (Fig. 1). The rapid increases observed in 2007 and 2009 are due to the fragments produced by the Chinese FY-1C anti-satellite missile test, and the collision of the Iridium33 and Cosmos satellites. The orbital velocities of the small objects,  $\sim 10$  km/s, may cause severe or catastrophic damage to functional satellites.

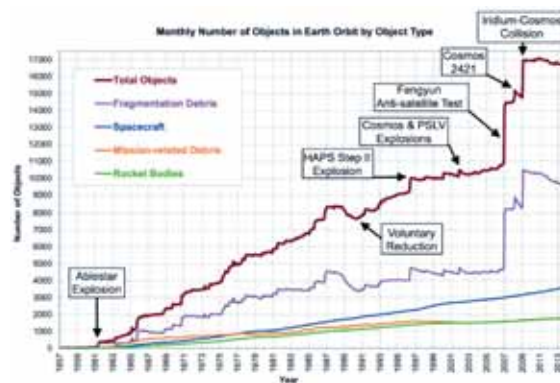


Figure 1: The evolution of the different debris populations since the first satellite launch by the URSS, Sputnik-1 in 1957.<sup>1</sup>

In the initial year of the New Reflection project, a simulation program was developed to assess the performance required by ground and space laser systems to lower the orbital altitude of debris to the height of the upper atmosphere (200 km), in terms of the debris mass and orbit (Battiston et al. 2017b).

The IdEA laboratory of the University of Trento has joined the group in the current year. The Pulsed Laser Deposition (PLD) facility of the IdEA laboratory is equipped with a nanosecond pulse width KrF excimer laser, with a variable 1-100 Hz repetition rate. The group has an important experience, theoretical as well as experimental, in the field of laser ablation.

The important parameters for debris mitigation are the ablation threshold and the pulse-energy-to-impulse coupling coefficient of aluminum, a common space construction material. The coupling coefficient has been measured at

<sup>†</sup>Contact Author: [william.burger@tifpa.infn.it](mailto:william.burger@tifpa.infn.it)

<sup>1</sup>NASA (2014), <https://gizmodo.com/a-history-of-garbage-in-space-1572783046>

the PLD laboratory using the observed angular deflection of a  $1.5 \times 1.5 \times 0.5 \text{ cm}^3$  Al target mounted on a ballistic pendulum in a vacuum chamber. The experimental set-up is shown in Fig. 2.



Figure 2: The Al target mounted on the ballistic pendulum in the KrF laser beam, blue arrow (left). View of the PLD laboratory, the angular deflection of the target is obtained from the displacement of a second, reflected laser beam, in the vertical direction, red arrows (right).

A preliminary result for the coupling coefficient,  $5.3 \cdot 10^{-5} \text{ N/W}$  obtained with a laser pulse energy density of  $0.8 \text{ GW/cm}^2$ , may be compared to the values used in (Battiston et al. 2017b) for the evaluation of the ground and space laser configurations,  $2 \cdot 10^{-5} \text{ N/W}$  between  $0.5$  and  $0.8 \text{ GW/cm}^2$ .

The primary objectives for the coming year are the optimization of the coupling coefficient measurement, and an extension of the measurement to materials suited to the applications of propulsion and asteroid deflection.

Fig. 3 shows the evolution with time of the number of detected near Earth asteroids (NEA). In 2005, NASA set the goal to detect 90% of the NEA with a diameter greater than 1 km. The impact of a 1 km diameter asteroid is expected to have an important regional effect,

while diameters exceeding 10 km would produced world-wide consequences.

Laser ablation is one option considered for asteroid impact avoidance. In order to be effective, the counter-measures considered should be applied well in advance of the expected impact date. Consequently the laser system should be deployed in space.

Ablation also plays an important role during the breakup of meteorites in the atmosphere. The ablation threshold and coupling coefficient of meteorites are important input parameters for simulations which trace the meteorites through the atmosphere to predict the mass, velocity and trajectory of the remnants which represent a risk for commercial aircraft,<sup>2</sup> as well as for populated regions on the ground.

We have recently received from the University of Central Florida in Orlando, USA, in collaboration with NASA, samples of asteroid simulant material, which mimic the mineralogy of the type C1 carbonaceous chondrite meteorites. For the propulsion application, the candidate materials will be evaluated in terms of efficiency and required launch mass. Laser propulsion may be considered for satellites in space, small or micro satellite launches and interplanetary travel.

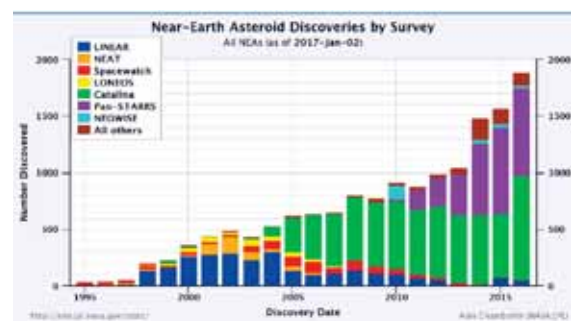


Figure 3: The time evolution of the number of detected NEA.<sup>3</sup>

## Selected Papers

Battiston, R., Burger, W., Cafagna, C., Manea, C., and Spataro, B. (2017b). *A Systematic Study of Laser Ablation for Space Debris Mitigation*. *Journal of Space Safety Engineering* **4**, pp. 36–44.

<sup>2</sup>Emanuelli, M. (2014), <http://www.spacesafetymagazine.com/space-on-earth/malaysia-flight-370/space-debris-meteorite-forecast-safer-aviation/>.

<sup>3</sup>Chamberlin, A. (2017), <https://commons.wikimedia.org/w/index.php?curid=5041231>

## Redsox2

Irina Rashevskaya,<sup>†</sup> Giacomo Borghi, Francesco Ficorella, Giancarlo Pepponi, Antonino Picciotto, Nicola Zorzi

The collaboration of the REDSOX project worked on several avenues pertaining to the development of silicon drift detectors (SDDs). In 2017 a lot of work was done by the TIFPA group in the REDSOX2 collaboration for the characterisation of a large number of sensors produced by FBK in 2016. These activities required the execution of a large quantity and variety of measures. The measurements on all Redsox lots have made an important contribution to the development of the FBK drift chamber production process on 6-inch wafers and resulted in an increase of the production yield up to 80% in the two batches fabricated in 2016.

In 2017 the activities on detector characterisation and qualification has been focused on the optimisation of test equipment and automatisa-tion of the test procedure.

The important work is in progress for the realization of the SESAME detectors that INFN will realise for the XAFS line at Jordanian synchrotron facility, which will be the first major international research center in the Middle East. The XAFS prototype was built around a linear array of eight  $9\text{ mm}^2$  SDD cells specifically designed for the high event rate of the beam line. The new support kits for testing XAFS structures were designed and produced. To optimize the test process and apply a bias on all eight cells of the structures at the same time, a new probe-card has been designed and produced. Eight prototypes were installed and tested on the beam lines in different beam tests at the XAFS line at the Elettra synchrotron in Trieste .

The sensors with new improved version of the TwinMic detector based on the 8 square cell array (3+5) have been tested. The best sensors were mounted and implemented in beam test at the end of 2017 at the Elettra synchrotron in Trieste.

Some tested sensors were used as proto-types for future experiments with possible as-trophysical applications (THESEUS and XGS). (Campana et al. 2016) The Redsox detectors were implemented in FLARES to demonstrate the high potential of a technique that combines ultra-pure scintillating crystals with arrays of high performance silicon drift detectors. (Capelli et al. 2017)

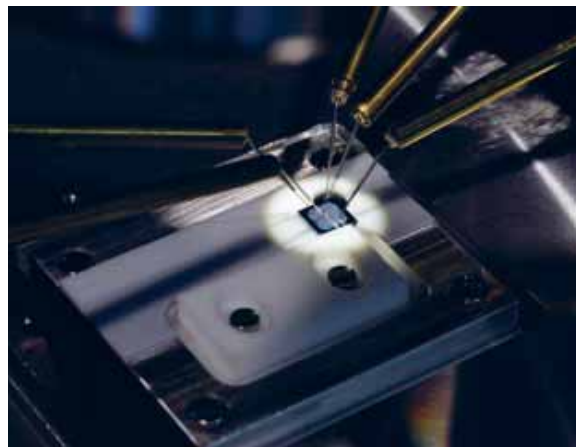


Figure 1: PixDD array of  $4\times 4$  under test.

The PixDD is designed to address low-energy X-ray imaging applications where fast read out is important for the performance. Two devices having pixel sides of 500 and 300  $\mu\text{m}$  have been designed in arrays of  $4\times 4$  and  $32\times 32$

<sup>†</sup>Contact Author: [irina.rashevskaya@tifpa.infn.it](mailto:irina.rashevskaya@tifpa.infn.it)

respectively.

The  $4\times 4$  array PixDD produced in 2016 were measured at the probe station after implementation of new support kits (see Fig. 1), and then sent to Karlsruhe Institute for Technology (KIT) for the first stub bump bonding test. This consisted in depositing gold balls on the anodes of two sensors, using a ball bonder, and then bonding the two devices together by means of a dedicated machine that aligns the chips before proceeding with the mating. The parameters for the deposition of the gold balls were tuned using different devices available at KIT, and this resulted in a non-optimized proce-

dure. The bonded devices failed after the chips separation. In a meeting at KIT in February we reviewed the bonding process and decided to use the larger PixDDs ( $32\times 32$  array) to allow our KIT collaborators to optimize the parameters with a device having the same material layer stack. Other  $4\times 4$  PixDDs were also sent to KIT for a new test.

A new production run is programmed for 2018 to implement design optimizations of the detectors. New devices and new test structures are conceived and introduced in the wafer layout in a forthcoming production.

## Selected Papers

Campana, R. et al. (2016). *A compact and modular X and gamma-ray detector with a CsI scintillator and double-readout Silicon Drift Detectors*. Proc. SPIE Int. Soc. Opt. Eng. **9905**, p. 99056I.

Capelli, S. et al. (2017). *The FLARES project: An innovative detector technology for rare events searches*. Nucl. Instrum. Meth. **A845**, pp. 334–337.

# SEED

Lucio Pancheri,<sup>†</sup> Fabio Acerbi, Alessandro Ferri, Damiano Martorelli, Matteo Perenzoni

SEED project was born with a two-fold objective: to develop an innovative technology for monolithic sensors in CMOS technology and, at the same time, to demonstrate the possibility of a technology transfer between INFN and industry in the field of microelectronics. From the technology point of view, the goal of the project is the development of a monolithic fully-depleted sensor suitable for a wide range of energies, embedding different dedicated IP blocks. This achievement will demonstrate how monolithic CMOS can meet different requirements in radiation detection applications with a performance that goes beyond the current state of the art. At the same time, the active participation of an industrial partner (LFoundry) providing support on process technology, offers the unique opportunity to create a synergy between microelectronic designers and a silicon foundry, which has been sought for a long time by the national scientific community.

The first phase of the project has been devoted to the tailoring of the CMOS fabrication technology to include the particle sensors. The optimal substrate doping and process parameters have been identified by means of an extensive TCAD device simulation campaign, which was carried out at TIFPA, in tight collaboration with the foundry process engineers.

In parallel, a first test chip including pixels with different geometry parameters has been designed at INFN Torino. This chip was conceived as a first test bench for the proposed technology, suitable for an experimental char-

acterization with particles, X-rays and optical sources. A layout of the implemented pixel, featuring  $50\mu\text{m} \times 50\mu\text{m}$  area, is shown in Fig. 1.

A first MPW run has been produced in 2017 on wafers with a thickness of  $300\mu\text{m}$ . The first tests demonstrated the possibility of fully depleting the sensors and the complete functionality of electronics (Olave et al. 2017). A first test campaign showed a depletion voltage lower than 200V and a pixel electronic noise of 40 electrons rms. The first spectra were acquired with an X-ray source of  $^{55}\text{Fe}$  and with a pulsed laser source. A complete characterization campaign of the produced sensors is currently under way.

A new MPW run is currently under way, with the objective of further optimizing the production process.

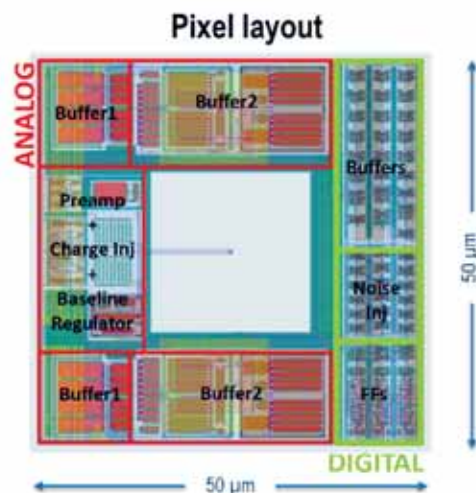


Figure 1: SEED prototype pixel layout

## Selected Papers

Olave, E. J., Panati, S., Cossio, F., Rivetti, A., Da Rocha Rolo, M., Demaria, N., Pancheri, L., Mattiazzo, S., Giubilato, P., and Pantano, D. (2017). “MATISSE: A Low power front-end electronics for MAPS characterization”. *TWEPP-17*. POS.

<sup>†</sup>Contact Author: lucio.pancheri@unitn.it

# SICILIA

Maurizio Boscardin,<sup>†</sup> Pierluigi Bellutti, Giacomo Borghi, Sabina Ronchin

The scientific goal of the SICILIA project is to detect high fluxes (about  $10^7$  pps/m<sup>2</sup>) and fluences (about  $10^{14}$ ) of heavy-ions in order to determine the cross sections of very rare nuclear phenomena, such as double charge exchange reactions, of impact for determining nuclear matrix elements entering in the expression of the neutrino-less double beta decay half-life. The main issues for these experiments are the high energy ( $\Delta E/E \sim 1/1000$ ), mass ( $\Delta m/m \sim 1/200$ ) and angular resolution ( $\Delta\theta \sim 0.1^\circ$ ) required in order to unambiguously select the reaction channels of interest and extract the relevant information from energy spectra and absolute cross section angular distributions. Due to the very low cross sections, these features must be guaranteed at fluences which exceed by far those tolerated in state-of-the-art solid state detectors, typically used in present experiments of this kind.

The Silicon Carbide technology offers today an ideal response to such challenges, since it gives the opportunity to combine the excellent properties of silicon detectors (resolution, efficiency, linearity, compactness) with a much larger radiation hardness (up to five orders of magnitudes for heavy ions), thermal stability and insensitivity to visible light. However, no commercial detector exists and a significant upgrade of present devices is required in terms of the thickness of the active region and of the dimension of the detection area.

The role of INFN - TIPFA in the project concerns the design, the development of the fabri-

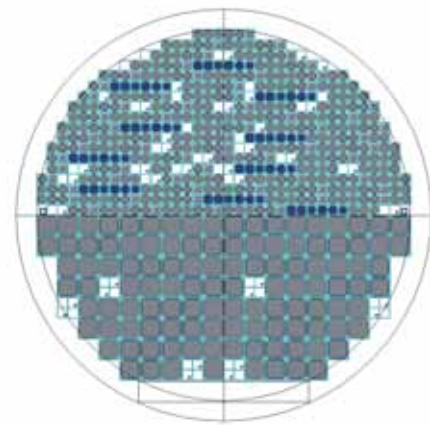


Figure 1: Wafer layout drawing

cation technology, the production, and the preliminary characterization of detectors based on a Schottky diode realized on a silicon carbide substrate. In detail, the fabrication process has been defined in partnership with INFN Catania and CNR IMM and the process flow has been optimized in order to adapt the technologies developed at CNR to the FBK capability.

The main process steps which have been defined for the production of SiC sensors in FBK are:

- (i) the use of a boron implant to define a junction termination extension (JTE) structure all around the diode;
- (ii) the deposition of Au or Pt as metal for the rectifier barrier.

An original layout was then developed to test the new fabrication process in a dedicated production run. The main goals of this layout are:

<sup>†</sup>Contact Author: boscardi@fbk.eu

- (i) test the process flow of the technology and measure the main parameters of the process
- (ii) produce detectors having different JTE structure designs and investigate how these structures can be used to control the electric field along the device edge and to maximize the breakdown voltage of the devices
- (iii) study if it is necessary to have a guard ring (GR) structure around the diode to define the active area of the sensor

To achieve these goals, we designed differ-

ent small test diodes and test structures and six different detector layouts, which have been produced in two different dimension:  $2.5 \text{ mm} \times 2.5 \text{ mm}$  and  $5 \text{ mm} \times 5 \text{ mm}$ . These layouts combined different solutions for the JTE structure and the GR structure.

The first wafers have been processed on 4-inch SiC material with an epitaxial layer of  $10 \mu\text{m}$  so due to the thin epi layer the device realized on the first batch could be used as for the process assessment but also as detectors for low energy particles. The electrical tests are ongoing.

# Activities starting in 2018

## ASAP

**Research outline** The ASAP project aims at improving the technology demonstrated in the APiX2 project with the goal of building a buttable module of suitable area, in the order of 20 mm<sup>2</sup>, and of reducing the noise characteristics and the thickness of the sensor. As for the APiX2 demonstrator, the ASAP sensor is based on the concept of vertically-integrated avalanche pixels made of two layers, using coincidence to reject thermally-generated spurious signals.

In the ASAP project, the vertical interconnection of the two layers is carried out by propagating the electrical signals from the upper layer to the lower layer with the technique of hybrid bonding. In contrast with the technique of bump-bonding, that requires a separate post-processing stage whereby the upper and lower chips are aligned and paired together (a technique employed successfully for the prototypes developed in APiX2 project), the possibility to perform the bonding at wafer level allows the thinning of the upper layer down to 10 μm or less. This possibility is particularly appealing for the ASAP detector because it allows the detection of ionizing radiation down to very low energies (hundreds of keV), a crucial feature for the imaging of beta-emitters. In addition, a more scaled technology will be adopted, offering the opportunity of minimizing the area of the readout circuitry, and thus improving the pixel area efficiency. The chosen technology will be also optimized for imaging applications, thus intrinsically offering a reduced thermal generation rate and therefore a lower noise. The ASAP project will further explore the application of the technology in particle tracking for HEP and space applications, as well as in the imaging of beta-tracers for radio-guided surgery.

**INFN groups** Pisa, TIFPA, Pavia, Padova.

**Principal Investigator** Pier Simone Marrocchesi, INFN Pisa

**TIFPA team** Lucio Pancheri (coordinator), Andrea Ficorella, David Macii, Marco Zanolì, Majid Zarghami.

## DEEP 3D

**Research outline** In the past decade thermal neutron tomography has been used from high technological industries in non-destructive testing (NDT). Neutron imaging provides information on materials and structures otherwise opaque to X-rays and this makes neutron radiography and tomography quite powerful for a number of applications: cracks and heterogeneities in metal components, water contamination in mechanical structures, internal structures within geological samples, oil and fuel distribution in car engines and fuel injectors, safety-sensitive aircraft or automotive components, archaeological samples and many others.

Despite silicon is not sensitive to neutrons, by using converter materials it is possible to convert neutrons in charged reaction products that can be easily detected by silicon. In order to increase the reaction products detection probability, 3D geometries have been previously developed by the

Trento group in the CSN5 HYDE project. In particular, the 3D sensors have cavities obtained by DRIE (Deep Reactive Ion Etching) with a depth of about  $25\ \mu\text{m}$ , that will be filled with the converter.

The DEEP 3D (Detectors for neutron imaging with Embedded Electronics Produced in 3D technology) project plans two branches of parallel activities: the first part aims at building a hybrid detector module consisting of a 3D detector connected to a Medipix read-out, whereas the second part aims at the development of a monolithic detector. The first part represents an important step forward in the current state of the art in thermal neutron detectors at relatively low cost, while the second part is a more futuristic solution able to exceed the limits of hybrid 3D neutron detectors, thanks to the reduction of the pixel size flanked by an incomparable gamma-ray rejection ratio while maintaining the same high neutron detection efficiency.

The final demonstrator for the first part of the project will be a 3D silicon detector filled with enriched LiF coupled with a Medipix-2 chip, that will be characterized under neutron fluxes and, as final goal, by capturing images of small objects. LiF filling of the cavities will be performed on the assemblies in collaboration with the Czech Technical University in Prague, by pressing the enriched LiF powder, with average grain size smaller than  $1\ \mu\text{m}$ , inside the cavities of the detector.

For the second part, the demonstrator will have smaller area and a less sophisticated electronics as compared to the hybrid detector, in order to maximize the flexibility in the testing, but it will have globally a better performance. The final goal is to characterize the performance of the device under neutron fluxes.

The monolithic design is expected to increase the spatial resolution performance by a reduction of the pixel pitch and by changing the converter material from lithium fluoride to enriched Boron. The Boron converter allows to obtain better spatial resolution for reaction products having a shorter range. Boron deposition cannot be performed after the assembly with the chip due to the relatively high temperature required in LPCVD ( $\sim 400\ ^\circ\text{C}$ ). On the other hand, the minimum pixel size is constrained by the bump dimensions that makes it difficult to shrink values much below  $50\times 50\ \mu\text{m}^2$ . The pad and the bump bonding, moreover, contribute to the input capacitance that affects the noise performance. The monolithic approach is intrinsically not affected by these problems.

3D technology applied to monolithic detectors for neutron imaging can be considered a revolutionary development, and paves the way also to the application of this approach to other types of radiation detectors, making it possible to add attractive options, such as 3D electrodes and Slim/Active edges on top of the intrinsic features of monolithic detectors, so as to further improve their performance, e.g., in terms of radiation hardness, speed, etc.

**involved external institutions** Leibniz Institute of Photonic Technology (IPHT) Jena (Germany), Institute of Experimental and Applied Physics — Czech Technical University in Prague

**INFN groups** TIFPA, gruppo collegato di Cosenza

**Principal Investigator** Roberto Mendicino, TIFPA

**TIFPA team** Roberto Mendicino (coordinator), Gian-Franco Dalla Betta, Alberto Quaranta, Matteo Perenzoni, Giacomo Borghi

## ELOFLEX

**Research outline** The aim of the 2-year experiment ELOFLEX (Electro-Optical FLEXible detectors for mixed radiation fields) is to study the feasibility for the realization of flexible detectors for real-time dose measurements in mixed radiation fields. Such detectors should be obtained by combining organic semiconductor detectors (OSD) with quantum dots based scintillators (QDS). OSD have been demonstrated to be cheap and effective systems for the fabrication of flexible X-ray detectors suitable for measuring the real time irradiation dose at rates of mGy/s. On the other side, during the last years the interest on QDS is increasing owing to the stability of the luminescent nanocrystals

and to the possibility to tune their emission wavelength in order to match the efficiencies of different photo-detectors. Moreover, during the experiment NADIR the possibility to use QD for the off-line evaluation of the dose released within nanoscale volumes has been explored with promising results. In the first part, ELOFLEX experiment will test the response of both detecting systems to different radiations, namely therapeutic proton beams, X-rays and gamma-rays at different energies. Both the response intensity and its evolution with the radiation dose will be measured. It is worth noting that in most cases such systems have been never tested before with all of these radiations. After this study, it will be possible to select the best conditions for the preparation of innovative detectors that will be obtained by joining OSD and QDS in order to realize a novel hybrid flexible detector systems. As a first approach, electrical and optical signals will be collected separately from each detector during the irradiation. A more ambitious device will be developed, as a proof of principle, by directly integrating the QDS onto OSD device in such a way that the scintillation light is directly detected and converted into an electrical signal by the organic semiconductor layer.

**involved external institutions** University of Trento — Department of Industrial Engineering, University of Bologna — Department of Physics and Astronomy.

**INFN groups** TIFPA, Bologna.

**Principal Investigator** Alberto Quaranta, TIFPA

**TIFPA team** Alberto Quaranta (coordinator), Enrico Zanazzi, Matteo Favaro, Andrea Ficorella, Viviana Mulloni.

## ISOLPHARM-Ag

**Research outline** The INFN ISOLPHARM project aims to go beyond the state of the art by developing GMP grade radiopharmaceuticals prototypes exploiting RIBs produced in the second generation Italian ISOL facility, now in the construction phase, named SPES, which will make use of a recently acquired and installed 70 MeV cyclotron. The driving idea is the production of high specific activity, carrier-free radionuclides thanks to the extreme purity of the ISOL radioactive beams.  $^{111}\text{Ag}$  is regarded as a very promising radionuclide for therapy. Its decay properties make it, without any doubt, a very good candidate for internal radiotherapy. It is a  $\beta$ -emitter with medium half-life (7.45 d), convenient  $\beta$ -energy and medium tissue penetration (average  $\beta$ -energy 360 keV and average tissue penetration  $1.8\ \mu\text{m}$ ) and low percentage of associated  $\gamma$ -emission. The ISOLPHARM\_AG project for CSN5 will have three main goals, based on the application of the Isolpharm method to the production of  $^{111}\text{Ag}$  radionuclides as radiopharmaceuticals precursors:

- Proof of principle of the possibility of producing and releasing  $^{111}\text{Ag}$  from the SPES fission target, using production, diffusion and effusion complex Monte Carlo codes on a dedicated grid computing infrastructure
- Study of the Ag chemistry with the aim of developing purification techniques from contaminants, synthesizing suitable chelators for  $\text{Ag}^+$  with controlled thermodynamic, kinetic and toxicity properties
- Development of targeting agents to transport  $^{111}\text{Ag}$  to defined tumor cells

**involved external institutions** University of Padova — Department of Physics and Astronomy, University of Trento — Department of Industrial Engineering, University of Padova — Dipartimento di Scienze del Farmaco.

**INFN groups** Laboratori Nazionali di Legnaro, Padova, TIFPA.

**Principal Investigator** Alberto Andrichetto, LNL

**TIFPA team** Antonella Motta (coordinator), Walter Tinganelli, Devid Maniglio, Alberto Quaranta.

## TIMESPOT

**Research outline** This is a 3-year project approved as a CSN5 “Call”. The goal is the development and implementation of a complete integrated system for tracking having very high precision both in space (100  $\mu\text{m}$  or less) and in time (100 ps or less) per detection channel. The main use and scope is in HEP experiments at high luminosity (e.g., upgrade of LHCb VELO), where the high density tracking, both in space and time, is an issue. The approach is based on 3D geometry Silicon and Diamond pixelated sensors, dedicated integrated front-end and pre-processing chip (time measurement electronics) in 28 nm CMOS, and real-time processors for data elaboration both at front-end and back-end level (fast tracking algorithms). TIFPA is responsible for WP1: 3D Si sensors development and characterization, and is also involved in WP6: System integration and tests.

**involved external institutions** CERN, FBK, GSI, Augsburg University, Manchester University.

**INFN groups** Bologna, Cagliari, Ferrara, Firenze, Genova, Milano, Padova, Perugia, TIFPA, Torino.

**Principal Investigator** Adriano Lai, INFN Cagliari

**TIFPA team** Gian-Franco Dalla Betta (coordinator), Giacomo Baldi, Maurizio Boscardin, Mostafa El-Khatib, Roberto Iuppa, David Macii, Giulio Monaco, Kenji Nardone, Giovanni Verzellesi.

## XDET

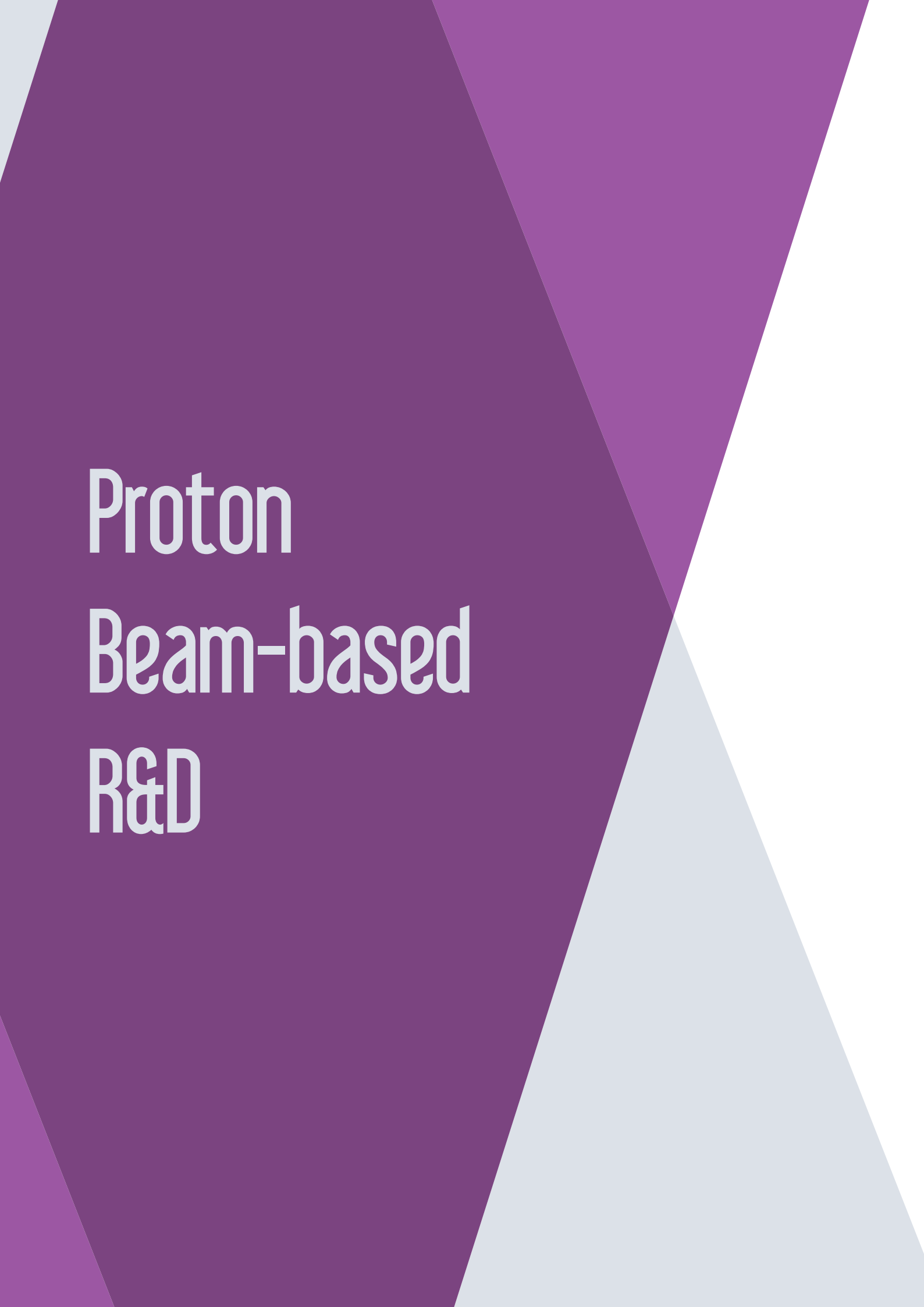
**Research outline** The use of large accelerator-driven X-ray sources, such as synchrotron light and free-electron lasers (FEL) facilities, continues to grow and expand to many scientific disciplines. A large number of synchrotron radiation sources is available around the world. Each of them features a large number of beam-lines, providing photons with wavelengths spanning from the atomic level to biological cells, which can be used as probes for advanced research in material science, physical and chemical science and in the medical and pharmaceutical fields. On the other hand, newly proposed X-ray FELs, with their outstanding properties in terms of brilliance and pulse duration, can offer unprecedented capabilities in penetrating the microscopic structure of organic and inorganic systems, new materials and matter under extreme conditions and in recording and understanding time evolution of fast biochemical phenomena at the nanoscale. These facilities are now driving the state of the art of X-ray science, therefore shaping the requirements for many types of detectors.

The XDET project aims to develop advanced instrumentation for X-ray imaging applications compliant with the very challenging specifications set by the FEL environment in terms of input dynamic range, processing speed, amplitude resolution and radiation hardness. The collaboration also plans to extend the use of the developed instrument to synchrotron light source experiments. The research will be pursued by following two different approaches, one based on hybrid, the other based on monolithic sensor technology. The final deliverable for the monolithic sensor research line will consist of a detector prototype based on a two-tier structure and including a monolithic pixel sensor layer with integrated analog front-end and a digital layer incorporating high density memories and readout circuits. For the hybrid sensor research line, the collaboration will finally deliver the main building blocks for the construction of an X-ray camera based on hybrid technology. Vertical integration processes, in particular those enabling the fabrication of peripheral, low density through silicon vias (TSV), will also be explored by the collaboration in view of the design of a 2-tier, 4 side buttable detector tile.

**INFN groups** TIFPA, Pavia, Torino, Pisa.

**Principal Investigator** Lodovico Ratti, INFN Pavia

**TIFPA team** Lucio Pancheri (coordinator), Giulio Monaco, Giacomo Baldi, Maurizio Boscardin, Sabina Ronchin, Giovanni Verzellesi, Majid Zarghami.



# Proton Beam-based R&D

Francesco Tommasino

francesco.tommasino@unitn.it

Coordinator,

TIFPA Protontherapy Experimental Room Activities



During 2017 the activities in the Experimental Room of the Trento Proton Therapy Centre (PTC) reached full operation. The experimental campaign dedicated to the characterization of the fixed proton beam at the  $30^\circ$  beam line has been completed, and results are summarized in a NIM A publication (Tommasino et al. 2017b). At the same time, after preliminary design and simulation work, a single scattering system has been tested at the  $0^\circ$  beam line, which allows obtaining large field irradiation (i.e.  $6 \times 6 \text{ cm}^2$ ) with a homogeneity in the order of 90%. This allows expanding the spectrum of experiments that can be performed at the PTC, paving the way for radiobiology research. Importantly, the geometry of the passive scattering beam line will be part of the Hadrontherapy class of the Geant4 Monte Carlo code, thus being available to the users' community.

The number of proposals received by external users strongly increases in the last year. Consequently, a Program Advisory Committee (PAC) has been officially set up in order to evaluate beam time requests and assign beam time to interested users. The PAC meets three times per year, and the documentation needed for proposal preparation can be found online (<http://www.tifpa.infn.it/sc-init/med-tech/p-beam-research/>).

Research activities performed in the Experimental Room by guest groups in 2017 range from physics measurements of interest for therapy (BUILDING, MOPET), to detector testing for medical (iMPACT, DP-MONDO, Prima-RDH-IRPT, profiling activities within MoVe IT, GammaRad), space applications (LIDAL, ROSSINI) and material science (ELOFLEX). An industrial proposal (KI-MARK) has been also presented by Kayser Italia. RIGHTABOVE is instead the first project performed at PTC dedicated to the study of combined radio- and immune-therapy. Finally, the PLANT experiment aims at the investigation of genomic alterations induced by proton irradiation in tomato plants.

Finally, we are glad to announce that the Experimental Room is now acknowledged among ESA ground based irradiation facilities and is part of the CORA-IBER program dedicated to the study of biological effects of space radiation.

# BUILDING: Dose Build-up effects in proton Bragg curves

Tabea Pfuhl,<sup>1,4</sup> Felix Horst,<sup>1,2,3</sup> Christoph Schuy,<sup>1</sup> Joachim Stroth,<sup>1,4</sup> Marta Rovituro,<sup>5</sup> Uli Weber<sup>1†</sup>

Target fragments are considered to deliver a relevant contribution to the total dose in the entrance channel of proton beams. Especially, due to their low energy and higher LET target fragments can increase the biological efficiency and justify also in the entry channel the commonly applied RBE of 1.1.

Direct measurements of the energy spectra and of the yields of target fragments via detection of single particles require a carefully designed and complex setup due to their low energy. For instance, the FOOT cooperation actu-

ally plans such a complex single-particle detector system, whereas for the BUILDING experiment a complimentary approach is intended: We expect to yield information about target fragmentation by precise measurements of the build-up region of the Bragg curves.

The build-up region consists of two different contributions. First, the  $\delta$ -electron build-up effect takes place in the first few millimeters of the target, until an equilibrium state of the forwards scattered  $\delta$ -electrons is reached.

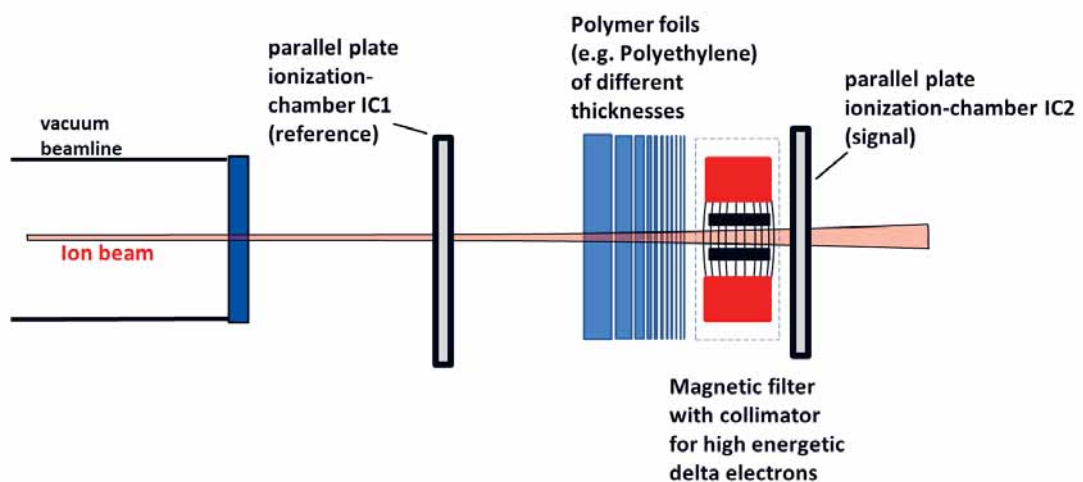


Figure 1: Schematic setup for the measurement of Bragg curves at low penetration depth in order to measure the  $\delta$ -electron and target fragment build-up effect.

<sup>†</sup>Contact Author: u.weber@gsi.de

<sup>1</sup>GSI Darmstadt, Germany

<sup>2</sup>JLU Gießen, Germany

<sup>3</sup>THM, Gießen, Germany

<sup>4</sup>University of Frankfurt, Germany

<sup>5</sup>INFN TIFPA, Trento, Italy

Secondly, the target fragment build-up effect covers the first centimeters of the entrance channel and is a result of target fragments created by inelastic interactions of the beam particles with the target atoms. These fragments have a low kinetic energy and partly high atomic numbers compared to the beam protons which results in increased RBE values. However, the relevant production cross sections for ion beam therapy still have large uncertainties.

As the direct measurement of target fragments is extremely difficult the target fragment production is examined indirectly by investigating the target fragment build-up effect in proton Bragg curves.

Therefore, the build-up region ( $<12 \text{ g/cm}^2$ ) of the Bragg curve was measured using two parallel plate ionization chambers and a series of solid polyethylene targets (foils) of different thicknesses. In order to avoid geometric effects (scattering losses) by larger air gaps, we minimized the gap and shifted the targets as close as possible to the second ionization chamber.

As a second option (see Fig. 1), we used a magnetic dipole (permanent magnets of NdFeB) in order to filter out the high-energetic  $\delta$ -electrons. By introducing the magnets, it can be better differentiated between the  $\delta$ -electron build-up and the nuclear build-up effect, where the latter

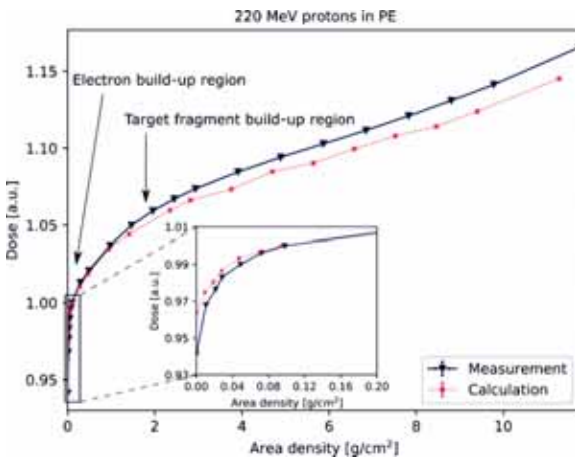


Figure 2: Precise Bragg curve measurement (build-up region) in polyethylene for a 220 MeV proton beam.

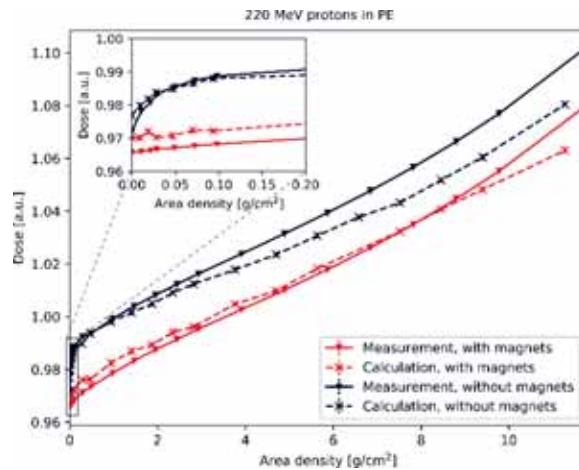


Figure 3: Same measurement as in figure 2 but using a magnetic filter for suppressing the  $\delta$ -electron build-up effect.

gives the relevant information about the production of target fragments. The exact geometry (distances of the targets, magnetic field size, and collimator size) was optimized in advance by Monte Carlo simulations, in order to enable a measurement of an optimal pronounced build-up effect and differentiation between the  $\delta$ -electron and nuclear build-up region. In the experiment of November 2017 at the Trento proton therapy facility a pencil beam with an energy of 220 MeV (clinical maximum) was used.

Fig. 2 shows the dose build-up (without magnets) for the proton beam in comparison with FLUKA simulations. Fig. 3 shows the same measurement using the magnetic filter for suppressing the  $\delta$ -electron build-up effect.

In addition, extensive FLUKA Monte Carlo simulations were carried out for benchmarking of the experiment. A comparison of the experimental results with calculated Bragg curves is also shown in Fig. 2 and Fig. 3.

The setup enabled a precise measurement of the build-up region. The data points show a very low noise (fluctuation). The magnetic filter could suppress the build-up effect by the  $\delta$ -electrons. The FLUKA MC simulations show a satisfying agreement with the measurement, however, at deeper penetration depths a difference occurred that might be explained by a geometrical cut-off effect of the second ionization chamber.

# ELOFLEX

Alberto Quaranta,<sup>1,2†</sup> Enrico Zanazzi,<sup>1,2</sup> Andrea Ficorella,<sup>1,2</sup> Marta Rovituso<sup>2</sup>

During the first run performed at the APSS-TIFPA facility, irradiation tests were performed on polysiloxane samples containing different concentrations of quantum dots (QD). The samples were disks of 2.2 cm of diameter and 4 mm thick. The QD concentrations were  $10^{14}$ ,  $10^{13}$  and  $10^{12}$  QD/ml for CdSeS/ZnS dots and were  $10^{14}$  and  $10^{13}$  QD/ml for CdSe/ZnS dots. The samples were irradiated with an energy of 70 MeV and a current of  $3 \times 10^8$  p/s.

During irradiation light emission tests were performed in order to check if any scintillation light is emitted by the samples. The light was collected both by a SiPM detector connected on the edge of the disc and by an optical fibre in front of the sample. The fibre was connected to an optical spectrometer Ocean Optics QE6500 in order to collect the whole spectrum.

During the irradiation tests no significant light emission was detected. This can be due to the lack of energy transfer between the matrix and the dots, which has to be improved through an addition of dye molecules suitable for this process.

Post-irradiation optical analyses were per-

formed on samples irradiated with a total fluence of  $7.2 \times 10^{10}$  p. The analyses were performed at DII with a pulsed laser (470 nm with pulse width 300 ps). In this case changes of both light yield and lifetime were detected. All the samples exhibited a slight decrease of the peak intensity and a concentration effect, due to the formation of quenching defects in the dots, was observed only for samples with  $10^{13}$  QD/ml. This concentration effect is worth of further investigation and it can be related to both to the average number of ionizations per QD and to the shield effect of the QD themselves.

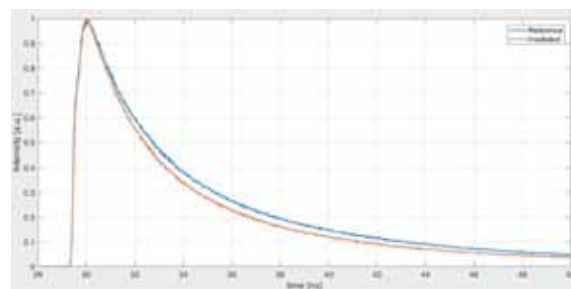


Figure 1: Lifetime of reference and irradiated samples with  $10^{13}$  QD/ml and after an irradiation of  $7.2 \times 10^{10}$  p.

<sup>†</sup>Contact Author: [alberto.quaranta@unitn.it](mailto:alberto.quaranta@unitn.it)

<sup>1</sup>University of Trento, Italy

<sup>2</sup>INFN TIFPA, Trento, Italy

# GammaRad

Alberto Gola,<sup>1,2†</sup> Veronica Regazzoni,<sup>1,2</sup> Daniele Rucatti,<sup>1</sup> Christian Manea,<sup>2</sup> Enrico Verroi,<sup>2</sup> Marta Rovituso<sup>2</sup>

Although proton therapy beams offer the possibility to accurately target tumors, thanks to the narrow dose distribution around the Bragg peak, different sources of range uncertainty have been identified. They include non-uniformity and x-ray computed tomography (CT) artefacts, conversion of Hounsfield units to proton stopping power, and anatomical variations (weight change, tumor reduction) as well as patient misplacement and internal organ motion. All these sources can add up to a maximum uncertainty of 10-15 mm. To reduce the safety margins associated with these uncertainties and allow more optimal treatment strategies, a reliable device for real-time monitoring of the range inside the patient would be valuable and different solutions are being investigated. Among different techniques, positron emission tomography (PET) and prompt gamma imaging (PGI) are the most promising methods for in vivo range verification. PET imaging detects coincidence gamma rays due to the production of positron emitters and requires some minutes to achieve enough statistics to have a sufficient signal to noise ratio. PGI instead uses prompt gamma rays generated by de-excitation of target nuclei; the quantity of these rays and their temporal emission (few nanoseconds) allow to perform a range verification during treatment with the PGI. Several research groups are evaluating different approaches to realize a prompt gamma imaging system suitable for the use in clinical condition

and the optimization of a gamma-ray detector for PGI is still ongoing.

In this context, the scientific objective of the GammaRad project is the development of an innovative high-performance, solid-state gamma-ray detection module (GDM) and its validation as a prompt gamma imager in proton therapy. The GDM will be used in a slit-camera configuration. Fig. 1 shows the concept of the slit-camera technique for prompt gamma imaging, which provides a 1-D projection of emitted prompt gamma-rays on the GDM.

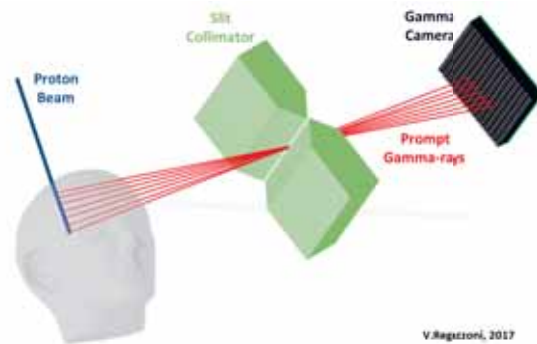


Figure 1: Concept of the gamma of the slit-camera technique for prompt gamma imaging

**GammaRad Activity at TIFPA** TIFPA started the GammaRad activity in 2014, collaborating with Fondazione Bruno Kessler (FBK), Politecnico di Milano and the Proton Therapy Center of Trento. The most innovative part of the gamma-ray detector developed for the project is the photo-sensor used for the scintillation light

<sup>†</sup>Contact Author: gola@fbk.eu  
<sup>1</sup>FBK, Trento, Italy

<sup>2</sup>INFN TIFPA, Trento, Italy

readout which is composed of SiPMs. These SiPMs were developed and produced in FBK and feature high cell density together with high Photon Detection Efficiency (PDE), in order to improve linearity of the detector in high-dynamic range applications such as PGI. After careful evaluation of preliminary test data, the  $15\ \mu\text{m}$  cell of the RG-HD technology was selected for the GammaRad project. In addition to the photo-sensor, the GammaRad system is composed of a readout ASIC and an acquisition system, both provided by Politecnico di Milano. During 2017, TIFPA activity was focused on testing the photodetector with the proton beam, for the final optimization of its operating parameters and to understand its performance and the optimal beam configuration before the final PGI measurements. The tests were carried out in the experimental room managed by TIFPA and located in the Proton therapy center of Trento. More in detail, the test were carried out to:

- Optimize the experimental setup of the GammaRad project;
- Evaluate the rate of Prompt Gamma photons (PG) vs. beam current;
- Optimize the beam (in terms of current and energy) and the acquisition parameters to obtain the best measurement con-

ditions of the PGs;

- Test the acquisition software for single-channel measurements;
- Acquire a preliminary spectrum of PG that was analyzed offline by applying an energy calibration made in the FBK laboratories;
- Acquire PG spectra with different detectors (SiPM) used in various polarization conditions.

These tests provided useful information for the final development of the photo-sensor module (see Fig. 2), that will be tested in 2018.

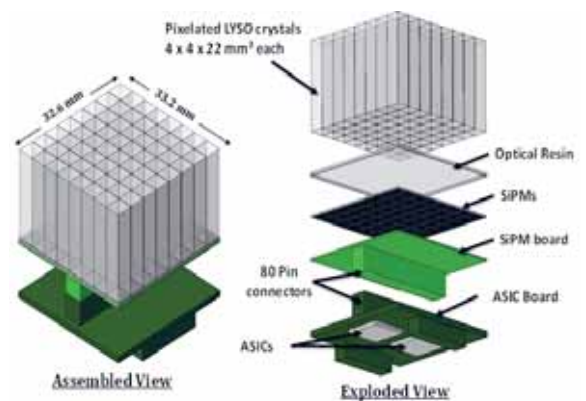


Figure 2: Photo-detector module for the GammaRad project. It consists of a tile of 64 photo-sensors coupled to a LYSO crystal with 64 pixels.

# iMPACT calorimeter prototype testing

Piero Giubilato,<sup>1†</sup> Serena Mattiazzo,<sup>1</sup> Nicola Pozzobon,<sup>1</sup> Devis Pantano,<sup>1</sup> Mario Tessaro,<sup>2</sup> Filippo Baruffaldi,<sup>1</sup> Jeffery Wyss,<sup>3</sup> Roberto Iuppa,<sup>4,5</sup> Ester Ricci,<sup>4,5</sup> Benedetto di Ruzza,<sup>5</sup> Chiara La Tessa<sup>4,5</sup>

The iMPACT project, funded by ERC grant 649031, aims at realizing a proton scanner for a proton Computed Tomography (pCT) system. A pCT scanner is composed by a *tracker* and a *calorimeter*. The tracker must provide the particles position and angle before and after they pass through the target (the human body), while the calorimeter has to measure the residual energy of the passing particles. By combining the track and energy information of about one billion protons passing through the target from different directions, it is possible to reconstruct a 3D image of the target itself.

The main differences respect to the well-established x-rays CT are:

- More difficult computing to reconstruct the 3D image, as protons scatter randomly in their path through the target.
- Less spatial resolution for a given number

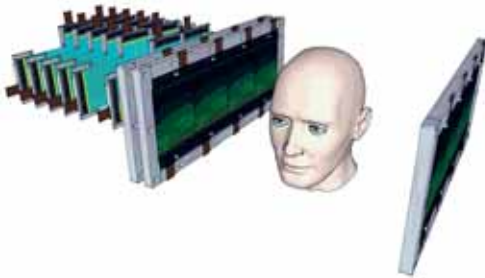


Figure 1: iMPACT pCT scanner representation.

<sup>†</sup>Contact Author: piero.giubilato@pd.infn.it

<sup>1</sup>University of Padua, Italy

<sup>2</sup>INFN Padua, Italy

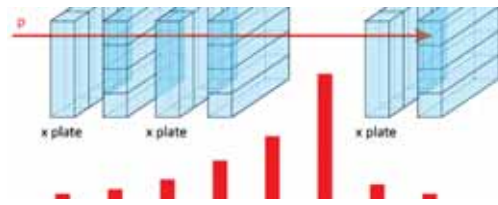


Figure 2: Achromatic calorimeter pictorial layout.

of particles, always because of the protons scattering.

- *Much less dose delivered to the patient* for an equivalent image quality respect to traditional x-rays CT (protons ionize little while travelling through the body at the employed energies).
- *Much better tissue density resolution*, which is the key point in providing a realistic 3D model for therapy beam targeting.

**Test beam goals and results** The iMPACT pCT scanners employs a fast achromatic calorimeter to measure the protons energy after they passed through the target. The achromatic calorimeter derives the particle energy by measuring its travel range within an absorber of known characteristics instead that measuring its released energy, like in traditional setups.

The TIFPA irradiation facility, set within the APSS Proton Therapy Centre in Trento, has been used to perform a realistic test of

<sup>3</sup>University of Cassino, Italy

<sup>4</sup>University of Trento, Italy

<sup>5</sup>INFN TIFPA, Trento, Italy

the calorimeter first prototype building blocks (called stations, see Fig. 3).



Figure 3: Experimental setup installed at the TIFPA irradiation facility. The tracker ALPIDE sensor sits in the leftmost instalment, followed by the first calorimeter station with the one-plane front-end electronic visible. After the plastic absorber, the second calorimeter station is visible. Both the calorimeter stations and the plastic absorber were arranged in different positions during testing.

Each calorimeter prototype station, simulating a set of 4 adjacent planes, was moved respect a plastic absorber, to check the signal output both before and after the protons going through the target (Fig. 3). Each configuration has been tested with protons at 228 MeV, 70 MeV and 36 MeV. Results confirmed how distinguishing the different regions of the Bethe Block curve the proton is in (Plateau, Bragg Peak) while passing a specific finger is actually possible and robust, and therefore represents an effective way to build a fast calorimeter for a pCT scanner.

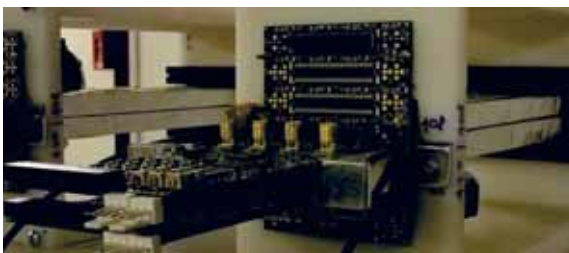


Figure 4: Detail of tested a two-plane readout arrangement, front-end electronics in front and wrapped scintillator fingers on the foreground/right. Numbers marking the scintillator type (BC408 and BC420) are visible.

Fig. 5 shows one of the system configuration installed in the experimental area simulated in Geant 4. Using an absorber (Polycarbonate) before the measuring planes reproduces the pro-

tons straggling, which intrinsically sets a limit to the maximum theoretical resolution a range calorimeter can achieve.

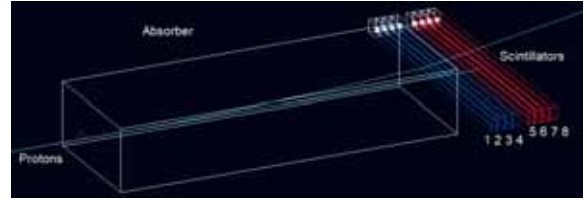


Figure 5: Fingers arrangement used to determine realistic values of the maximum light output at the Bragg Peak (here the GEANT4 model used for simulations). Having an absorber before the detection planes ensures protons straggling degrades the measure, as it will happen in the real application.

In Fig. 6 the blue curve represents the light signal intensity distribution for protons with still enough energy to be in the plateau region of the Bethe-Block after passing through the absorber. Considering only those protons generating the Bragg Peak in the penultimate scintillator enforced this specific energy selection. The distribution shows how an adequate threshold can effectively filter out all the signals generated by protons traversing the finger still in the Bethe Block plateau region, drastically reducing the number of data to record.

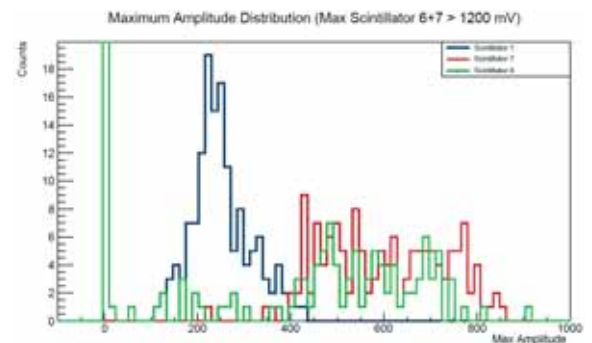


Figure 6: Light output distribution for scintillators 1 (blue), 7 (red) and 8 (green) in the configuration of Figure 5, considering events generating a signal greater than 400 mV in scintillator 7 (hence having only protons in the plateau region in scintillator 1). The blue distribution from scintillator 1 shows a threshold system can effectively suppress protons out of the Bragg Peak region.

By delaying the signal from each finger is possibly to visualize the Bragg Peak energy deposition, as done in Fig. 7 In the picture time-slicing of the scintillator signals is used to depict the energy deposition envelope across the eight

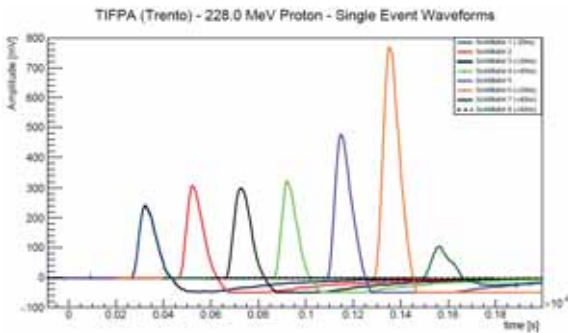


Figure 7: The delayed signals from the eight scintillating fingers help visualizing the energy deposition of a proton arriving from the left and stopping in the penultimate finger (finger 8 shows no signal).

scintillators: with reference to Fig. 5, the left-most peak representing the energy deposited in scintillator #1, se second from the left the energy deposited in scintillator #2, and so on.

Fig. 8 superimposes the signal values distributions registered on stations 1, 3 (blue and red curves) and 6, 7 (green and black curves) for

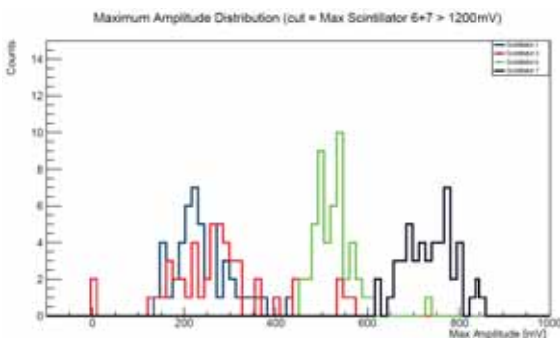


Figure 8: Distribution of the measured output signal for proton traversing a calorimeter finger in the plateau energy region (blue and green curves), before the Bragg peak (green curve) and at the Bragg peak (black curve). The peaks distance is much larger than the distribution width, making possible distinguishing the different regimes with a threshold system.

proton having the Bragg peak in scintillator 7. The distributions do not overlap, clearly illustrating how a thresholds system can effectively distinguish the different regions of proton energy realise, therefore correctly reconstructing its range and energy.

**Further outcome of the test-beam** The second component of the iIMPACT scanner is a fast pixel tracker, whose first prototype will be realized using the ALPIDE sensor developed by the ALICE collaboration. The ALPIDE chip is a MAPS of  $30 \times 15 \text{ mm}^2$  active area, with  $28 \times 28 \mu\text{m}^2$  big pixels, realized in the same Tower Jazz process used for the OrthoPix prototype (with which it shares a very similar pixel cell).

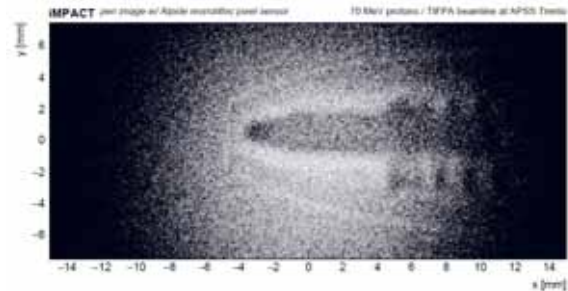


Figure 9: Proton radiography of a pen with the ALPIDE sensor, taken during the TIFPA test beam.

The ALPIDE sensor has been tested together with the calorimeter stations, during the same test beam. While not being the first goal of the shift, it nevertheless provided insightful information about the potentiality of MAPS sensor for non-minimum ionizing particles tracking and imaging. A quick demonstrative radiography of a ball pen performed with the ALPIDE sensor and 70 MeV protons clearly illustrates the potential of a large area MAPS sensors in imaging applications (Fig. 9).

# KI-MARK

Alessandra Tortora,<sup>1</sup> Devitt Dini,<sup>1</sup> Alessio Pannocchia,<sup>1</sup> Luca Pieroni,<sup>1†</sup> Simone Gerardin,<sup>2</sup> Marta Bagatin,<sup>2</sup> Francesco Tommasino,<sup>3,4</sup> Chiara La Tessa,<sup>3,4</sup> Marta Rovituso<sup>4</sup>

Kayser Italia has performed in 2017 a radiation test session on an ARM microcontroller manufactured in a standard CMOS process, in the Proton Beam facility at the Centro di Protonterapia in Trento. The facility is managed by Trento Institute for Fundamental Physics and Applications (TIFPA), a Science and Technology National Center for research in fundamental physics. The tests have been performed by Kayser Italia in collaboration with University of Padova, Dept. of Information Engineering who has a strong background in radiation testing of electronics devices.

The main objective of the test was acquiring information on the behavior of the selected

ARM microcontroller in the presence of radiation comparable to the International Space Station environment. ISS Columbus module requirements were used as baseline for the definition of radiation test parameters and configuration but the tests were limited to evaluate the ARM microcontroller for SEEs.

The executed procedure has been elaborated according to the following relevant ESA standards and guidelines:

- Single Event Effects Test Method and Guidelines, ESCC Basic Specification No. 25100
- Space Station Ionizing Radiation Design Environment, SSP 30512

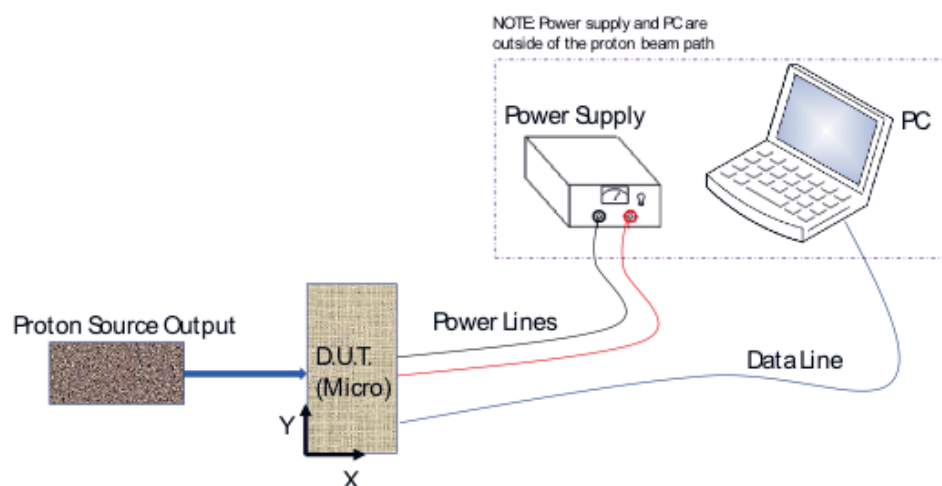


Figure 1: ARM Radiation Test Setup (simplified).

<sup>†</sup>Contact Author: [l.pieroni@kayser.it](mailto:l.pieroni@kayser.it)

<sup>1</sup>Kayser Italia, Livorno, Italy

<sup>2</sup>University of Padua, Italy

<sup>3</sup>University of Trento, Italy

<sup>4</sup>INFN TIFPA, Trento, Italy

The test setup was arranged as schematically shown in Fig. 1.

The Device Under Test (DUT) (see Fig. 2) is the ARM microcontroller that was soldered on a specifically designed and developed test board. According to the good practice, the area around (and behind) the DUT has to be left free of sensitive components and with the smallest amount of heavy materials, in order to minimize the board activation.

Irradiation tests were performed into two different configurations:

1. static conditions; microprocessor idle
2. dynamic conditions: microprocessor running a Kayser Italia custom application.

The DUT has been irradiated with the proton beam at four selected energies (70 MeV, 119 MeV, 169 MeV, 228 MeV) for well-defined lapse of time. Irradiations under protons has been performed in air with the device normal to the beam.

Static tests were providing a worst-case estimation of the device sensitivity for SEU and MBU and are effective in evidencing small latch-up phenomena (due to low currents at play). The ARM microcontroller was idle during the exposure and its memory filled and registers configured with known patterns. The Kayser Italia custom test board contained another microcontroller outside the exposed area that acted as “supervisor” and data acquisition system for detecting the occurrence of latch-up and protecting the DUT itself quickly cutting off the power supply. All software and firmware used during the radiation tests was specifically developed by Kayser Italia.

Dynamic tests make it possible to evaluate

derating factors, i.e. the fact that not all corrupted bits result in an application error (e.g. an upset in a register about to be rewritten has no impact on the application results), for a specific set of routines. Typically, dynamic tests provide smaller error rates, but their validity is limited to the code tested under exposure to radiation. The ARM microcontroller executed a representative set of software routines in a loop during the exposure to radiation. At the same time, the supply current was monitored by the supervisor for the occurrence of latch-up. Real time checking (i.e. with the proton beam on) of the results or signatures was done and a full initialization of the application upon error detection. In any case off-line data was downloaded from the safe area with the beam off.

The radiation tests were successfully performed between January and February 2017 and have finally lead to the use of selected and tested ARM microcontroller within a biological incubator to be flown on International Space Station in 2018-2019.



Figure 2: Test Board mounted on the XY translation stage.

# LIDAL: Light Ion Detector for ALTEA

Alessandro Rizzo,<sup>1,2†</sup> Carolina Berucci,<sup>1</sup> William Burger,<sup>3,4</sup> Cinzia de Donato,<sup>2</sup> Luca di Fino,<sup>1</sup> Marco Durante,<sup>4</sup> Chiara la Tessa,<sup>5,4</sup> Christian Manea,<sup>4</sup> Livio Narici,<sup>1,2</sup> Marta Rovituso,<sup>4</sup> Francesco Tommasino<sup>5,4</sup>

The LIDAL (Light Ion Detector for ALTEA) is a compact Time-of-Flight detector designed to work paired with three silicon detector units of ALTEA (Anomalous Long Term Effects on Astronauts) system. The LIDAL prototype has been tested at TIFPA proton beam line in order to study the temporal performances of the ToF system and fast FEE (Front end Electronics). A time resolution below 80 ps has been evaluated for proton with kinetic energy till 221 MeV.

**The ALTEA-LIDAL system and LIDAL prototype** LIDAL is a compact detector designed to measure in detail the low-Z part of the particle spectrum inside the International Space Station (ISS) through ToF technique. LIDAL detector will consist of three modules: two LDU (LIDAL Detector Unit) with 8 scintillators each, and one LCU (LIDAL Collector Unit), for data acquisition. In between the two LDU modules, three Silicon Detector Unit (SDU) of the ALTEA system will take place. In addition to the study of the low-Z part of the particle spectrum measuring the velocity  $\beta$  of the passing through particle, the second task of the ALTEA-LIDAL system is the Particle IDentification (PID). Indeed, matching  $\beta$  measured by LIDAL detector with the deposited energy ( $dE/dx$ ) measured by ALTEA for each event, it will be possible to efficiently discriminate the different elemental species for a reliable risk assessment for astro-

nauts in space.

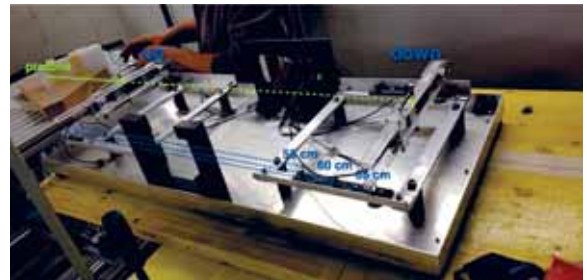


Figure 1: Picture of test setup at TIFPA. Two LIDAL scintillators are placed in front of the proton beam line at a distance between them of 60 and 65 cm.

LIDAL first prototype (see Fig. 1) has been developed using plastic scintillator ( $90 \times 25 \times 8$  mm) EJ230 (Eljen Technologies) for fast timing application coupled with two PMMA light guides and two HAMAMATSU PMTs RS9880U210.

The plastic scintillators are characterized by a rise time of 500 ps and a good light output of 9700 photons for 1 MeV electron. The PMTs, with a rise time of 520 ps and high quantum efficiency, assure the required fast response to perform ToF measurements with the needed detail. The generated signal is then processed by FEE, in particular by the NINO chip.

## The LIDAL test at TIFPA proton beam line

The runs at TIFPA proton beam line, have been taken with protons at different energies with

<sup>†</sup>Contact Author: [alessandro.rizzo@roma2.infn.it](mailto:alessandro.rizzo@roma2.infn.it)

<sup>1</sup>University of Rome “Tor Vergata”, Italy

<sup>2</sup>INFN Rome Tor Vergata, Italy

<sup>3</sup>FBK, Trento, Italy

<sup>4</sup>INFN TIFPA, Trento, Italy

<sup>5</sup>University of Trento, Italy

a rate below 10 kHz, a condition which requires the dark current working mode for the cyclotron. The main goal of the measurement campaign is the evaluation of the time resolution for protons at different energies, fixing the baseline between the two scintillators at 65 and 60 cm.

The secondary goal is the study of time resolution of the system as a function of the impinging point of the incident particles. Data have been acquired at five different beam energies for the 65 cm baseline configuration (100, 131, 159, 193 and 228 MeV) and at three energies for the 60 cm baseline configuration (100, 159 and 228 MeV). An example of these ToF measurements is given in Fig. 2.

The time resolution has been evaluated as the  $\sigma$  of the Gaussian function used to fit the temporal distributions. The resulting average time resolution for protons in the considered energy range has been evaluated as  $73 \pm 3$  ps for the baseline 65 cm long and  $78 \pm 6$  ps for the baseline 60 cm long.

In order to evaluate the other performances of detector, kinetic energy of the beam and beam profile have been reconstructed in the configuration with baseline 60 cm long. Three runs with beam impinging in the center of the detector at different energies have been acquired.

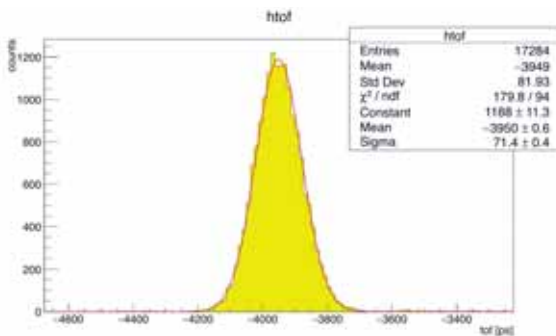


Figure 2: ToF distribution obtained for 65 cm long baseline with a proton beam of 159 MeV.

Concerning the beam profile measurements, the isocenter of the beam falls in the center of the detector, in between the two scintillators. Nominally beam dimension at isocenter has an average value of 12 mm (sigma) in the considered energy range and rate (below 2 kHz). The transversal (horizontal) dimension of the beam has been reconstructed in each scintillator by means of left-right arrival time difference recorded by the system. In the table below the obtained results of kinetic energy and beam spot dimension are summarized.

Measurements	I	II	III
$T_{nominal}[MeV]$	100	159	228
$T_{degraded}[MeV]$	85	153	226
$T_{meas}[MeV]$	$84 \pm 3$	$150 \pm 7$	$225 \pm 10$
beam spot front [mm]	21	17	14
beam spot rear [mm]	30	18	15

The dimension of the spot is getting bigger on the rear scintillator because of the interaction of the protons with the front scintillator. The larger energy deposited in the rear scintillator due to the degrading effect of the first scintillator on the beam, is clearly visible by correlating the QDC values measured for each event.

Tests at TIFPA proton beam line have shown that the time resolution values is well below the design goal of 100 ps for LIDAL prototype. For protons with a kinetic energy that ranges from 100 to 228 MeV, the time resolution of the detector results in  $73 \pm 3$  ps for a baseline 65 cm long, and  $78 \pm 8$  ps for a baseline 60 cm long.

The measurements have also shown that the light collected at the extremities is plenty, so smaller dimensions of scintillators for the final detector has been chosen in order to further enhance performances in terms of time resolution.

# Dose Profiler and MONDO tracker characterisation

G. Battistoni,<sup>1</sup> Y. Dong,<sup>2,1</sup> M. De Simoni,<sup>3,4</sup> R. Faccini,<sup>3,4</sup> M. Fischetti,<sup>5,4</sup> V. Giacometti,<sup>6,4</sup> E. Gioscio,<sup>6</sup> C. La Tessa,<sup>7,8</sup> C. Mancini-Terracciano,<sup>4</sup> M. Marafini,<sup>6,4</sup> I. Mattei,<sup>1</sup> R. Mirabelli,<sup>3,4</sup> S. Muraro,<sup>9</sup> D. Pinci,<sup>4</sup> M. Rovituso,<sup>8</sup> A. Sarti,<sup>5,10,6</sup> A. Sciubba,<sup>5,4,6</sup> E. Solfaroli Camillocci,<sup>11,3</sup> F. Tommasino,<sup>7,8</sup> G. Traini,<sup>3,4</sup> S.M. Valle,<sup>2,1</sup> V. Patera<sup>5,4,6†</sup>

In 9-15 May 2017 and 29-30 June 2017 two data-taking campaigns have been performed at the experimental cave of the Trento proton-therapy center. Proton beams at different energies have been used to characterise the response of the *Dose Profiler* (DP) and the MONDO (MONitor of Neutron Dose in hadrOn-therapy) tracker. A short summary of the activity is reported hereafter.

The DP is a detector specifically designed to monitor the beam range in particle therapy treatments exploiting the secondary charged fragments (G. Traini et al. 2017). Six planes of plastic scintil-

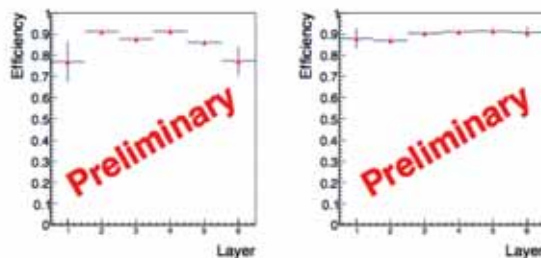


Figure 1: Detection efficiency per single layer, in the horizontal view (left) and the vertical view (right).

† Contact Author: vincenzo.patera@roma1.infn.it

<sup>1</sup>INFN Milan, Italy

<sup>2</sup>University of Milan, Italy

<sup>3</sup>Physics Dept., Sapienza University of Rome, Italy

<sup>4</sup>INFN Rome, Italy

<sup>5</sup>Dept. of Fundamental and Applied Engineering Sciences, Sapienza University of Rome, Italy

<sup>6</sup>Enrico Fermi Historical Museum of Physics and Study and Research Centre, Rome, Italy

<sup>7</sup>University of Trento, Italy

<sup>8</sup>INFN TIFPA, Trento, Italy

<sup>9</sup>INFN Pisa, Italy

<sup>10</sup>INFN LNF, Frascati, Italy

<sup>11</sup>Center for Life Nano Science, IIT@Sapienza, Rome, Italy

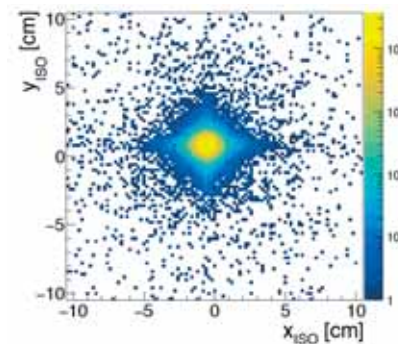


Figure 2: Reconstructed beam spot with proton beam at 169 MeV.

lating fibres, read-out by Silicon Photomultipliers, provide the incident fragment trajectories to reconstruct the emission points. Two additional layers of plastic scintillator, placed over the last fibre plane, are used to measure the kinetic energy. The DP has been tested using proton beams at intensities of the order of  $10^3$  p/s, directly impinging the detector entrance surface. Two plastic scintillators have been positioned between the beam exit window and the DP, to independently monitor the beam intensity and provide an external trigger for data

acquisition. The detection efficiency and the spatial resolution have been investigated using protons at the energies of interest for particle therapy monitoring applications. A single layer detection efficiency of the order of  $\sim 90\%$  has been measured for each fibre plane, as shown in Fig. 1. The spatial resolution on a single reconstructed proton track has been evaluated at 50 cm from the DP entrance face, obtaining values between 3 mm and 5 mm, depending on the beam energy. In Fig. 2 an example of reconstructed beam spot is shown. Data are still preliminary, and further analysis are ongoing.

The MONDO (MONitoring for Neutron Dose in hadrOntherapy) project aims to perform a characterisation of the primary neutrons emitted in PT treatments, in the energy range of 20-400 MeV, to improve the Monte Carlo models currently embedded in the TPS software (Marafini et al. 2017b). The MONDO detector is designed to track secondary neutrons pro-

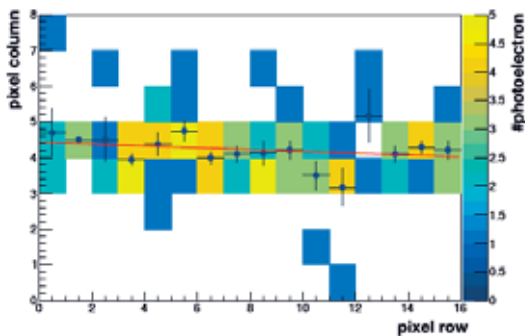


Figure 3: Example of a 140 MeV proton track reconstructed by the SPAD-net sensor. The beam is coming from left to right.

## References

- Marafini, M. et al. (2017b). *MONDO: a neutron tracker for Particle Therapy secondary emission characterisation*. *Phys. Med. Biol.* **62**, pp. 3299–3312.
- Traini, G. et al. (2017). *Design of a new tracking device for on-line beam range monitor in carbon therapy*. *Physica Medica* **34**, pp. 18–27.

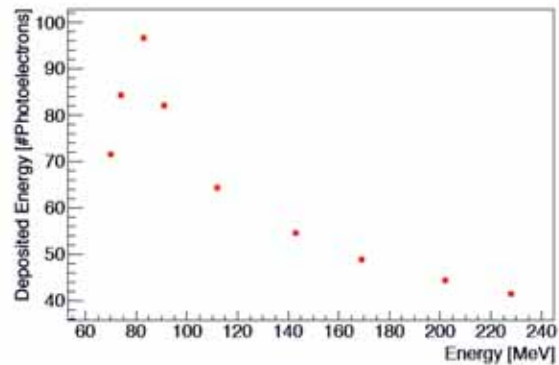


Figure 4: Top: Number of photoelectrons produced by a proton track reconstructed by the SPAD-net sensor as a function of the proton beam nominal kinetic energy

duced in nuclear interactions of PT heavy ion beam with patient tissues, reconstructing the neutron four-momentum exploiting the Double Elastic Scattering (DES) in the tracker interacting material. A tracker prototype, made by scintillating fibres, has been tested using proton beams at different energies, directly impinging on the detector. Two different read-out systems have been used: a standard multi-anode photomultiplier (PMT), and a sensor developed by FBK named *SPAD-net*, based on SPAD technology, whose layout (pixel size and trigger strategy) was not optimised for the MONDO needs. The tracker prototype response has been studied, in terms of released charge and signal topology. In Figs. 3 and 4 an example of proton reconstructed track and the number of photoelectrons detected in the SPAD-net as a function of the beam energy sensor are shown, respectively.

# MOPET: Measurement of crOss section data relevant for PET range verification in proton therapy

Felix Horst,<sup>1,2,3</sup> Christoph Schuy,<sup>1</sup> Claire-Anne Reidel,<sup>1,5</sup> Wihan Adi,<sup>2</sup> Kai-Thomas Brinkmann,<sup>2</sup> Lukas Nies,<sup>2</sup> Marta Rovituso,<sup>4</sup> Hans-Georg Zaunick,<sup>2</sup> Christian Finck,<sup>6</sup> Klemens Zink,<sup>3</sup> Uli Weber<sup>1†</sup>

The analysis of PET activation patterns is an established technique for range verification in proton and heavy ion therapy. For this method, the distribution of the positron emitters within the irradiated tissue needs to be calculated for each individual treatment plan. Such transport calculations require a precise knowledge of the underlying nuclear reactions, i.e. the production cross sections for the isotopes of interest (mainly  $^{10}\text{C}$ ,  $^{11}\text{C}$  and  $^{15}\text{O}$ ).

A detector system to measure such cross sections, consisting of three  $\text{BaF}_2$  scintillators for the detection of the 511 keV annihilation photons in coincidence, was developed and characterized (Fig. 1). A short proton or heavy ion pulse impinges on a target (e.g. graphite or Beryllium oxide) and activates the material. Two scintillators measure the rate of 511 keV photons emitted in  $180^\circ$  and the third scintillator is used to measure the random coincidence rate. The initial activities of the generated target fragments ( $^{10}\text{C}$ ,  $^{11}\text{C}$ ,  $^{15}\text{O}$ ) can be obtained by fitting the measured decay curve with a superposition of multiple exponential functions with different half-lives corresponding to the different isotopes (Fig. 2). Finally, the produc-

tion cross sections can be calculated from these initial activities.

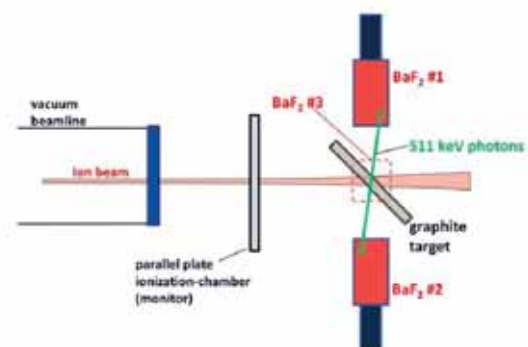


Figure 1: Setup for detection of 511 keV photons

The developed setup was used in an experiment (November 2017) with protons conducted at the Trento proton therapy Center to measure  $^{12}\text{C}(p,pn)^{11}\text{C}$  and  $^{12}\text{C}(p,p2n)^{10}\text{C}$  cross sections in the energy range of 50–230 MeV. The obtained cross sections are in good agreement with literature data (Fig. 3). Future measurements with  $^{12}\text{C}$  projectiles, where the available cross section data are more sparse than for protons, are planned for the future.

<sup>†</sup>Contact Author: u.weber@gsi.de

<sup>1</sup>GSI Darmstadt, Germany

<sup>2</sup>JLU Gießen, Germany

<sup>3</sup>THM, Gießen, Germany

<sup>4</sup>INFN TIFPA, Trento, Italy

<sup>5</sup>Strasbourg University, Strasbourg, France

<sup>6</sup>IPHC, Strasbourg, France

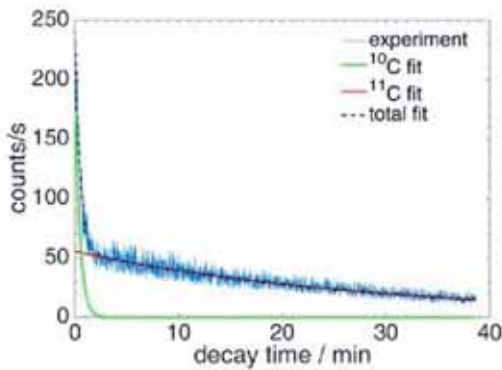


Figure 2: Measured decay curves for  $^{10}\text{C} / ^{11}\text{C}$

**Beam profile and envelope measurements using MIMOSA28 CMOS sensors** The PET activation experiments (but also other experiments using the proton pencil beams) require the precise information of the beam spot geometry at the target and the envelope in order to model the geometrical correction factors due to the limited detector sizes. The MIMOSA28 CMOS sensor system can be used for this purpose. The active area of the chip is composed of 928 rows x 960 columns with a pixel size of  $20.7 \mu\text{m}$  and has a readout time of  $186.5 \mu\text{s}$  per frame. To reach a track resolution under  $5 \mu\text{m}$ , the sensors need first to be aligned.

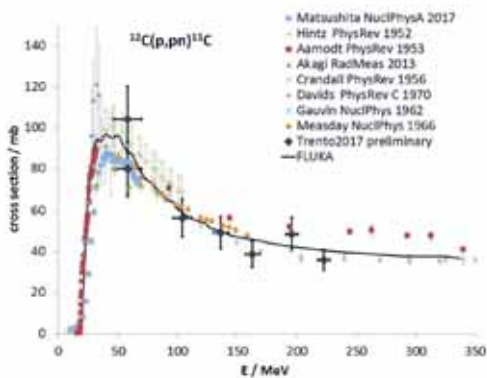


Figure 3: Measured production cross section ( $^{11}\text{C}$  target fragments) for protons on a graphite target, compared to literature data.

An alignment algorithm has been implemented for the data analysis with the minimiza-

tion of a complex chi square function, based on a linear regression analysis. This algorithm was tested with proton beams (Trento June 2017) in the range of 70 to 220 MeV and shows significantly better results than older alignment algorithms. Using the precise alignment of the sensors, the lateral fluence distribution at different z positions could be measured. Fig. 4 shows the beam width at the region of interest for a 125 MeV beam with  $10^3$ - $10^4$  protons per second.

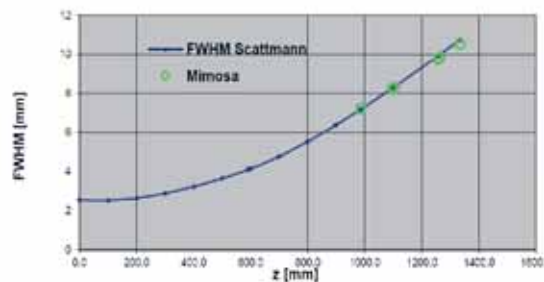


Figure 4: Photo (above) of the setup in the Trento proton therapy facility, using the MIMOSA28 detector system with 6 sensors; diagram (below) of the measured beam spot sizes (FWHM) at different distances from the vacuum window .

The experiments for PET isotope production could be successfully conducted in the beam times of June (test with one energy) and for a series of energies in November 2017. The accuracy of the cross sections is satisfactory. Also the test for the MIMOSA28 sensors was successful. The envelope of the beam with low intensity could be precisely measured. This can serve in future as an excellent preparation for other experiments but also for the alignment of dedicated research projects with the MIMOSA28 system.

# PLANT: Genomic analysis of tomato plants upon exposure to radiation

Alexander Helm,<sup>1†</sup> Walter Sanseverino,<sup>2†</sup> Veronica De Micco,<sup>3</sup> Carmen Arena,<sup>3</sup> Riccardo Aiese Cigliano,<sup>3</sup> Luis Matias Hernandez,<sup>2</sup> Francesco Tommasino,<sup>4,1</sup> Emanuele Scifoni,<sup>1</sup> Valentina Marchesano,<sup>1,4</sup> Alessandra Bisio,<sup>4</sup> Marco Durante,<sup>1</sup> Walter Tinganelli<sup>1</sup>

This experiment is part of an international collaboration. It involves institutes from Italy and Spain. Along with TIFPA and the Center for Integrative Biology (CIBIO, Trento), Sequentia Biotech SL (Barcelona, Spain), the Departments of Agricultural Sciences and Biology (University of Naples Federico II), as well as Telespazio SpA are essential parts of this collaboration. The aim of the project is to analyze the effects of different radiation types (photons and particles) on plants and to study the genomic modifications occurring thereafter, with the further idea to create new useful phenotypes, which could be used either in agriculture or for putative future space colonies, where radio resistant plants are advantageous. Here we present an exploratory study that has been performed using M82 tomato seeds. Seeds were irradiated with a proton beam at the Proton Therapy Center in Trento and, following germination analyzed applying next generation sequencing (NGS). New phenotypes might be advantageous with respect to an increased amount of specific edible products, higher resistance to pathogens or for example an increased radio resistance. The latter is of particular interest for possible space colonization of e.g. the Moon a project that international space agencies are aiming at in future. Briefly, to determine whether the

radiation received had effects on germination and the genome, seeds (irradiated and control) were shipped to the Centre for Research in Agricultural Genomics (CRAG) in Barcelona (Fig. 1, Fig. 2) and subjected to a germination test.



Figure 1: CRAG building.

Additionally, an NGS analysis was performed. From two seeds irradiated with 50 Gy and two control seeds (sham-irradiated) DNA was extracted and sequenced using Illumina HiSeq 2500, producing about 20 Gb of sequences per sample (Pair-end 2 × 150). Both samples were mapped against the Heinz tomato reference genome 1706 v3.2 and a variant calling analysis was performed. To perform a sensitive variant calling Sequentia developed a cus-

<sup>†</sup>Contact Author: alexander.helm@unitn.it

<sup>†</sup>Contact Author: wsanseverino@sequentiabiotech.com

<sup>1</sup>INFN TIFPA, Trento, Italy

<sup>2</sup>Sequentia Biotech, Barcelona, Spain

<sup>3</sup>University of Naples, Italy

<sup>4</sup>University of Trento, Italy

tom pipeline called SUPER-W. SUPER is an easy and user-friendly workflow written in python to call SNPs, DIPs and Structural variations (SV) using NGS resequencing data and a reference sequenced genome. It works with single (SE) and paired-end (PE) reads of any size. The structural variations calling works only with PE data. SUPER-W allows choosing the step in which the analysis will start. SUPER-W automatically recognizes the input file format Using the fastq file as input, SUPER-W starts from the mapping step, While the bam file directly calls the variations and with the vcf file to produce the superb results. SUPER-W is, to date, the only file format that merges the power of Mpileup results with the depth of information of the single pileup (for example the possibility of knowing the allele frequency of a variation in Mpileup format with great precision). Finally, all the pipeline steps have been developed to work in a multi-threaded environment allowing the user to analyze many samples together (Fig. 3).



Figure 2: PIs at Sequentia Biotech, working in a greenhouse.

by the irradiation event. These analyses served to eliminate the mutations produced by the genetic background. Moreover, the mutations of the control sample were subtracted. Currently a list of mutations induced by radiation has been created. In January 2018, the third phase of the project will begin, where the control and irradiated tomato seeds will be cultivated and taken to the F2 generation to study the effects of the radiation on the phenotype. Samples from adult plants will be also subjected to morpho-functional analyses to evaluate possible radiation-induced alterations of traits linked to plant productivity.

The results of this analysis were used to perform a comparative analysis and to highlight the mutations that were produced specifically

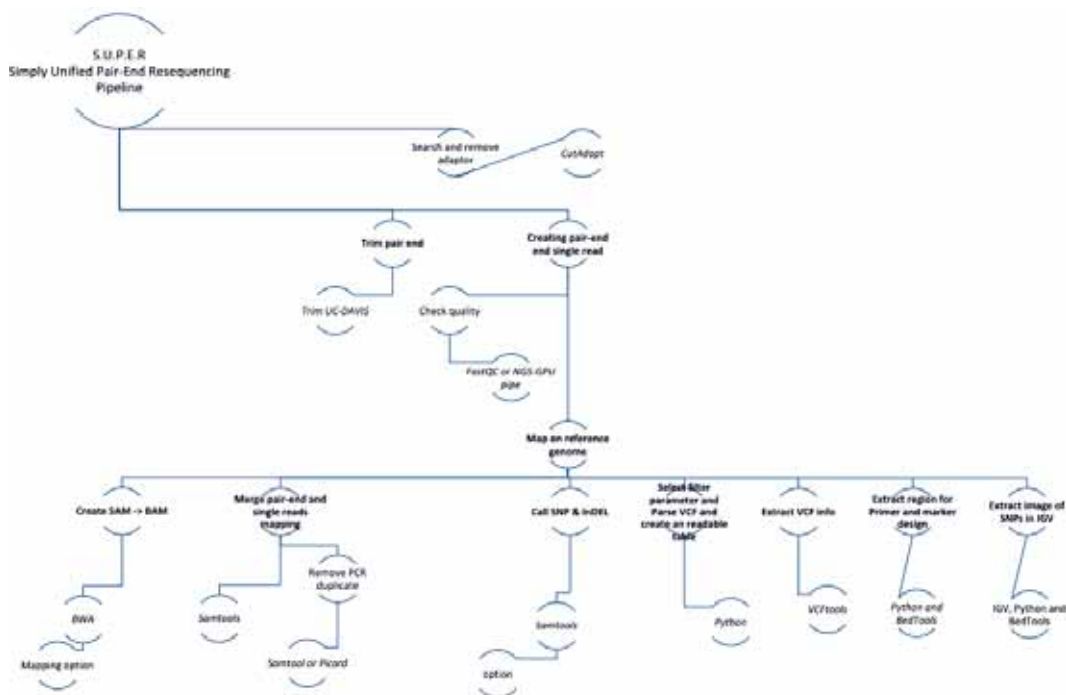


Figure 3: The SUPER pipeline workflow.

# Prima-RDH-IRPT

Mara Bruzzi,<sup>1,2</sup> Carlo Civinini,<sup>1†</sup> Nunzio Randazzo,<sup>3</sup> Marta Rovituro,<sup>4</sup> Monica Scaringella,<sup>1</sup> Valeria Sipala,<sup>5,6</sup> Francesco Tommasino<sup>7,4</sup>

In hadron therapy a highly conformed irradiation field is delivered to the target by moving the beam and, at the same time, modulating its energy. To setup a treatment plan, which efficiently covers the tumor volume with the required dose sparing as much as possible adjacent healthy tissues, the patients' Stopping Power (SP) maps should be precisely measured. These maps are presently extracted from X-rays tomographies converting the photon attenuation coefficients into SP thus introducing unavoidable uncertainties. A direct measurement of the SP maps using protons (proton Computed Tomography - pCT), could mitigate this source of errors. To be effective in reducing the uncertainties in dose distribution, this method should keep the SP map position error below one millimeter and density error below one percent. The position resolution obtained by a pCT system is essentially limited by the Multiple Coulomb Scattering (MCS). In a typical target (20 cm water equivalent) a 200 MeV proton undergoes an rms MCS angle of about 30 mrad which corresponds to an rms of the projected displacement of 3 mm or more; this effect excludes the use of simple radiographies to extract sub-millimeter SP maps. A solution is to reconstruct the most likely proton path (MLP) of each particle crossing the object under test (phantom). The MLP could be determined measuring the proton segments up- and down-stream the target. With this method the maximum error on the MLP of a 200 MeV energy proton in 20 cm of water is about 0.5 mm. In a pCT dataset single

event information is then composed by the proton MLP measured by a tracker associated to the proton energy loss as measured by a calorimeter or range counter. Data is taken with the phantom rotated at different angles and an algebraic tomographic reconstruction techniques is then used to reconstruct the 3D SP maps. Furthermore pCT images can be of paramount importance when the region to be irradiated is close to metal prosthesis. In this case the direct measurement of the SP of the prosthesis could overcome the problems coming from poor X-CT imaging of metal structures.

The pCT system (Fig. 1), built by the Prima-RDH-IRPT collaboration,<sup>1</sup> is composed by a four planes silicon microstrip tracker followed by a YaG:Ce scintillating calorimeter. The apparatus field of view



Figure 1: The Prima-RDH-IRPT pCT system mounted on the Trento Proton Therapy center experimental beam line. The four tracker planes (green boards), the anthropomorphic phantom and the calorimeter (inside the grey box) are visible. The proton beam enters the apparatus from left.

<sup>†</sup>Contact Author: [Carlo.Civinini@fi.infn.it](mailto:Carlo.Civinini@fi.infn.it)

<sup>1</sup>INFN Florence, Italy

<sup>2</sup>University of Florence, Italy

<sup>3</sup>INFN Catania, Italy

<sup>4</sup>INFN TIFPA, Trento, Italy

<sup>5</sup>University of Sassari, Italy

<sup>6</sup>INFN LNS, Catania, Italy

<sup>7</sup>University of Trento, Italy

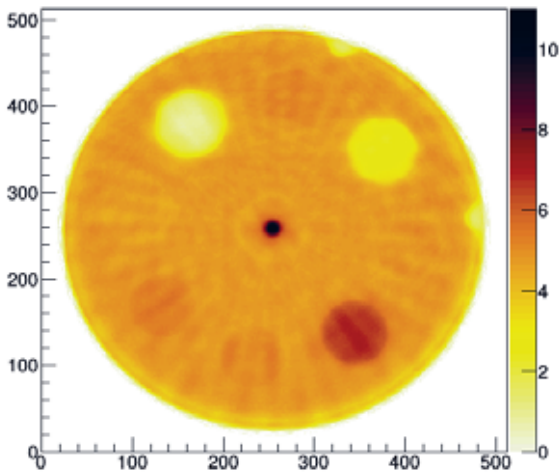


Figure 2: Tomographic reconstruction of the axial view of the electron density phantom. The color scale correspond to the proton SP [MeV/cm]. The x-y axes units are number of pixels ( $400 \times 400 \mu\text{m}^2$  each).

is about  $20 \times 5 \text{ cm}^2$ . The phantom is placed between the second and third plane, the calorimeter just after the fourth plane. A remotely controlled rotating platform and a vertical stage are used to move the phantom during data taking without the need to enter the beam area.

During July 2017 a test of the complete pCT apparatus has been performed at the Trento Proton Therapy center experimental beam line; data for two tomographies have been acquired using an anthropomorphic head phantom and a 9 cm radius electron density cylindrical phantom. The calorimeter energy response has been calibrated using six different beam energies in the range 83-228 MeV while the tracker planes have been aligned with a high statistics run at 228 MeV. The proton beam has been widened to cover the entire system field of view placing a 5 mm Tantalum scattering foil just after the beam pipe exit. Tomography data has been taken at 40 different phantom angles, about  $5 \times 10^6$  protons per projection, and analyzed using an iterative Algebraic Reconstruction Technique algorithm running on a GPU.<sup>2</sup>

A preliminary image of the electron density phantom is shown in Fig. 2. In this phantom eight different radial inserts are plugged into a water equivalent bulk material. A central tita-

anium insert (with a density of  $4.51\text{g/cm}^3$ ), to simulate a metal prosthesis, is also present. The insert located around 12 o'clock has a density of  $1.07\text{g/cm}^3$  (liver) and it is clearly visible; on the contrary the adipose insert ( $0.96\text{g/cm}^3$ ) in position around three o'clock could not be resolved.

A 1 mm thick axial slice of the anthropomorphic head at the level of the lower jaw is shown in Fig. 3. The jaw's bone as well as a vertebral section are clearly visible together with the pharynx channel. A section of a titanium prosthesis located near the vertebral bone could be identified. Both pictures exhibit radially shaped artifacts which presently limit the SP and position resolutions. Further studies are needed to fully understand this issue.

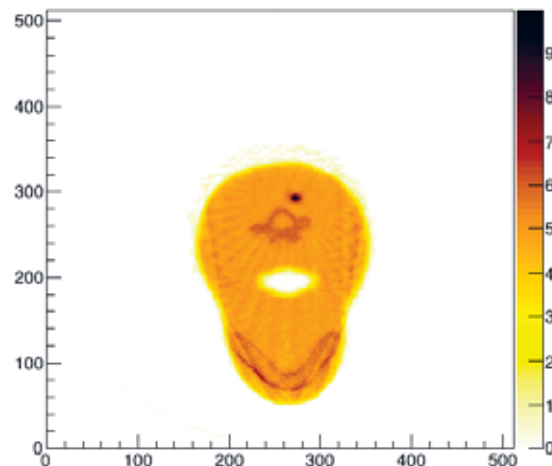


Figure 3: Tomographic reconstruction of a 1 mm thick axial slice of an anthropomorphic phantom. Axes units are the same of Fig. 2 except for pixel dimension which in this case is  $600 \times 600 \mu\text{m}^2$ .

**Acknowledgements** The authors wish to thank Dr. Marco Schwarz of Trento Proton Therapy Center, for having made available to us the anthropomorphic phantom. In addition, we gratefully acknowledge the help of the IBA and TIFPA personnel at the Trento Proton Therapy Center for quickly setting up the cyclotron to produce a reliable proton beam with the required intensity and quality. This work has been supported by INFN CSN5 Prima-RDH and MIUR IRPT experiments.

<sup>1</sup>Civinini, C. et al. (2013), Nucl. Inst. and Meth. A 732, pp. 573–576.

<sup>2</sup>Civinini, C. et al. (2016), 2016 IEEE Nuclear Science Symposium, Medical Imaging Conference, and Room-Temperature Semiconductor Detector Workshop, pp. 1–6.

# Detectors for lateral dose distributions: an intercomparison

G. Petringa,<sup>1</sup> R. Catalano,<sup>1</sup> S. Puglia,<sup>1</sup> F. Tommasino,<sup>2</sup> M. Rovituso,<sup>2</sup> S. Colombi,<sup>2</sup> E. Scifoni,<sup>2</sup> G. A. P. Cirrone<sup>1†</sup>

Relative dosimetry in terms of beam profile measurement, is a fundamental step in the quality procedures for radiotherapy. In particular for proton/ion beams, characterised by sharp dose gradients, detectors with an high spatial resolution result necessary for a correct beam characterisation. The MoVe IT (Modeling and Verification for Ion beam Treatment planning) project aims at allowing accurate description and testing of radiobiological particle beam effects, hence a precise characterization of the physical beam properties is essential. In this framework, among the possible choices, systems based on the use of scintillating screen coupled with CCD cameras can guarantee a sufficient spatial resolution and a relatively easy simplicity of use. The main aim of this work, has been investigated the suitability of a thin 2D plastic scintillator coupled to a high resolution CCD camera (Charged Coupled Device) with high energy proton beams at TIFPA facility of INFN (Istituto Nazionale di Fisica Nucleare). The device and the acquisition software has been entirely realized at LNS (Laboratori Nazionali del Sud) of INFN. In order to validate the measurements performed radiochromic EBT3 films were used as a reference.

**The functioning principle** The functioning principle of the system is based on the detection of the light emitted when a scintillator is hit by the proton beam. The system, in fact, consists of a scintillating screen mounted perpendicularly to the beam axis at a fixed distance and observed by a highly sensitive charge-coupled device camera. The basic idea is the

possibility to obtain real time information about the relative spatial dose distribution delivered through the measurement of the light emission in the scintillating screen. The main advantages of such a device are the relative simplicity of assembly and the extreme velocity into the profile acquisition. These kind of devices have been already extensively tested under passive 60 MeV proton and Carbon beams at the INFN-LNS facility and under 230 MeV active proton beams at the CNAO facility. Never this approach has been applied for large (up to  $10 \times 10 \text{ cm}^2$ ) passively transported high-energy (up to 230 MeV) therapeutic beams, like those available at the TIFPA facility. In case of large beams one limitation that must be investigated and, eventually, corrected is related to the possible image distortion at the image edges.

**Detector characteristics** The scintillator system, consists of a thin EJ204 (Scionix, Bunnik, The Netherland) plastic scintillator sheet (0.5 and 1 mm in thickness), coupled with a 12 bit Smartek Digital CCD CMOS GCP2061M with a resolution of  $2464 \times 1544$  pixels. The picture of prototype is shown in Fig. 1.

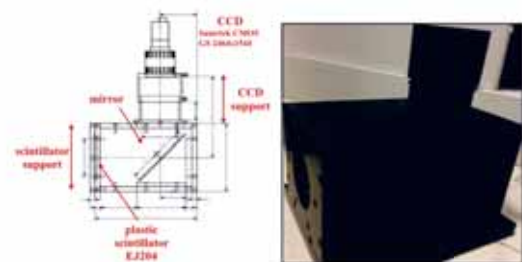


Figure 1: Schematic layout of the beam profile system (left) and its real picture .

<sup>†</sup>Contact Author: pablo.cirrone@lns.infn.it

<sup>1</sup>INFN LNS, Catania, Italy

<sup>2</sup>INFN TIFPA, Trento, Italy

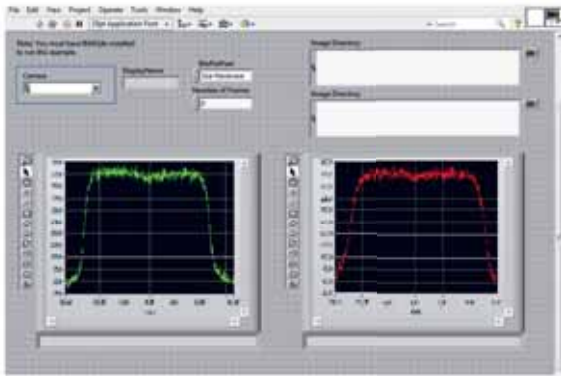


Figure 2: Panel of the preliminary version of the analysis software .

The plastic scintillator surface is placed perpendicular to the beam direction inserted in a support with a diameter of 60 mm. Behind the scintillator, at a 80 mm distance, the 45° mirror reflects the light coming from the scintillator itself in the direction perpendicular to the beam axis. The purpose of reflecting mirror is, in fact, to avoid direct irradiation of the CCD-chip. In this setup, the role of the high resolution CCD camera is to record the light signal from the mirror. The CCD is firmly fixed with some adjustment screws, allowing for an accurate alignment. All the components of the system are made of Teflon with a black surface to avoid photon scattering. The real-time data acquisition and processing is performed by in-house custom application developed with LabView 2016 (National Instruments, Austin, TX, USA). A sketch of the preliminary version of the software is shown in Fig. 2. A first preliminary experimental test of this device has been done at LNS with a proton beam of 62 MeV.

**Experimental set-up** The geometrical configuration of the elements involved in the experimental campaign performed at TIFPA protontherapy facility is reported in the Fig. 3. Accelerated protons exit in air through 70 μm Titanium window. In order to monitor the beam stability and the beam fluence during the irradiation, a detector, called MiniQ (DE.TEC.TOR., Turin, I), has been placed at 5.5 cm from the beam exit window. The beam profiling system has been placed at the isocenter with its surface perpendicular to the beam axis after a PMMA collimator with a square aperture of 1 cm and a thickness able to stop a proton beam until 150

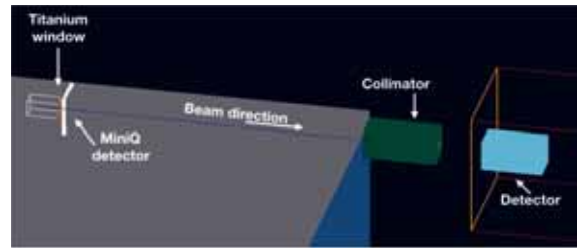


Figure 3: Schematic representation of the experimental setup.

MeV of energy.

In Fig. 4 a comparison between transversal beam profiles measured with the beam profiling system and EBT3 Gafchromic film is shown. A good agreement, with differences in terms of FWHM within 2% for the investigated proton beam energy of 150 MeV, has been found. A big discrepancy can be observed as respect lateral penumbras. This is due to the low efficiency of the employed CCD that obliged to use a thicker scintillator and to increase the beam intensity and the acquisition time of each frame; this causes a general increment of the noise. We are sure to eliminate this problem when the final, high sensitivity CCD camera will be ready.

**Conclusions** In the future, the presented instrument could be a good quality control system for clinical proton beams. Nevertheless, a more accurate investigation has to be performed in order to determine the detector operative range and increase the spatial resolution as well as the signal-to-noise ratio.

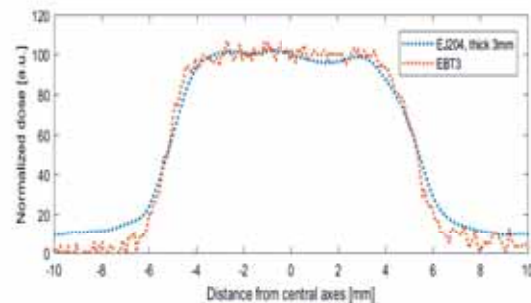


Figure 4: Horizontal profile of a mono-energetic proton beam of 150 MeV of energy. Profiles are normalized at isocenter.

**Credits** This work was done in the framework of the Move-it INFN Call-project funded by the INFN V Committee and of ASIF INFN activity.

# RIGHTABOVE: Optimizing the combination of charged particle therapy with immunotherapy for the treatment of metastatic cancer disease

Alexander Helm,<sup>1†</sup> Walter Tinganelli,<sup>1</sup> Palma Simoniello,<sup>2</sup> Alessandra Bisio,<sup>3</sup> Valentina Marchesano,<sup>1,3</sup> Rikako Azuma,<sup>4</sup> Daniel Ebner,<sup>5</sup> Shigeru Yamada,<sup>4</sup> Tadashi Kamada,<sup>4</sup> Marco Durante,<sup>1</sup> Takashi Shimokawa<sup>4</sup>

Ionizing radiation as applied in radiotherapy regimens is generally acknowledged to be immunogenic. This is discussed to be related with a specific immunogenic cell death and molecular pattern triggered by irradiation, which is hypothesized to be particularly differential following the exposure to charged particles, i.e. protons or carbon ions (Durante et al. 2016). Clinical cases in which a regression of metastatic cancer disease outside the radiation field was found after radiotherapy have been reported (Durante et al. 2013; Demaria et al. 2016) and are generally termed as abscopal effects. However, the precise mechanisms remain to be elucidated. A better understanding of these may well contribute to an effective application of immunotherapeutic drugs to boost the immunogenic effects of charged particle radiation, finally resulting in a protocol for clinical studies.

TIFPA is the integral part of an international collaboration aiming at finding such protocol. This includes the search for an efficient *in vivo* cancer model and suitable cancer type as well as the characterization of the molecular effects *in vitro*, in order to better understand the un-

derlying mechanisms. Moreover, the radiation type favorable for such treatment regimens is in the focus of the research. The collaboration includes, among others, the NIRS-QST in Chiba, Japan (Shimokawa Lab), where the accelerator HIMAC is used to expose *in vivo* and *in vitro* samples to carbon ions under medical conditions. Comparative exposures to protons and X-rays are performed at TIFPA.

**Methods** Briefly, two types of cancer and mouse models, respectively, have been investigated in preliminary studies so far: an osteosarcoma model including C3H mice and a melanoma model based on C57BL/6 mice. Tumor cells are injected in both hind limbs of mice resembling an exposed and an abscopal tumor. Whereas the osteosarcoma model is favorable for its spontaneous and easy to investigate formation of lung metastases, melanoma is a cancer type typically treated already with immunotherapeutic drugs. Such drugs are e.g. Nivolumab and Ipilimumab, which are applied in these studies, too. The aim is to determine

<sup>†</sup>Contact Author: alexander.helm@tifpa.infn.it

<sup>1</sup>INFN TIFPA, Trento, Italy

<sup>2</sup>University of Naples Parthenope, Naples, Italy

<sup>3</sup>CIBIO, Trento, Italy

<sup>4</sup>NIRS-QST, Chiba, Japan

<sup>5</sup>Brown Univ., Alpert Med. School, Providence, RI, USA

a powerful treatment regimen, i.e. the proper timing and sequence of immune therapeutics application before and/or following exposure to charged particles or X-rays. For the in vitro characterization of the molecular mechanisms and effects, the tumor cell lines will be exposed and subsequently subjected to gene expression studies using RNA-seq, a next generation sequencing method. A polysomal profiling allows to distinguish which genes are expressed more actively following irradiation. In order to determine a proper time point of investigation after exposure for this comprehensive analysis, preliminary experiments are currently being performed. These include expression studies for certain candidate genes applying qPCR after different time points following exposure as well as the influence of fractionation.

#### **Highlights of research activities in 2017**

The results of the pilot studies, which were necessary to find the correct experimental set-up are currently analyzed. Briefly, the research activity took place as follows. Three beam times have been performed in 2017 (February, October and November) at the HIMAC in Japan using carbon ions. These include in vivo and in vitro studies. Furthermore, in vitro studies, i.e. the exposure of tumor cell lines have been performed at TIFPA with X-rays and protons, applying for the first time the experimental room at the Trento Proton Therapy Center for purely biological studies in November 2017. While preliminary studies are being performed and data currently being under analysis and evaluation, the research collaboration has been screening literature in the field and has authored two reviews on the related research.

## **References**

- Demaria, S., Coleman, C. N., and Formenti, S. C. (2016). *Radiotherapy: Changing the Game in Immunotherapy*. *Trends in Cancer* **2**(6), pp. 286–294.
- Durante, M., Brenner, D. J., and Formenti, S. C. (2016). *Does Heavy Ion Therapy Work Through the Immune System?* *International Journal of Radiation Oncology\*Biophysics\*Physics* **96**(5), pp. 934–936.
- Durante, M., Reppingen, N., and Held, K. D. (2013). *Immunologically augmented cancer treatment using modern radiotherapy*. *Trends in Molecular Medicine* **19**(9), pp. 565–582.

# ROSSINI

Marta Rovituro,<sup>1</sup> Marco Durante,<sup>1</sup> Chiara La Tessa<sup>2,1†</sup>

The roadmap of space exploration foresees longer and further travels also outside the Earth orbit as well the establishment of permanent outposts on other planets like the Moon or Mars. The design of spacecrafts and habitats depends heavily on the mission scenario and must take into account the radioprotection properties of both the structural components as well as dedicated shielding. In fact, late effects caused by exposure to cosmic radiation are nowadays considered the main health risks of space travel. The combination of increased mission length with the radiation environment in deep space will result in exceeding the currently accepted radiation dose limits. As time in space should be increased, rather than decreased, according to the plans of exploration and colonization, the best tools for minimizing the risk to the crew members are the mission planning and spacecraft design.

Among the strategies currently available, passive systems seem to be the only realistic option, as active shielding and biology-based countermeasures are both still in a preliminary phase. The current trend is to find multifunctional materials that combine excellent mechanical properties with a high shielding effectiveness to minimize the overall load. The greatest challenge is posed by the high-energetic component of the Galactic Cosmic Rays (GCR), which require a very thick shielding ( $>20 \text{ g cm}^{-2}$ ) to be fully stopped and thus call for an alternative approach to reduce its contribution to the total dose. The optimal ap-

proach is to exploit nuclear fragmentation for breaking up the ions into lighter species with lower biological effects. Following this idea, several studies have been focused on characterizing the fragmentation power of a variety of materials either of current use in space or potential candidates. Measurements available from literature have been mostly performed with  $\approx 1000 \text{ MeV/u } ^{56}\text{Fe}$  ions, chosen as a proxy for the high-energy and heavy-ions (HZE) of the GCR spectrum. Nevertheless, the shielding effectiveness of a given material has been proven to change dramatically depending on the beam species and energy and to obtain an overall rank of the materials a comprehensive study is needed.

The ROSSINI project of the European Space Agency (ESA) is a ground-based study of shielding for space travel. Its approach is based on the use of a single high-energy heavy ion beam attenuation to estimate the shielding effectiveness of different materials. (Zeitlin et al. 2008) Its test campaign has included target materials currently used in different mission scenarios for structural or shielding functions as well as promising alternative candidates. The main rationale behind the selection was to find multifunctional materials which represent an optimal compromise between mechanical properties and radioprotection performances. Simulants of in-situ resources have been studied too because they are considered the best option for building permanent habitats on other planets.

The shielding effectiveness of all materi-

<sup>†</sup>Contact Author: chiara.latessa@tifpa.infn.it

<sup>1</sup>INFN TIFPA, Trento, Italy

<sup>2</sup>University of Trento, Italy

als has been assessed by measuring their performance in reducing the dose when exposed to high-energy charged particles. The samples were exposed to 1000 MeV/u  $^4\text{He}$  and 962-972 MeV/u  $^{56}\text{Fe}$  beams at the NASA Space Radiation Laboratory (NSRL) in Brookhaven National Laboratory (Upton NY, USA) and to 430 MeV/u  $^{12}\text{C}$  ions at the Heavy Ion Therapy (HIT) center (Heidelberg, Germany). The beams selected for the test campaign were identified as a proxy for the GCRs.

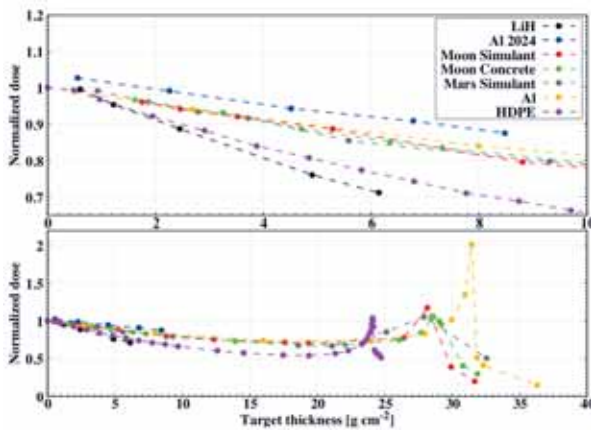


Figure 1: Partial or full Bragg curves of 968 MeV/u  $^{56}\text{Fe}$  ions in Aluminum, High Density Polyethylene (HDPE), Moon and Mars simulants and 972 MeV/u  $^{56}\text{Fe}$  ions in Aluminum 2024, Lithium Hydride (LiH) and Moon concrete. The upper plot is a zoom of the datasets up to  $10\text{ g cm}^{-2}$  of depth.

The dose reduction (partial or full Bragg curves when enough material was available) were measured for all selected candidates to obtain their shielding effectiveness. Results obtained with Iron are shown in Fig. 1.

The shielding effectiveness of all materials have been obtained with the methods described in (Zeitlin et al. 2008) and are shown in Fig. 2 for some selected materials. The values have been normalized to the material area density.

The findings indicate that the best shielding is lithium hydride, which performs better

## References

Agostinelli, S. et al. (2003). *GEANT4—a simulation toolkit*. Nucl. Inst. Meth. A **506**, p. 250.  
 Sato, T. et al. (2013). *Particle and Heavy Ion Transport Code System PHITS, Version 2.52*. J. Nucl. Sci. Technol. **50**, pp. 913–923.  
 Zeitlin, C. et al. (2008). *Shielding experiments with high-energy heavy ions for spaceflight applications*. New J. Phys. **10**(7), p. 075007.

than polyethylene (the current shielding material used on the ISS). For this reason, the addition of lithium hydride to multi-layer samples caused a much stronger dose decrease than other materials of comparable area density. The results also show that the classification of all candidates in term of shielding effectiveness is not influenced by the ion species, but the value changes dramatically depending on the beam energy. All in-situ resources have a similar shielding effectiveness around  $3\% \text{ cm}^2 \text{ g}^{-1}$ .

The output of this investigation has provided guidelines and recommendations for the design of space vessels, inflatable habitats and permanent outposts in different space environments. Additionally, the results represent a rich dataset for benchmarking Monte Carlo codes currently used for space applications. In fact, a task of ROSSINI has been dedicated to the comparison of all experimental data with simulations from GRAS(Agostinelli et al. 2003) and PHITS(Sato et al. 2013) Monte Carlo transport codes.

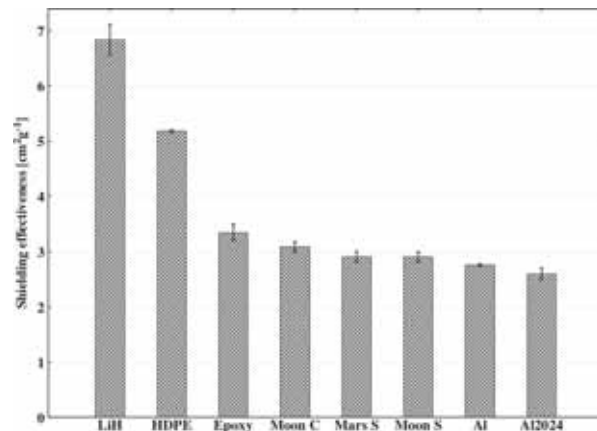


Figure 2: Shielding effectiveness of Aluminum (Al), High Density Polyethylene (HDPE), Moon (Moon S) and Mars (Mars S) simulants exposed to 968 MeV/u  $^{56}\text{Fe}$  ions and Aluminum 2024 (Al2024), Lithium Hydride (LiH) and Moon concrete (Moon C) exposed to 972 MeV/u  $^{56}\text{Fe}$  ions. All values have been normalized to the target area density.

# TIFPA Services



### **Giuliana Pellizzari**

giuliana.pellizzari@tifpa.infn.it

direction secretariat, scientific associations, Personnel selection procedures, agreements, Personnel training courses, safety matters

### **Laura Chilovi**

laura.chilovi@tifpa.infn.it

travel support, scientific secretariat, seminars, shipment service

### **Marta Perucci**

marta.perucci@tifpa.infn.it

Head of service, Personnel affairs, budget management, purchases, payments, event organization, external funds



### **Alberto Franzoi**

alberto.franzoi@tifpa.infn.it

design and realization of silicon chips for radiation detection

### **Piero Spinnato**

piero.spinnato@tifpa.infn.it

Head of service, general technical management, coordination with UniTN services, IT infrastructure management and development, TIFPA website and publications editor

### **Christian Manea**

christian.manea@tifpa.infn.it

laboratories technical management, electronics development, user support at Protontherapy experimental room, technology transfer, Personnel delegate at TIFPA board, Personnel safety delegate

### **Enrico Verroi**

enrico.verroi@tifpa.infn.it

Facility planning for Protontherapy experimental beam-lines, coordination of user support at Protontherapy experimental room

# TIFPA Services

Marta Perucci, Piero Spinnato

**Administration** In 2017, the SIGEA service has increased his general activities. The service is composed by 3 employees. The general budget for the year 2017, compared with 2016, is displayed in the table below:

year	total funds [k€]	external funds [k€]
2017	1800	476
2016	1600	205

Table 1: TIFPA budget.

TIFPA was awarded in 2017 the EU Horizon2020 Infrastructure INSPIRE project and the MIUR-Premiale SPARE project (along with ASI and Centro Fermi) thanks to the proton facility and they will go into the 2018 budget.

The number of administrative procedures of the service in 2017 amounts to approximately 600 travels and 130 orders of purchase. Concerning personnel, in 2017 TIFPA substantially increased its permanent staff, which now amounts to 5 units, thanks to the recruitment of 3 permanent staff members (2 new and 1 from temporary staff). The number of temporary employees has been increased to 12, under various types of contracts, e.g., research fellowships and post-docs. We also host students from Trento University master courses. Concerning research associates, their number at the end of the year amounts to 151. During 2017, we organized 17 scientific seminars. The SIGEA service has provided support for two new scientific boards: the *Gruppo di Sorveglianza* (GdS) and the Proposal Advisory Committee (PAC). The GdS has been appointed by the INFN man-

agement with the duty of coordinating the experimental requests for INFN scientific groups who need to collaborate with FBK. The PAC is a board internal to TIFPA, wich manages and evaluates proposals from national and international scientific groups or companies for irradiation experiment requests at the APSS proton therapy center.

**Technical Services** Following the startup phase of 2015-16, the activities of the TIFPA Technical Services in 2017 have been mainly oriented to the consolidation of the research infrastructure built over the previous years. The clean room within the headquarters in Povo has been made fully operational and began hosting activities in both performance testing of microelectronics for particle detection in Space, which also uses the facilities in the electronics lab, and for radiobiology *in vitro* experiments. Researchers working in the latter area are also heavily exploiting the X-ray radiogenic machine installed in December 2016.

The experimental room at the APSS proton-therapy centre has been extensively used for a wide spectrum of activities based on the two proton beamlines hosted therein (accounts of such activities are collected in the *Proton Beam-based R&D Part*).

In order to meet the need for a transparent interconnection to the wireless network of the external users of the beamline facility, we set-up the wireless network infrastructure of the protontherapy centre to provide the pan-european eduroam network. As usual for the IT infras-

structure at the protontherapy centre, the setup of the eduroam network is an excellent example of harmonic coordination among partners. The wireless infrastructure is under the administrative responsibility of APSS, the authentication process is managed by UniTN, passing from ether to copper, the network traffic travels across INFN devices.

The service is developing an environment for scientific computing, based on hardware acquired by research groups. An initial nucleus consisting of two storage and computing nodes, including 48 TB of raw storage, 80 hy-

perthreaded cores and four 10 Gb/s network interfaces has been provided by the MoVe-IT project. Over this physical substrate, we will build a middleware environment which will manage the provisioning of virtualized computing resources that users will access transparently through usual batch submission tools.

A non negligible fraction of our time has been devoted to user support in technical matters and administrative tasks for purchasing procedures. Finally, with much enjoyment we fulfilled the task of editing and publishing this Annual Report.

# TIFPA Publications

## Virtual Labs

### Medical Technologies

- Baselet, B., Azimzadeh, O., Erbedinger, N., Bakshi, M., Dettmering, T., Janssen, A., Ktitareva, S., Lowe, D., Michaux, A., Quintens, R., Raj, K., Durante, M., Fournier, C., Benotmane, M., Baatout, S., Sonveaux, P., Tapio, S., and Aerts, A. (2017). *Differential impact of single-dose Fe ion and X-ray irradiation on endothelial cell transcriptomic and proteomic responses*. *Frontiers in Pharmacology* **8**(9).
- Durante, M., Cucinotta, F., and Loeffler, J. (2017a). *Editorial: Charged particles in oncology*. *Frontiers in Oncology* **7**(12).
- Durante, M., Forte, G., and Russo, G. (2017b). *Radiobiological models towards a personalized radiation oncology*. *Translational Cancer Research* **6**, S759–S760.
- Durante, M., Orecchia, R., and Loeffler, J. (2017c). *Charged-particle therapy in cancer: Clinical uses and future perspectives*. *Nature Reviews Clinical Oncology* **14**(8), pp. 483–495.
- Ebner, D., Tinganelli, W., Helm, A., Bisio, A., Simoniello, P., Natale, F., Yamada, S., Kamada, T., Shimokawa, T., and Durante, M. (2017a). *Generating and grading the abscopal effect: Proposal for comprehensive evaluation of combination immunoradiotherapy in mouse models*. *Translational Cancer Research* **6**, S892–S899.
- Ebner, D., Tinganelli, W., Helm, A., Bisio, A., Yamada, S., Kamada, T., Shimokawa, T., and Durante, M. (2017b). *The immunoregulatory potential of particle radiation in cancer therapy*. *Frontiers in Immunology* **8**(2).
- Erbedinger, N., Rapp, F., Ktitareva, S., Wendel, P., Bothe, A., Dettmering, T., Durante, M., Friedrich, T., Bertulat, B., Meyer, S., Cardoso, M., Hehlhans, S., Rödel, F., and Fournier, C. (2017). *Measuring leukocyte adhesion to (primary) endothelial cells after photon and charged particle exposure with a dedicated laminar flow chamber*. *Frontiers in Immunology* **8**(6).
- Kreuzer, M., Auvinen, A., Cardis, E., Durante, M., Harms-Ringdahl, M., Jourdain, J., Madas, B., Ottolenghi, A., Pazzaglia, S., Prise, K., Quintens, R., Sabatier, L., and Bouffler, S. (2017). *Multidisciplinary European Low Dose Initiative (MELODI): strategic research agenda for low dose radiation risk research*. *Radiation and Environmental Biophysics*. Article in Press, pp. 1–11.
- Luft, S., Arrizabalaga, O., Kulish, I., Nasonova, E., Durante, M., Ritter, S., and Schroeder, I. (2017). *Ionizing Radiation Alters Human Embryonic Stem Cell Properties and Differentiation Capacity by Diminishing the Expression of Activin Receptors*. *Stem Cells and Development* **26**(5), pp. 341–352.
- Natale, F., Rapp, A., Yu, W., Maiser, A., Harz, H., Scholl, A., Grulich, S., Anton, T., Hörl, D., Chen, W., Durante, M., Taucher-Scholz, G., Leonhardt, H., and Cardoso, M. (2017). *Identification of the elementary structural units of the DNA damage response*. *Nature Communications* **8**.
- Richter, D., Lehmann, H., Eichhorn, A., Constantinescu, A., Kaderka, R., Prall, M., Lugenbiel, P., Takami, M., Thomas, D., Bert, C., Durante, M., Packer, D., and Graeff, C. (2017). *ECG-based 4D-dose reconstruction of cardiac arrhythmia ablation with carbon ion beams: Application in a porcine model*. *Physics in Medicine and Biology* **62**(17), pp. 6869–6883.

- Rovituso, M., Schuy, C., Weber, U., Brons, S., Cortés-Giraldo, M., La Tessa, C., Piasetzky, E., Izraeli, D., Schardt, D., Toppi, M., Scifoni, E., Krämer, M., and Durante, M. (2017). *Fragmentation of 120 and 200 MeV u-14He ions in water and PMMA targets*. *Physics in Medicine and Biology* **62**(4), pp. 1310–1326.
- Schneider, C., Newhauser, W., Wilson, L., Schneider, U., Kaderka, R., Miljanić, S., Knežević, Ž., Stolarczyk, L., Durante, M., and Harrison, R. (2017). *A descriptive and broadly applicable model of therapeutic and stray absorbed dose from 6 to 25 MV photon beams*: *Medical Physics* **44**(7), pp. 3805–3814.
- Sokol, O., Scifoni, E., Tinganelli, W., Kraft-Weyrather, W., Wiedemann, J., Maier, A., Boscolo, D., Friedrich, T., Brons, S., Durante, M., and Kämer, M. (2017). *Oxygen beams for therapy: Advanced biological treatment planning and experimental verification*. *Physics in Medicine and Biology* **62**(19), pp. 7798–7813.
- Tommasino, F., Durante, M., D’Avino, V., Liuzzi, R., Conson, M., Farace, P., Palma, G., Schwarz, M., Cella, L., and Pacelli, R. (2017a). *Model-based approach for quantitative estimates of skin, heart, and lung toxicity risk for left-side photon and proton irradiation after breast-conserving surgery*. *Acta Oncologica* **56**(5), pp. 730–736.
- Tommasino, F., Rovituso, M., Fabiano, S., Piffer, S., Manea, C., Lorentini, S., Lanzone, S., Wang, Z., Pasini, M., Burger, W., La Tessa, C., Scifoni, E., Schwarz, M., and Durante, M. (2017b). *Proton beam characterization in the experimental room of the Trento Proton Therapy facility*. *Nuclear Instruments and Methods in Physics Research, Section A: Accelerators, Spectrometers, Detectors and Associated Equipment* **869**, pp. 15–20.
- Vanstalle, M., Mattei, I., Sarti, A., Bellini, F., Bini, F., Collamati, F., De Lucia, E., Durante, M., Faccini, R., Ferroni, F., Finck, C., Fiore, S., Marafini, M., Patera, V., Piersanti, L., Rovituso, M., Schuy, C., Sciubba, A., Traini, G., Voena, C., and La Tessa, C. (2017). *Benchmarking Geant4 hadronic models for prompt- $\gamma$  monitoring in carbon ion therapy*. *Medical Physics* **44**(8), pp. 4276–4286.

## Sensors and detectors

- Benkechkache, M., Latreche, S., Ronchin, S., Boscardin, M., Pancheri, L., and Dalla Betta, G.-F. (2017). *Design and First Characterization of Active and Slim-Edge Planar Detectors for FEL Applications*. *IEEE Trans. Nucl. Sci.* **64**(4), pp. 1062–1070.
- Cartiglia, N., Arcidiacono, R., Baldassarri, B., Boscardin, M., Cenna, F., Dellacasa, G., Dalla Betta, G.-F., Ferrero, M., Fadeyev, V., Galloway, Z., Garbolino, S., Grabas, H., Monaco, V., Obertino, M., Pancheri, L., Paternoster, G., Rivetti, A., Rolo, M., Sacchi, R., Sadrozinski, H., Seiden, A., Sola, V., Solano, A., Staiano, A., Ravera, F., and Zatserklyaniy, A. (2017). *Tracking in 4 dimensions*. *Nucl. Instrum. Methods A* **845**, pp. 47–51.
- Lodola, L., Batignani, G., Benkechkache, M., Bettarini, S., Casarosa, G., Dalla Betta, G.-F., Fabris, L., Forti, F., Giorgi, M., Grassi, M., Malcovati, P., Manghisoni, M., Morsani, F., Paladino, A., Pancheri, L., Paoloni, E., Ratti, L., Re, V., Rizzo, G., Traversi, G., Vacchi, C., Verzellesi, G., and Xu, H. (2017a). “PixFEL: development of an X-ray diffraction imager for future FEL applications”. *Proceedings of Science - 25th Workshop on Vertex Detectors (Vertex 2016)*. Ed. by F. Forti and F. Palla. Trieste, Italy: Sissa, 065(1–10).
- Lodola, L., Ratti, L., Comotti, D., Fabris, L., Grassi, M., Malcovati, P., Manghisoni, M., Re, V., Traversi, G., Vacchi, C., Batignani, G., Bettarini, S., Forti, F., Casarosa, G., Morsani, F., Paladino, A., Paoloni, E., Rizzo, G., Benkechkache, M., Dalla Betta, G.-F., Mendicino, R., Pancheri, L., Verzellesi, G., and Xu, H. (2017b). “A pixelated X-ray detector for diffraction imaging at next-generation high-rate FEL sources”. *Proc. SPIE 10392 (Hard X-ray, Gamma-ray, and Neutron detector physics XIX)*. SPIE, p. 103920D.

- Paternoster, G., Arcidiacono, R., Boscardin, M., Cartiglia, N., Cenna, F., Dalla Betta, G.-F., Ferrero, M., Malaria, M., Obertino, M., Pancheri, L., Piemonte, C., and Sola, V. (2017a). *Developments and first measurements of Ultra-Fast Silicon Detectors produced at FBK*. *Journal Instrum.* **12**, p. C02077.
- Ratti, L., Comotti, D., Fabris, L., Grassi, M., Lodola, L., Malcovati, P., Manghisoni, M., Re, V., Traversi, G., Vacchi, C., Batignani, G., Bettarini, S., Casarosa, G., Forti, F., Morsani, F., Paladino, A., Paoloni, E., Rizzo, G., Benkechache, M., Dalla Betta, G.-F., Mendicino, R., Pancheri, L., Verzellesi, G., and Xu, H. (2017). “PFM2: a 32x32 readout chip for the PixFEL X-ray imager demonstrator”. *IEEE Nuclear Science Symposium and Medical Imaging Conference (NSS - MIC’16)*. Ed. by C. Da Via.
- Staiano, A., Arcidiacono, R., Boscardin, M., Dalla Betta, G.-F., Cartiglia, N., Cenna, F., Ferrero, M., Ficorella, F., Mandurrino, M., Obertino, M., Pancheri, L., Paternoster, G., and Sola, V. (2017). *Development of Ultra-Fast Silicon Detectors for 4D Tracking*. *Journal Instrum.* **12**, p. C12012.
- Acerbi, F., Davini, S., Ferri, A., Galbiati, C., Giovanetti, G., Gola, A., Korga, G., Mandarano, A., Marcante, M., Paternoster, G., Piemonte, C., Razeto, A., Regazzoni, V., Sablone, D., Savarese, C., Zappalà, G., and Zorzi, N. (2017a). *Cryogenic Characterization of FBK HD Near-UV Sensitive SiPMs*. *IEEE Transactions on Electron Devices* **64**(2), pp. 521–526.
- Regazzoni, V., Acerbi, F., Cozzi, G., Ferri, A., Fiorini, C., Paternoster, G., Piemonte, C., Rucatti, D., Zappalà, G., Zorzi, N., and Gola, A. (2017b). *Characterization of high density SiPM non-linearity and energy resolution for prompt gamma imaging applications*. *Journal of Instrumentation* **12**, P07001.
- Abba, A., Caponio, F., Citterio, M., Coelli, S., Fu, J., Lazzaroni, M., Merli, A., Monti, M., Neri, N., Petruzzo, M., Rashevskaya, I., and Terzi, D. (2017). *Silicon telescope for prototype sensor characterization using particle beams and cosmic rays*. *Journal of Instrumentation* **12**(03), p. C03060.
- Adamczyk, K. et al., Belle-II SVD (2017). *The Belle II silicon vertex detector assembly and mechanics*. *Nucl. Instrum. Meth.* **A845**, 38–42.
- Alfonsi, L., Ambroglini, F., Ambrosi, G., Ammendola, R., Assante, D., Badoni, D., Belyaev, V., Burger, W., Cafagna, A., Cipollone, P., Consolini, G., Conti, L., Contin, A., De Angelis, E., De Donato, C., De Franceschi, G., De Santis, A., De Santis, C., Diego, P., and Zoffoli, S. (2016). *The HEPD particle detector and the EFD electric field detector for the CSES satellite*. **137**.
- Caria, G. et al., Belle-II SVD (2017). *The Software Framework of the Belle II Silicon Vertex Detector and its Development for the 2016 Test-Beam at DESY*. *PoS Vertex2016*, p. 060.
- Dutta, D. et al. (2017). *Belle II Silicon Vertex Detector*. *JINST* **12**(02), p. C02074.
- Lück, T. et al., Belle-II SVD (2017). *Performance studies of the Belle II Silicon Vertex Detector with data taken at the DESY test beam in April 2016*. *PoS Vertex2016*, p. 057.
- Nakamura, K. R. et al., Belle-II SVD (2017). *The Belle II SVD detector*. *PoS Vertex2016*, p. 012.
- Rashevskaya, I. et al. (2017). *Double-sided strip sensors for the Limadou-CSES project*. *PoS Vertex2016*, p. 064.
- Vitale, L. et al., Belle-II SVD (2017). *The Monitoring System of the Belle II Vertex Detector*. *PoS Vertex2016*, p. 051.

## Particle Physics

- Chatrchyan, S. et al., CMS collaboration (2017). *Measurement of the mass difference between top quark and antiquark in pp collisions at  $\sqrt{s} = 8$  TeV*. *Phys. Lett.* **B770**, pp. 50–71.

## ATLAS

- Aaboud, M. et al., The ATLAS Collaboration (2017[a]). *A measurement of the calorimeter response to single hadrons and determination of the jet energy scale uncertainty using LHC Run-1 pp-collision data with the ATLAS detector*. European Physical Journal C **77**(1).
- The ATLAS Collaboration (2017[b]). *Analysis of the  $Wtb$  vertex from the measurement of triple-differential angular decay rates of single top quarks produced in the  $t$ -channel at  $\sqrt{s}=8$  TeV with the ATLAS detector*. Journal of High Energy Physics (12).
  - The ATLAS Collaboration (2017[c]). *Determination of the strong coupling constant  $\alpha(s)$  from transverse energy-energy correlations in multijet events at  $\sqrt{s}=8$  TeV using the ATLAS detector*. European Physical Journal C **77**(12).
  - The ATLAS Collaboration (2017[d]). *Electron efficiency measurements with the ATLAS detector using 2012 LHC proton-proton collision data*. European Physical Journal C **77**(3).
  - The ATLAS Collaboration (2017[e]). *Evidence for light-by-light scattering in heavy-ion collisions with the ATLAS detector at the LHC*. Nature Physics **13**(9), pp. 852+.
  - The ATLAS Collaboration (2017[f]). *Evidence for the  $H \rightarrow b\bar{b}$  decay with the ATLAS detector*. Journal of High Energy Physics (12).
  - The ATLAS Collaboration (2017[g]). *Femtoscopy with identified charged pions in proton-lead collisions at  $\sqrt{s_{NN}}=5.02$  TeV with ATLAS*. Physical Review C **96**(6).
  - The ATLAS Collaboration (2017[h]). *Fiducial, total and differential cross-section measurements of  $t$ -channel single top-quark production in pp collisions at 8 TeV using data collected by the ATLAS detector*. European Physical Journal C **77**(8).
  - The ATLAS Collaboration (2017[i]). *High- $E-T$  isolated-photon plus jets production in pp collisions at  $\sqrt{s}=8$  TeV with the ATLAS detector*. Nuclear Physics B **918**, 257–316.
  - The ATLAS Collaboration (2017[j]). *Identification and rejection of pile-up jets at high pseudorapidity with the ATLAS detector*. European Physical Journal C **77**(9).
  - The ATLAS Collaboration (2017[k]). *Identification and rejection of pile-up jets at high pseudorapidity with the ATLAS detector (vol 77, 580, 2017)*. European Physical Journal C **77**(10).
  - The ATLAS Collaboration (2017[l]). *Jet energy scale measurements and their systematic uncertainties in proton-proton collisions at  $\sqrt{s}=13$  TeV with the ATLAS detector*. Physical Review D **96**(7).
  - The ATLAS Collaboration (2017[m]). *Jet reconstruction and performance using particle flow with the ATLAS Detector*. European Physical Journal C **77**(7).
  - The ATLAS Collaboration (2017[n]). *Measurement of  $b$ -hadron pair production with the ATLAS detector in proton-proton collisions at  $\sqrt{s}=8$  TeV*. Journal of High Energy Physics (11).
  - The ATLAS Collaboration (2017[o]). *Measurement of charged-particle distributions sensitive to the underlying event in  $\sqrt{s}=13$  TeV proton-proton collisions with the ATLAS detector at the LHC*. Journal of High Energy Physics (3).
  - The ATLAS Collaboration (2017[p]). *Measurement of detector-corrected observables sensitive to the anomalous production of events with jets and large missing transverse momentum in pp collisions at  $\sqrt{s}=13$  TeV using the ATLAS detector*. European Physical Journal C **77**(11).
  - The ATLAS Collaboration (2017[q]). *Measurement of forward-backward multiplicity correlations in lead-lead, proton-lead, and proton-proton collisions with the ATLAS detector*. Physical Review C **95**(6).
  - The ATLAS Collaboration (2017[r]). *Measurement of inclusive and differential cross sections in the  $H \rightarrow ZZ^* \rightarrow 4l$  decay channel in pp collisions at  $\sqrt{s}=13$  TeV with the ATLAS detector*. Journal of High Energy Physics (10).
  - The ATLAS Collaboration (2017[s]). *Measurement of jet activity produced in top-quark events with an electron, a muon and two  $b$ -tagged jets in the final state in pp collisions  $\sqrt{s}=13$ TeV with the ATLAS detector*. European Physical Journal C **77**(4).

- The ATLAS Collaboration (2017[t]). *Measurement of jet fragmentation in Pb + Pb and pp collisions at  $\sqrt{s_{NN}}=2.76$  TeV with the ATLAS detector at the LHC.* European Physical Journal C **77**(6).
- The ATLAS Collaboration (2017[u]). *Measurement of jet  $p(T)$  correlations in Pb + Pb and pp collisions at  $\sqrt{s_{NN}}=2.76$  TeV with the ATLAS detector.* Physics Letters B **774**, 379–402.
- The ATLAS Collaboration (2017[v]). *Measurement of lepton differential distributions and the top quark mass in  $t\bar{t}$  production in pp collisions at a  $\sqrt{s}=8$  TeV with the ATLAS detector.* European Physical Journal C **77**(11).
- The ATLAS Collaboration (2017[w]). *Measurement of multi-particle azimuthal correlations in pp, p + Pb and low-multiplicity Pb + Pb collisions with the ATLAS detector.* European Physical Journal C **77**(6).
- The ATLAS Collaboration (2017[x]). *Measurement of the cross section for inclusive isolated-photon production in pp collisions at  $\sqrt{s}=13$  TeV using the ATLAS detector.* Physics Letters B **770**, 473–493.
- The ATLAS Collaboration (2017[y]). *Measurement of the cross-section for electroweak production of dijets in association with a Z boson in pp collisions at  $\sqrt{s}=13$  TeV with the ATLAS detector.* Physics Letters B **775**, 206–228.
- The ATLAS Collaboration (2017[z]). *Measurement of the Drell-Yan triple-differential cross section in pp collisions at  $\sqrt{s}=8$  TeV.* Journal of High Energy Physics (12).
- The ATLAS Collaboration (2017[aa]). *Measurement of the inclusive cross-sections of single top-quark and top-antiquark t-channel production in pp collisions at  $\sqrt{s}=13$  TeV with the ATLAS detector.* Journal of High Energy Physics (4).
- The ATLAS Collaboration (2017[ab]). *Measurement of the inclusive jet cross-sections in proton-proton collisions at  $\sqrt{s}=8$  TeV with the ATLAS detector.* Journal of High Energy Physics (9).
- The ATLAS Collaboration (2017[ac]). *Measurement of the  $k(t)$  splitting scales in  $Z \rightarrow ll$  events in pp collisions at  $\sqrt{s}=8$  TeV with the ATLAS detector.* Journal of High Energy Physics (8).
- The ATLAS Collaboration (2017[ad]). *Measurement of the prompt  $J/\psi$  pair production cross-section in pp collisions at  $\sqrt{s}=8$  TeV with the ATLAS detector.* European Physical Journal C **77**(2).
- The ATLAS Collaboration (2017[ae]). *Measurement of the  $t\bar{t}\gamma$  production cross section in proton-proton collisions at  $\sqrt{s}=8$  TeV with the ATLAS detector.* Journal of High Energy Physics (11).
- The ATLAS Collaboration (2017[af]). *Measurement of the  $t\bar{t}$  production cross section in the tau plus jets final state in pp collisions at  $\sqrt{s}=8$  TeV using the ATLAS detector.* Physical Review D **95**(7).
- The ATLAS Collaboration (2017[ag]). *Measurement of the  $t\bar{t}Z$  and  $t\bar{t}W$  production cross sections in multilepton final states using  $3.2 \text{ fb}^{-1}$  of pp collisions at  $\sqrt{s}=13$  TeV with the ATLAS detector.* European Physical Journal C **77**(1).
- The ATLAS Collaboration (2017[ah]). *Measurement of the W boson polarisation in  $t\bar{t}$  events from pp collisions at  $\sqrt{s}=8$  TeV in the lepton plus jets channel with ATLAS.* European Physical Journal C **77**(4).
- The ATLAS Collaboration (2017[ai]). *Measurement of the  $W^+ W^-$  production cross section in pp collisions at a centre-of-mass energy of  $\sqrt{s}=13$  TeV with the ATLAS experiment.* Physics Letters B **773**, 354–374.
- The ATLAS Collaboration (2017[aj]). *Measurement of the ZZ production cross section in proton-proton collisions at  $\sqrt{s}=8$  TeV using the  $ZZ \rightarrow \ell^-\ell^+\ell'^-\ell'^+$  and  $ZZ \rightarrow \ell^-\ell^+\nu\bar{\nu}$  decay channels with the ATLAS detector.* Journal of High Energy Physics (1).
- The ATLAS Collaboration (2017[ak]). *Measurement of W boson angular distributions in events with high transverse momentum jets at  $\sqrt{s}=8$  TeV using the ATLAS detector.* Physics Letters B **765**, 132–153.
- The ATLAS Collaboration (2017[al]). *Measurement of  $W^\pm W^\pm$  vector-boson scattering and limits on anomalous quartic gauge couplings with the ATLAS detector.* Physical Review D **96**(1).

- Aaboud, M. et al., The ATLAS Collaboration (2017[am]). *Measurement of  $WW/WZ \rightarrow \ell \nu qq'$  production with the hadronically decaying boson reconstructed as one or two jets in  $pp$  collisions at  $\sqrt{s}=8$  TeV with ATLAS, and constraints on anomalous gauge couplings*. European Physical Journal C **77**(8).
- The ATLAS Collaboration (2017[an]). *Measurements of  $\psi(2S)$  and  $X(3872) \rightarrow J/\psi \pi^+ \pi^-$  production in  $pp$  collisions at  $\sqrt{s}=8$  TeV with the ATLAS detector*. Journal of High Energy Physics (1).
  - The ATLAS Collaboration (2017[ao]). *Measurements of charge and CP asymmetries in  $b$ -hadron decays using top-quark events collected by the ATLAS detector in  $pp$  collisions at  $\sqrt{s}=8$  TeV*. Journal of High Energy Physics (2).
  - The ATLAS Collaboration (2017[ap]). *Measurements of integrated and differential cross sections for isolated photon pair production in  $pp$  collisions at  $\sqrt{s}=8$  TeV with the ATLAS detector*. Physical Review D **95**(11).
  - The ATLAS Collaboration (2017[aq]). *Measurements of long-range azimuthal anisotropies and associated Fourier coefficients for  $pp$  collisions at  $\sqrt{s}=5.02$  and 13 TeV and  $p + Pb$  collisions at  $\sqrt{s_{NN}}=5.02$  TeV with the ATLAS detector*. Physical Review C **96**(2).
  - The ATLAS Collaboration (2017[ar]). *Measurements of the production cross section of a  $Z$  boson in association with jets in  $pp$  collisions at  $\sqrt{s}=13$  TeV with the ATLAS detector*. European Physical Journal C **77**(6).
  - The ATLAS Collaboration (2017[as]). *Measurements of top quark spin observables in  $tt$  events using dilepton final states in  $\sqrt{s}=8$  TeV  $pp$  collisions with the ATLAS detector*. Journal of High Energy Physics (3).
  - The ATLAS Collaboration (2017[at]). *Measurements of top-quark pair differential cross-sections in the  $e\mu$  channel in  $pp$  collisions at  $\sqrt{s}=13$  TeV using the ATLAS detector*. European Physical Journal C **77**(5).
  - The ATLAS Collaboration (2017[au]). *Measurements of top-quark pair differential cross-sections in the lepton plus jets channel in  $pp$  collisions at  $\sqrt{s}=13$  TeV using the ATLAS detector*. Journal of High Energy Physics (11).
  - The ATLAS Collaboration (2017[av]). *Measurements of top-quark pair to  $Z$ -boson cross-section ratios at  $\sqrt{s}=13, 8, 7$  TeV with the ATLAS detector*. Journal of High Energy Physics (2), 1–54.
  - The ATLAS Collaboration (2017[aw]). *Performance of the ATLAS track reconstruction algorithms in dense environments in LHC Run 2*. European Physical Journal C **77**(10).
  - The ATLAS Collaboration (2017[ax]). *Performance of the ATLAS Transition Radiation Tracker in Run 1 of the LHC: tracker properties*. Journal of Instrumentation **12**.
  - The ATLAS Collaboration (2017[ay]). *Precision measurement and interpretation of inclusive  $W^+$ ,  $W^-$  and  $Z/\gamma^*$  production cross sections with the ATLAS detector*. European Physical Journal C **77**(6).
  - The ATLAS Collaboration (2017[az]). *Reconstruction of primary vertices at the ATLAS experiment in Run 1 proton-proton collisions at the LHC*. European Physical Journal C **77**(5).
  - The ATLAS Collaboration (2017[ba]). *Search for a scalar partner of the top quark in the jets plus missing transverse momentum final state at  $\sqrt{s}=13$  TeV with the ATLAS detector*. Journal of High Energy Physics (12).
  - The ATLAS Collaboration (2017[bb]). *Search for anomalous electroweak production of  $WW/WZ$  in association with a high-mass dijet system in  $pp$  collisions at  $\sqrt{s}=8$  TeV with the ATLAS detector*. Physical Review D **95**(3).
  - The ATLAS Collaboration (2017[bc]). *Search for dark matter at  $\sqrt{s}=13$  TeV in final states containing an energetic photon and large missing transverse momentum with the ATLAS detector*. European Physical Journal C **77**(6).

- The ATLAS Collaboration (2017[bd]). *Search for dark matter in association with a Higgs boson decaying to  $b$ -quarks in  $pp$  collisions at  $\sqrt{s}=13$  TeV with the ATLAS detector.* Physics Letters B **765**, 11–31.
- The ATLAS Collaboration (2017[be]). *Search for dark matter in association with a Higgs boson decaying to two photons at  $\sqrt{s}=13$  TeV with the ATLAS detector.* Physical Review D **96**(11).
- The ATLAS Collaboration (2017[bf]). *Search for Dark Matter Produced in Association with a Higgs Boson Decaying to  $b\bar{b}$  Using  $36\text{ fb}^{-1}$  of  $pp$  Collisions at  $\sqrt{s}=13$  TeV with the ATLAS Detector.* Physical Review Letters **119**(18).
- The ATLAS Collaboration (2017[bg]). *Search for direct top squark pair production in final states with two leptons in  $\sqrt{s}=13$  TeV  $pp$  collisions with the ATLAS detector.* European Physical Journal C **77**(12).
- The ATLAS Collaboration (2017[bh]). *Search for Heavy Higgs Bosons  $A/H$  Decaying to a Top Quark Pair in  $pp$  Collisions at  $\sqrt{s}=8$  TeV with the ATLAS Detector.* Physical Review Letters **119**(19).
- The ATLAS Collaboration (2017[bi]). *Search for heavy resonances decaying to a  $W$  or  $Z$  boson and a Higgs boson in the  $q\bar{q}^{(\prime)}b\bar{b}$  final state in  $pp$  collisions at  $\sqrt{s}=13$  TeV with the ATLAS detector.* Physics Letters B **774**, 494–515.
- The ATLAS Collaboration (2017[bj]). *Search for heavy resonances decaying to a  $Z$  boson and a photon in  $pp$  collisions at  $\sqrt{s}=13$  TeV with the ATLAS detector.* Physics Letters B **764**, 11–30.
- The ATLAS Collaboration (2017[bk]). *Search for new high-mass phenomena in the dilepton final state using  $36\text{ fb}^{-1}$  of proton-proton collision data at  $\sqrt{s}=13$  TeV with the ATLAS detector.* Journal of High Energy Physics (10).
- The ATLAS Collaboration (2017[bl]). *Search for new phenomena in a lepton plus high jet multiplicity final state the ATLAS experiment using  $\sqrt{s}=13$  TeV proton-proton collision data.* Journal of High Energy Physics (9).
- The ATLAS Collaboration (2017[bm]). *Search for new phenomena in dijet events using  $37\text{ fb}^{-1}$  of  $pp$  collision data collected at  $\sqrt{s}=13$  TeV with the ATLAS detector.* Physical Review D **96**(5).
- The ATLAS Collaboration (2017[bn]). *Search for new phenomena in events containing a same-flavour opposite-sign dilepton pair, jets, and large missing transverse momentum in  $\sqrt{s}=13$  TeV  $pp$  collisions with the ATLAS detector.* European Physical Journal C **77**(3).
- The ATLAS Collaboration (2017[bo]). *Search for new phenomena in high-mass diphoton final states using  $37\text{ fb}^{-1}$  of proton-proton collisions collected at  $\sqrt{s}=13$  TeV with the ATLAS detector.* Physics Letters B **775**, 105–125.
- The ATLAS Collaboration (2017[bp]). *Search for new phenomena with large jet multiplicities and missing transverse momentum using large-radius jets and flavour-tagging at ATLAS in 13 TeV  $pp$  collisions.* Journal of High Energy Physics (12).
- The ATLAS Collaboration (2017[bq]). *Search for new resonances decaying to a  $W$  or  $Z$  boson and a Higgs boson in the  $\ell^+\ell^-b\bar{b}$ ,  $\ell\nu b\bar{b}$ , and  $\nu\bar{\nu}b\bar{b}$  channels with  $pp$  collisions at  $\sqrt{s}=13$  TeV with the ATLAS detector.* Physics Letters B **765**, 32–52.
- The ATLAS Collaboration (2017[br]). *Search for pair production of heavy vector-like quarks decaying to high- $p(T)$   $W$  bosons and  $b$  quarks in the lepton-plus-jets final state in  $pp$  collisions at  $\sqrt{s}=13$  TeV with the ATLAS detector.* Journal of High Energy Physics (10).
- The ATLAS Collaboration (2017[bs]). *Search for pair production of vector-like top quarks in events with one lepton, jets, and missing transverse momentum in  $\sqrt{s}=13$  TeV  $pp$  collisions with the ATLAS detector.* Journal of High Energy Physics (8), 1–40.
- The ATLAS Collaboration (2017[bt]). *Search for squarks and gluinos in events with an isolated lepton, jets, and missing transverse momentum at  $\sqrt{s}=13$  TeV with the ATLAS detector.* Physical Review D **96**(11).

- Aaboud, M. et al., The ATLAS Collaboration (2017[bu]). *Search for super symmetry in events with  $b$ -tagged jets and missing transverse momentum in  $pp$  collisions at  $\sqrt{s}=13$  TeV with the ATLAS detector.* Journal of High Energy Physics (11).
- The ATLAS Collaboration (2017[bv]). *Search for supersymmetry in final states with two same-sign or three leptons and jets using  $36\text{ fb}^{-1}$  of  $\sqrt{s} = 13$  TeV  $pp$  collision data with the ATLAS detector.* Journal of High Energy Physics (9).
  - The ATLAS Collaboration (2017[bw]). *Search for the Dimuon Decay of the Higgs Boson in  $pp$  Collisions at  $\sqrt{s}=13$  TeV with the ATLAS Detector.* Physical Review Letters **119**(5).
  - The ATLAS Collaboration (2017[bx]). *Search for top quark decays  $t \rightarrow qH$ , with  $H \rightarrow \gamma\gamma$ , in  $\sqrt{s}=13$  TeV  $pp$  collisions using the ATLAS detector.* Journal of High Energy Physics (10).
  - The ATLAS Collaboration (2017[by]). *Search for triboson  $W^{\pm}W^{\pm}W^{\mp}$  production in  $pp$  collisions at  $\sqrt{s}=8$  TeV with the ATLAS detector.* European Physical Journal C **77**(3).
  - The ATLAS Collaboration (2017[bz]). *Searches for the  $Z\gamma$  decay mode of the Higgs boson and for new high-mass resonances in  $pp$  collisions at  $\sqrt{s}=13$  TeV with the ATLAS detector.* Journal of High Energy Physics (10).
  - The ATLAS Collaboration (2017[ca]). *Studies of  $Z\gamma$  production in association with a high-mass dijet system in  $pp$  collisions at  $\sqrt{s}=8$  TeV with the ATLAS detector.* Journal of High Energy Physics (7).
  - The ATLAS Collaboration (2017[cb]). *Study of ordered hadron chains with the ATLAS detector.* Physical Review D **96**(9).
  - The ATLAS Collaboration (2017[cc]). *Study of the material of the ATLAS inner detector for Run 2 of the LHC.* Journal of Instrumentation **12**.
  - The ATLAS Collaboration (2017[cd]). *Study of  $WW\gamma$  and  $WZ\gamma$  production in  $pp$  collisions at  $\sqrt{s}=8$  TeV and search for anomalous quartic gauge couplings with the ATLAS experiment.* European Physical Journal C **77**(9).
  - The ATLAS Collaboration (2017[ce]). *Top-quark mass measurement in the all-hadronic  $t\bar{t}$  decay channel at  $\sqrt{s}=8$  TeV with the ATLAS detector.* Journal of High Energy Physics (9).
- Aad, G. et al., The ATLAS Collaboration (2017[a]). *Measurement of the charge asymmetry in top-quark pair production in the lepton-plus-jets final state in  $pp$  collision data at  $\sqrt{s} = 8$  TeV with the ATLAS detector.* European Physical Journal C **77**(8).
- The ATLAS Collaboration (2017[b]). *Performance of algorithms that reconstruct missing transverse momentum in  $\sqrt{s}=8$  TeV proton-proton collisions in the ATLAS detector.* European Physical Journal C **77**(4).
  - The ATLAS Collaboration (2017[c]). *Search for lepton-flavour-violating decays of the Higgs and  $Z$  bosons with the ATLAS detector.* European Physical Journal C **77**(2).
  - The ATLAS Collaboration (2017[d]). *Topological cell clustering in the ATLAS calorimeters and its performance in LHC Run 1.* European Physical Journal C **77**(7).
- Angerami, A. et al., The ATLAS Collaboration (2017). *Measurements of photo-nuclear jet production in  $Pb + Pb$  collisions with ATLAS.* Nuclear Physics A **967**. 26th International Conference on Ultrarelativistic Nucleus-Nucleus Collisions (Quark Matter), Chicago, IL, FEB 05-11, 2017, 277–280.
- Iuppa, R. (2017). *New Physics in di-boson resonances and long-lived particles with ATLAS and CMS: Latest Run 1 and early Run 2 results.* Nuovo Cimento C - Colloquia and Communications in Physics **40**(1).
- Jia, J. et al., The ATLAS Collaboration (2017). *Heavy Ion Results from ATLAS.* Nuclear Physics A **967**. 26th International Conference on Ultrarelativistic Nucleus-Nucleus Collisions (Quark Matter), Chicago, IL, FEB 05-11, 2017, 51–58.

**RD-FASE2**

- Dalla Betta, G.-F., Mendicino, R., Boscardin, M., Hoferkamp, M., Mendicino, R., Seidel, S., and Sultan, D. (2017a). *Electrical characterization of FBK small-pitch 3D sensors after  $\gamma$ -ray, neutron and proton irradiations*. *Journal Instrum.* **12**, p. C11028.
- Dalla Betta, G.-F., Mendicino, R., Boscardin, M., Ronchin, S., and Zorzi, N. (2017b). “Small-pitch 3D devices”. *Proceedings of Science - 25th Workshop on Vertex Detectors (Vertex 2016)*. Ed. by F. Forti and F. Palla. Trieste, Italy: Sissa, 028(1–10).
- Ducourthial, A., Bomben, M., Calderini, G., D’Eramo, L., Marchiori, G., Luise, I., Bagolini, A., Boscardin, M., Bosisio, L., Darbo, G., Dalla Betta, G.-F., Giacomini, G., Meschini, M., Messineo, A., Ronchin, S., and Zorzi, N. (2017). *Thin and edgeless sensors for ATLAS pixel detector upgrade*. *Journal Instrum.* **12**, p. C12038.
- Moscatelli, F., Passeri, D., Morozzi, A., Dalla Betta, G.-F., Mattiazzo, S., Bomben, M., and Bilei, G. (2017a). *Surface damage characterization of FBK devices for High Luminosity LHC (HL-LHC) operations*. *Journal Instrum.* **12**, P12010.
- Moscatelli, F., Passeri, D., Morozzi, A., Mattiazzo, S., Dalla Betta, G.-F., Dragicevic, M., and Bilei, G. M. (2017b). *Effects of Interface Donor Trap States on Isolation Properties of Detectors Operating at High-Luminosity LHC*. *IEEE Trans. Nucl. Sci.* **64(8)**, pp. 2259–2267.
- Moscatelli, F., Passeri, D., Morozzi, A., Mattiazzo, S., Dragicevic, M., Dalla Betta, G.-F., and Bilei, G. M. (2017c). “Radiation damage effects on p-type silicon detectors for high-luminosity operations: test and modeling”. *Proc. of the Workshop on Radiation Effects on Components and Systems (RADECS 2016)*. IEEE.
- Sultan, D., Dalla Betta, G.-F., Mendicino, R., Boscardin, M., Ronchin, S., and Zorzi, N. (2017a). *First Production of New Thin 3D Sensors for HL-LHC at FBK*. *Journal Instrum.* **12**, p. C01022.

**Astroparticle Physics**

- Abrescia, M. et al., EEE collaboration (2017). *Operation and performance of the EEE network array for the detection of cosmic rays*. *Nucl. Instrum. Meth.* **A845**, pp. 383–386.
- Nozzoli, F. (2017a). *A balance for Dark Matter bound states*. *Astropart. Phys.* **91**, pp. 22–33.
- Nozzoli, F. (2017b). *On  $^{146}\text{Nd}$ ,  $^{144}\text{Sm}$  and other unexplored  $2\beta$  decay isotopes*. *Phys. Rev. C*, in press.

**AMS-02**

- Aguilar, M. et al., AMS collaboration (2017). *Observation of the Identical Rigidity Dependence of He, C, and O Cosmic Rays at High Rigidities by the Alpha Magnetic Spectrometer on the International Space Station*. *Phys. Rev. Lett.* **119(25)**, p. 251101.
- AMS collaboration (2016). *Precision Measurement of the Boron to Carbon Flux Ratio in Cosmic Rays from 1.9 GV to 2.6 TV with the Alpha Magnetic Spectrometer on the International Space Station*. *Phys. Rev. Lett.* **117(23)**, p. 231102.
- Nozzoli, F. (2016). “Precision measurement of antiproton to proton ratio with the Alpha Magnetic Spectrometer on the International Space Station”. *25th European Cosmic Ray Symposium (ECRS 2016) Turin, Italy, September 04-09, 2016*.

**DarkSide**

- Aalseth, C. E., Acerbi, F., et al. (2017). *Cryogenic Characterization of FBK RGB-HD SiPMs*. *JINST* **12**, P09030.
- Acerbi, F., Davini, S., et al. (2017b). *Cryogenic Characterization of FBK HD Near-UV Sensitive SiPMs*. *IEEE Transactions on Electron Devices* **64**, pp. 521–526.

## FISH

- Bienaimé, T., Fava, E., Colzi, G., Mordini, C., Serafini, S., Qu, C., Stringari, S., Lamporesi, G., and Ferrari, G. (2016). *Spin-Dipole Oscillation and Polarizability of a Binary Bose-Einstein Condensate near the Miscible-Immiscible Phase Transition*. Phys. Rev. A **94**, p. 063652.
- Fava, E., Bienaimé, T., Mordini, C., Colzi, G., Qu, C., Stringari, S., Lamporesi, G., and Ferrari, G. (2017). *Spin Superfluidity of a Bose Gas Mixture at Finite Temperature*. arXiv:1708.03923.

## HUMOR

- Kralj, N., Rossi, M., Zippilli, S., Natali, R., Borrielli, A., Pandraud, G., Serra, E., Di Giuseppe, G., and Vitali, D. (2017). *Enhancement of three-mode optomechanical interaction by feedback-controlled light*. Quantum Science and Technology **2**(3).
- Pontin, A., Bonaldi, M., Borrielli, A., Marconi, L., Marino, F., Pandraud, G., Prodi, G., Sarro, P., Serra, E., and Marin, F. (2017). “Quantum nondemolition measurement of light intensity fluctuations in an optomechanical experiment”. *2017 European Conference on Lasers and Electro-Optics and European Quantum Electronics Conference*. Vol. F81-EQEC 2017. Optical Society of America, IEEE.
- Rossi, M., Kralj, N., Zippilli, S., Natali, R., Borrielli, A., Pandraud, G., Serra, E., Di Giuseppe, G., and Vitali, D. (2017). *Enhancing Sideband Cooling by Feedback-Controlled Light*. Physical Review Letters **119**(12).

## LISA Pathfinder

- Armano, M. et al., LISA Pathfinder Collaboration (2018). *Beyond the Required LISA Free-Fall Performance: New LISA Pathfinder Results down to 20  $\mu$  Hz*. Physical Review Letter **120**, p. 061101.
- LISA Pathfinder Collaboration (2017a). *Capacitive sensing of test mass motion with nanometer precision over millimeter-wide sensing gaps for space-borne gravitational reference sensors*. Physical Review D **96**(6), p. 062004.
- LISA Pathfinder Collaboration (2017b). *Charge-Induced Force Noise on Free-Falling Test Masses: Results from LISA Pathfinder*. Physical Review Letters **118**(17), p. 171101.

## QUAX

- Crescini, N., Braggio, C., Carugno, G., Falferi, P., Ortolan, A., and Ruoso, G. (2017b). *The QUAX- $g_p$   $g_s$  experiment to search for monopole-dipole Axion interaction*. Nucl. Instrum. Meth. **A842**, pp. 109–113.

## VIRGO

- Abbott, B. P., Abbott, R., Abbott, T. D., Acernese, F., Ackley, K., Adams, C., Adams, T., Addesso, P., Adhikari, R. X., Adya, V. B., et al. (2017a). *A gravitational-wave standard siren measurement of the Hubble constant*. Nature **551**, pp. 85–88.
- (2017b). *All-sky search for periodic gravitational waves in the O1 LIGO data*. Phys. Rev. D **96**(6), 062002, p. 062002.
- (2017c). *Estimating the Contribution of Dynamical Ejecta in the Kilonova Associated with GW170817*. The Astrophysical Journal Letters **850**, L39, p. L39.
- (2017d). *Gravitational Waves and Gamma-Rays from a Binary Neutron Star Merger: GW170817 and GRB 170817A*. The Astrophysical Journal Letters **848**, L13, p. L13.
- (2017e). *GW170104: Observation of a 50-Solar-Mass Binary Black Hole Coalescence at Redshift 0.2*. Physical Review Letters **118**(22), 221101, p. 221101.

- (2017f). *GW170814: A Three-Detector Observation of Gravitational Waves from a Binary Black Hole Coalescence*. *Physical Review Letters* **119**(14), 141101, p. 141101.
  - (2017g). *GW170817: Observation of Gravitational Waves from a Binary Neutron Star Inspiral*. *Physical Review Letters* **119**(16), 161101, p. 161101.
  - (2017h). *Multi-messenger Observations of a Binary Neutron Star Merger*. *The Astrophysical Journal Letters* **848**, L12, p. L12.
  - (2017i). *On the Progenitor of Binary Neutron Star Merger GW170817*. *The Astrophysical Journal Letters* **850**, p. L40.
  - (2017j). *Search for gravitational waves from Scorpius X-1 in the first Advanced LIGO observing run with a hidden Markov model*. *Phys. Rev. D* **95**(12), 122003, p. 122003.
  - (2017k). *Search for intermediate mass black hole binaries in the first observing run of Advanced LIGO*. *Phys. Rev. D* **96**(2), 022001, p. 022001.
  - (2017l). *Upper Limits on Gravitational Waves from Scorpius X-1 from a Model-based Cross-correlation Search in Advanced LIGO Data*. *The Astrophysical Journal* **847**, 47, p. 47.
- Acernese, F., Adams, T., Agatsuma, K., Aiello, L., Allocca, A., Amato, A., Antier, S., Arnaud, N., Ascenzi, S., Astone, P., et al. (2017). *Status of the Advanced Virgo gravitational wave detector*. *International Journal of Modern Physics A* **32**, 1744003, p. 1744003.
- Albert, A., André, M., Anghinolfi, M., Ardid, M., Aubert, J.-J., Aublin, J., Avgitas, T., Baret, B., Barrios-Martí, J., Basa, S., et al. (2017). *Search for High-energy Neutrinos from Binary Neutron Star Merger GW170817 with ANTARES, IceCube, and the Pierre Auger Observatory*. *The Astrophysical Journal Letters* **850**, L35, p. L35.
- Pian, E., D’Avanzo, P., Benetti, S., Branchesi, M., Brocato, E., Campana, S., Cappellaro, E., Covino, S., D’Elia, V., Fynbo, J. P. U., Getman, F., Ghirlanda, G., Ghisellini, G., Grado, A., Greco, G., Hjorth, J., Kouveliotou, C., Levan, A., Limatola, L., Malesani, D., Mazzali, P. A., Melandri, A., Møller, P., Nicastro, L., Palazzi, E., Piranomonte, S., Rossi, A., Salafia, O. S., Selsing, J., Stratta, G., Tanaka, M., Tanvir, N. R., Tomasella, L., Watson, D., Yang, S., Amati, L., Antonelli, L. A., Ascenzi, S., Bernardini, M. G., Boër, M., Bufano, F., Bulgarelli, A., Capaccioli, M., Casella, P., Castro-Tirado, A. J., Chassande-Mottin, E., Ciolfi, R., Copperwheat, C. M., Dadina, M., De Cesare, G., di Paola, A., Fan, Y. Z., Gendre, B., Giuffrida, G., Giunta, A., Hunt, L. K., Israel, G. L., Jin, Z.-P., Kasliwal, M. M., Klose, S., Lisi, M., Longo, F., Maiorano, E., Mapelli, M., Masetti, N., Nava, L., Patricelli, B., Perley, D., Pescalli, A., Piran, T., Possenti, A., Pulone, L., Razzano, M., Salvaterra, R., Schipani, P., Spera, M., Stamerra, A., Stella, L., Tagliaferri, G., Testa, V., Troja, E., Turatto, M., Vergani, S. D., and Vergani, D. (2017). *Spectroscopic identification of r-process nucleosynthesis in a double neutron-star merger*. *Nature* **551**, pp. 67–70.

## Nuclear Physics

### AEGIS

- Aghion, S. et al. (2017). *Characterization of a transmission positron/positronium converter for anti-hydrogen production*. *Nucl. Instrum. Methods Phys. Res. B* **407**, p. 55.
- Brusa, R. S. et al. (2017). *The AEGIS experiment at CERN: Measuring antihydrogen free-fall in earth’s gravitational field to test WEP with antimatter*. *J. of Phys. Conf* **791**, p. 012014.
- Caravita, R. et al. (2017). *Advances in Ps Manipulations and Laser Studies in the AEGIS Experiment*. *Acta Phys Pol B* **48**, p. 1583.

## FOOT

- Alexandrov, A., Argirò, S., Battistoni, G., Belcari, N., Biondi, S., Giuseppina, M., Bruni, G., Brambilla, S., Camarlinghi, N., Cerello, P., Ciarrocchi, E., Clozza, A., De Lellis, G., Di Crescenzo, A., Durante, M., Faccini, R., Ferrero, V., Ferroni, F., Finck, C., et al. (2017). “The FOOT (Fragmentation Of Target) Experiment”. *Proc. of the 55th International Winter Meeting on Nuclear Physics*. PoS.
- Argirò, S., Battistoni, G., Belcari, N., Biondi, S., Giuseppina, M., Bruni, G., Brambilla, S., Camarlinghi, N., Cerello, P., Ciarrocchi, E., Clozza, A., De Lellis, G., Di Crescenzo, A., Durante, M., Faccini, R., Ferrero, V., Ferroni, F., Finck, C., et al. (2016). “The FOOT (Fragmentation Of Target) Experiment”. *Proc. of the 26th International Nuclear Physics Conference*. PoS.

## Theoretical Physics

### BELL

- Dappiaggi, C., Moretti, V., and Pinamonti, N. (2017). *Hadamard States from Light-like Hypersurfaces*. Springer Brief in Mathematical Physics **25**, pp. 1–106.
- Ghiloni, R., Moretti, V., and Perotti, A. (2017). *Spectral representations of normal operators via Intertwining Quaternionic PVMs*. *Reviews in Mathematical Physics* **29**(10), p. 1750034.
- Mazzucchi, S. (2017). *Infinite Dimensional Oscillatory Integrals with Polynomial Phase and Applications to Higher-Order Heat-Type Equations*. *Potential Analysis*.
- Moretti, V. and Oppio, M. (2017). *Quantum theory in real Hilbert space: How the complex Hilbert space structure emerges from Poincaré symmetry*. *Reviews in Mathematical Physics* **29**(06), p. 1750021.
- Pastorello, D. (2017a). *A geometric approach to quantum control in projective Hilbert spaces*. *Reports in Mathematical Physics* **79**, pp. 53–56.
- (2017b). *A quantum key distribution scheme based on tripartite entanglement and violation of CHSH inequality*. *International Journal of Quantum Information* **15**, p. 1750040.

### BIOPHYS

- Alberga, D., Ciofini, I., Mangiatordi, G. F., Pedone, A., Lattanzi, G., Roncali, J., and Adamo, C. (2017a). *Effects of Substituents on Transport Properties of Molecular Materials for Organic Solar Cells: A Theoretical Investigation*. *Chemistry of Materials* **29**, pp. 673–681.
- Alberga, D., Trisciuzzi, D., Lattanzi, G., Bennet, J. L., Verkman, A. S., Mangiatordi, G. F., and Nicolotti, O. (2017b). *Comparative molecular dynamics study of neuromyelitis optica-immunoglobulin G binding to aquaporin-4 extracellular domains*. *Biochimica et Biophysica Acta (BBA)-Biomembranes* **1859**, pp. 1326–1334.
- Azzolini, M., Morresi, T., Garberoglio, G., Calliari, L., Pugno, N. M., Taioli, S., and Dapor, M. (2017a). *Monte Carlo simulations of measured electron energy-loss spectra of diamond and graphite: Role of dielectric-response models*. *Carbon* **118**, p. 299.
- Garberoglio, G., Jankowski, P., Szalewicz, K., and Harvey, A. H. (2017). *All-dimensional H<sub>2</sub>-CO potential: Validation with fully quantum second virial coefficients*. *J. Chem. Phys.* **146**(5), p. 054304.
- Lepore, E., Bosia, F., Bonaccorso, F., Bruna, M., Taioli, S., Garberoglio, G., Ferrari, A. C., and Pugno, N. M. (2017a). *Spider silk reinforced by graphene or carbon nanotubes*. *2D Materials* **4**(3), p. 031013.
- Mangiatordi, G. F., Alberga, D., Pisani, L., Gadaleta, D., Trisciuzzi, D., Farina, R., Carotti, A., Lattanzi, G., Catto, M., and Nicolotti, O. (2017). *A rational approach to elucidate human monoamine oxidase molecular selectivity*. *European Journal of Pharmaceutical Sciences* **101**, pp. 90–99.
- Pedrielli, A., Taioli, S., Garberoglio, G., and Pugno, N. (2017a). *Designing graphene based nanofoams with nonlinear auxetic and anisotropic mechanical properties under tension or compression*. *Carbon* **111**. Erratum. *Carbon*, **116**, (2017), p. 20. arXiv:1606.05494, pp. 796–806.

**FBS**

- Bacca, S. and Orlandini, G. (2016). *Electric dipole polarizability from first principles calculations*. Phys. Rev. C **41**, p. 034317.
- Deflorian, S., Efras, V., and Leidemann, W. (2017). *Calculation of the Astrophysical S-Factor S-12 with the Lorentz Integral Transform*. Few-Body Syst. **58**, pp. 1–12.
- Ferrari Ruffino, F., Lonardonì, D., Barnea, N., Deflorian, S., Leidemann, W., Orlandini, G., and Pederiva, F. (2017). *Benchmark Results for Few-Body Hypernuclei*. Few-Body Syst. **58**, UNSP 113.
- Leidemann, W., Deflorian, S., and Efras, V. (2017). *Determination of S-Factors with the LIT Method*. Few-Body Syst. **58**, UNSP 27.
- Orlandini, G. and Turro, F. (2017). *Integral Transform Methods: A Critical Review of Various Kernels*. Few-Body Syst. **58**, UNSP 76.

**FLAG**

- Chinaglia, S., Colléaux, A., and Zerbini, S. (2017). *A non-polynomial gravity formulation for Loop Quantum Cosmology bounce*. Galaxies **5**, p. 51.
- Chinaglia, S. and Zerbini, S. (2017). *A note on singular and non-singular black holes*. Gen. Rel. Gravitation **49**, p. 75.
- Cisterna, A., Hassaine, M., Oliva, J., and Rinaldi, M. (2017). *Axionic black holes in the K-essence sector of the Horndeski model*. Phys. Rev. D, in press.
- Cisterna, A., Delsate, T., Ducobu, L., and Rinaldi, M. (2016). *Slowly rotating neutron stars in the nonminimal derivative coupling sector of Horndeski gravity*. Phys. Rev. **D93**(8), p. 084046.
- Odintsov, S. D., Oikonomou, V., and Sebastiani, L. (2017). *Unification of Constant-roll Inflation and Dark Energy with Logarithmic  $R^2$ -corrected and Exponential  $F(R)$  Gravity*. Nuclear Physics B **923**, p. 608.
- Rinaldi, M. (2017a). *Mimicking dark matter in Horndeski gravity*. Phys. Dark Universe **16**, pp. 14–21.
- (2017b). “Quasi Scale-Invariant Inflationary Attractors”. *Fourteenth Marcel Grossmann Meeting on General Relativity*. Ed. by M. Bianchi, R. Jantzen, and R. Ruffini. Singapore: World Scientific.
- Rinaldi, M. and Vanzo, L. (2016). *Inflation and reheating in theories with spontaneous scale invariance symmetry breaking*. Phys. Rev. **D94**(2), p. 024009.
- Rinaldi, M., Vanzo, L., Zerbini, S., and Venturi, G. (2016a). *Inflationary quasi scale-invariant attractors*. Phys. Rev. **D93**, p. 024040.
- Sebastiani, L. (2017). “Thermodynamical aspects of black holes in modified gravity”. *3rd Karl Schwarzschild Meeting - Gravity and the Gauge/Gravity Correspondence*. Ed. by P. Nicolini, M. Kaminski, J. Mureika, and M. Bleicher. Singapore: IOP publishing Ltd.
- Tambalo, G. and Rinaldi, M. (2017). *Inflation and reheating in scale-invariant scalar-tensor gravity*. Gen. Rel. Gravitation **49**, p. 52.

**MANYBODY**

- Contessi, L., Lovato, A., Pederiva, F., Roggero, A., Kirscher, J., and van Kolck, U. (2017). *Ground-state properties of  $^4\text{He}$  and  $^{16}\text{O}$  extrapolated from lattice QCD with pionless EFT*. Phys. Lett. **B772**, pp. 839–848.
- Ferrari Ruffino, F., Lonardonì, D., Barnea, N., Deflorian, S., Leidemann, W., Orlandini, G., and Pederiva, F. (2017). *Benchmark Results for Few-Body Hypernuclei*. Few-Body Systems **58**(3). 23rd European Conference on Few-Body Problems in Physics, Aarhus, DENMARK, AUG 08-12, 2016.

## NEMESYS

- Azzolini, M., Morresi, T., Garberoglio, G., Calliari, L., Pugno, N. M., Taioli, S., and Dapor, M. (2017b). *Monte Carlo simulations of measured electron energy-loss spectra of diamond and graphite: Role of dielectric-response models*. Carbon **118**(Supplement C), pp. 299–309.
- Lepore, E., Bosia, F., Bonaccorso, F., Bruna, M., Taioli, S., Garberoglio, G., Ferrari, A. C., and Pugno, N. M. (2017b). *Spider silk reinforced by graphene or carbon nanotubes*. 2D Materials **4**(3), p. 031013.
- Pedrielli, A., Taioli, S., Garberoglio, G., and Pugno, N. M. (2017b). *Designing graphene based nanofoams with nonlinear auxetic and anisotropic mechanical properties under tension or compression*. Carbon **111**(Supplement C), pp. 796–806.
- Pedrielli, A., Taioli, S., Garberoglio, G., and Pugno, N. M. (2018). *Gas adsorption and dynamics in Pillared Graphene Frameworks*. Microporous and Mesoporous Materials **257**(Supplement C), pp. 222–231.
- Segatta, F., Cupellini, L., Jurinovich, S., Mukamel, S., Dapor, M., Taioli, S., Garavelli, M., and Men-  
nucci, B. (2017). *A Quantum Chemical Interpretation of Two-Dimensional Electronic Spectroscopy of Light-Harvesting Complexes*. Journal of the American Chemical Society **139**(22). PMID: 28513172, pp. 7558–7567.
- Signetti, S., Taioli, S., and Pugno, N. M. (2017). *2D Material Armors Showing Superior Impact Strength of Few Layers*. ACS Applied Materials & Interfaces **9**(46). PMID: 29120161, pp. 40820–40830.

## NINPHA

- Rinaldi, M., Scopetta, S., Traini, M., and Vento, V. (2016b). *Correlations in double parton distributions: perturbative and non-perturbative effects*. Journal of High Energy Physics **10**, 063 (35 pages).
- Traini, M. (2017). *Generalized parton distributions: confining potential effects within AdS/QCD*. European Physics Journal C **77**, pp. 246–260.
- Traini, M., Rinaldi, M., Scopetta, S., and Vento, V. (2017). *The effective cross section for double parton scattering within a holographic AdS/QCD approach*. Physics Letter B **768**, pp. 270–273.

## TEONGRAV

- Ciolfi, R., Kastaun, W., Giacomazzo, B., Endrizzi, A., Siegel, D. M., and Perna, R. (2017). *General relativistic magnetohydrodynamic simulations of binary neutron star mergers forming a long-lived neutron star*. Phys. Rev. D **95**(6), 063016, p. 063016.
- Kastaun, W., Ciolfi, R., Endrizzi, A., and Giacomazzo, B. (2017). *Structure of stable binary neutron star merger remnants: Role of initial spin*. Phys. Rev. D **96**(4), 043019, p. 043019.
- Kelly, B. J., Baker, J. G., Etienne, Z. B., Giacomazzo, B., and Schnittman, J. (2017). *Prompt Electromagnetic Transients from Binary Black Hole Mergers*. Phys. Rev. D **96**(12), 123003, p. 123003.
- Piro, A. L., Giacomazzo, B., and Perna, R. (2017). *The Fate of Neutron Star Binary Mergers*. The Astrophysical Journal Letters **844**, L19, p. L19.

## Technological and Interdisciplinary Physics

### APiX2

- Ficorella, A., Pancheri, L., Brogi, P., Collazuol, G., Dalla Betta, G.-F., Marrocchesi, P., Morsani, F., Ratti, L., and Savoy-Navarro, A. (2018). *Crosstalk Characterization of a Two-Tier Pixelated Avalanche Sensor for Charged Particle Detection*. IEEE Journal of Selected Topics in Quantum Electronics **24**(2).

- Pancheri, L., Brogi, P., Collazuol, G., Dalla Betta, G.-F., Ficorella, A., Marrocchesi, P., Morsani, F., Ratti, L., and Savoy-Navarro, A. (2017a). *First prototypes of two-tier avalanche pixel sensors for particle detection*. Nuclear Instruments and Methods in Physics Research, Section A: Accelerators, Spectrometers, Detectors and Associated Equipment **845**, pp. 143–146.
- Pancheri, L., Ficorella, A., Brogi, P., Collazuol, G., Dalla Betta, G.-F., Marrocchesi, P., Morsani, F., Ratti, L., Savoy-Navarro, A., and Sulaj, A. (2017b). *First Demonstration of a Two-Tier Pixelated Avalanche Sensor for Charged Particle Detection*. IEEE Journal of the Electron Devices Society **5**(5), pp. 404–410.
- Pancheri, L., Ficorella, A., Brogi, P., Collazuol, G., Dalla Betta, G.-F., Marrocchesi, P. S., Morsani, F., Ratti, L., and Savoy-Navarro, A. (2017c). “Two-Tier Geiger-Mode Avalanche Detector for Charged Particle Imaging”. *2017 International Image Sensor Workshop (IISW)*. International Image Sensor Society, pp. 101–104.

## ARDESIA

- Bellotti, G., Butt, A., Carminati, M., Fiorini, C., Balerna, A., Piemonte, C., Zorzi, N., and Bombelli, L. (2017). “The Detection Module of ARDESIA: A New, Versatile Array of SDDs for X-Ray Spectroscopy Synchrotron Applications”. *Conference Record of the 2016 Nuclear Science Symposium (NSS/MIC/RTSD), Strasbourg (France)*. IEEE.

## MoVe-IT

- Ferruz, M. B., Ivošev, V., Haume, K., Ellis-Gibblings, L., Traore, A., Thakare, V., Rosa, S., de Vera, P., Tran, V.-L., Mika, A., et al. (2017). “New research in ionizing radiation and nanoparticles: the ARGENT project”. *Nanoscale Insights into Ion-Beam Cancer Therapy*. Springer, pp. 379–434.
- Hespeels, F., Heuskin, A., Scifoni, E., Kraemer, M., and Lucas, S. (2017). *Backscattered electron emission after proton impact on carbon and gold films: experiments and simulations*. Nuclear Instruments and Methods in Physics Research Section B: Beam Interactions with Materials and Atoms **401**, pp. 8–17.
- Lacombe, S., Porcel, E., and Scifoni, E. (2017). *Particle therapy and nanomedicine: state of art and research perspectives*. Cancer nanotechnology **8**(1), p. 9.
- Tommasino, F., Nahum, A., and Cella, L. (2017c). *Increasing the power of tumour control and normal tissue complication probability modelling in radiotherapy: recent trends and current issues*. Translational Cancer Research **6**(S5), S807–S821.

## NEWREFLECTIONS

- Battiston, R., Burger, W., Cafagna, C., Manea, C., and Spataro, B. (2017b). *A Systematic Study of Laser Ablation for Space Debris Mitigation*. Journal of Space Safety Engineering **4**, pp. 36–44.

## Redsox2

- Bufon, J., Gianoncelli, A., Ahangarianabhari, M., Altissimo, M., Bellutti, P., Bertuccio, G., Borghes, R., Carrato, S., Caetero, G., Cicuttin, A., Crespo, M. L., Fabiani, S., Gandola, M., Giacomini, G., Giuressi, D., Kourousias, G., Menk, R. H., Picciotto, A., Piemonte, C., Rachevski, A., Rashevskaya, I., Schillani, S., Stolfa, A., Vacchi, A., Zampa, G., Zampa, N., and Zorzi, N. (2017b). *Towards a multi-element silicon drift detector system for fluorescence spectroscopy in the soft X-ray regime*. X-Ray Spectrometry **46**(5). XRS-16-0088.R1, pp. 313–318.
- Campana, R. et al. (2016). *A compact and modular X and gamma-ray detector with a CsI scintillator and double-readout Silicon Drift Detectors*. Proc. SPIE Int. Soc. Opt. Eng. **9905**, p. 99056I.

Capelli, S. et al. (2017). *The FLARES project: An innovative detector technology for rare events searches*. Nucl. Instrum. Meth. **A845**, pp. 334–337.

## SEED

Olave, E. J., Panati, S., Cossio, F., Rivetti, A., Da Rocha Rolo, M., Demaria, N., Pancheri, L., Mattiazzo, S., Giubilato, P., and Pantano, D. (2017). “MATISSE: A Low power front-end electronics for MAPS characterization”. *TWEPP-17*. POS.

## Proton Beam-based R&D

### GammaRad

Cozzi, G., Busca, P., Carminati, M., Fiorini, C., Gola, A., Piemonte, C., and Regazzoni, V. (2016). “Development of a SiPM-based detection module for prompt gamma imaging in proton therapy”. *2016 IEEE Nuclear Science Symposium, Medical Imaging Conference and Room-Temperature Semiconductor Detector Workshop (NSS/MIC/RTSD)*, pp. 1–5.

Regazzoni, V., Acerbi, F., Cozzi, G., Ferri, A., Fiorini, C., Paternoster, G., Piemonte, C., Rucatti, D., Zappalà, G., Zorzi, N., and Gola, A. (2017a). *Characterization of High Density SiPM Non-linearity and Energy Resolution for Prompt Gamma Imaging Applications*. *Journal of Instrumentation* **12**(07), P07001.

### RIGHTABOVE

Ebner, D. K., Tinganelli, W., Helm, A., Bisio, A., Yamada, S., Kamada, T., Shimokawa, T., and Durante, M. (2017). *The Immunoregulatory Potential of Particle Radiation in Cancer Therapy*. *Frontiers in Immunology* **8**, p. 99.

# Seminars

## TIFPA Guest Seminars

- Tim Dietrich, Albert Einstein Institute, Potsdam, Germany, *Simulating generic binary neutron star mergers*, Feb. 9, 2017.
- Edoardo Vescovi, Humboldt-University, Berlin, Germany, *Heat kernel spectroscopy for Wilson loops in  $AdS_5 \times S^5$* , Mar. 27, 2017.
- Irene Maier, University of Vienna, UCLA and UCR, *Osteo-immunogenicity and intestinal microbiota in radiotherapy*, Apr. 3, 2017.
- Emilio Bellini, Beecroft Institute of Particle Astrophysics and Cosmology, University of Oxford, United Kingdom, *Maximal freedom at minimum cost: efficient description of general scalar-tensor theories*, Apr. 12, 2017.
- Alberto Andrighetto, INFN, Laboratori Nazionali di Legnaro, Italy, *The ISOLPHARM project: production of high purity radionuclides for nuclear medicine applications*, May 26, 2017.
- C.-J. Yang, Institut de Physique Nucléaire d'Orsay, France, *Toward the implementation of EFT concepts in density functional theory*, May 29, 2017.
- Walter Sanseverino, Sequentia Biotech, Barcelona, Spain, *Next Generation Bioinformatics: unleashing genomics potential*, June 15, 2017.
- Valerio Faraoni, Bishop's University, Sherbrooke, Canada, *Three cosmological applications of the quasilocal energy*, June 22, 2017.
- Ira-Ida Skvortsova, Medizinische Universität, Dept. of Therapeutic Radiology and Oncology, Innsbruck, Austria, *Cancer stem cells and radiation resistance*, July 10, 2017.
- Xavier Mougeot, CEA, LIST, Laboratoire National Henri Becquerel, Gif-sur-Yvette, France, *How the current high-precision experiments challenge the usual beta decay and electron capture models*, July 20, 2017.
- Marco Bruni, Institute of Cosmology and Gravitation, University of Portsmouth, United Kingdom, *Weak Field and Full GR Cosmological Simulations*, July 21, 2017.
- Werner Egger, Universität der Bundeswehr München, Neubiberg, Germany, *The pulsed low-energy positron beam system PLEPS for defect structure investigations: Principles and applications in materials sciences*, Sept. 11, 2017.
- Alessio Marrani, "Enrico Fermi" Center, Roma, INFN and University of Padova, Italy, *U-Duality and F-Duality : Linear and Non-Linear Symmetries of Black Hole Entropy*, Sept. 28, 2017.
- Alessandro Davoli, SISSA, Trieste, Italy, *Displaced vertices from pseudo-Dirac dark matter*, Oct. 24, 2017.
- Roberto Percacci, SISSA, Trieste, Italy, *Classical and quantum unimodular gravity and the cosmological constant*, Oct. 26, 2017.
- Ippocratis Saltas, Central European Institute for Cosmology and Fundamental Physics, Czech Republic, *Aspects of quantum stability and consistency of theories for dark energy*, Nov. 16, 2017.
- Sara Pozzi, Department of Nuclear Engineering and Radiological Sciences, University of Michigan, Ann Arbor, USA, *Neutron Detection in Proton Therapy for Cancer Treatment*, Dec. 21, 2017.

## Particle Physics

### ATLAS

Roberto Iuppa, invited talk: *Measurements of exclusive production in ATLAS*, At: Low x 2017, Bisceglie, Italy, June 12-18, 2017.

### RD-FASE2

Gian-Franco Dalla Betta, invited talk: *3D pixels sensors in Trento: update on activities and plans*, At: AIDA 2020 Second Annual Meeting, LPNHE, Paris, France, Apr. 4-7, 2017.

Gian-Franco Dalla Betta, invited talk: *Small pitch, thin 3D pixel sensors for phase 2 upgrades at LHC*, At: Journée thématique: Fabrication de détecteurs semiconducteurs, LPNHE, Paris, France, June 14, 2017.

Gian-Franco Dalla Betta, *Electrical characterization of FBK small-pitch 3D sensors after  $\gamma$ -ray, neutron and proton irradiations*, At: 19th International Workshop on Radiation Imaging Detectors (IWORID2017), AGH University of Science and Technology, Krakow, Poland, July 2-6, 2017.

Gian-Franco Dalla Betta, invited talk: *Sensor developments for Phase 2 ATLAS and CMS pixel detectors*, At: SIF 2017, Trento, Italy, Sept. 11-15, 2017.

Gian-Franco Dalla Betta, *Progress in Small-Pitch, Thin 3D Pixel Sensors for HL-LHC*, At: 2017 IEEE Nuclear Science Symposium and Medical Imaging Conference (NSS - MIC'17), Atlanta, USA, Oct. 21-28, 2017.

Gian-Franco Dalla Betta, *A three-dimensional gated diode structure for surface parameter characterization in a 3D sensor technology*, At: 2017 IEEE Nuclear Science Symposium and Medical Imaging Conference (NSS - MIC'17), Atlanta, USA, Oct. 21-28, 2017.

Roberto Mendicino, *Development of Thin, Narrow-Pitch 3D Pixel Sensors for HL-LHC*, At: 12th Trento Workshop on Advanced Silicon Radiation Detectors, Fondazione Bruno Kessler, Trento, Italy, Feb. 20-22, 2017.

## Astroparticle Physics

### AMS-02

Francesco Nozzoli, invited talk: *Alpha Magnetic Spectrometer, stato e prospettive dopo sei anni in orbita*, At: 103° Congresso Nazionale SIF, Società Italiana di Fisica, Trento, Italy, Sept. 11-15, 2017.

Francesco Nozzoli, *A Balance for Dark Matter Bound States*, At: 103° Congresso Nazionale SIF, Società Italiana di Fisica, Trento, Italy, Sept. 11-15, 2017.

### DarkSide

Marco Marcante, Poster: *Caratterizzazione criogenica da 300 K a 40 K di NUV-HD Silicon Photomultipliers*, At: XVI Incontri di Fisica della Alte Energie, Università degli Studi di Trieste, Trieste, Italia, Dec. 18-21, 2017.

### HUMOR

Antonio Pontin, *Quantum nondemolition measurement of light intensity fluctuations in an optomechanical experiment*, At: 2017 Conference on Lasers and Electro-Optics Europe & European Quantum Electronics Conference (CLEO/Europe-EQEC), International Congress Centre (ICM), Munich, Germany, June 25-29, 2017.

**LIMADOU**

Francesco Maria Follega, *Performance tests for the Limadou HEPD flight-model*, At: 103° Congresso Nazionale SIF, Società Italiana di Fisica, Trento, Italy, Sept. 11-15, 2017.

Ester Ricci, *Strategy for the Limadou HEPD event reconstructon*, At: 103° Congresso Nazionale SIF, Società Italiana di Fisica, Trento, Italy, Sept. 11-15, 2017.

**LISA Pathfinder**

Rita Dolesi, invited talk: *Gravitational Waves Space Detectors: status and science*, At: GWPAW 2017, Annecy, France, May 30, 2017.

Rita Dolesi, *Brownian noise and other stray forces introduced by residual gas surrounding geodesic reference masses: the experience of LISA Pathfinder*, At: Amaldi Meeting, Pasadena, USA, July 9-14, 2017.

Valerio Ferroni, *The challenge to fly at zero g. The case of LISA Pathfinder*, At: International Symposium on Gravitational Waves, Beijing, China, May 25-29, 2017.

Valerio Ferroni, *Measurement and compensation of the electrostatic patch effect on board LISA Pathfinder*, At: 3rd HUST-UNITN Workshop on inertial sensing for gravitational experiments in space, Wuhan, China, May 29, 2017.

Valerio Ferroni, *The challenge to fly at zero g. The case of LISA Pathfinder*, At: CNES CCT Workshop, Toulouse, France, Sept. 6-7, 2017.

Ferran Gilbert, *Temperature noise effects on LISA Pathfinder's GRS: preliminary results*, At: Temperature noise effects on LISA Pathfinder's GRS: preliminary results, Pasadena, USA, June 9, 2017.

Ferran Gilbert, *Special experiments on LISA Pathfinder*, At: 50th Rencontres de Moriond - Gravitation Session, La Thuile, Italy, Mar. 29, 2017.

Giuliana Russano, *Measurements of subfemto-g acceleration noise with parabolic flights in pico-g for space based gravitational wave observatory: LISA Pathfinder free-fall experiment results*, At: 12th Amaldi Conference on Gravitational Waves, Pasadena, USA, July 9-14, 2017.

Daniele Vetrugno, *LISA Pathfinder workflow: from a space based laboratory to the sub femto-g acceleration noise*, At: International Symposium on Gravitational Waves, Beijing, China, May 25-28, 2017.

Daniele Vetrugno, invited talk: *Measuring the differential force disturbances between two test-masses orbiting L1: Data analysis and results from the LISA Pathfinder satellite*, At: UNITN-HUST Workshop, Wuhan, China, May 29, 2017.

Daniele Vetrugno, invited talk: *LISA Pathfinder results: a ticket to listen to the music of the Universe ... from space!*, At: Wilhelm und Else Heraeus-Seminar, Gravitational decoherence Physikzentrum, Bad Honnef, Germany, Sept. 25-28, 2017.

Stefano Vitale, Special open event on Gravitational waves: *LISA and LISA Pathfinder*, At: Annual Gathering of the American Association for the Advancement of Science, Boston, USA, Feb. 20, 2017.

Stefano Vitale, General Lecture: *LISA Pathfinder*, At: International Symposium on gravitational waves, Beijing, China, May 26, 2017.

Stefano Vitale, General lecture: *LISA e LISA Pathfinder*, At: Fermi school on gravitational waves, Varenna, Italy, July 3-12, 2017.

Stefano Vitale, *LISA Pathfinder results*, At: LISA Pathfinder and Microscope Workshop, Toulouse, France, Sept. 6-7, 2017.

Stefano Vitale, Plenary Talk: *LISA e LISA Pathfinder*, At: 103° Congresso SIF, Trento, Italy, Sept. 11-15, 2017.

Bill Weber, *The physics of the LISA Pathfinder experiment*, At: International Symposium on gravitational waves, Beijing, China, May 26, 2017.

Bill Weber, *LISA Pathfinder: sub-femto-g differential accelerometry for gravitational wave observation from space*, At: Amaldi Meeting, Pasadena, USA, July 12, 2017.

Bill Weber, *LISA Pathfinder; LISA and the Gravitational Astronomy from the Dawn of the Universe*, At: A Decade of Agile, Rome, Italy, Dec. 13, 2017.

## Theoretical Physics

### BELL

Sonia Mazzucchi, invited talk: *Projective systems of functionals and generalized Feynman-Kac formulae*, At: Mathematical Congress of the Americas, Montreal U. Montreal, Canada, July 24-28, 2017.

Alberto Melati, *Renormalization of vector fields in locally covariant AQFT*, At: Microlocal analysis: a tool to explore a quantum world, Genova U, Genova, Italia, Jan. 13, 2017.

Alberto Melati, *Renormalization of vector fields in locally covariant AQFT*, At: Fundamental problems of quantum physics, Milano U, Milano, Italia, Mar. 13, 2017.

Valter Moretti, *Why quantum mechanics is complex?*, At: Physics and Geometry, Bologna U and INFN, Bologna Department of Physics, Italy, Nov. 20-21, 2017.

Marco Oppio, *Why do we need complex Hilbert spaces?*, At: XXVth International Conference on Integrable Systems and Quantum Symmetries, Prague, Czech Republic, June 6-10, 2017.

Marco Oppio, *Why do we need complex Hilbert spaces?*, At: Xth International Symposium on Quantum Theory and Symmetries, Varna, Bulgaria, June 19-25, 2017.

Davide Pastorello, invited talk: *Two-way quantum key distribution based on tripartite entanglement*, At: International Workshop Quantum Physics and Geometry, Trento U, CIRM, INFN, Levico Terme, Italia, July 4-6, 2017.

Alessandro Perotti, *Left and right eigenvalues of quaternionic matrices are not unrelated*, At: 11th International Conference on Clifford Algebras and Their Applications in Mathematical Physics, Ghent University, Ghent, Belgium, Aug. 7-11, 2017.

### BIOPHYS

Pietro Faccioli, invited talk: *Self-Consistent Atomistic Calculation of Protein Folding Pathways*, At: Challenges across Large-Scale Biomolecular and Polymer Simulations, Erwin Schroedinger Institute for Mathematics and Physics, Vienna, Austria, Feb. 21-24, 2017.

Pietro Faccioli, invited seminar: *Investigating Dynamics of Biomolecules with Theoretical Physics Methods*, At: Seminar, Pisa University and INFN, Pisa, Italy, Mar. 3, 2017.

Pietro Faccioli, invited talk: *Folding mechanism of knotted proteins*, At: DPG Spring Meeting, University of Dresden, Dresden, Germany, Mar. 23-24, 2017.

Pietro Faccioli, *Quantum Dynamics of molecular excitations in non-equilibrium*, At: Seeking synergy between dynamics and statistics for non-equilibrium quantum processes, Ecole Normal Superior, Paris, France, June 6-9, 2017.

Pietro Faccioli, invited talk: *Self-Consistent Atomistic Calculation of Protein Folding Pathways*, At: Computational approaches to investigating allostery, CECAM Headquarter, Lausanne, Switzerland, Oct. 20-1, 2017.

Pietro Faccioli, invited talk: *Instantons and topology in protein folding*, At: Gauge topology: from lattice to collider, ECT\*, Villazzano (Trento), Italy, Nov. 11-13, 2017.

Gianluca Lattanzi, *Challenges in computational biophysics: from membrane proteins to biosensors*, At: Challenges across Large-Scale Biomolecular and Polymer Simulations, Erwin Schroedinger Institute for Mathematics and Physics, Vienna, Austria, Feb. 21-24, 2017.

Gianluca Lattanzi, invited talk: *Challenges in computational biophysics: from membrane proteins to biosensors*, At: Basel Postdoc Network Retreat, Basel Postdoc Network, Zermatt, Switzerland, June 21-23, 2017.

Gianluca Lattanzi, invited talk: *My journey in Biophysics*, At: Frey Alumni Event, Department of Physics, Ludwig Maximilians Universitaet, Munich, Germany, July 8, 2017.

## FBS

Winfried Leidemann, invited talk: *Ab initio calculations for non-strange and strange few-baryon systems*, At: Fustipen Topical Meeting on “ Nuclear Structure and Reaction Theories: Building Together for the Future on Selected Topics in Nuclear and Atomic Physics”, GANIL, Caen, France, Oct. 9-13, 2017.

Giuseppina Orlandini, *Reactions to continuum with bound state methods: the integral transform approach*, At: Workshop on Selected Topics in Nuclear and Atomic Physics, University of Padova, Fiera di Primiero, Italy, Oct. 1-5, 2017. (Series of 4 invited talks).

## FLAG

Stefano Chinaglia, *A model of regular black hole (satisfying the Weak Energy Condition)*, At: IV Edition - Cosmology and the Quantum Vacuum, ICE-CSIC/IIEC and ICREA, Spain, Segovia, Spain, Sept. 4-8, 2017.

Massimiliano Rinaldi, invited talk: *Scale invariant inflationary universe*, At: collaboration seminar, Helsinki University, Helsinki, Finland, Jan. 25-28, 2017.

Massimiliano Rinaldi, invited talk: *Scale invariant gravity and inflation*, At: collaboration seminar, Oskar Klein Centre, Stockholm, Sweden, June 13-14, 2017.

Massimiliano Rinaldi, invited talk: *Scale invariant inflation*, At: collaboration Seminar, Dipartimento di Astronomia, Padova university, Padova, Italy, June 16, 2017.

Lorenzo Sebastiani, *Thermodynamical aspects of black holes in modified gravity*, At: Karl Schwarzschild meeting, Frankfurt University, FIAS, conference location, Germany, July 24-28, 2017.

## MANYBODY

Alessandro Lovato, invited talk: *A unified description of the nuclear EOS and neutrino responses*, At: Nuclear Astrophysics in the Gravitational Wave Astronomy Era, ECT\*, Trento, Italy, June 12-16, 2017.

Alessandro Lovato, invited talk: *Electromagnetic and neutral-current responses from Quantum Monte Carlo*, At: 11th International Workshop on Neutrino-Nucleus Scattering in the Few-GeV Region, University of Toronto, Toronto, Canada, June 25-30, 2017.

Alessandro Lovato, invited talk: *Nuclei from Lattice-QCD data*, At: Ab initio nuclear structure and electroweak response: current status and future prospects, Thomas Jefferson National Accelerator facility, Newport News, USA, Aug. 7-11, 2017.

Alessandro Lovato, invited talk: *Electron scattering within ab-initio approaches*, At: The 19th International Workshop on Neutrinos from Accelerators, Uppsala University, Uppsala, Sweden, Sept. 25-30, 2017.

Alessandro Lovato, invited talk: *Electron scattering within ab-initio approaches*, At: XIV Conference on Theoretical Nuclear Physics in Italy, Cortona, Italy, Oct. 3-5, 2017.

Alessandro Lovato, invited talk: *Nuclei from Lattice-QCD data*, At: UK nuclear theory meeting, University of York, York, UK, Nov. 2-3, 2017.

Alessandro Lovato, invited talk: *Quantum Monte Carlo predictions for electron- and neutrino-nucleus scattering*, Fermilab, Batavia, USA, Nov. 16, 2017.

Alessandro Lovato, invited talk: *Quantum Monte Carlo results for electron- and neutrino-nucleus scattering*, At: MANYBODY collaboration meeting, University of Torino, Torino, Italy, Dec. 12-13, 2017.

Alessandro Lovato, invited talk: *MANYBODY Theory of nuclear quantum many-body systems*, At: SM&FT 2017 High Performance Computing in Theoretical Physics, Bari, Italy, Dec. 13-15, 2017.

Francesco Pederiva, invited talk: *Pushing QMC beyond locality and time reversal: the nuclear physics case*. At: Sign Problem 2017, Institute of Nuclear Theory, University of Washington, Seattle, USA, Mar. 22-24, 2017.

Francesco Pederiva, invited talk: *Neutron Equation of State from QMC Calculations*, At: Transport 2017, FRIB - Michigan State University, East Lansing, Michigan, USA, Mar. 27-30, 2017.

Francesco Pederiva, invited talk: *TDLDA density and spin density response functions in neutron matter based on QMC calculations of the equation of state*, At: Landau Fermi Liquid Theory in Nuclear and Many-Body Systems, ECT\*, Trento, Italy, May 22-26, 2017.

Francesco Pederiva, invited talk: *Hypernuclei and Hypermatter: Quantum Monte Carlo Studies*, At: Nuclear Astrophysics in the Gravitational Wave Astronomy Era, ECT\*, Trento, Italy, June 12-16, 2017.

Francesco Pederiva, invited talk: *Bridging LQCD and Many-Body Nuclear Physics with a Pionless Effective Field Theory*, At: Workshop on Neutrino-less Double-beta Decay, Institute of Nuclear Theory, University of Washington, Seattle, USA, July 6-7, 2017.

Francesco Pederiva, invited talk: *Microscopic Theories of Strongly Interacting Many-Body Systems*, At: Theoretical Nuclear Physics in Italy, INFN, Cortona, Italy, Oct. 3-5, 2017.

Francesco Pederiva, invited talk: *Progress in the understanding of the role of hyperons in the inner core EOS*, At: ASTRA: Advances and open problems in low-energy nuclear and hadronic STRAngeness physics, ECT\*, Trento, Italy, Oct. 23-27, 2017.

Francesco Pederiva, invited talk: *Progress in the understanding of the role of hyperons in the inner core EOS*, At: COMPSTAR Working Group 2 Meeting, INFN - Sezione di Catania, Catania, Italy, Nov. 7-9, 2017.

## NEMESYS

Simone Taioli, *Synthesis of carbon-based materials by SuMBE: theory and experiment*, At: Synthetic methods across the flagship, University of Barcelona, Puerto de La Cruz, Tenerife, Spain, Feb. 05-10, 2017.

Simone Taioli, *Graphene synthesis, carbon foams, pillared graphene, pseudospheres and all that from first-principles, multiscale simulations and experiments*, At: 1st European Conference on Chemistry of Two-Dimensional Materials (Chem2DMat), University of Strasbourg, Strasbourg, France, Aug. 22-26, 2017.

Simone Taioli, *Graphene synthesis, carbon foams, pillared graphene, pseudospheres and all that from first-principles, multiscale simulations and experiments*, At: Recent Progress in Graphene & 2D Materials Research 2017, National University of Singapore, Singapore, Singapore, Sept. 19-22, 2017.

## TEONGRAV

Riccardo Ciolfi, invited talk: *Binary neutron star mergers as multimessenger sources*, INAF-IASF, Bologna, Italy, Mar. 15, 2017.

Riccardo Ciolfi, invited talk: *Multimessenger astrophysics with binary neutron star mergers*, IST, University of Lisbon, Lisbon, Portugal, Apr. 13, 2017.

- Riccardo Ciolfi, invited talk: *Gravitational wave sources and multimessenger astronomy*, At: 18th Lomonosov Conference on Elementary Particle Physics, Moscow State University, Moscow, Russia, Aug. 24 -30, 2017.
- Riccardo Ciolfi, invited talk: *X-ray emission from gravitational wave sources*, At: THESEUS Workshop, INAF, Osservatorio Astronomico di Napoli, Napoli, Italy, Oct. 05 -06, 2017.
- Riccardo Ciolfi, invited talk: *Coalescing neutron stars: theoretical models and perspectives*, At: LXI Congress of the Italian Astronomical Society, Padova University and INAF-Osservatorio Astronomico di Padova, Padova, Italy, Oct. 12 -15, 2017.
- Andrea Endrizzi, *Numerical Simulations of Binary Neutron Stars in GRMHD*, At: 2017 PhD Workshop, University of Trento, Trento, Italy, Nov. 29, 2017.
- Andrea Endrizzi, *Binary Neutron Star Mergers: Effects of Magnetic Fields in the Post-Merger Evolution*, At: NewCompStar Annual Conference, University of Warsaw, Warsaw, Poland, Mar. 27-31, 2017.
- Andrea Endrizzi, *Binary Neutron Star Mergers: Effects of Magnetic Fields in the Post-Merger Evolution*, At: Bridging Nuclear and Gravitational Physics: the Dense Matter Equation of State, ECT\*, Trento, Italy, June 05-09, 2017.
- Andrea Endrizzi, *Effects of the BL microphysical Equation of State on Binary Neutron Star Mergers*, At: 108th National Congress of the Italian Physics Society (SIF), SIF, Trento, Italy, Sept. 11-17, 2017.
- Andrea Endrizzi, *GRMHD simulations of binary neutron star mergers forming a long-lived neutron star*, At: EU Einstein Toolkit 2017 & EdFest, University of Mallorca, Palma de Mallorca, Spain, Oct. 11-13, 2017.
- Bruno Giacomazzo, invited talk: *Magnetic Field Effects in Merging Binary Neutron Stars*, Stony Brook University, Stony Brook, NY, USA, Jan. 25, 2017.
- Bruno Giacomazzo, “*General Relativistic Simulations of Low-Mass Magnetized Binary Neutron Star Mergers*”, At: “April Meeting” of the American Physical Society, Washington DC, USA, Jan. 28-31, 2017.
- Bruno Giacomazzo, invited talk: *Merging Neutron Stars as Tools for Fundamental Physics*, At: European Week of Astronomy and Space Science, Prague, Czech Republic, June 26, 2017.
- Bruno Giacomazzo, invited talk: *General Relativistic MagnetoHydroDynamic Simulations: a Review and Status Report*, At: European Physical Society 44TH CONFERENCE ON PLASMA PHYSICS, Belfast, UK, June 30, 2017.
- Bruno Giacomazzo, *Magnetic Field Effects in the Post-Merger Phase of Binary Neutron Stars*, At: INT Workshop “Observational Signatures of r-process Nucleosynthesis in Neutron Star Mergers”, Seattle, WA, USA, Aug. 1-4, 2017.
- Bruno Giacomazzo, invited talk: *GRMHD simulations of binary NS mergers and possible future directions*, At: The Astrophysics of NS Mergers, Flatiron Institute, New York, NY, USA, Nov. 20-22, 2017.
- Bruno Giacomazzo, invited talk: *Simulating Binary Neutron Star Mergers in the Multi-Messenger Era*, University of Pisa, Pisa, Italy, Nov. 30, 2017.
- Bruno Giacomazzo, invited talk: *Simulating Binary Neutron Star Mergers in the Multi-Messenger Era*, Friedrich Schiller Universität, Jena, Germany, Dec. 5, 2017.

## Technological and Interdisciplinary Physics

### APiX2

- Lucio Pancheri, invited talk: *State of the art and perspectives of CMOS avalanche detectors*, CERN, Geneva, CH, Jan. 20, 2017.

## ARDESIA

Giovanni Bellotti, *Silicon Drift Detectors and Readout ASICs for High-Resolution and High-Count Rate X-Ray Spectroscopy*, At: 12th “Trento” Workshop on Advanced Silicon Radiation Detectors (TREDI2017), Trento, Italy, Feb. 20-22, 2017.

Giovanni Bellotti, *ARDESIA: 4-Channels Fast SDD X-ray Spectrometer for Synchrotron Applications*, At: 24th International Congress on X-ray Optics and Microanalysis (ICXOM24), Trieste, Italy, USA, Sept. 25-29, 2017.

Giovanni Bellotti, *ARDESIA: 4-Channels Fast SDD X-ray Spectrometer for Synchrotron Applications*, At: IEEE Nuclear Science Symposium and Medical Imaging Conference (NSS/MIC), Atlanta, GA, USA, Oct. 21-28, 2017.

## MoVe-IT

Emanuele Scifoni, invited talk: *Research possibilities in quantum technology at TIFPA irradiation facilities*, At: Workshop Q@TN - Quantum Science and Technology in Trento, Università di Trento, Trento, Italy, Jan. 20, 2017.

Emanuele Scifoni, invited talk: *Radiobiology of particle beams: Basics and Hot Topics*, At: OMA International School on Medical Accelerators, CNAO, Pavia, Italy, June 5-9, 2017.

Emanuele Scifoni, invited talk: *Ion beam Biophysics: Fundamentals and Research Challenges at GSI/FAIR*, At: Fifth International FAIR School, Castiglione della Pescaia, Italy, Sept. 3-10, 2017.

Emanuele Scifoni, invited talk: *Single and multi-ion biologically optimized treatment planning with oxygen beams*, At: SIF, 103° Congresso Nazionale della Società Italiana di Fisica, Università di Trento, Trento, Italy, Sept. 11-15, 2017.

Emanuele Scifoni, invited talk: *Le Particelle nel Ritrattamento: Razionale radiobiologico*, At: 3° Corso Avanzato AIRB: La moderna reirradiazione, Centro Protonterapia APSS, Trento, Italy, Oct. 6-7, 2017.

Emanuele Scifoni, invited talk: *Missing Physics Data for Treatment Planning Systems*, At: International Symposium of Ion Therapy (ISIT), UT Southwestern Medical Center, Dallas, USA, Nov. 1-3, 2017.

Emanuele Scifoni, invited talk: *Biologically oriented treatment planning*, At: MICROS, 17th International Symposium on Microdosimetry, Venice, Italy, Nov. 5-10, 2017.

Emanuele Scifoni, invited talk: *MoVe IT - Modeling and Verification of Ion beam Treatment planning: an overview*, At: PRESS, Proton Therapy Research Seminars, IFJ PAN, Krakow, Poland, Nov. 24, 2017.

## NEWREFLECTIONS

William J. Burger, *Radiation Shielding for Long-Term Manned Space Mission*, At: 9th IAASS Conference, Toulouse, France, Oct. 18-20, 2017.

## Proton Beam-based R&D

### GammaRad

Veronica Regazzoni, poster: *Characterization of High Density SiPM Non-linearity and Energy Resolution for Prompt Gamma Imaging Applications*, At: New Developments in Photodetection (NDIP) 2017, Tours, France, July 3-7, 2017.

**RIGHTABOVE**

Walter Tinganelli, invited talk: *Radiobiology projects*, At: Meet the Professor, Istituto Scientifico Romagnolo per lo Studio e la Cura dei Tumori (IRST), Meldola, Italy, Apr. 18, 2017.

Walter Tinganelli, invited talk: *Radiobiology project at TIFPA*, University of Naples Parthenope, Naples, Italy, Dec. 21, 2017.

**ROSSINI**

Chiara La Tessa, *Innovative shielding materials for radioprotection in space*, At: NASA Human Research Program Investigators' Workshop (HRP), NASA, Galveston, TX, US, Jan. 23-26, 2017.

Chiara La Tessa, invited talk: *The role of detectors in nuclear physics measurements for radiotherapy and space applications*, At: 12th Trento Workshop on Advanced Silicon Radiation Detectors, Fondazione Bruno Kessler (FBK), Trento, Italy, Feb. 20-22, 2017.

Chiara La Tessa, invited talk: *Fisica applicata alla medicina*, At: VII International Course "Detectors and Electronics for High Energy Physics, Astrophysics, Space and Medical Physics", Legnaro National Laboratories (LNL), Legnaro, Italy, Apr. 7, 2017.

Chiara La Tessa, invited talk: *Fisica applicata alla medicina*, At: XXIX National School of Nuclear and Subnuclear Physics "Francesco Romano", Otranto, Italy, May 27, 2017.

Chiara La Tessa, contributed: *A new experimental facility at the Trento Protontherapy center*, At: 63th Radiation Research Society (RADRES), Cancun, Mexico, Oct. 15-18, 2017.

Chiara La Tessa, invited talk: *The role of microdosimetry in hadrontherapy and space radioprotection*, At: 17th International Symposium on Microdosimetry (MICROS), Venice, Italy, Nov. 5-10, 2017.

Marta Rovituso, *Una nuova facility di irraggiamento presso il Centro di Protonterapia di Trento*, At: Giornata SIRR, SIRR, Napoli, Italy, May 31, 2017.

Marta Rovituso, *Fragmentation and lateral scattering of 120 and 200 MeV/u  $^4\text{He}$  ions in water targets*, At: 103° Congresso Nazionale della SIF, SIF, Trento, Italy, Sept. 11-16, 2017.

Marta Rovituso, contributed: *Characterization of innovative shielding materials for radioprotection in deep-space travels*, At: 63th Radiation Research Society (RADRES), Cancun, Mexico, Oct. 15-18, 2017.

## Events

Marco Durante, round table: *Conoscere l'Universo, esplorare il corpo umano*, at Festival delle Scienze, Rome, 14 May 2017.

Marco Durante, invited talk: *Curare con le particelle. Dalla ricerca fondamentale alle terapie oncologiche*, at Incontri Uomo-Virtuale a Palazzo Blu, Pisa, 18 May 2017.

Marco Durante, round table: *Economia della salute e protonterapia*, at 12° Festival dell'Economia, Trento, 3 June 2017.

Marco Durante, invited talk: *Ioni pesanti: dalla terapia del cancro alla missione su Marte*, at “Sapere e Futuro”, Trento, 24 Nov. 2017.

Marco Durante, Outreach Fringe Program “Fisicittà” within 103° Congresso Nazionale SIF, “Science on screen”, Trento, 12 Sept. 2017.

Marco Durante, Outreach Fringe Program “Fisicittà” within 103° Congresso Nazionale SIF, “E.R. fisici in prima linea”, Trento, 13 Sept. 2017.

Roberto Iuppa, Ester Ricci, *International Masterclasses — hands on particle physics*, in collaboration with CERN, Trento, 16 Mar. 2017.

Roberto Iuppa, *Protoni sempre in giro lungo un tubo del raggio d'un canederlo trentino*, at Pint of Science Festival, Trento, 17 May 2017.

Roberto Iuppa, Chiara La Tessa, Massimiliano Rinaldi, Walter Tinganelli, Outreach Fringe Program “Fisicittà” within 103° Congresso Nazionale SIF, *Particelle*, series of talks in collaboration with TEDx Trento, Trento, 14 Sept. 2017.

Massimiliano Rinaldi, seminar: *Einstein, buchi neri e onde gravitazionali*, Università della Libera Età, Novellara (RE), 9 Jan. 2017.

Emanuele Scifoni, Organizer Meeting *ARGENT, Advanced Radiotherapy Generated by Nanoprocesses and Technologies*, Centre for Cancer Research and Cell Biology, Queen University Belfast, (UK), 22-24 Feb. 2017.

Emanuele Scifoni, Outreach Lecture: *La ricerca in Adroterapia*, Visit to Protontherapy Center of Liceo Prati, Trento, 6 Mar. 2017.

Emanuele Scifoni, Outreach Lecture: *La ricerca in Adroterapia*, Visit to Protontherapy Center of Liceo Arcivescovile of Trento and Liceo Rosmini of Rovereto, Trento, 3 May 2017.

Emanuele Scifoni, Outreach Lecture: *MoVe IT, Modeling and Verification for Ion beam Treatment planning An Overview*, Visit to Protontherapy Center of UniTN Biology students, Trento, 3 May 2017.

Emanuele Scifoni, Organizer *MoVe IT 1st annual Meeting*, Università Federico II, Naples, 31 May-1 June 2017.

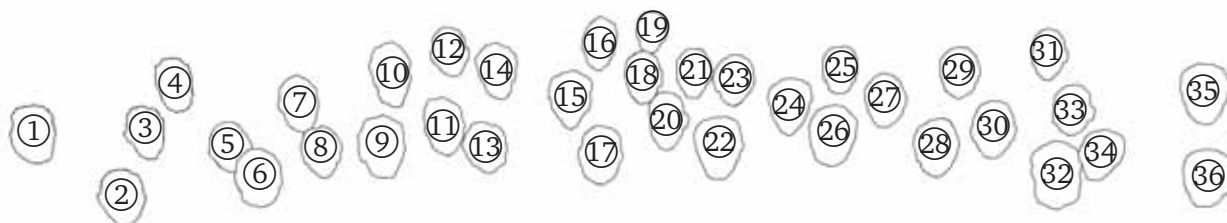
Emanuele Scifoni, LOC member, 103° Congresso Nazionale SIF, Università di Trento, 11-15 Sept. 2017.

Emanuele Scifoni, Organizer Outreach Fringe Program “Fisicittà” within 103° Congresso Nazionale SIF, *La fisica come non la avete mai vista*, Trento, 11-15 Sept. 2017.

Emanuele Scifoni, invited talk: *Particelle sempre più brave: La Ricerca in Fisica Nucleare per avanzare la Terapia con Protoni e altre Particelle cariche* to outreach event “Notte dei Ricercatori”, Muse, Trento, 29 Sept. 2017.

Emanuele Scifoni, invited talk: *Charged particles radiation biophysics: from cancer therapy to space research* to outreach event: “Porte Aperte all'Università di Trento”, 20 Oct. 2017.





① Enrico Serra

② Ignazio Lazzizzera

③ Marta Perucci

④ Emanuele Scifoni

⑤ Laura Chilovi

⑥ Gian-Franco Dalla Betta

⑦ Alexander Helm

⑧ Valentina Marchesano

⑨ Alberto Quaranta

⑩ Alessandro Lovato

⑪ Christian Manea

⑫ Piero Spinnato

⑬ Chiara La Tessa

⑭ Francesco Tommasino

⑮ Marco Schwarz

⑯ Paolo Falferi

⑰ Marco Durante

⑱ Walter Tinganelli

⑲ Lucio Pancheri

⑳ Enrico Verroi

㉑ Maurizio Boscardin

㉒ Graziano Fortuna

㉓ Alberto Gola

㉔ Giovanni Andrea Prodi

㉕ Nicola Zorzi

㉖ Stefano Vitale

㉗ Francesco Pederiva

㉘ Giuseppina Orlandini

㉙ Roberto Iuppa

㉚ Pierluigi Bellutti

㉛ Matteo Puel

㉜ William Jerome Burger

㉝ Laurent Basara

㉞ Giuliana Pellizzari

㉟ Francesco Dimiccoli

㊱ Irina Rashevskaya





*TIFPA group photograph 2017. See previous page for who's who.*



Trento Institute for  
Fundamental Physics  
and Applications

## **TIFPA - INFN**

c/o Dipartimento di Fisica  
Università di Trento  
Via Sommarive, 14  
38123 Povo (Trento), Italy  
tel.: +39 0461 281500  
fax: +39 0461 282000  
email: [info@tifpa.infn.it](mailto:info@tifpa.infn.it)  
[www.tifpa.infn.it](http://www.tifpa.infn.it)